

**CRANFIELD UNIVERSITY**



**JASON COLTON**

**MINIMISING PARTICULATE PASSAGE DURING RIPENING OF  
DIRECT FILTERS**

**SCHOOL OF WATER SCIENCES**

**PhD THESIS**

ProQuest Number: 10832178

All rights reserved

INFORMATION TO ALL USERS

The quality of this reproduction is dependent upon the quality of the copy submitted.

In the unlikely event that the author did not send a complete manuscript and there are missing pages, these will be noted. Also, if material had to be removed, a note will indicate the deletion.



ProQuest 10832178

Published by ProQuest LLC (2018). Copyright of the Dissertation is held by Cranfield University.

All rights reserved.

This work is protected against unauthorized copying under Title 17, United States Code  
Microform Edition © ProQuest LLC.

ProQuest LLC.  
789 East Eisenhower Parkway  
P.O. Box 1346  
Ann Arbor, MI 48106 – 1346

**CRANFIELD UNIVERSITY**

**SCHOOL OF WATER SCIENCES**

**PhD THESIS**

**ACADEMIC YEAR: 1996-1997**

**JASON COLTON**

**MINIMISING PARTICULATE PASSAGE DURING RIPENING OF DIRECT  
FILTERS**

**SUPERVISOR: Dr C.S.B. FITZPATRICK**

**DECEMBER 1996**

## ABSTRACT

A significant consideration in forward planning for water treatment works design and operation concerns the effectiveness of filtration plant in providing a barrier to particulates in the low micron size range, including *Cryptosporidium* oocysts. The filter ripening period has long been identified as a cause for concern with respect to particulate passage into the filtrate, this work has shown that up to 54% of all particles that pass into supply during a 48 hour run, do so in the first hour of operation

The aim of this study was to investigate methods of reducing particulate passage into the filtrate during ripening and identify optimum. Thus strengthening the filtration barrier to *Cryptosporidium* oocysts. The work was carried out on a large direct filtration pilot plant treating an upland lake source. Variables investigated included, filter media type and size, backwash regimes and durations, start-up strategies such as slow-start, and filtration rate.

The two filter media types and configurations that gave best removal were 1m beds of 0.5-1.0mm silica sand and 2m beds of 2.0-3.35mm quartz sand. A combined air/water backwash, at rates to achieve collapse-pulsing, reduced the numbers of particles in the filtrate during ripening and increased runlengths when compared to water only wash and air followed by water wash. Optimum backwash durations identified for the 0.5-1.0mm sand and 2.0-3.35mm sand were 4 and 3 minutes respectively.

The effect of start-up strategies on the numbers of particles in the filtrate during ripening was found to be variable. Slow start (both 1/2 hour and 1 hour) performed well under normal conditions experienced at the plant but performance was adversely affected by deteriorating raw water conditions. Delayed start was not as effective as slow start under normal conditions but was much more effective during periods of poorer raw water quality. Higher filtration rates (10 and 20m/h) resulted in much greater numbers of particles in the filtrate during ripening, thus fast-start was not a viable option.

Cost benefit analysis of the technical options showed backwash optimisation and delayed start to be attractive retro-fit options in terms of cost effective reduction of particulate passage during filter ripening.

## AKNOWLEDGEMENTS

I would like to acknowledge the support I have received from everyone in the Technology Development Team (Water) at North West Water Ltd. Special thanks to my company supervisor, Pete Hillis, without whose help and guidance this project would not have been possible.

I would like to thank my supervisor, Dr. Caroline Fitzpatrick, for her assistance. Thanks also to the other members of my steering committee, Dr. Hoi Yeung and Dr. Kazim Chaharabaghi.

Thanks to Fiona Shaw for all her effort and diligent work in sometimes trying conditions at the Lostock pilot plant.

I would like to thank Tanya Kent for all her faith, support and encouragement.

I am grateful to my sister, Sharon, for the loan of her computer and to my mother for all her support down the years.

Finally, thanks to all my friends at the School of Water Sciences, Cranfield, for their support.

## CONTENTS

<b>ABSTRACT</b>	i
<b>ACKNOWLEDGEMENTS</b>	ii
<b>CONTENTS</b>	iii
<b>LIST OF FIGURES</b>	xi
<b>LIST OF TABLES</b>	xxi
<b>CHAPTER 1 INTRODUCTION</b>	1
<b>CHAPTER 2 LITERATURE REVIEW</b>	4
<b>2.1 Historical perspective</b>	4
2.1.1.. <i>The Earliest Records</i>	4
2.1.2.. <i>The Seventeenth and Eighteenth Centuries</i>	4
2.1.3.. <i>The Nineteenth and Twentieth Centuries</i>	5
<b>2.2 Filtration Theory</b>	6
2.2.1 <i>Macroscopic filter behaviour</i>	7
2.2.1.1 <i>Transport mechanisms</i>	8
2.2.2 <i>Microscopic filter behaviour</i>	11
2.2.2.1 <i>Modeling the flow through a clean filter bed</i>	11
2.2.2.2 <i>Attachment mechanisms</i>	12
2.2.3 <i>Headloss build-up</i>	13
2.2.3.1 <i>Clean bed headloss prediction</i>	14
2.2.3.2 <i>Clogged bed headloss prediction</i>	15
2.2.4 <i>..Detachment mechanisms</i>	16
<b>2.3 Factors that play a key role in filtration</b>	17
2.3.1.. <i>Influent quality</i>	17
2.3.2.. <i>Pre - treatment</i>	18
2.3.3 <i>Filtration rate</i>	19
2.3.4 <i>Filter media</i>	20
<b>2.4..Filter Backwashing</b>	20
2.4.1 <i>Fluidised bed behavior</i>	21
2.4.2 <i>Backwash system development</i>	22

2.4.2.1	<i>Water only backwash</i>	23
2.4.2.2	<i>Water only backwash with surface wash auxiliary</i>	24
2.4.2.3	<i>Air scour followed by water backwash</i>	25
2.4.2.4	<i>Simultaneous air and water backwash</i>	26
2.4.3	<i>Other factors affecting particle detachment</i>	31
2.4.3.1	<i>Interaction forces between particles and collectors</i>	31
2.4.3.2	<i>Backwash duration</i>	32
<b>2.5</b>	<b>Start-Up and Filter Ripening</b>	33
<b>2.6</b>	<b>Filtrate quality concerns</b>	37
<b>2.7..</b>	<b>Monitoring filtrate quality</b>	38
2.7.1..	<i>The relationship between turbidity and particle counts</i>	39
2.7.2..	<i>Particle counting technology</i>	39
3.7.3..	<i>Applications in water management</i>	40
2.7.4..	<i>On - line monitoring</i>	40
<b>CHAPTER 3</b>	<b>OBJECTIVES</b>	43
<b>CHAPTER 4</b>	<b>PILOT PLANT SYSTEM</b>	45
<b>4.1</b>	<b>Location</b>	45
<b>4.2</b>	<b>Pilot pant complex</b>	47
<b>4.3</b>	<b>Operational procedure</b>	47
4.3.1	<i>Raw water delivery</i>	47
4.3.2	<i>pH control</i>	49
4.3.3	<i>Coagulation and flocculation</i>	49
4.3.4	<i>Normal operation</i>	51
4.3.5	<i>Backwash</i>	52
<b>4.4</b>	<b>Plant monitoring</b>	54
4.4.1	<i>Influent monitoring</i>	54
4.4.2	<i>Effluent monitoring</i>	54
4.4.3	<i>Headloss monitoring</i>	55
4.4.4	<i>Backwash water monitoring</i>	55
<b>4.5</b>	<b>Appurtenances</b>	55

<b>CHAPTER 5 MEDIA TESTING</b>	58
<b>5.1 Introduction</b>	58
<b>5.2 Experimental procedure</b>	58
5.2.1 <i>Media particle size distribution</i>	58
5.2.2 <i>Settling velocity measurement</i>	58
5.2.3 <i>Fluidised bed behaviour assessment</i>	59
5.2.4 <i>Collapse-pulsing backwash determination</i>	60
5.2.5 <i>Scanning electron microscope examination</i>	60
<b>5.3 Results</b>	60
5.3.1 <i>Media particle size distribution</i>	60
5.3.2 <i>Settling velocity measurement</i>	61
5.3.3 <i>Fluidised bed behaviour assessment</i>	62
5.3.4 <i>Collapse-pulsing backwash determination</i>	65
5.3.5 <i>Scanning electron microscope examination</i>	66
<b>5.4 Discussion</b>	70
5.4.1 <i>Media particle size distribution</i>	70
5.4.2 <i>Settling velocity measurement</i>	70
5.4.3 <i>Fluidised bed behaviour assessment</i>	71
5.4.4 <i>Collapse-pulsing backwash determination</i>	71
<b>CHAPTER 6 MEDIA PERFORMANCE ASSESSMENT</b>	74
<b>6.1 Introduction</b>	74
<b>6.2 Experimental procedure</b>	74
<b>6.3 Results</b>	78
6.3.1 <i>Influent conditions</i>	78
6.3.2 <i>Filter performance</i>	78
6.3.2.1 <i>1m bed of 0.5-1.0mm sand</i>	79
6.3.2.2 <i>2m beds of 2.0-3.35mm sand</i>	81
6.3.2.3 <i>1.5m bed of 1.18-2.8mm sand</i>	84
6.3.2.4 <i>0.5m bed of 0.35-0.6mm sand</i>	87
6.3.2.5 <i>1.5m 2-3.35mm sand and 0.5m 2.5-5mm anthracite</i>	90
6.3.2.6 <i>0.5m 2-3.35mm sand and 1.5m 2.5-5mm anthracite</i>	92
6.3.2.7 <i>0.3m of .6-1.4mm garnet and 1.7m of 2.5-5.0mm anthracite</i>	95



6.3.2.8 <i>Filter performance summary</i>	98
<b>6.4 Discussion</b>	101
6.4.1 <i>Performance monitoring</i>	101
6.4.2 <i>Filtrate quality</i>	104
6.4.1.1 <i>Filtrate quality during steady state operation</i>	104
6.4.1.2 <i>Filtrate quality during the ripening period</i>	106
6.4.2 <i>Headloss development</i>	112
6.4.3 <i>Solids removal during backwash</i>	113
6.4.3.1 <i>Turbidity washout curves</i>	113
6.4.3.2 <i>Clean bed headloss</i>	114
6.4.3.3 <i>Problems with the backwashing process</i>	115
6.4.5 <i>Media selection</i>	116
<b>6.5 Conclusions</b>	117

## **CHAPTER 7 THE EFFECT OF BACKWASH STRATEGY**

<b>ON PERFORMANCE</b>	119
<b>7.1 Introduction</b>	119
<b>7.2 Experimental Procedures</b>	119
7.2.1 <i>Backwash regime assessment</i>	119
7.2.2 <i>Backwash duration assessment</i>	120
<b>7.3 Results</b>	120
7.3.1 <i>Backwash regime assessment</i>	121
7.3.1.1 <i>Influent quality</i>	121
7.3.1.2 <i>1m beds of 0.5-1.0mm sand</i>	121
7.3.1.3 <i>2m beds of 2.0-3.35mm sand</i>	124
7.3.1.3 <i>Backwash regime summary</i>	126
7.3.2 <i>Backwash duration assessment</i>	127
7.3.2.1 <i>Influent conditions</i>	127
7.3.2.2 <i>1m bed of 0.5-1.0mm sand</i>	128
7.3.2.3 <i>2m beds of 2.0-3.35mm sand</i>	135
<b>7.4 Discussion</b>	142
7.4.1 <i>Backwash effectiveness</i>	142
7.4.1.1 <i>Backwash regime</i>	142

7.4.1.2 <i>CP backwash duration</i>	143
7.4.2 <i>Filter performance during ripening</i>	144
7.4.2.1 <i>Backwash regime</i>	144
7.4.2.2 <i>Backwash duration</i>	145
7.4.3 <i>Backwash selection</i>	147
<b>7.5 Conclusions</b>	148
<b>CHAPTER 8 START-UP STRATEGY ASSESSMENT</b>	150
<b>8.1 Introduction</b>	150
<b>8.2 Experimental methods</b>	150
<b>8.3 Results</b>	151
8.3.1 <i>Influent quality</i>	151
8.3.2 <i>Filter performance</i>	155
8.3.2.1 <i>The effect of poor raw water quality and increased ferric on filtrate quality</i>	156
8.3.2.2 <i>1m beds of 0.5 -1.0mm sand</i>	156
8.3.2.3 <i>2m beds of 2.0 -3.35mm sand</i>	163
8.3.3 <i>Filter headloss development</i>	170
8.3.3.1 <i>1m beds of 0.5 -1.0mm sand</i>	170
8.3.3.2 <i>2m beds of 2.0 -3.35mm sand</i>	170
8.3.4 <i>Relationship between raw water quality and NPFR</i>	171
<b>8.4 Discussion</b>	177
8.4.1 <i>The effect of start-up strategies on filter performance</i>	177
8.4.1.1 <i>Performance under “normal conditions” with 1.0mg/l ferric dose</i>	178
8.4.1.2 <i>Performance under “extreme conditions” with 1.5mg/l ferric dose</i>	185
8.4.1.3 <i>Summary of start-up strategy performance</i>	189
8.4.2 <i>The effect of start-up strategies on headloss development</i>	190
8.4.3 <i>Relationship between raw water quality and NPFR</i>	190
<b>8.5 Conclusions</b>	192

<b>CHAPTER 9 THE EFFECT OF FILTRATION RATE ON PERFORMANCE</b>	<b>194</b>
<b>9.1 Introduction</b>	<b>194</b>
<b>9.2 Experimental procedures</b>	<b>194</b>
<b>9.3 Results</b>	<b>195</b>
<i>9.3.1 Influent quality</i>	<b>195</b>
<i>9.3.2 Filter performance</i>	<b>196</b>
<i>9.3.2.1 1m beds of 0.5-1.0mm sand</i>	<b>196</b>
<i>9.3.2.2 2m beds of 2.0 - 3.35mm sand</i>	<b>201</b>
<b>9.4 Discussion</b>	<b>207</b>
<i>9.4.1. The effect of filtration rate on filtrate quality</i>	<b>207</b>
<i>9.4.2 The effect of filtration rate on runlength</i>	<b>210</b>
<i>9.4.3 The effect of higher filtration rates on water production</i>	<b>211</b>
<b>9.5 Conclusions</b>	<b>213</b>
<b>CHAPTER 10 ECONOMIC ASSESSMENT OF TECHNICAL OPTIONS</b>	<b>215</b>
<b>10.1 Introduction</b>	<b>215</b>
<b>10.2 The Research Drivers - Water quality regulations and regulators</b>	<b>215</b>
<b>10.3 Public Health Risk - The Threat of <i>Cryptosporidium</i></b>	<b>217</b>
<i>10.3.1 Occurrence of oocysts in raw water</i>	<b>217</b>
<i>10.3.2 Epidemiology of cryptosporidiosis</i>	<b>218</b>
<i>10.3.3 History of waterborne cryptosporidiosis outbreaks</i>	<b>219</b>
<i>10.3.4 Infectious dose of <i>Cryptosporidium</i> oocysts</i>	<b>220</b>
<i>10.3.5 Surrogate measures of water quality that allow</i> <i>assessment of public health risk</i>	<b>221</b>
<b>10.4 Treatment Options</b>	<b>222</b>
<i>10.4.1 Option 1 - Water only backwash</i>	<b>223</b>
<i>10.4.2 Option 2 - Air followed by water backwash</i>	<b>223</b>
<i>10.4.3 Option 3 - Combined air/water "collapse-pulsing" backwash</i>	<b>223</b>
<i>10.4.4 Option 4 - Backwash (Opt 3) duration optimisation</i>	<b>223</b>
<i>10.4.5 Options 5 and 6 - Backwash optimisation and Delayed start</i>	<b>224</b>
<i>10.4.6 Options 7 and 8 - Backwash optimisation and Slow-start</i>	<b>224</b>
<b>10.5 Treatment option costing system</b>	<b>224</b>
<i>10.5.1 Full-scale plant details</i>	<b>225</b>

10.5.2	<i>Capital cost of treatment options</i>	225
10.5.2.1	<i>Option 1 - Water only backwash</i>	225
10.5.2.2	<i>Option 2 - Air followed by water backwash</i>	225
10.5.2.3	<i>Option 3 - Combined air/water "collapse-pulsing" backwash</i>	226
10.5.2.4	<i>Option 4 - Backwash (Opt 3) duration optimisation</i>	226
10.5.2.5	<i>Options 5 and 6 - Backwash optimisation and Delayed start</i>	226
10.5.2.6	<i>Options 7 and 8 - Backwash optimisation and Slow-start</i>	227
10.5.3	<i>Operating costs of treatment options</i>	228
10.5.3.1	<i>Operating cost of different backwash regimes - Options 1,2 and 3</i>	229
10.5.3.5	<i>Option 4 - Backwash (Opt 3) duration optimisation</i>	231
10.5.3.2	<i>Options 5 and 6 - Backwash optimisation and Delayed start</i>	234
10.5.3.3	<i>Options 7 and 8 - Backwash optimisation and Slow-start</i>	235
10.5.4	<i>Total cost of treatment options for 5 year period</i>	237
<b>10.6</b>	<b>Performance measure</b>	238
<b>10.7</b>	<b>Cost Benefit Analysis</b>	239
10.7.1	<i>1m beds of 0.5-1.0mm sand</i>	240
10.7.2	<i>2m beds of 2.0-3.35mm sand</i>	242
<b>10.8</b>	<b>Conclusions/Recommendations</b>	245
<b>CHAPTER 11</b>	<b>CONCLUDING DISCUSSION</b>	247
11.1	<b>Problems encountered working under "real" conditions</b>	247
11.2	<b>Implications of the work</b>	249
<b>CHAPTER 12</b>	<b>FURTHER WORK</b>	253
<b>LIST OF SYMBOLS</b>		254
<b>LIST OF ABBREVIATIONS</b>		255

<b>REFERENCES</b>	256
<b>APPENDIX A</b>	268

## LIST OF FIGURES

### Chapter 2

Figure 2.1 Mechanisms of filtration (adapted from Amirtharajah, 1988).	7
Figure 2.2 Transport mechanisms of filtration (Ives, 1982).	9
Figure 2.3 Comparison of theoretical model and experimental data (Yao <i>et al.</i> , 1971).	10
Figure 2.4 Happel's sphere-in-cell model.	12
Figure 2.5 Characteristics of a fluidised bed (adapted from Cleasby, 1977).	22
Figure 2.6 Schematic of an air water distribution nozzle (Haarhoff and Malan, 1983).	25
Figure 2.7 Schematic of air motion corresponding to conditions below, at and exceeding collapse-pulsing. (McNelly and Amirtharajah, 1991).	27
Figure 2.8 Cleaning efficiencies and backwash parameters as functions of air and water flowrates shown in 3D plots (Fitzpatrick, 1991).	28
Figure 2.9 Recommended air and water backwashing flowrates for sand and 36 dual media filter beds (Amirtharajah <i>et al.</i> , 1991).	29
Figure 2.10 Formation of particle chains or dendrites during filtration (O'Melia and Ali 1978).	33
Figure 2.11 Schematic showing poor filtrate quality during ripening period (Adapted from Amirtharajah and Wetstein, 1980).	36

### Chapter 4

Figure 4.1 The pilot plant building at Lostock WTW.	45
Figure 4.2 Schematic diagram of Lostock direct filtration pilot plant (not to scale).	46
Figure 4.3 Schematic diagram of a lostock pilot plant filter column (not to scale).	48
Figure 4.4 Photograph showing four of the lostock pilot plant filter columns.	48
Figure 4.5 Photograph showing backwash water tank, pump and compressors.	49
Figure 4.6 Coagulant optimisation using particle count and turbidity - 1m deep 0.5-1.0mm sand filter.	50
Figure 4.7 Coagulant optimisation using colour and iron content - 1m deep 0.5-1.0mm sand filter.	50

Figure 4.8 Coagulant optimisation using particle count and turbidity - 2m deep 2.0-3.35 mm sand filter.	50
Figure 4.9 Coagulant optimisation using colour and iron content- 2m deep 2.0-3.35 mm sand filter.	50
Figure 4.10 Photograph showing pre-treatment chemicals and dosing pumps.	51
Figure 4.11 Pre-treatment system, showing dosing points, in-line mixers and pH control system.	52
Figure 4.12 Photograph showing electrically actuated v-notch ball valves on filter outlet	53

## Chapter 5

Figure 5.1 Schematic of testing apparatus used in media studies.	59
Figure 5.2 Media Settling velocities at 10°C.	61
Figure 5.3 Headloss and bed expansion curves for water only backwash - 0.355-0.6mm sand.	63
Figure 5.4 Headloss and bed expansion curves for water only backwash- 0.5-1.0mm sand	63
Figure 5.5 Headloss and bed expansion curves for water only backwash- 1.18-2.8mm sand	63
Figure 5.6 Headloss and bed expansion curves for water only backwash - 2.0-3.35mm sand	64
Figure 5.7 Headloss and bed expansion curves for water only backwash- 0.3-0.6mm garnet.	64
Figure 5.8 Headloss and bed expansion curves for water only backwash - 2.5-5.0mm anthracite.	64
Figure 5.9 Air and water backwash rates that cause collapse-pulsing.	66
Figure 5.10 Air rates and % $V_{mf}$ that cause collapse-pulsing.	66
Figure 5.11 Scanning electron micrograph of 0.5-1.0mm sand, x 50 magnification.	67
Figure 5.12 Scanning electron micrograph of 0.5-1.0mm sand, x 500 magnification.	67
Figure 5.13 Scanning electron micrograph of 1.18-2.0mm sand, x 30 magnification.	68
Figure 5.14 Scanning electron micrograph of 1.18-2.0mm sand, x 500 magnification.	68
Figure 5.15 Scanning electron micrograph of 2.0-3.35mm sand, x 20 magnification.	69

Figure 5.16 Scanning electron micrograph of 2.0-3.35mm sand, x 500 magnification 69

## Chapter 6

Figure 6.1	Illustration of how theoretical detention times were determined.	76
Figure 6.2	Mean filtrate 2-5 $\mu$ m particle count during ripening - 0.5-1.0mm sand	80
Figure 6.3	Headloss development during 48 hour run - 0.5-1.0mm sand	80
Figure 6.4	Backwash water turbidity during backwashing of 0.5-1.0mm sand filter.	80
Figure 6.5	Mean filtrate 2-5 $\mu$ m particle count during ripening - 2.0-3.35mm sand	83
Figure 6.6	Headloss development during 48 hour run - 2.0-3.35mm sand.	83
Figure 6.7	Backwash water turbidity during backwashing of 2.0-3.35mm sand filter.	83
Figure 6.8	Mean filtrate 2-5 $\mu$ m particle count during ripening - 1.18-2.8mm sand	86
Figure 6.9	Headloss development during 48 hour run - 1.18-2.8mm sand filter	86
Figure 6.10	Backwash water turbidity during backwashing of 1.18-2.8mm sand filter.	86
Figure 6.11	Mean filtrate 2-5 $\mu$ m particle count during ripening - 0.35-0.6mm sand.	88
Figure 6.12	Headloss development during 48 hour run - 0.35-0.6mm sand filter	88
Figure 6.13	Backwash water turbidity during backwashing of 0.35-0.6mm sand filter.	88
Figure 6.14	Mean filtrate 2-5 $\mu$ m particle count during ripening - 1.5m 2.0-3.35mm sand and 0.5m 2.5-5.0mm anthracite.	91
Figure 6.15	Headloss development during 48 hour run -1.5m 2.0-3.35mm sand and 0.5m 2.5-5.0mm anthracite filter.	91
Figure 6.16	Backwash water turbidity during backwashing of 1.5m 2.0-3.35mm sand and 0.5m 2.5-5.0mm anthracite filter.	91
Figure 6.17	Mean filtrate 2-5 $\mu$ m particle count during ripening - 0.5m of 2.0-3.35mm sand and 1.5m of 2.5-5.0mm.	94
Figure 6.18	Headloss development during 48 hour run - 0.5m of 2.0-3.35mm sand and 1.5m of 2.5-5.0mm filter.	94
Figure 6.19	Backwash water turbidity during backwashing of 0.5m of 2.0-3.35mm sand and 1.5m of 2.5-5.0mm filter.	94
Figure 6.20	Mean filtrate 2-5 $\mu$ m particle count during ripening -0.3m of 0.6-1.4mm garnet and 1.7m of 2.5-5.0mm anthracite.	96
Figure 6.21	Headloss development during 48 hour run - 0.3m of 0.6-1.4mm garnet and 1.7m of 2.5-5.0mm anthracite filter.	96



Figure 6.22 Backwash water turbidity during backwashing of 0.3m of 0.6-1.4mm garnet and 1.7m of 2.5-5.0mm anthracite filter.	96
Figure 6.23 Comparison of mean filtrate particle counts.	98
Figure 6.24 Comparison of total number of 2-5 $\mu$ m particles in first 420l of filtrate.	99
Figure 6.25 Comparison of headloss development during 48 hour run.	100
Figure 6.26 Comparison of backwash water turbidities	100
Figure 6.27 Comparison of particle count and particle volume of filtrate during ripening - 2m 2.0-3.35mm sand filter.	102
Figure 6.28 Particle size distribution of raw and filtered water (from 1m 0.5-1.0mm sand filter).	103
Figure 6.29 Percentage removals at steady state for a range of sand sizes.	105
Figure 6.30 Filter ripening for 2-5 $\mu$ m and 2-200 $\mu$ m particles.	107
Figure 6.31 Filter ripening for 2-5 $\mu$ m and 5-10 $\mu$ m particles.	107
Figure 6.32 Filter ripening for 10-15 $\mu$ m and 15-20 $\mu$ m particles.	107
Figure 6.33 Filter ripening for 20-25 $\mu$ m and 25-50 $\mu$ m particles.	107
Figure 6.34 Relationship between media size and ripening time.	108
Figure 6.34 Backwash water turbidities Vs. backwash water volume.	114

## Chapter 7

Figure 7.1 Fraction of 2-5 $\mu$ m particles remaining in filtrate after different backwash regimes.	122
Figure 7.2 Backwash water turbidities during different backwash regimes.	123
Figure 7.3 Headloss development during filter run following different backwash regimes.	124
Figure 7.4 Fraction of 2-5 $\mu$ m particles remaining in filtrate after different backwash regimes.	125
Figure 7.5 Backwash water turbidities during different backwash regimes.	126
Figure 7.6 Headloss development during filter run following different backwash regimes.	126
Figure 7.7 Filtrate 2-5 $\mu$ m particle count following 1 minute CP backwash - 0.5-1.0mm sand	129
Figure 7.8 Filtrate 2-5 $\mu$ m particle count following 2 minute CP backwash -	

0.5-1.0mm sand.	129
Figure 7.9 Filtrate 2-5 $\mu$ m particle count following 3 minute CP backwash - 0.5-1.0mm sand.	129
Figure 7.10 Filtrate 2-5 $\mu$ m particle count following 4 minute CP backwash - 0.5-1.0mm sand.	130
Figure 7.11 Filtrate 2-5 $\mu$ m particle count following 5 minute CP backwash 0.5-1.0mm sand.	130
Figure 7.12 Comparison of filtrate particles counts following a range of CP backwash durations - 0.5-1.0mm sand filter	132
Figure 7.13 Numbers of 2-5 $\mu$ m particles in the components of ripening following a range of CP backwash durations - 0.5-1.0mm sand filter	133
Figure 7.14 How the NPF following a range of CP backwash was affected by total backwash remnants and influent - 0.5-1.0mm sand	134
Figure 7.15 Headloss development following a range of CP backwash - 0.5-1.0mm sand.	134
Figure 7.16 Filtrate 2-5 $\mu$ m particle count following 1 minute CP backwash - 2.0-3.35mm sand	136
Figure 7.17 Filtrate 2-5 $\mu$ m particle count following 2 minute CP backwash - 2.0-3.35mm sand	136
Figure 7.18 Filtrate 2-5 $\mu$ m particle count following 3 minute CP backwash - 2.0-3.35mm sand.	136
Figure 7.18 Filtrate 2-5 $\mu$ m particle count following 4 minute CP backwash - 2.0-3.35mm sand	137
Figure 7.19 Filtrate 2-5 $\mu$ m particle count following 5 minute CP backwash - 2.0-3.35mm sand	137
Figure 7.20 Comparison of filtrate particles counts following a range of CP backwash durations - 2.0-3.35mm sand filter	139
Figure 7.21 Numbers of 2-5 $\mu$ m particles in the components of ripening following a range of CP backwash durations - 2.0-3.35mm sand filter.	140
Figure 7.22 How the NPF following a range of CP backwash was affected by total backwash remnants and influent - 2.0-3.35mm sand.	141
Figure 7.23 Headloss development following a range of CP backwash - 2.0-3.35mm sand.	141

## Chapter 8

Figure 8.1 Filtration flowrates (measured by digital flowmeters) for slow start strategies.	151
Figure 8.2 The effect of ferric (III) sulphate coagulation and flash mixing on the particle size distribution of high quality raw water (mean of 20 samples).	153
Figure 8.3 The effect of ferric (III) sulphate flocculation and flash mixing on the particle diameter of high quality raw water (mean of 20 samples).	154
Figure 8.4 The effect of ferric (III) sulphate flocculation and flash mixing on the power law slope coefficient ( $\beta$ ).	154
Figure 8.5 The effect of ferric (III) sulphate flocculation and flash mixing on the particle size Distribution of low quality raw water (mean of 8 samples).	155
Figure 8.6a Filtrate particle count vs. time - 1m beds of 0.5-1.0mm sand, 1.0mg/l ferric sulphate, 1 hour slow start, 1/2 hour delayed start	158
Figure 8.6b Filtrate particle count vs. volume of filtrate produced - 1m beds of 0.5-1mm sand, 1.0mg/l ferric sulphate, 1 hour slow start, 1/2 hour delayed start.	158
Figure 8.6c Cumulative number of 2-5 $\mu$ m particles in filtrate vs. volume filtrate produced 1m beds of 0.5-1.0mm sand, 1.0mg/l ferric sulphate, 1 hour slow , 1/2 hour delayed start	158
Figure 8.7a Filtrate particle count vs. time - 1m beds of 0.5-1.0mm sand, 1.5mg/l ferric sulphate, 1 hour slow start, 1/2 hour delayed start.	159
Figure 8.7b Filtrate particle count vs. volume of filtrate produced - 1m beds of .5-1mm sand, 1.5mg/l ferric sulphate, 1 hour slow start, 1/2 hour delayed start.	159
Figure 8.7c Cumulative number of 2-5 $\mu$ m particles in filtrate vs. volume filtrate produced 1m beds of 0.5-1.0mm sand, 1.5mg/l ferric sulphate, 1 hour slow , 1/2 hour delayed start	159
Figure 8.8a Filtrate particle count vs. time - 1m beds of 0.5-1.0mm sand, 1.0mg/l ferric sulphate, 1/2 hour slow start, 1 hour delayed start.	161
Figure 8.8b Filtrate particle count vs. volume of filtrate produced - 1m beds of .5-1mm sand, 1.0mg/l ferric sulphate, 1/2 hour slow start, 1 hour delayed start.	161
Figure 8.8c Cumulative number of 2-5 $\mu$ m particles in filtrate vs. volume filtrate produced 1m beds of 0.5-1.0mm sand, 1.0mg/l ferric sulphate, 1/2 hour slow, 1 hour delayed start.	161

Figure 8.9a	Filtrate particle count vs. time - 1m beds of 0.5-1.0mm sand, 1.5mg/l ferric sulphate, 1/2 hour slow start, 1 hour delayed start.	162
Figure 8.9b	Filtrate particle count vs. volume of filtrate produced - 1m beds of .5-1mm sand, 1.5mg/l ferric sulphate, 1/2 hour slow start, 1 hour delayed start.	162
Figure 8.9c	Cumulative number of 2-5 $\mu$ m particles in filtrate vs. volume filtrate produced 1m beds of 0.5-1.0mm sand, 1.5mg/l ferric sulphate, 1/2 hour slow, 1 hour delayed start.	162
Figure 8.10a	Filtrate particle count vs. time - 2m beds of 2.-3.35 sand, 1.0mg/l ferric sulphate, 1 hour slow start, 1/2 hour delayed start.	165
Figure 8.10b	Filtrate particle count vs. volume of filtrate produced - 2m beds of 2.0-3.35mm sand, 1.0mg/l ferric sulphate, 1 hour slow start, 1/2 hour delayed start.	165
Figure 8.10c	Cumulative number of 2-5 $\mu$ m particles in filtrate vs. volume of filtrate produced 2m beds of 2.0-3.35mm sand, 1.0mg/l ferric sulphate, 1 hour slow start, 1/2 hour delayed start.	165
Figure 8.11a	Filtrate particle count vs. time - 2m beds of 2.0-3.35mm sand, 1.5mg/l ferric sulphate, 1 hour slow start, 1/2 hour delayed start.	166
Figure 8.11b	Filtrate particle count vs. volume of filtrate produced - 2m beds of 2.-3.35mm sand, 1.5mg/l ferric sulphate, 1 hour slow start, 1/2 hour delayed start.	166
Figure 8.11c	Cumulative number of 2-5 $\mu$ m particles in filtrate vs. volume of filtrate produced beds of 2.0-3.35mm sand, 1.5mg/l ferric sulphate, 1 hour slow start, 1/2 hour delayed start	166
Figure 8.12a	Filtrate particle count vs. time - 2m beds of 2.0-3.35mm sand, 1.0mg/l ferric sulphate, 1/2 hour slow start, 1 hour delayed start.	168
Figure 8.12b	Filtrate particle count vs. volume of filtrate produced - 2m beds of 2.0-3.35mm sand, 1.0mg/l ferric sulphate, 1/2 hour slow start, 1 hour delayed start.	168
Figure 8.12c	Cumulative number of 2-5 $\mu$ m particles in filtrate vs. volume of filtrate produced 2m beds of 2.0-3.35 sand, 1.0mg/l ferric sulphate, 1/2 hour slow start, 1 hour delayed start	168
Figure 8.13a	Filtrate particle count vs. time - 2m beds of 2.0-3.35mm sand, 1.5mg/l ferric sulphate, 1/2 hour slow start, 1 hour delayed start	169

Figure 8.13b Filtrate particle count vs. volume of filtrate produced - 2m beds of 2.0-3.35mm sand, 1.5mg/l ferric sulphate, 1 hour slow start, 1/2 hour delayed start	169
Figure 8.13c Cumulative number of 2-5µm particles in filtrate vs. volume of filtrate produced 2m beds of 2.0-3.35mm sand, 1.0mg/l ferric sulphate, 1/2 hour slow start, 1 hour delayed start	.169
Figure 8.14a Headloss development -1m beds 0.5-1.0mm sand, 1.0mg/l ferric.	172
Figure 8.14b Headloss development-1m beds of 0.5-1.0mm sand,1.5mg/l ferric.	172
Figure 8.14c Headloss development-1m beds of 0.5-1.0mm sand,1.0mg/l ferric	172
Figure 8.14d Headloss development-1m beds of 0.5-1.0mm sand,1.5mg/l ferric	172
Figure 8.15a Headloss development-2m beds of 2.0-3.35mm sand,1.0mg/l ferric.	173
Figure 8.15b Headloss development - 2m beds of 2.0-3.35mm sand, 1.5mg/l ferric.	173
Figure 8.15c Headloss development-2m beds of 2.0-3.35mm sand,1.0 mg/l ferric.	173
Figure 8.15d Headloss development-2m bedsof 2.0-3.35mm sand, 1.5mg/l ferric.	173
Figure 8.16 Relationship between NPFR from 1m beds of 0.5-1.0mm sand and raw water quality. *Polynomial best fit line is for control only.	175
Figure 8.17 Relationship between NPFR from 2m beds of 2.0-3.35mm sand and raw water quality. *Polynomial best fit line is for control only.	175
Figure 8.18 Comparison of relationships between NPFR and raw water quality.	176
Figure 8.19 Particle size distribution data for 0.5-1.0mm sand filter, 1/2 hour slow start.	184
Figure 8.20 Backwash water turbidities under different loading rates - 1m beds of 0.5-1.0mm sand.	187

## Chapter 9

Figure 9.1 Real time filtrate particle count data at 6 and 10m/h (0.5-1.0mm sand).	197
Figure 9.2 Volume corrected filtrate particle count at 6 and 10m/h (.5-1mm sand).	197
Figure 9.3 Cumulative number of 2-5µm particles in filtrate (0.5-1.0mm sand)	197
Figure 9.4 Headloss development at 6 and 10m/h (0.5-1.0mm sand).	198
Figure 9.5 Real time filtrate particle count data at 6 and 20m/h (0.5-1.0mm sand).	199
Figure 9.6 Volume corrected filtrate particle count at 6 and 20m/h (.5-1mm sand).	199
Figure 9.7 Cumulative number of 2-5µm particles in filtrate (0.5-1.0mm sand).	199

Figure 9.8 Headloss development at 6 and 20m/h (0.5-1.0mm sand).	201
Figure 9.9 Real time filtrate particle count data at 6 and 10m/h (2.0-3.35mm sand).	202
Figure 9.10 Volume corrected filtrate particle count at 6, 10m/h (2-3.35mm sand).	202
Figure 9.11 Cumulative number of 2-5 $\mu$ m particles in filtrate (2.0-3.35mm sand).	202
Figure 9.12 Headloss development at 6 and 10m/h (2.0-3.35mm sand).	203
Figure 9.13 Real time filtrate particle count data at 6 and 20m/h (2.0-3.35mm sand).	205
Figure 9.14 Volume corrected filtrate particle count at 6, 20m/h (2.0-3.35mm sand).	205
Figure 9.15 Cumulative number of 2-5 $\mu$ m particles in filtrate (2.0-3.35mm sand).	205
Figure 9.16 Headloss development at 6 and 10m/h (2.0-3.35mm sand).	206
Figure 9.17 % Removal at steady state for a range of filtration rates (1m of 0.5-1.0 mm sand).	207
Figure 9.18 % Removal at steady state for a range of filtration rates (2m of 2.-3.35 mm sand).	207
Figure 9.19 Cumulative number of 25-400 $\mu$ m particles in filtrate (0.5-1.0mm sand).	209
Figure 9.20 Cumulative number of 25-400 $\mu$ m particles in filtrate (2.0-3.35mm sand).	209
Figure 9.21 Headloss development for 0.5-1.0mm sand at 10m/h.	210
Figure 9.22 Headloss development for 0.5-1.0mm sand at 20m/h.	210
Figure 9.23 Headloss development for 2-3.35mm sand at 10m/h.	210
Figure 9.24 Headloss development for 2-3.35mm sand at 20m/h.	210

## Chapter 10

Figure 10.1 Relationship of influent <i>Cryptosporidium</i> concentration and log reduction by treatment necessary to produce acceptable water (Haas <i>et al.</i> , 1996).	221
Figure 10.2 How start-up strategies affect water production during the start of filter run.	228
Figure 10.3 Annual operating costs, not incorporating production - 1m 0.5-1.0mm sand filters	240
Figure 10.4 Annual operating costs, incorporating production - 1m 0.5-1.0mm sand filters	240
Figure 10.5 Capital costs of technical options - 1m 0.5-1.0mm sand filter.	240
Figure 10.6 Performance of technical options - 1m 0.5-1.0mm sand filters	240
Figure 10.7 Cost benefit analysis not incorporating production -	

1m 0.5-1.0mm sand filter.	242
Figure 10.8 Cost benefit analysis incorporating production - 1m 0.5-1.0mm sand filter.	242
Figure 10.9 Annual operating costs, not incorporating production - 2m 2.0-3.35 mm sand filters	243
Figure 10.10 Annual operating costs, incorporating production - 2m 2.0-3.35 mm sand filters	243
Figure 10.11 Capital costs of technical options - 2m 2.0-3.35mm sand filter	243
Figure 10.12 Performance of technical options - 2m 2.0-3.35mm sand filters	243
Figure 10.13 Cost benefit analysis not incorporating production - 2m 2.0-3.35 mm sand filter	244
Figure 10.14 Cost benefit analysis incorporating production - 2m 2.0-3.35 mm sand filter	244

## Chapter 11

Figure 11.1 Effect of landslide at lake Thirlmere on raw water quality	247
Figure 11.2 The effect of temperature on filtrate quality during ripening	248
Figure 11.3 The effect of media age on filtrate quality during ripening	248
Figure 11.4. Particle count during ripening	249
Figure 11.5 Combined filtrate particle count	249

## LIST OF TABLES

### Chapter 4

Table 4.1 Appurtenances used in the Lostock pilot plant.	56
--	----

### Chapter 5

Table 5.1 Sieve analysis results.	61
Table 5.2 Media settling velocities at 10°C.	62
Table 5.3 Experimentally and theoretically determined values of $V_{mf}$ .	65

### Chapter 6 - need to change in chap and text!

Table 6.1 Media sizes and bed depths.	74
Table 6.2 Collapse-pulsing and rinse flowrates for all media.	75
Table 6.4 Theoretical detention times for all the filter media/configurations.	77
Table 6.5 Summary of influent quality during trial.	78
Table 6.6 Summary performance data for 1m bed of 0.5-1.0mm sand.	81
Table 6.7 Summary performance data for 2m bed of 2.0-3.35mm sand	84
Table 6.8 Summary performance data for 1.5m bed of 1.18-2.8mm sand.	87
Table 6.9 Summary performance data for 0.5m bed of 0.35-0.6mm sand.	89
Table 6.10 Summary performance data for 1.5m 2.0-3.35mm sand and 0.5m 2.5-5.0mm anthracite.	92
Table 6.11 Summary performance data for 0.5m 2.0-3.35mm sand and 1.5m 2.5-5.0mm anthracite.	95
Table 6.12 Summary performance data for 0.3m of 0.35-0.6mm garnet and 1.7m of 2.5-5.0mm anthracite.	97
Table 6.13 Mean steady state particle counts and % removals.	105
Table 6.14 Comparison of actual and predicted clean bed headloss	115



## Chapter 7

Table 7.1	Filter media and filter operating details	119
Table 7.2	Backwash flowrates and durations used in backwash regime assessment.	120
Table 7.3	Summary of influent conditions during backwash regime trial.	121
Table 7.4	Average NPF values for backwash components after different backwash regimes.	127
Table 7.5	Summary of influent conditions during trial.	127
Table 7.7	Filter performance parameters for a range of CP backwash durations - 1m beds of 0.5-1.0mm sand.	131
Table 7.8	Filter performance parameters for a range of CP backwash durations - 2m bed of 2.0-3.35mm sand	

## Chapter 8

Table 8.1	A summary of the raw water quality during the trial (before ferric dose increase)..	152
Table 8.2	A summary of the raw water quality during the trial (after ferric dose increase)..	152
Table 8.3	The effect of start-up strategy on daily performance in terms of NPF for 1m beds of 0.5-1.0mm sand.	163
Table 8.4	The effect of start-up strategy on daily performance in terms of NPF for 2m beds of 2.0-3.35mm sand.	170
Table 8.5	The overall effect of start-up strategies on performance of 1m beds of 0.5-1.0mm sand	177
Table 8.6	The overall effect of start-up strategies on performance of 2m beds of 2.0-3.35mm sand.	177

## Chapter 9

Table 9.1	Operational filter runlengths for a range of filtration rates.	195
Table 9.2	Summary of influent conditions during backwash regime trial.	196

Table 9.3	The effect of 10m/h filtration rate upon performance of 1m beds of 0.5-1.0mm sand filters during ripening.	198
Table 9.4	The effect of 20m/h filtration rate upon performance of 1m beds of 0.5-1.0mm sand filters during ripening.	200
Table 9.5	The effect of 10m/h filtration rate upon performance of 2m bed of 2.0-3.35mm sand filters during ripening.	203
Table 9.6	The effect of 20m/h filtration rate upon performance of 2m bed of 2.0-3.35mm sand filters during ripening.	204
Table 9.7	Approximation of hydraulic shear forces over a range of filtration rates.	205
Table 9.8	Summary of filter performance during ripening, as a function of filtration rate.	209
Table 9.9	Effect of filtration rate of water production parameters.	212

## Chapter 10

Table 10.1	Counts of <i>Cryptosporidium</i> oocysts from the National Monitoring Survey (Quennell and West, 1995).	218
Table 10.2	Capital cost for installation of delayed start control systems.	226
Table 10.3	Capital costs for installation of slow start valves and control systems	227
Table 10.4	Water production and backwash consumption - 1m 0.5-1.0mm sand filter.	229
Table 10.5	Operating costs for backwash regimes - 1m bed of 0.5-1.0mm sand.	230
Table 10.6	Water production and backwash consumption - 2m 2.0-3.35mm sand filter.	230
Table 10.7	Operating costs for backwash regimes - 2m bed of 2.0-3.35mm sand.	231
Table 10.8	Water consumption's ( $m^3/m^2$ ) during backwashing -1m bed of 0.5-1.0mm sand	231
Table 10.9	Water production and backwash consumption statistics for a 1m bed of 0.5-1.0mm sand.	232
Table 10.10	Total operating cost for different CP backwash durations - 1m of 0.5-1.0mm sand.	232
Table 10.11	Water consumption's ( $m^3/m^2$ ) during backwashing -2m bed of 2.0-3.35mm sand.	233
Table 10.12	Water production and backwash consumption statistics for a 2m bed of 2.0-3.35mm sand	233

Table 10.13	Total operating cost for different CP backwash durations - 2m of 2.0-3.35mm sand.	233
Table 10.14	Water production and backwash usage when using delayed start - 1m beds of 0.5-1.0mm sand	234
Table 10.15	Annual and total project operating costs of delayed start options - 1m beds of 0.5-1.0mm sand.	234
Table 10.16	Water production and backwash usage when using delayed start - 2m beds of 2.0-3.35mm sand.	235
Table 10.17	Annual and total project operating costs of delayed start options - 2m beds of 2.0-3.35mm sand.	235
Table 10.18	Water production and backwash consumption figures when using low-start options - 1m beds of 0.5-1.0mm sand.	236
Table 10.19	Annual and total project operating costs of slow start options - 1m beds of 0.5-1.0mm sand.	236
Table 10.20	Water production and backwash consumption figures when using slow-start options - 2m beds of 2.0-3.35mm sand.	236
Table 10.21	Annual and total project operating costs of slow start options - 2m beds of 2.0-3.35mm sand.	237
Table 10.22	Summary of operating and capital costs - 1m beds of 0.5-1.0mm sand	237
Table 10.23	Summary of operating and capital costs - 2m beds of 2.0-3.35 mm sand	238
Table 10.24	Relative performance of Technical Options - 1m beds of 0.5-1.0mm sand	259
Table 10.25	Relative performance of Technical Options - 2m beds of 2.0-3.35mm sand	259
Table 10.26	Pay-back time for invested capital - 1m 0.5-1.0mm sand filter	241
Table 10.27	Pay-back time for invested capital - 2m 2.0-3.35mm sand filter	244

## INTRODUCTION

In 1989 there was a waterborne outbreak of cryptosporidiosis in Swindon and parts of Oxfordshire. Five hundred people caught the disease, a self-limiting diarrhea, which can be life threatening to immuno-suppressed individuals. The disease was caused by a parasitic protozoan, *Cryptosporidium parvum*, which has a hardy, environmental resistant form called an oocyst. Following the Swindon outbreak the government commissioned a study on *Cryptosporidium* in water supplies by a group of experts, chaired by Sir John Badenoch. The Badenoch report (DoE/DoH, 1990) highlighted rapid gravity filtration as a key process stage since *Cryptosporidium* oocysts are resistant to chlorine and other forms of disinfection used in water treatment.

Rapid gravity filtration removes particles from suspension by attaching them to media or to previously retained particles. Because of the latter mode of attachment, the removal efficiency of filters improves over time after backwashing, this improvement is known as filter ripening. The period of high particulate passage, or ripening, was flagged in the Badenoch report as a particular cause for concern. The report detailed work on the effectiveness of filtration plants in providing a barrier to particulates in the low micron size band, including *Cryptosporidium* oocysts (LeChevallier *et al.*, 1991; and Ives *et al.*, 1993). Removals ranged from 75% to 99.999% (5 log). However, all reported significantly more oocysts and oocyst-sized particles entering supply during the ripening period.

Two possible methods of reducing the passage of particulates into supply during the ripening period were presented in the Badenoch report. The first was filter to waste, which is rarely an option when retro-fitting old plants. The second was slow start - gradual opening of the filter inlet/outlet valves so as to avoid any surges in flow. Slow start was taken up in parts of the UK water industry with some plants being retro-fitted. However, the effect of slow start on performance during the ripening period was still largely unknown.

North West Water decided that pilot plant trials were necessary in order to comply with recommendations in the Badenoch report. The trials would provide comprehensive performance data for a range of rapid gravity filtration options which would allow optimisation of existing plants and produce a basis for the selection and design of future plants.

The trials were designed to address the specific problems with raw waters that have been classified as 'clean waters' - thin, low alkalinity, upland waters, for which a filtration barrier against *Cryptosporidium* might be required.

The site chosen for the trials was Lostock Water Treatment Works (WTW) taking water from the Thirlmere Aqueduct (TA). This 200Ml/d supply from Lake Thirlmere is treated with lime and dosed with chlorine at the head of the aqueduct at Dunmail Raise. There is no treatment other than re-chlorination at the 22 take-offs, of which Lostock is the largest. The main perceived improvement for these types of waters was the provision of a barrier for *Cryptosporidium* species; non-compliance with manganese and tri-halo methanes (THM) were marginal issues. It was therefore seen as a suitable model for 'clean waters'. The Lostock site in particular offered a building capable of holding pilot rigs and a ready means of disposing of the test flow.

The particular intention of carrying out trials with ferric coagulation and direct conventional single stage filtration was to find the operating conditions under which passage of particulates into the treated water would be minimised. Although monitoring is regular, *Cryptosporidium* has rarely been found in TA water, numbers have been low when samples were positive. It was therefore accepted that performance with respect to *Cryptosporidium* removal would be through measurement of a surrogate, viz. particles of a similar size.

The reported size of *Cryptosporidium* oocysts in the literature is 3-6 $\mu$ m, the light extinction sensor-based particle counters used in these trials size oocysts in the range 2-4 $\mu$ m - due to their low refractive index. Thus monitoring particles in the 2-5 $\mu$ m size range provided a suitable surrogate for single oocysts. In addition the 2-5 $\mu$ m size range is the one closest to the particle size of minimum removal efficiency for rapid gravity filtration, which is 1 $\mu$ m.

# *CHAPTER 2*

## LITERATURE REVIEW

### 2.1 Historical perspective

#### 2.1.1 *The Earliest Records*

Sanskrit medical lore and Egyptian inscriptions provide the earliest recorded details on the use of filtration in water treatment.

The *Sus'rata Samhita*, a body of medical lore said to date from 2000 B.C (Baker, 1949) states: "Impure water should be purified by being boiled over a fire, or being heated in the sun, or by dipping a heated iron into it, or it may be purified by filtration through sand and coarse gravel and then allowed to cool."

The first depiction of filtration apparatus was found on the walls of Rameses II's tomb in the thirteenth century B.C. The picture shows wick siphons of assorted sizes. Wick siphons were also known to be commonly used in the days of Socrates (468-399 B.C) and Plato (427-347 B.C). By the time of Aristotle (384-322 B.C), a common knowledge of filtration through porous vessels existed, as detailed in his *De Generatione Animalium* (Baker, 1949).

It was a Roman who produced the first known detailed description of a water works system. Sextus Julius Frontinus, who in 97 A.D became the water commissioner of Rome, wrote a treatise on the Roman public water supply.

#### 2.1.2 *The Seventeenth and Eighteenth Centuries*

Some sixteen centuries after Frontinus, in 1685, the first known illustrated description of sand filters was published. The author was Luc Antonio Porzio, an Italian physician (Baker, 1949). Porzio proposed multiple filtration through sand, preceded by straining and sedimentation. His inspiration came from the filter-cisterns of the Venetian Ducal Palace, which led him to believe that filtration was " a very efficacious method of correcting the bad qualities of water".

There was little advancement in water treatment technology in the eighteenth century, with the possible exception of work carried-out by the French. The scientist Plüche published the first clear-cut recognition of the slowness of sedimentation compared with filtration, and of the need to periodically clean the sand in filters, in 1732. In the 1760's and 1780's, two French promoters obtained licenses for filter plants. One of these promoters built a filter plant and organised a city-wide carrier system to convey the treated water.

### 2.1.3 *The Nineteenth and Twentieth Centuries*

After the turn of the century, it was the English and Scottish who carried-out the pioneering work in filtration.

The first filter to supply water to a whole town was completed at Paisley, Scotland, in 1804, but the water it supplied was carted to consumers. Three years later in Glasgow filtered water was piped to consumers by two competing water companies. In 1810, one of these companies built the first recorded filter gallery. The two companies constructed six filter plants in total, however, none of them was a success.

In 1827, slow sand filters designed by Robert Thom were installed at Greenock, Scotland. Similar slow sand filters designed by James Simpson were installed at London in 1829. Thom's filters were cleaned by reverse-flow wash; Simpson's by surface scraping. Simpson's design became the model for sand filters throughout the world, whereas Thom's was followed in only a very few places.

It was not until the 1880's that a new sand filtration process appeared. The new process was rapid filtration, an American development. Four men were responsible for the evolution of the rapid sand filter: Patrick Clark, John Hyatt, Col. L.H. Gardner and Isaiah Smith Hyatt. The chief mechanical devices employed were jets of water applied on or just below the surface; reverse-flow wash, which operated through the whole depth of the filter; and revolving sand agitators or stirrers, which loosened the media from top to bottom. The first rapid filtration plant was installed in 1882, at Somerville, U.S.A. (Baker, 1949).



However, despite numerous designs the rapid sand filter was not adopted as the successor to slow sand filtration until the pioneering work by George W. Fuller was completed in 1897. Fuller compared the performance of slow sand filtration with rapid sand filtration for the treatment of turbid Ohio river water at Louisville. Rapid sand filtration was represented by four competing companies, who each supplied, installed and operated a 0.25-mgd. unit. Fuller concluded that rapid sand filtration, with its physico-chemical action, was far more suited to removing particulates from turbid river water than slow sand filtration - with its associated biological action.

After Fullers work was published many rapid sand filtration plants were installed throughout the U.S.A.. The "new" process was soon well ahead of its rival, it forged ahead until adoptions of the older process virtually ceased. Meanwhile old plants of the slow sand type either had their burdens lessened by the addition of rapid sand filters or else were abandoned.

The rapid sand filter became an integral part of the water treatment process.

## 2.2 Filtration Theory

Deep bed filtration has the characteristic feature that the suspended particles are deposited within a highly porous layer, leading to a high degree of particle removal from the water passing the filter. In most cases, the filter layer consists of a packing of filter grains (typically 0.5-4.0mm), which can be backwashed after a given runlength. During the filter run the capacity of the filter bed for the uptake of particles becomes exhausted, leading to either particulate breakthrough or an unacceptable increase of headloss.

In a deep bed filter, the deposition of particles requires two successive steps. A "transport mechanism" must first bring the small particles from the bulk of the fluid within the interstices close to the surfaces of the media. As a particle approaches the surface of the media, or of previously deposited particles on the media, an "attachment mechanism" is required to retain the particle. Both steps (shown in Fig 2.1) are the result of several forces and torques acting on the particles, such as drag and gravity forces, stochastic forces by Brownian motion, and physio-chemical surface forces. Thus, there exists an extremely complex situation, especially

under the practical conditions of water treatment. It is for this reason that there are still many unanswered questions concerning the particle removal process and why a comprehensive theory of deep bed filtration is still lacking. Despite this, the understanding of this process up to now is a very important basis for the optimization of the design and operation of deep bed filters.

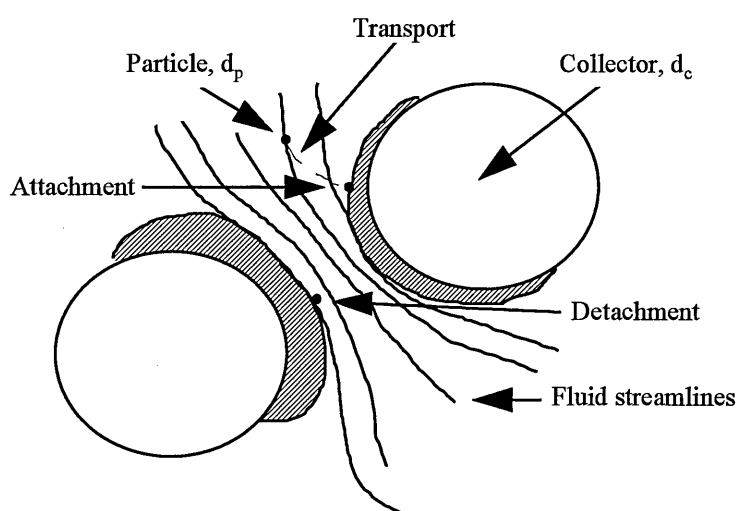


Figure 2.1. Mechanisms of filtration (adapted from Amirtharajah, 1988).

Numerous mathematical models have been put forward to explain filter behaviour, and they can in general, be classified into two groups: macroscopic description of filter behaviour, and microscopic filtration theory. The first describes, for practical means only, the relevant parameters like filtrate quality and headloss development as a function of time on an experimental basis. The second is strictly based on fundamental physio-chemical mechanisms, thus needing relatively little experimental information.

### 2.2.1 Macroscopic filter behaviour

The first mathematical model, based on material balance and kinetic equations, was proposed by Iwasaki (1935):

$$\frac{\partial C}{\partial L} = -\lambda.C \quad (1)$$

In this first order kinetic equation,  $C$  is the concentration of particulate matter at any depth or time,  $L$  is the bed depth, and  $\lambda$  is the filter coefficient. The equation states that the change in

particle concentration with depth is directly proportional to the bulk concentration of suspended material. In this equation, and indeed for macroscopic modelling in general a number of assumptions are made: that particle concentration over the filter cross section is homogeneous, and that the flow pattern is one-dimensional plug flow.

Iwasaki (1935) also proposed that:

$$\lambda = \lambda_0 + k_1\sigma \quad (2)$$

Where,  $\lambda_0$  is the clean bed filter coefficient,  $\sigma$  is the specific deposit, or volume of solids deposited per unit volume of bed, and  $k_1$  is a constant. This equation describes how the filter coefficient improves as deposited material accumulates. Follow-up work by Ives (1960), Ives and Sholji (1965), Ives and Gregory (1967) and Ison and Ives (1969) again showed and tried to describe the initial increase and eventual decrease in filter removal efficiency. Ives and co-workers concluded that the initial improvement was caused by an initial increase in surface area available for removal and then deterioration as the interstitial velocities became larger due to the clogging of filter pores. [ the increase in filter removal efficiency as a result of deposited material will be covered in more detail in a later section]

Ives and co-workers recognized the importance of viewing filtration as involving fluid transport of suspended particles to the media surfaces, or indeed the surfaces of previously captured particles.

#### 2.2.1.1 *Transport mechanisms*

A means of quantitatively describing transport mechanisms is the single collector efficiency,  $\eta$ , which is defined as the ratio of the rate at which suspended particles strike the collector to the rate at which suspended particles approach the collector. This is equivalent to the ratio of the area of streamlines cleared of particles to the projected area of the collector in the direction of flow (Tobiason and O'Melia, 1982).

Many forces can be considered in calculating the single collector efficiency. These include

hydrodynamic forces caused by disturbances in the flow regime near the collector, molecular diffusion (Brownian motion), gravity (sedimentation), and inertia. Removal may also occur by direct interception of particles with the collector surface as the particles follow streamlines. These transport mechanisms are shown schematically in Fig 2.2. It is generally accepted that under the laminar flow conditions of water filtration the dominant mechanisms are diffusion, sedimentation and interception.

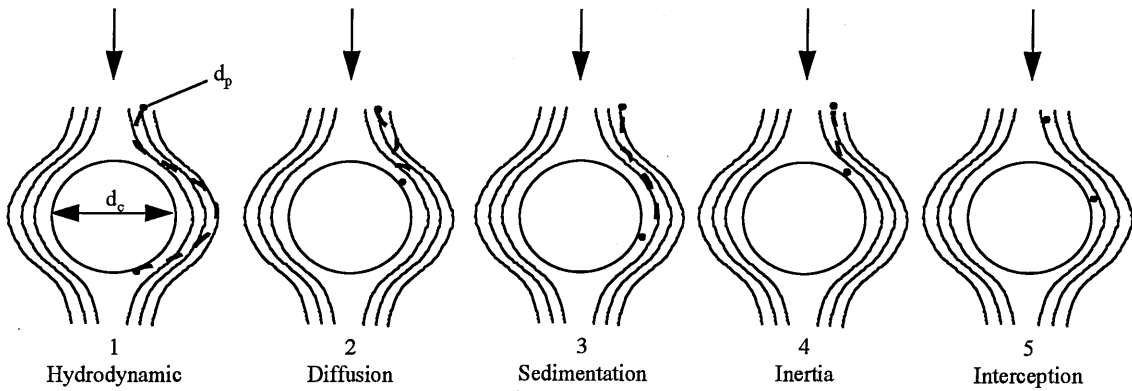


Figure 2.2 Transport mechanisms of filtration (Ives, 1982).

Many efforts have been made to describe each mechanism separately or a small group of mechanisms, the most notable contribution was by Yao *et al.*, (1971). They presented collection efficiencies for interception ( $\eta_I$ ), sedimentation ( $\eta_s$ ) and diffusion ( $\eta_D$ ) for spherical particles:

$$\eta_I = \frac{3}{2} \left( \frac{d_p}{d_c} \right)^2 \quad (3)$$

$$\eta_s = \frac{(\rho_p - \rho_l) g d_p^2}{18 \mu V_0} \quad (4)$$

$$\eta_D = 4.04 N_{Pe}^{\frac{2}{3}} = 0.9 \left( \frac{KT}{\mu d_p d_c V_0} \right)^{\frac{2}{3}} \quad (5)$$

Where  $K$  is the Boltzman's constant,  $T$  is the absolute temperature,  $\rho_p$  is the suspended particle density,  $\rho_l$  is the liquid density,  $d_p$  is the suspended particle diameter,  $d_c$  is the collector diameter,  $V_0$  is the filtration velocity,  $\mu$  is the water viscosity, and  $N_{Pe}$  is the Peclect number.

Yao *et al.*, (1971) also showed that the three single collection efficiencies for interception, sedimentation and diffusion could reasonably be assumed to be additive, so that the overall collector efficiency could be approximately expressed as:

$$\eta = \eta_I + \eta_S + \eta_D \quad (6)$$

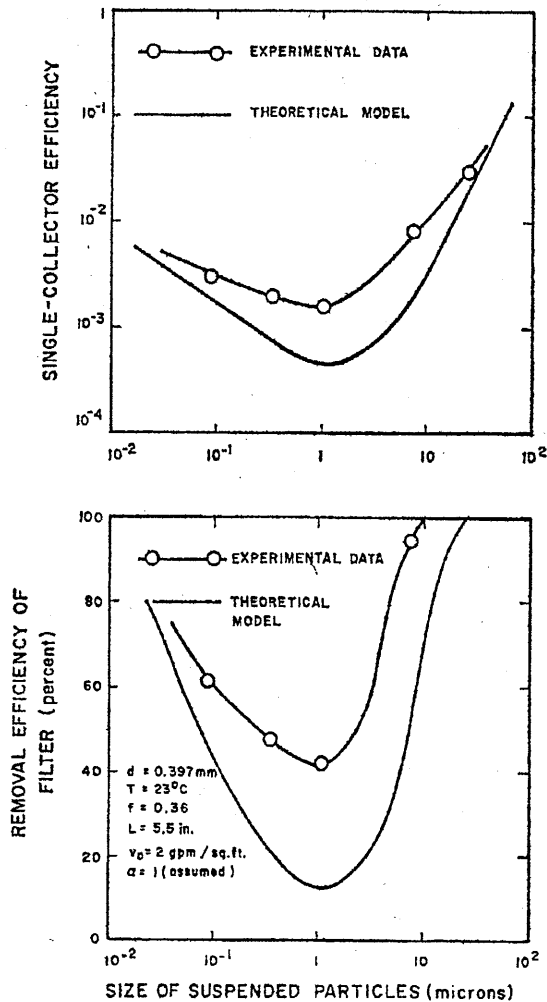


**Figure 2.3 Comparison of theoretical model and experimental data (Yao *et al.*, 1971).**

In the same piece of work, Yao *et al.* (1971) found that a minimum collector efficiency occurs for particles with a diameter of 1  $\mu\text{m}$ . For smaller particles diffusion is dominant, whereas for larger particles sedimentation and interception are the most important mechanisms, this is illustrated in Fig 2.3.

### *2.2.2 Microscopic filter behaviour*

Whereas the macroscopic approach is based on strongly simplified models, the microscopic approach attempts to address all forces and torques acting on particles that are transported from the bulk solution in the filter pores to the surface of the filter material to achieve stable deposition there.

A basis for a good prediction of particle behaviour is the realistic description of the structure of the filter bed. As this is a very difficult process for practical conditions, suitable models are used to approximately describe the geometric structure of the clean filter bed with regard to the properties influencing the particle deposition.

To describe the deposition process in the initial filtration phase the interactions of the particles with the collector surface have to be considered in addition to the behaviour of a particle in the pore space. In the subsequent dynamic filtration phase, where the deposit increasingly influences the deposition mechanisms, interactions between depositing particles and deposits on the collector surface also have to be considered. In this dynamic period detachment of previously deposited particles may occur.

#### *2.2.2.1 Modeling the flow through a clean filter bed*

When modelling the flow through a clean filter bed laminar, axially symmetrical flow conditions are considered. This allows the introduction of a stream function to simplify the description of the flow fields of interest. A good example of this is Happel's sphere-in-cell model (Happel, 1958). In this model, shown schematically in Fig 2.4, a representative spherical collector of the filter bed is considered to be surrounded by a liquid envelope that is taken to be frictionless along its outer surface. The diameter of the envelope is so chosen that the porosity of the combined entity (namely, the spherical grain and the liquid envelope) is equal to the macroscopic porosity of the filter bed. The limiting trajectory shown in Fig 2.4 is defined as the trajectory that separates the trajectories that intercept the collector from those that do not (Rajagopalan and Tien, 1976).

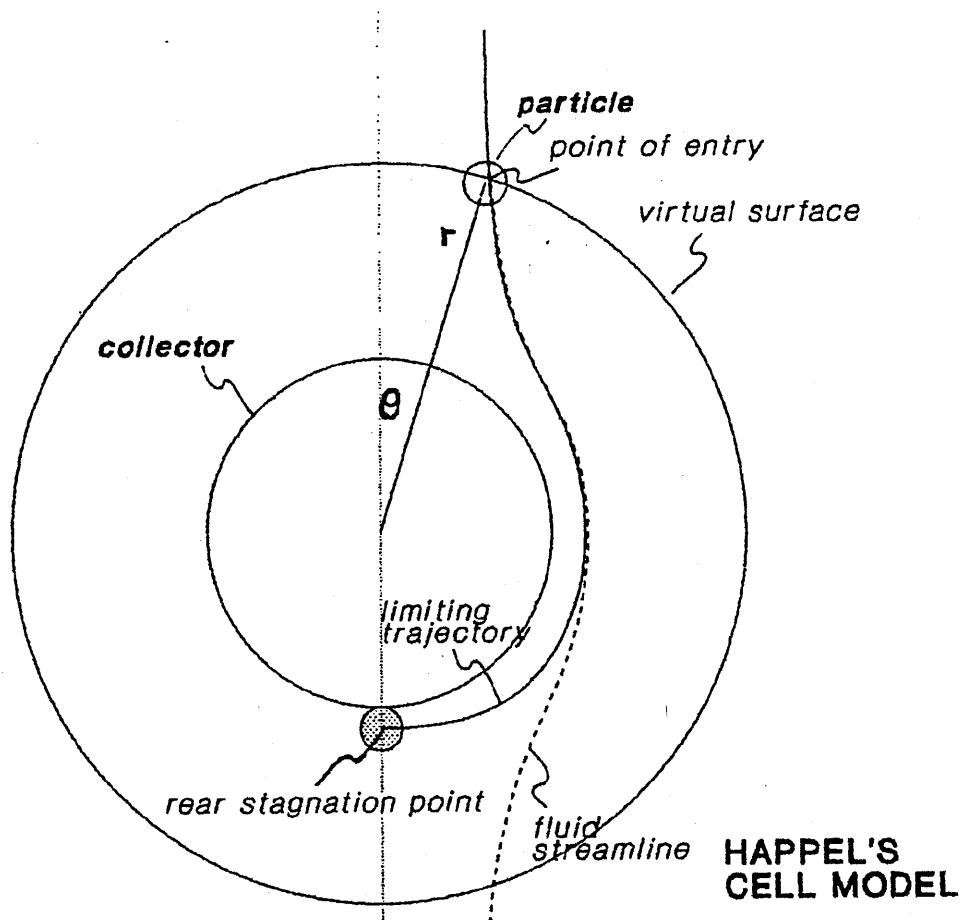


Figure 2.4 Happel's sphere-in-cell model.

#### 2.2.2.2 Attachment mechanisms

Suspended particles that are transported to the surface of the collector must adhere there to be removed. The chemistry of the filtration system is of great importance in determining how well particles attach. In fact, Adin *et al.* (1979) concluded that transport considerations are relatively unimportant as compared to chemical alterations which greatly affect the attachments of solids in the bed.

The attachment mechanisms that have been extensively studied are the interactions of double layers and the London-Van der Waals or dispersion force. Some other less understood and less quantified forces of significance, highlighted by Tobiasson and O'Melia (1988), include those due to the hydration of ions at surfaces, the steric interactions of adsorbed macromolecules, and the interactions of hydrophobic surfaces.

The electric double layer occurs because solids dispersed in water commonly bear an electrical surface charge arising, for example, from the dissociation of surface groups or from the specific adsorption of ions. The effect of the electric double layer is therefore dependent on the surface charges of the suspended particles, and the collector surface, as well as the ionic strength of the suspending fluid. The effects of changes in these characteristics have been studied by O'Melia and Crapps (1964), Ives and Gregory (1967), O'Melia and Stumm (1967), Ghosh *et al.* (1975), Davis and Borchardt (1966), Wang *et al.* (1986) and others.

Several of these studies have shown that, for particles and collectors with negative surface charges, low ionic strength causes lower collection efficiencies which improve with increasing ionic strength up to a point, after which there is little effect.

Modifying the surface charge of the suspension and the collector has also been observed to be of great importance. Davis and Borchardt (1966) found that coagulant dose affected the removal of algae in a sand filter but not in a consistent manner. Ghosh *et al.* (1975), Glasser and Edzwald (1978), and Adin and Rebhun (1974) have shown that when using synthetic polymers as filter aids, an optimum dose exists which provides the highest initial filter coefficients.

London-Van der Waals force is the result of the interaction between fluctuating dipoles of atoms, due to the rotation of their electrons. It is usually an attractive force between solid surfaces and it applies over very small distances, of the order of a few hundred nm (Ives and Gregory, 1967).

In addition to the electric double layer and London forces, Ives and Gregory (1967) also postulated hydrogen bonding and mutual adsorption of polymeric species as attachment forces. Other special chemical interactions may also play an important role (O'Melia and Stumm, 1967). Once the filter has accumulated some solid matter it seems that mechanical support may cause the attachment to occur. Also, mechanical support on the top or forward stagnation point of a collector should be important (Yao *et al.*, 1971).

### 2.2.3 Headloss build-up

The development of pressure drop or headloss is another important parameter in describing the



behaviour in deep bed filters. Knowledge of the headloss development is important for the design and operation of a filter with respect to the determination of the maximum headloss and the avoidance of negative head within the filter layers.

When water passes through a granular bed, energy losses occur due to both form and drag friction at the surface of the media. In addition, losses occur due to continuous contraction and expansion experienced by the fluid phase as it passes through pore openings in the media. The headloss will depend on a wide range of variables, such as porosity, particle shape, roughness, size and size distribution of the granular media, and the type of fluid flow, i.e. laminar, transitional or turbulent. Models have been developed for the prediction of headloss through clean filter media as a function of the relevant physical parameters.

### 2.2.3.1 Clean bed headloss prediction

Darcy, in a classic study, observed that the hydraulic gradient,  $\frac{\Delta p}{l}$ , under laminar conditions (Reynold's number less than 10) in porous media was given by:

$$\frac{\Delta p}{l} = \frac{V_0 \mu}{k} \quad (7)$$

Where,  $V_0$  is the superficial velocity and  $k$  is the hydraulic permeability, which needs to be determined by experiment. This empirical relationship states that the pressure drop through porous media is directly proportional to the superficial velocity, the depth of the media and the viscosity.

Following on from this work, Carman developed a theoretical expression for the hydraulic permeability by postulating a physical model of the porous media. The resulting equation became known as the Carman-Kozeny equation:

$$\frac{\Delta p}{l} = \frac{k\mu S^2 V_0}{\varepsilon_0^3} \quad (8)$$

Where,  $\varepsilon_0$  is the initial porosity,  $S$  is the specific surface of the media and  $k$  is the dimensionless Kozeny constant (close to 5 under most conditions). For spherical particles the Carman-Kozeny equation becomes:

$$\frac{\Delta H}{l} = \frac{180(1 - \varepsilon_0)^2 \mu V_0}{\varepsilon_0^3 d_p \rho l g} \quad (9)$$

Where,  $\Delta H$  is the headloss in units of length (of the water column) and  $g$  is the gravitational constant.

#### 2.2.3.2 Clogged bed headloss prediction

As particulate matter is captured in a granular media filter, interstitial pore space will decrease. In addition the media size will change due to accumulation of particulate matter on the media surfaces. Generally, it has been shown that the increase in headloss due to accumulation of solids in the pore spaces can be approximated as (Ives, 1982):

$$\frac{\Delta H}{\Delta H_0} = 1 + \gamma_1 \sigma \quad (10)$$

Where,  $\Delta H_0$  is the clean bed headloss at time  $t=0$ ,  $\sigma$  is the mass specific deposit and  $\gamma$  is an empirical constant.

#### 2.2.4 Detachment mechanisms

In an attempt to model the entire cycle of filtration, researchers have included terms for particle breakthrough. Ives (1960) and Mackie *et al.*, (1987) attributed breakthrough to a lack of particle attachment, whereas other researchers attributed it to particle detachment. Mints and Krishtal (1960) described detachment as directly proportional to the accumulated deposit:

$$\left(\frac{\partial \sigma}{\partial t}\right)_{\text{detachment}} = -a\sigma \quad (11)$$

Where,  $a$  is the rate constant. Vigneswaran and Chang (1986) and Adin and Rebhun (1987) incorporated terms into their models that assume that the amount of breakoff is directly proportional to the product of the hydraulic gradient and the amount of deposited material on the filter grain, so that:

$$\left(\frac{\partial \sigma}{\partial t}\right)_{\text{detachment}} = -k\alpha J \quad (12)$$

Where,  $k$  is the detachment coefficient, and  $J$  is the hydraulic gradient.

Vigneswaran and Tulachan (1988) examined a model based on the idea that only a limited quantity of particles, termed the ultimate specific deposit, can be deposited on a filter grain. Vigneswaran and Chang (1989) performed experimental analysis on two types of model. The first was based on the assumption of detachment, and the second was based on the concept of the saturation of sites on a filter grain on which particle deposition occurs. The model based on detachment more closely matched experimental data.

A number of researchers have made qualitative investigations into the phenomenon of breakoff. Payatakes *et al.*, (1981) witnessed particle reentrainment in a specially designed apparatus. They observed that the tops of grains initially accumulated "snowcaps", later on in a filter run they observed that parts of the snowcaps became reentrained as the fluid shear forces overcame the attachment forces. Ives (1989), using endoscopes, also observed the formation of "snowcaps". Particle detachment was seen to take place as a result of instabilities caused by arriving particles. An analogy was made to snow deposition on mountainsides, with occasional occurrences of avalanches.

Lawler and co-workers (Darby and Lawler, 1990 and Lawler and Kau, 1992) had found indications that breakoff contributed to decreasing removal efficiency in latter stages of laboratory filter runs; yet had no real proof. It was not until a carefully designed follow-up study by Moran *et al.*, (1993) that direct evidence of floc breakoff was found. They found that detachment greatly influenced particle breakthrough. Detachment was found to be highly

dependent on specific deposit. For a specified section of filter, increased deposit resulted in increased detachment.

## 2.3 Factors that play a key role in filtration

### 2.3.1 *Influent quality*

It has been a long established fact that the size of suspended particles is a crucial factor in determining the effectiveness of rapid gravity filtration (Cookson, 1970; O'Melia and Stumm, 1967; and Yao *et al.*, 1971). O'Melia and Ali (1978) carried out experiments to find out the effect of particle size throughout the filtration run, using three monodisperse suspensions of 0.1, 1.0 and 7.6 $\mu\text{m}$ . They found in accordance with Yao *et al* that the 1 $\mu\text{m}$  suspension gave the lowest removal throughout the filter run.

While most of the detailed experimental work on filtration has concentrated on monodisperse suspensions there have been a number of studies that have looked at the effect of particle size distribution on filtration performance. Darby and Lawler (1990) carried out experiments with bimodal and trimodal suspensions of latex particles. They concluded that the removal of particles of one size is influenced by both the presence of particles of other sizes, and by surface chemistry. They stated that particles of one size were preferentially captured by the particles of a similar size. Vigneswaran *et al.*, (1990) also used bimodal and trimodal suspensions, but using pollen grains, and found that the presence of coarse particles improved fine particle removal. This improvement was more pronounced the greater the ratio of coarse to fine particles, and the greater the relative size difference. Tobiason (1990), again using bimodal and trimodal suspensions of latex particles, reported that the removal of smaller particles was reduced by the presence of larger ones and that the presence of smaller particles improved the removal of larger ones.

There is therefore substantial evidence that particle size distribution plays an important role in filtration performance but recent work is contradictory as to the true effect.

### 2.3.2 *Pre - treatment*

The importance of adequate and continuous pre-treatment was recognized as early as 1898 by Fuller to be essential to producing good filtrate.

Pre-treatment usually consists of addition of metallic coagulant, for example aluminium sulphate, ferric sulphate and ferric chloride. Following the proper mixing of coagulants with raw water, there are a number of complex reactions that take place with suspended particles and some of the dissolved and organic matter. These coagulation reactions take place in less than 1 second (Culp, 1977).

At this point in the process, the particles formed are very small, and the colloids are destabilized. When the destabilized particles collide, they stick together (Culp, 1977). In a still body of water agglomeration takes place at a very slow rate. This rate can be increased by agitation or stirring of the water; in a well-designed flocculator, agglomeration of all particles might be completed in times varying from 5 to 45 minutes (Culp, 1977). At this point, enough collisions have occurred so that the floc particles have grown to a size that will settle rapidly.

Traditionally treatment plants consist of a pre-treatment stage followed by sedimentation - the majority of flocs are allowed to settle out - and then filtration of particulates.

A more recent advance for the treatment of low turbidity waters is the use of direct filtration (defined as a treatment system not preceded by sedimentation. When the elimination of the settling step is desired, the conventional method of flocculation can be eliminated (Culp, 1977). The water containing the destabilized particles can be taken directly to a granular filter where contact flocculation takes place as part of the filtration process at a greatly accelerated rate, because of the huge number of possible contacts afforded by the passage of the water through the granular filter bed. The floc particles become attached or adsorbed to the surface of the filter grains.

### 2.3.3 *Filtration rate*

For maximum particle removal efficiency plants should use low filtration rates. However, such a plan can not be adopted for economic reasons. In fact, the real trends in practice are just the opposite. Higher filtration rates are being used to reduce the size of plant and thereby reduce the capital investment.

Fuller is believed to be responsible for establishing a filtration rate of 4.9m/h for chemically pretreated surface waters. This rate remained the standard for at least half a century. However researchers began to realise that with properly pretreated water, higher rates gave virtually the same water quality (Brown, 1955; Bayliss 1956; Robeck et al., 1964; and Mosher and Hendrick, 1986).

Brown (1955) compared performances at filtration rates of 4.9, 7.3, and 9.8 m/h on full-scale filters treating a water that received conventional alum coagulation and sedimentation. He reported that the difference in effluent turbidity was considered insignificant.

Bayliss (1956) reported on seven years of testing of full-scale filters. performance at several rates from 4.9 - 12.2 m/h were compared. He concluded that 12.2m/h did produce a slightly poorer quality effluent.

Robeck et al. (1964) compared performance of pilot filters at 4.9, 9.8 and 14.6m/h when filtering alum-coagulated surface waters through single-medium and dual media filters. With proper coagulation, and sometime of polyelectrolyte filter aid, the effluent turbidity was the same at all filtration rates.

Mosher and Hendrick (1986) assessed the performance of field-scale pilot filters operated at 12.2m/h on low turbidity waters. They also concluded that with adequate pre-treatment a high quality effluent was achievable.

The highest reported filtration rate is 43.9m/h (Trussell et al. 1980) a low filtrate turbidity was obtained from coarse deep bed filters. However, the addition of cationic polymer as well as alum was required to achieve this.

It can therefore be seen that increasing the rate of filtration results in somewhat poorer filtrate as theory would predict. Filtration rates up to 9.8m/h appear reasonable with conventional pretreatment and without the use of filter aid polymers to increase filtration efficiency. However, with rates higher than this, filter aid polymers are usually required to maintain filtrate quality.

#### 2.3.4 *Filter media*

The size of the filter media was observed by Ives and Shoji (1965) to affect performance in conflicting ways. Generally, the smaller the filter media grain size the higher the percentage particulate removal. However, headloss increases are observed using smaller filter media at constant approach velocities. Conversely, larger grain sizes cause poorer particulate removal but lower the rate of headloss development. Ives and Shoji (1965) suggested that deeper bed depths can compensate for the use of coarser grain size.

The variable shape of filter media was shown by Ives and Shoji (1965) to affect filter performance. He compared the filter performance of glass beads, sand and anthracite. Under the same flow and with the same influent quality, anthracite performed the best followed by sand and finally glass. The differences were not due to surface electrochemical effects as all the media displayed very similar zeta potentials.

Observations by Trussell *et al* (1980) and Bablon *et al* (1988) also criticized highly rounded filter media. Angular grains have greater surface area than spherical grains which may account for improved filtration. However this is offset by the fact that fewer grains can fit into a unit volume of filter.

#### 2.4 **Filter Backwashing**

During the filtration run, sediment builds up in the filter, having been removed from the feed water by the afore mentioned mechanisms. The particles are retained within the filter in equilibrium with the hydraulic shear forces, which may overcome the attachment mechanisms

and wash them deeper into, or through the filter. As deposited particles build up, the interstitial spaces become smaller and therefore the fluid velocities increase in the upper part of the filter. Thus, the upper parts of the filter become less effective at removal. Therefore removal occurs deeper and deeper in the filter. Eventually, a point is reached when either clean bed depth is no longer available and particles begin to break through, or, the permeability of the filter is reduced causing a subsequent loss of head. It is then necessary to terminate the filter run and clean or "backwash" the filter.

There is a very wide selection of backwashing systems encountered throughout the U.K, Europe and the USA. However all backwashing systems employ the use of a reverse flow of water through the filter bed, usually at sufficient velocity to suspend the media particles in the fluid, in order to dislodge and remove attached impurities from the filter media.

#### 2.4.1 *Fluidised bed behavior*

In an ideal bed comprising single-sized spherical particles with no upward flow, gravity is the only force acting upon the particles. As the upflow of fluid is begun and increased through the bed, the particles exert a resistance to this flow, attributable to skin friction and form drag (Cleasby *et al*, 1975).

Energy loss, or pressure drop, is approximately a linear function of flow rate during flow through a fixed bed and is represented by line A-B in Fig 2.5. As the flowrate is increased further, the resistance of particles to flow increases until this resistance equals the gravitational force, and the particles become suspended in the fluid. Any further increase in flow rate causes the bed to expand and accommodate to the increased flow while effectively maintaining the same pressure drop. The fluidised bed thus formed closely resembles that of a liquid (Cleasby, 1977).



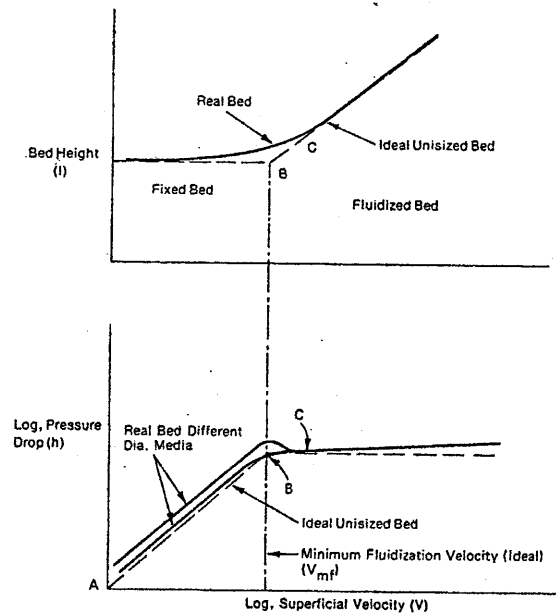


**Figure 2.5. Characteristics of a fluidised bed (adapted from Cleasby, 1977).**

The superficial fluid velocity required for the onset of fluidisation is called the minimum fluidisation velocity ( $V_{mf}$ ). It can be defined exactly as point B in Fig 2.5. for an idealized bed composed of unisized spherical particles. For a bed containing various particle sizes, the minimum fluidisation velocity is not the same for all particles. There is therefore a gradual change from the fixed bed to the totally fluidised state. For a real graded bed,  $V_{mf}$  is sometimes defined as the intersection of the two linear, discontinuous sections of the pressure drop curve although the entire bed is not fluidised at that flow rate and full-bed fluidisation would not occur until point C (Cleasby, 1977).

The common filter materials (sand, anthracites, garnet and GAC) are mostly spherical in shape. Some have low sphericity (very angular) while others have high sphericity. The sphericity of the material greatly influences the fluidization behavior of the media. It influences the fixed bed headloss, the  $V_{mf}$  and the expansion of the media as a function of backwash water velocity.

#### 2.4.2 Backwash system development

The use of a reverse flow backwash at sufficient velocity to fluidize the bed was the traditional

method of backwashing filters. However it was realised that this type of wash was inefficient and that supplementary washing techniques were required. The wide range of backwash systems that were developed and are currently in use can be categorized as follows:

- 2 phase systems:-
  1. Water only backwash
  2. Water backwash with surface water auxiliary
- 3 phase systems:-
  3. Water backwash with air auxiliary
    - a. air scour followed by water backwash
    - b. simultaneous air scour and water backwash
    - c. simultaneous air scour and water backwash followed by water wash

#### 2.4.2.1 *Water only backwash*

As stated this was the traditional method of backwashing, the British practice was to expand the bed by 20-30%, whereas the US practice leaned towards greater bed expansion - up to 50% (Bayliss, 1959). This type of backwash had been effective on high quality surface waters, however it was found to be ineffective on highly turbid waters due to mudball formation (Cleasby *et al*, 1975).

A large amount of research had gone into determining the cleaning or detachment mechanisms that occur during a water only fluidisation wash, and it was an area of contention in the scientific community (Cleasby *et al*, 1975; Cleasby *et al*, 1977; Cleasby and Lorence, 1978; Amirtharajah, 1978 and 1979). Theoretical detachment mechanisms include fluid shear, and grain collisions in this type of backwashing. There was a long held view among civil engineers, such as Fair and Geyer (1968), that collisions between the grains during fluidisation were responsible for the dislodgment of deposits.

It was not until the extensive research into fluidised beds by chemical engineers, such as Wen and Yu (1966), was utilized that opinion began to shift in favour of hydrodynamic shear forces being the predominant detachment mechanism in fluidised beds. It was studies published by

Cleasby *et al.*, (1975) and Amirtharajah (1978) that convinced the civil engineering community that particle collisions in fluidised beds were insignificant. Amirtharajah utilised the chemical engineering argument that during fluidisation the grains may not actually collide, but only approach extremely closely, due to the increased resistance of the water film as it thins. Two grains approaching one another have to displace the water between them, which flows away from the center of a diminishing gap, creating a high laminar shear stress.

Ives and Fitzpatrick (1989) in a much later piece of work made an interesting observation which seems to affirm the above. It was that experimental filter columns made from perspex do not become eroded following extensive sand fluidisation inside. If collisions take place, the hard quartz sand would be expected to erode the relatively soft perspex.

In a follow-up study Amirtharajah (1979), working on the principle that the optimum fluidised bed expansion will be the one that optimizes the shearing forces in the granular media, predicted that maximum hydraulic shear will occur at porosities of 0.68-0.7.

It should, however, be realised that there is no instant transition from a packed bed to a fluidised bed condition. Ives and Fitzpatrick (1989) using visual evidence provided by endoscopes, stated that "the initial reversal of flow with washwater detaches deposits by water shear. Then the sand grains commence intermittent movement whilst still in contact, resulting in rotation and other relative motion, which probably removes deposits by a grinding action. Further increases in flow intensifies these movements until the grains are lifted by the water drag into a fluidised mode".

In practice the water only wash is simple because only a single washwater distribution system is needed. However, it can be costly because large amounts of treated water are required (Cleasby, 1977), gravel support layer disturbance can occur (Haarhoff and Malan, 1983), and it has proved ineffective in washing filters treating highly turbid waters because it is an inherently weak cleaning process.

#### *2.4.2.2 Water only backwash with surface wash auxiliary*

This method of water backwash enhancement was, according to Bayliss (1959), first used in

method of backwashing filters. However it was realised that this type of wash was inefficient and that supplementary washing techniques were required. The wide range of backwash systems that were developed and are currently in use can be categorized as follows:

- 2 phase systems:-
  1. Water only backwash
  2. Water backwash with surface water auxiliary
- 3 phase systems:-
  3. Water backwash with air auxiliary
    - a. air scour followed by water backwash
    - b. simultaneous air scour and water backwash
    - c. simultaneous air scour and water backwash followed by water wash

#### 2.4.2.1 Water only backwash

As stated this was the traditional method of backwashing, the British practice was to expand the bed by 20-30%, whereas the US practice leaned towards greater bed expansion - up to 50% (Bayliss, 1959). This type of backwash had been effective on high quality surface waters, however it was found to be ineffective on highly turbid waters due to mudball formation (Cleasby, 1975).

A large amount of research had gone into determining the cleaning or detachment mechanisms that occur during a water only fluidisation wash, and it was an area of contention in the scientific community (Cleasby *et al.*, 1975; Cleasby *et al.*, 1977; Cleasby and Lawrence, 1978; Amirtharajah, 1978 and 1979). Theoretical detachment mechanisms include fluid shear, thinning water film and grain collisions in this type of backwashing. There was a long held view among civil engineers, such as Fair and Geyer (1968), that collisions between the grains during fluidisation were responsible for the dislodgment of deposits.

It was not until the extensive research into fluidised beds by chemical engineers, such as Wen and Yu (1966), was utilized that opinion began to shift in favour of hydrodynamic shear forces being the predominant detachment mechanism in fluidised beds. It was studies published by Cleasby *et*

*al.*, (1975) and Amirtharajah (1978) that convinced the civil engineering community that particle collisions in fluidised beds were insignificant. Amirtharajah utilised the chemical engineering argument that during fluidisation the grains may not actually collide, but only approach extremely closely, due to the increased resistance of the water film as it thins. Two grains approaching one another have to displace the water between them, which flows away from the center of a diminishing gap, creating a high laminar shear stress.

Ives and Fitzpatrick (1989) in a much later piece of work made an interesting observation which seems to affirm the above. It was that experimental filter columns made from perspex do not become eroded following extensive sand fluidisation inside. If collisions take place, the hard quartz sand would be expected to erode the relatively soft perspex.

In a follow-up study Amirtharajah (1979), working on the principle that the optimum fluidised bed expansion will be the one that optimizes the shearing forces in the granular media, predicted that maximum hydraulic shear will occur at porosities of 0.68-0.7.

It should, however, be realised that there is no instant transition from a packed bed to a fluidised bed condition. Ives and Fitzpatrick (1989) using visual evidence provided by endoscopes, stated that "the initial reversal of flow with washwater detaches deposits by water shear. Then the sand grains commence intermittent movement whilst still in contact, resulting in rotation and other relative motion, which probably removes deposits by a grinding action. Further increases in flow intensifies these movements until the grains are lifted by the water drag into a fluidised mode".

In practice the water only wash is simple because only a single washwater distribution system is needed. However, it can be costly because large amounts of treated water are required (Cleasby, 1977), gravel support layer disturbance can occur (Haarhoff and Malan, 1983), and it has proved ineffective in washing filters treating highly turbid waters because it is an inherently weak cleaning process.

#### *2.4.2.2 Water only backwash with surface wash auxiliary*

This method of water backwash enhancement was, according to Bayliss (1959), first used in

1908. However, its widespread adoption in the U.S. did not occur until much later. Surface wash is accomplished either with a grid of fixed pipes placed above the granular media, or with rotary water distribution arms, containing orifices or nozzles that supply high pressure jets of water above the fixed-bed surface prior to the backwash and into the upper layers of the media during part of the bed expansion (Cleasby chapter). The operation is relatively simple because only water is used and it has proved effective in eliminating some dirty filter problems. Yet media loss can occur, maintenance (especially of rotary-type washers) is high (Cleasby *et al.*, 1977) and it is not as effective for coarse media deep bed filters due to the greater solids penetration.

#### 2.4.2.3 Air scour followed by water backwash

When, as is the British practice, air is introduced prior to the water backwash a three phase system is produced. Plastic strainer nozzles (Fig 3.6) are used in the underdrains, which are generally covered by two or more layers of graded gravel to support the media (Haahroff and Malan, 1983).

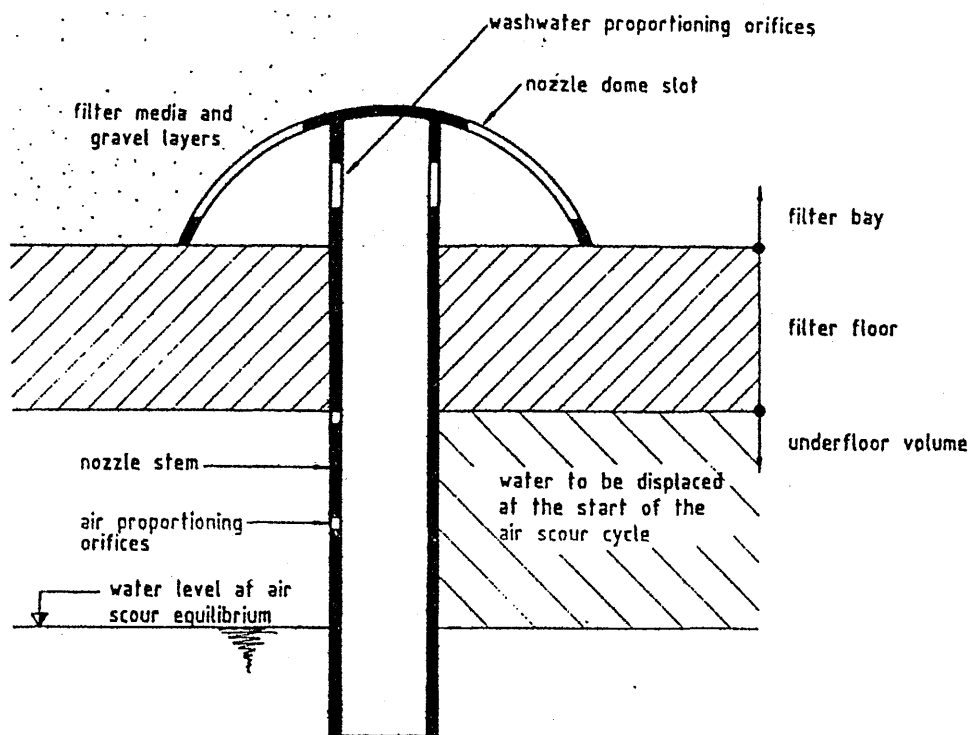


Figure 2.6. Schematic of an air water distribution nozzle (Haarhoff and Malan, 1983).

The action of an air scour prior to a water wash was described by Cleasby *et al.*, (1977):

" When the air is introduced at the bottom of the filter, the bubbles travel upward carrying some water and dirt particles as they pass through the bed and burst at the surface, where the maximum scouring action appears to be produced. Substantial agitation of the media near the bed's surface occurs and it is this action that provides the basis for air scour use in sand filters where minimum solids penetration occurs. Deeper agitation is also observed during the first minute or so of air scour. Thereafter, the bed apparently packs down, and the air seems to become more channeled as it passes through the bed ".

Air scour has been found to be effective at eliminating dirty filter problems such as mudball formation. Potential operational difficulties include gravel layer disturbance (Haarhoff and Malan, 1983), and media loss. Loss of sand can occur because air can be expelled from the bed at the onset of overflow into the backwash channel, and create sufficient turbulence to throw sand up to the overflow level (Cleasby *et al.*, 1977).

#### 2.4.2.4 Simultaneous air and water backwash

The use of simultaneous air and sub-fluidisation water backwash is a common practice on the European continent and has been for some time. The use of this type of backwash is a relatively recent advance in the U.S.

Hewitt and Amirtharajah (1984) performed an experimental characterization of air-water dynamics through filter media during backwashing of filters with air scour which showed that the flow patterns that developed when air and water flowed concurrently through porous media caused a condition where air pockets formed and collapsed within the bed. This motion appeared to provide the greatest amount of particle collisions and abrasions and was termed collapse-pulsing.

The air motion passing through a filter during air scour at a constant sub-fluidisation water flowrate and increasing air flow rate is depicted in Fig 2.7. The processes occurring in Fig 2.7 were described by McNelly and Amirtharajah (1991):

"At very low air flowrates, air travels in paths referred to as "veins" with tiny pockets within the veins forming occasionally (see Fig 2.7(a)). Due to the low air flow rate, only media in the immediate vicinity of the vein is displaced, resulting in conditions below collapse-pulsing. At slightly higher air flow rates but below the collapse-pulsing condition, air continues to travel in veins with an increased frequency of small pockets forming (see Fig 2.7(b)). Increasing the air flow rate further will result in an occasional air pocket forming and collapsing as it travels through the media. Fig 2.7(c) shows a microscopic view of the collapse-pulsing motion whereby an air pocket travels through the media, pauses, expands laterally, and then releases air from the top of the pocket to form a second pocket. Almost instantaneously, the lower pocket collapses. As the air flow rate is increased slightly, collapse-pulsing occurs more frequently (see Fig 2.7(d)). A further increase in the air flow rate will result in the collapse-pulsing motion to occur less frequently (Fig 2.7(e)). Finally, an even further increase in the air flow rate will cause the collapse-pulsing condition to be exceeded (Fig 2.7(f)).

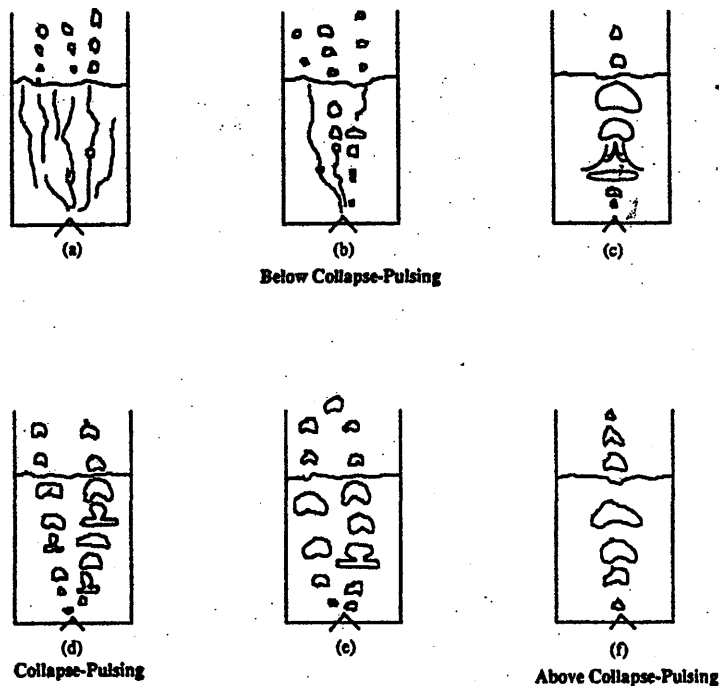


Figure 2.7. Schematic of air motion corresponding to conditions below, at and exceeding collapse-pulsing. (McNelly and Amirtharajah, 1991).



The initial studies carried out by Hewitt and Amirtharajah (1984) and Amirtharajah (1984) only dealt with the fluid and solid mechanics of the process of air scour. Studies on model systems by Regan and Amirtharajah (1984) showed that collapse-pulsing was also the condition of optimum removal of particles from the media grains during backwashing.

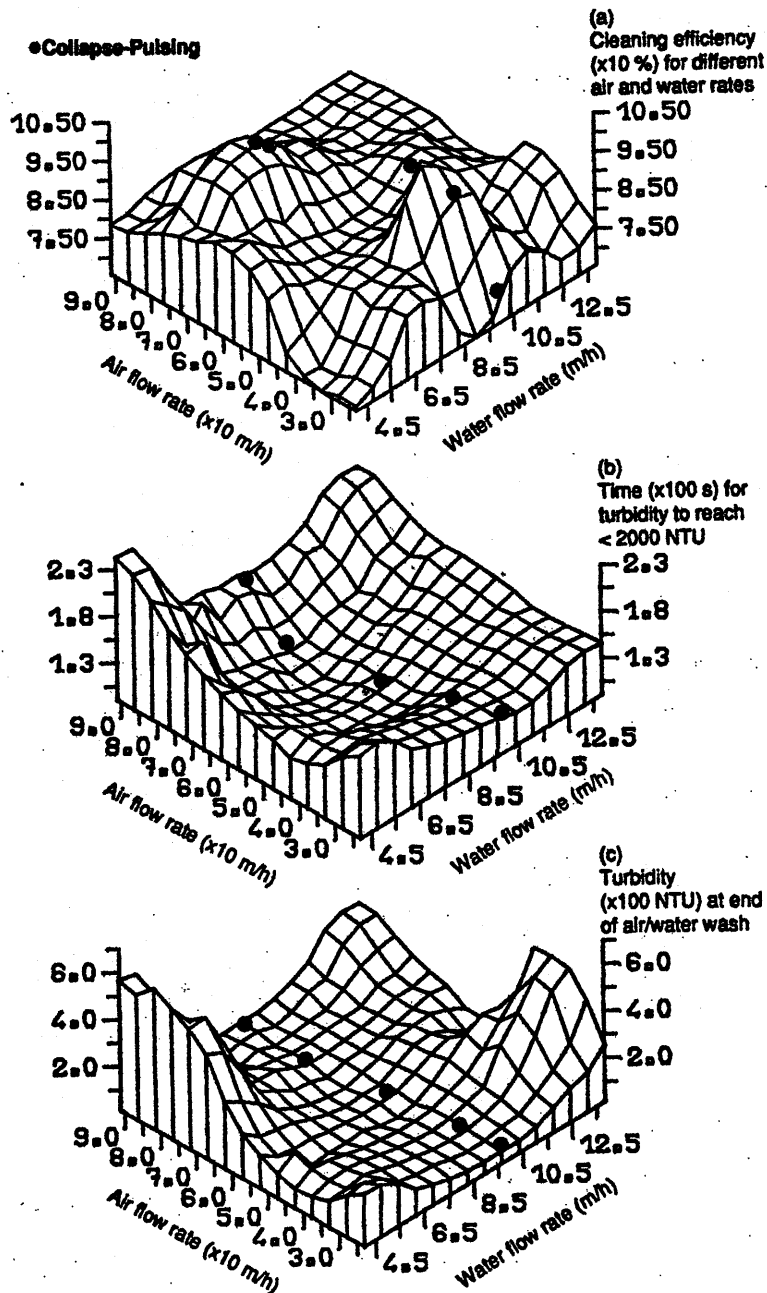


Figure 2.8. Cleaning efficiencies and backwash parameters as functions of air and water flowrates shown in 3D plots (Fitzpatrick, 1991).

The theoretical aspects of collapse-pulsing at the microscopic level were validated (Amirtharajah et al, 1991; Ives and Fitzpatrick (1989) using an experimental filter system developed by Ives (1989). The experimental system included an endoscope, high speed video with freeze frame capability for visual observations and an XY coordinator which enabled the determination of velocities of filter grains during air scour. The studies, carried out on a 0.115m diameter perspex filter column containing 0.5-1.0mm sand, indicated that collapse-pulsing theory gave best cleaning of media in terms of three variables: (1) overall removal of material from the filter media, (2) the cleaning time to a fixed backwash turbidity and (3) turbidity at the end of air-water backwash.

These results are shown in Fig 2.8, the graphs show a ridge in cleaning efficiency and valleys in time and turbidity corresponding closely to the collapse-pulsing condition. These studies were correlated with maxima in means and variances of grain speeds. A slow motion visual examination of video recordings of collapse-pulsing backwash indicated that the whole bed pulsed and grain movement was much more violent with rapid changes in magnitude and direction compared to water fluidisation alone.

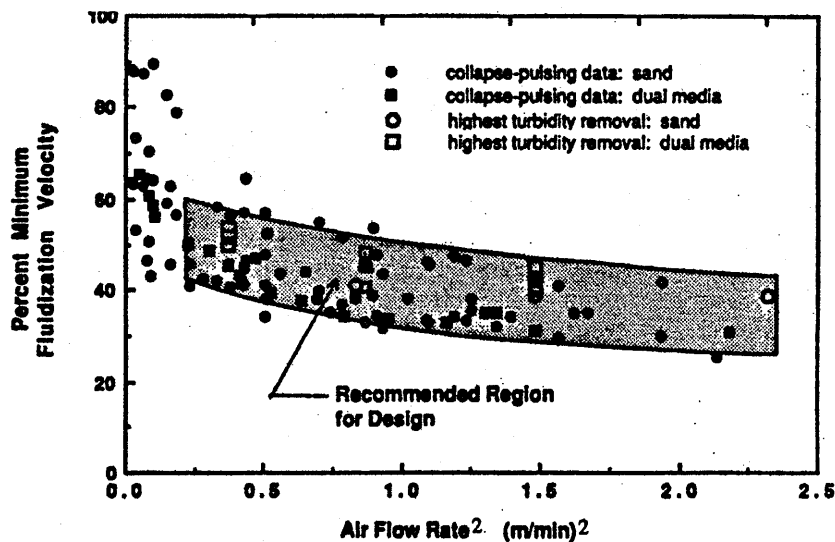


Figure 2.9 Recommended air and water backwashing flowrates for sand and dual media filter beds (Amirtharajah et al., 1991).

The fact that collapse-pulsing provides the optimum removal of particulates during backwash has also been illustrated at full scale for sand, GAC and dual media filters (Amirtharajah *et al*, 1991). Core samples were taken prior to and after a range of conditions of air- water backwash, the material removed from the core samples was measured in terms of turbidity and suspended solids. The optimum cleaning results at different air flowrates compared very favorably with the collapse-pulsing condition. These observations were summarised in the form of a design chart, shown in Fig 2.9. It shows the water flowrates as %  $V/V_{mf}$  that need to be combined with air flows.

It was a lack of adequate design information that resulted in the reluctance to adopt collapse-pulsing backwash. Bad design resulted in problems of media loss and destruction of gravel support layer.

Studies giving measurements on media loss from filters are rare. Trends observed in pilot-scale equipment using simultaneous air-water backwash of sand were presented by Amirtharajah and Trussler (1982). Full-scale work was carried out by Rauscher *et al.*, (1986) in plants showing high loss rates of anthracite media. In these plants, release of air during backwash was identified as a major cause of media disturbance that increased anthracite losses during the backwash cycle. In another full-scale study Amirtharajah *et al.*,(1991) showed that media loss during collapse-pulsing backwash was significant, however they noted that it was comparable to surface wash if these auxiliaries were operated whilst backwash water was overflowing into the backwash weirs. They went on to recommend that air scour be stopped prior to backwash water overflow into the backwash weir to minimise media loss.

Another problem associated with collapse-pulsing is that determination of flowrates to achieve collapse pulsing is carried out visually, determination is both difficult and subjective, since no mechanical/technical method is available. However, Amirtharajah (1984) developed a design equation to assist collapse pulsing flowrate determination:

$$a Qa^2 + \% \left( \frac{V}{V_{mf}} \right) = b \quad (13)$$

Where:

- $Q_a$  = air flow rate (m/min)  
 $V$  = backwash water velocity (m/min)  
 $V_{mf}$  = minimum fluidisation velocity (m/min)  
 $a, b$  = Constants

### 2.4.3 Other factors affecting particle detachment

The previous sections have shown that hydraulic shear forces are the dominant detachment mechanisms and the best backwash, in terms of removing deposits, is the one that maximizes these forces. The fact that hydraulic shear forces are the dominant detachment mechanisms means that the resistance of deposits and deposit attachments to shear stress seems to be a fundamental property governing the detachment process. Therefore both the interactive forces between particles and collectors at the microscopic level and the duration of the shear forces, i.e. the length of the backwash are key issues affecting particle detachment.

#### 2.4.3.1 Interaction forces between particles and collectors

There has been little research into the mechanics of particle detachment from filter media during backwashing in terms of the forces involved at the microscopic level. Recently, chemical aspects of filtration have been studied experimentally using the packed column technique by a number of researchers (McDowell-Bowyer, 1992; Ryan and Gschwend, 1994). Ionic strength and pH of the solution were identified as the important parameters affecting particle detachment when a constant hydrodynamic force was used to detach particles. Physical aspects of particle detachment have been experimentally and theoretically studied by varying the hydrodynamic force (Sharma *et al.*, 1992). Particles were attached onto a flat surface and particle detachment was studied under different flowrates. The particle detachment efficiency was found to increase with flow rates and particle size due to the hydrodynamic force.

Raveendran and Amirtharajah (1995) showed that higher pH and lower ionic strength enhanced detachment during backwash. The work was carried out on a lab scale model filter with well

defined spherical particle suspensions. Latex particles (5 $\mu$ m) were filtered in a packed bed of glass beads. The detachment of particles during filter backwashing under fluidization conditions was studied in relation to chemical characteristics of the backwash water. Theoretical calculations fitted the results only when short range forces, such as, Born repulsive forces and structural forces, were considered in addition to Van der Waals attractive forces and electrical double-layer interactive forces.

#### 2.4.3.2 Backwash duration

The time or duration of a backwash should be dependent on the extent to which a filter bed is clogged (the extent of clogging is a function of filtration rate and influent quality). Backwash durations used are based on several thumb-rule based criteria, Johnson and Cleasby (1966) reported that the range of actual cleaning components of backwash ranged from 3 to 12 minutes. The duration of backwash is very important because clean and filtered water is used for the purposes of backwashing. The total amount of clean water consumed in the backwash operation of a filter is usually 5%, although in badly managed filters, it can be seen to be as high as 15-20%.

Bhargarva and Ojha (1989) developed models that could pre-determine the backwash duration required to wash out a given amount of turbidity from a filter. However, the models worked on the volume of water required to rinse out a given amount of turbidity, they gave no consideration to the different efficiencies of different backwash regimes such as collapse-pulsing.

Amirtharajah *et al.*, (1991) recommended a collapse-pulsing backwash duration of 4 minutes, determined by the time taken for the water level to reach the backwash weir.

There are very few full-scale studies on the effect of backwash duration on plant performance. Only in a very recent study on full-scale plants by Chipps *et al.*, (1995) has the effect of the duration of the collapse-pulsing backwash on filter run length been considered. They found that the duration of collapse-pulsing backwash had a significant effect on filter performance; very short washes of 2 minutes were found to be ineffective, longer durations of 20 minutes were

found to result in a poor quality of filtrate. They failed to identify optimum durations but stated that 10 minutes was successful.

It has previously been assumed that optimum cleaning will result in optimum performance in terms of filtrate quality and run length. It is the writer's opinion that the backwash and start-up phases of the filtration cycle are inherently linked, and therefore the duration of the backwash will have a critical effect on filtrate quality when the filter is returned to service.

## 2.5 Start-Up and Filter Ripening

It is now well known that quality of the filtered water may be poorer at the beginning of the filtration cycle. However, it was not until O'Melia and Ali (1978) published their findings on the role of retained particles in deep bed filtration that any research addressed this poor initial effluent quality from a filter, frequently referred to as filter ripening. Then current theories described both the performance and removal efficiency of clean filters with some success. They did not, however, describe the initial degradation of effluent quality and the subsequent improvement. O'Melia and Ali (1978) developed a filter ripening model which incorporated the effects of suspended particle size. In this model, the fundamental concept of a single or unit collector was extended to include the effects of previously deposited particles.

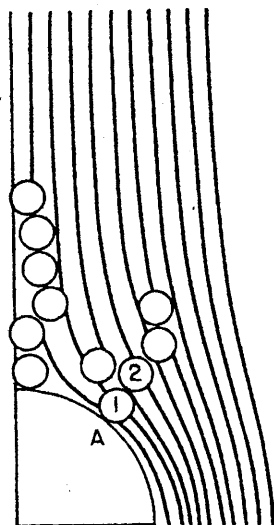


Figure 2.10 Formation of particle chains or dendrites during filtration (O'Melia and Ali 1978).

Adapting a theory from Tien *et al.*, (1977), who worked in aerosol filtration, O'Melia and Ali (1978) postulated that particle chains or dendrites are formed, enhancing the collector efficiency. A sketch of particle deposition during filtration is shown in Fig 2.10. The filter media is represented by a large sphere, termed the collector. Particles in suspension are depicted as smaller spheres of uniform size. Fluid streamlines for laminar flow are indicated. Particle removal by interception is also illustrated. For this case, suspended particles follow the fluid flow exactly and contact a collector because of their finite size. Removal by sedimentation and diffusion are not shown.

Particle 1 is removed on the spherical collector by interception at point A. This has two effects, first, it provides an additional contact site for further deposition by protruding into the original flow field. Particle 2, which would have been carried past the "clean" collector, can then be removed. Second, removal by the media grain in a shadow area downstream from point A is impaired, at least when removal is by direct interception or settling. The result of these effects is the formulation of a deposit consisting of chains or dendrites.

The resultant combined single collector efficiency,  $\eta_r$ , was defined mathematically, in the model of filter ripening that O'Melia and Ali (1978) developed, as:

$$\eta_r = \alpha\eta + N\alpha_p\eta_p\left(\frac{d_p}{d_c}\right)^2 \quad (14)$$

Where,  $\alpha$  is an attachment efficiency factor for particle-media contacts,  $\eta$  is the collision efficiency of particles with the clean media under favourable chemical conditions,  $N$  is the number of deposited particles on the surface of a single grain that act as collectors of additional particles,  $\alpha_p$  and  $\eta_p$  are the particle-particle attachment efficiency and collision efficiency, respectively, and  $d_p$  and  $d_c$  are the diameters of the suspended particles and filter media (collectors), respectively.

The O'Melia and Ali model was calibrated using the data of Habibian and O'Melia (1975) for experiments conducted with polystyrene particles. The model described the observed filter ripening for favourable chemical conditions as well as the marked effect of suspended particle size on headloss.

A key limitation of the original O'Melia and Ali model, as noted by the authors, is that the extent of deposition on the original filter media and the overall extent of deposition in the filter pores are unlimited. The removal efficiency of the filter always improves and filtered water quality cannot degrade. Several modifications of the model to address this problem have been made. Tare and Venkobachar (1985) assumed that because of finite media and retained particle surface area, the overall rate of removal was also decreasing in proportion to the number of particles deposited and included two additional terms and empirical constants in the removal equation.

Vigneswaran and Chang (1989) did not consider the surface coverage of the original media but they added a term to cause the rate of removal to decrease in proportion to the local hydraulic gradient and the extent of particle deposition.

Whilst this monodisperse suspension filtration modelling of the ripening period was going on other workers, most notably Amirtharajah and Wetstein (1980), began to address the ripening period in detail from an experimental viewpoint. Amirtharajah and Wetstein (1980) found that the initial poor quality of effluent is caused by remnants of the backwash water in the filtration system, and the initial stages of filtration i.e. the interface with the influent.

They reported that the backwash water remnants in the system can be subdivided into 3 types: 1) Clean backwash water in the underdrain and connecting pipework from the backwash water supply system up to the bottom of the media. 2) Backwash water remnants within the pores of the media, and 3) Backwash water remaining above the filter media up to the level of the backwash water overflow weir. This is illustrated in Fig 2.11.

Amirtharajah and Wetstein (1980) were the first to illustrate the presence of two turbidity peaks, they found that these peaks in filtrate turbidity corresponded to the detention times of the backwash components. This was re-iterated by a full-scale study by Quershi (1982) and in a follow up study by Cranston and Amirtharajah (1987). They found that the first turbidity peak occurs within the first few minutes and has a variable magnitude. They reported that the magnitude of solids passed during this initial peak is often small when compared to the total solids passed during the filter run. They believed the second peak is due to the interface between influent and coagulant-free, backwash remnant water above the media which partially destabilizes the influent particles.



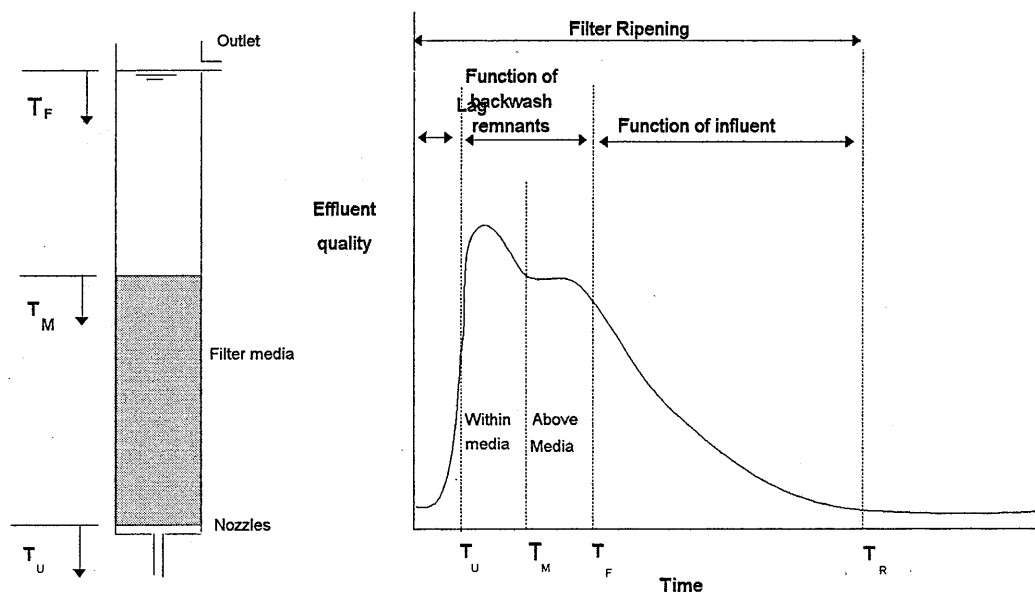


**Figure 2.11 Schematic showing poor filtrate quality during ripening period (Adapted from Amirtharajah and Wetstein (1980)).**

Bucklin *et al.*, (1988) in a study at two full-scale water treatment plants, observed that the magnitude and duration of the second turbidity peak was dependent upon the filter flow rate and the influent quality. At similar flow rates, the filter influent with the highest turbidity produced a turbidity peak of shorter duration. With similar turbidities, the filter with a higher flow rate recovered more quickly.

The duration of the ripening period under a variety of conditions (e.g. media size, flowrates) was investigated by Clarke *et al.*, (1992). They reported that ripening occurred for all particle sizes initially and continued for small particles in the range of  $1\mu\text{m}$  -  $6\mu\text{m}$  for several hours.

Darby and Lawler (1989) reported that the presence of previously retained particles are essential for minimizing the second peak in the ripening process and in the effective use of the full bed. They later reported (1990) that ripening, for the most part, was found to be strongly correlated

with the volume of previously captured particles but was strongly affected by the relative degree of particle-particle interactions versus particle-collector interactions.

In summary, after backwashing, the initial conditions - when a filter is put back into service - result in a relatively high level of particulates in the filtrate at the start of each run. One solution is to filter to waste initially, a second solution, based on theoretical work by Ives (DoE/DoH, 1990), is to restrict the rate of flow through the filter ("slow start") until filtrate quality is acceptable. The former procedure wastes water, which has been treated; the latter is largely untested and would require extensive flow controlling.

One of the few mentions of 'slow start' was in a study by Bucklin *et al.*, (1988); they found that on a full-scale filter incremental start-up conditions reduced the degradation period to 0.9 hours from 3.1 hours, while maintaining approximately the same magnitude of peak turbidity.

In a very recent study carried out by Hall and Pressdee (1995), slow start of pilot filters was monitored using particle counters. They found, in contradiction to Buckin *et al.*, (1988) that the length of the ripening period was increased. However, the peak of poor quality filtrate was reduced in magnitude. It should be noted that the slow start procedure used in this study was somewhat questionable; flow was increased from 1m/h to 5m/h in steps of 1m/h at 5 minute intervals using a manual valve.

The level of particulate passage into the filtrate during the ripening period is likely to be very dependent on backwash and start-up regimes. Therefore by monitoring particulate passage into the filtrate under a range of backwash and start-up regimes an optimum regime could be found that would minimize the passage of such particles.

## 2.6 Filtrate quality concerns

The period of high particulate passage, or ripening, has become a key issue within the water industry since the publication of the Badenoch Expert Group's report on *Cryptosporidium* in water supplies (DoE/DoH, 1990). The report was commissioned after an outbreak of Cryptosporidiosis in Swindon and parts of Oxfordshire in 1989. The organism responsible is a

small protozoan parasite with a complex life cycle. Following infection of a host, which may be man or livestock animals, a hardy form of the organism, known as an oocyst, is shed in large numbers in the host's faeces. The robust nature of the oocyst enables it to survive in the environment and it can be transmitted to humans via the water cycle.

The effectiveness of filtration plants providing a barrier to particulates in the low micron size band, including *Cryptosporidium* oocysts has been investigated by Lechevallier *et al.*, (1991), Gregory *et al.*, (1991), Ongerth (1991) and Ives *et al.*, (1993). Removals ranged from 75% to 99.999% (5 log). However all reported a significant decrease in removal during the ripening period.

Ives *et al.*, (1993) also reported that filters that can remove particles of about 4µm in size will also remove oocysts to the same degree since oocysts behave in many like typical aquatic microspherical particles, with a size of  $4.15\mu\text{m} \pm 0.4\mu\text{m}$  and a negative surface charge.

The filter ripening period was identified in the "Badenoch report" as a possible route for oocysts to pass into supply (Part II, Paper VIII, 1990). In an effort to address the problem the report recommended the use of "slow start".

## 2.7 Monitoring filtrate quality

Generally, a bank of filters are monitored collectively by turbidity measurements of the combined filtrate. However, more recently because of promulgated legislation it is the growing trend to monitor individual filters.

Although individual filter monitoring gives greater process control it is now thought that turbidity is not sensitive enough to give accurate measurements of filter performance. With the fairly recent development of particle size analysers their use within the water industry has been somewhat limited. Particle size analysis can provide accurate determinations of particle numbers and distributions. It is this ability which is a major advantage over turbidity.

### 2.7.1 *The relationship between turbidity and particle counts*

There is little consensus in the literature regarding the relationship between turbidity and particle counts. Mie theory (Garcia-Rubio, 1987; Treweek and Morgan, 1980) relates turbidity to number, size, and optical constants (refractive index, extinction coefficient) of spherical particles. Garcia-Rubio (1987) concluded that turbidity measured over several wavelengths could, in principle, yield information about the particle size distribution in water. In practice, however, many workers (Bishop, 1981; Logsdon *et al.*, 1981, 1985; Westerhoff, 1976) found little direct correlation between cumulative total particle per unit volume and turbidity.

In a study of commercially available particle counters Hargesheimer *et al.*, (1992) concluded that a single conversion factor cannot be developed to relate the turbidity and particle counting results because turbidity is a one-dimensional measure of water clarity and particle counting is a two-dimensional measure. The additional information provided by two dimensions (i.e. particle size and particle counts) in particle counting means that this technique can be used to identify differences undetected by turbidimetric measurement.

### 2.7.2 *Particle counting technology*

The particle counter differs from the traditional particulate measurement of turbidity, in that individual particles in a known volume sample are sized and the number within pre-defined size ranges are counted. This provides quantitative information on the concentration of particles within size ranges that correspond to different types of contaminants.

Optical particle counters employ a light extinction technique also referred to as light obscuration or light blockage to count and size particles. Various different calibration particles are available. As with the pharmaceutical industry, the preferred calibration material in the water industry is mono-dispersed latex beads.

It is important to note that the particle counter is being used to size naturally occurring real particles, i.e. particles that are not normally spheres, but are of varied shapes, different surface characteristics and light absorbancy capacities. As such the particle counters sizing of a real

particle is that which corresponds to the same projected area (shadow) of a latex bead (the unreal calibration material). This lack of a prime calibration standard of a known size distribution of naturally occurring real particles can result in a difference in the size reported in the literature (from microscopic analyses) for a semi-transparent type particle to that produced from an optical particle counter. This is clearly illustrated by the parasitic organism *Cryptosporidium*. The reported size in the literature for the oocysts is 3-6 $\mu\text{m}$  (Ongerth, 1991; Hargeshmeir *et al.*, 1992; Ives *et al.*, 1993; and Gregory *et al.*, 1994). They are sized by extinction sensors in the range 2-4 $\mu\text{m}$ .

### 2.7.3 *Applications in water management*

Most of the early work with particle counters in the 1970's looked into their general application within water treatment plants (Beard and Tanaka, 1977; Tate and Trussell, 1978). In recent years the particle counter has become more affordable and therefore available. It has been used in the research, development and validation of new processes (Cross and Rossi, 1992; Entwisle and Murray, 1993). It is also been used to enhance particulate removal and monitor process performance (Monscvitz and Rexing, 1983; Tunison, 1985). On-line particle counters are capable of alerting plant operators to deterioration in their processes, hours before traditional turbidity problems indicate a potential problem (Hargesheimer *et al.*, 1992). This is proving to be essential to help prevent *Cryptosporidium* oocysts entering the drinking water supply.

### 2.7.4 *On - line monitoring*

Real time monitoring of the final filtered water before distribution into the supply network is already regulated. In most countries this requires that the water is below a defined nephelometric turbidity limit (NTU). In America, the state of Georgia already requires that all surface water treatment plants have on-line particle counters, monitoring in the 3-15 $\mu\text{m}$  size range. Legislation in five other states (Massachusetts, New York, Ohio, Illinois and California) require pilot plants for surface waters to have particle counters.

Within the U.K the "Badenoch report" recommended that turbidity meters be installed on individual filters, as there was evidence that they were not sensitive enough to detect filter breakthrough on water pooled from multiple filters.

Recent studies have shown that *Cryptosporidium* breakthrough can be related to deterioration in plant performance (LeChevallier and Norton, 1992) or unusually high levels in the influent to the filter (Hargesheimer et al., 1993). In both studies the particle counters showed clear increases in the particle concentration  $> 2\mu\text{m}$  in the filter effluent.

# *CHAPTER 3*

## **OBJECTIVES**

The overall objective of the work was to minimise the passage of particulates into the filtrate during ripening of rapid gravity direct filters. A number of possible methods existed to achieve this overall objective, these were broken down into separate trials each with their own objective:

- 1) To assess the performance of a range of media types and configurations and to identify two that minimised particulate passage during ripening and performed in an operationally acceptable manner.
- 2) To assess the performance of different backwash regimes, to identify an optimum and to assess the effect of changing the backwash duration on particulate passage during ripening.
- 3) To assess the effect of start-up strategies upon particulate passage during ripening and identify optimum strategies.
- 4) To assess the effect of higher rate filtration on particulate passage during ripening.
- 5) To perform a cost benefit analysis of technical options and determine most cost effective solutions.



# *CHAPTER 4*

## **PILOT PLANT SYSTEM**

This chapter describes in detail the pilot plant on which all the experiments contained in this thesis were carried-out. The chapter covers the location, the layout of the pilot plant filter complex, and the design and operation of the pilot filter system. The experimental procedures used in each trial will be covered in the relevant chapters.

### **4.1 Location**

Lostock WTW is situated 5 miles west of Bolton, Greater Manchester. It takes water from the Thirlmere Aqueduct (TA). The 200ML/d supply from lake Thirlmere is treated with lime and dosed with chlorine at the head of the aqueduct at Dunmail Raise. There is no other treatment other than re-chlorination at the 22 take-offs, of which Lostock is the largest. The Lostock site (actually the middlebrook strainer plant) offered a building capable of holding pilot rigs (shown in Figure 4.1) and had a ready means of disposing of the whole of the test flow.



**Figure 4.1. The pilot plant building at Lostock WTW.**

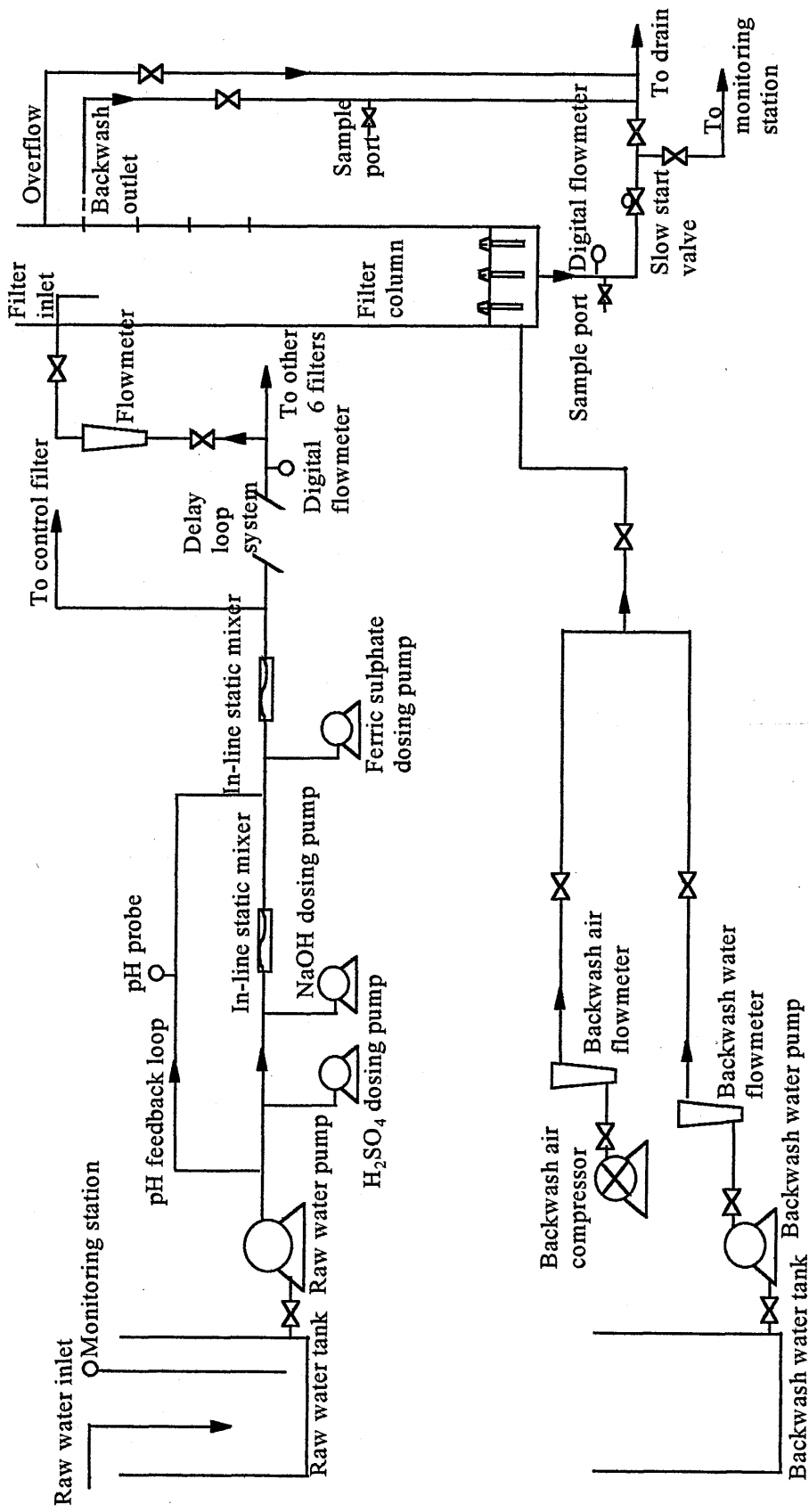


Figure 4.2. Schematic diagram of Lostock direct filtration pilot plant (not to scale).

## 4.2 Pilot Plant Complex

The pilot plant was designed by North West Water and Aston Dane Ltd and constructed by Plastic Systems. A schematic flowsheet is depicted in Figure 4.2. Raw water was drawn from the break tank by the raw water pump. Prior to filtration the raw water was treated by the addition of various chemicals. Delay loops could be brought into service to introduce additional residence time upstream of the main filtration system, which comprised seven filters manifolded on the water feed line. A separate stream was taken off upstream of the delay loops and passed through a control filter. Figure 4.3 is a schematic of one of the filter columns, and Figure 4.4 is a photograph of the columns. The filters were 3m in height and had an internal diameter of 300mm. Each filter had three filter nozzles in the base section, the filter nozzles were supplied by General Filter Company, Ames, Iowa, USA.

Water for backwashing was drawn from the existing treated water supply. It was held in the backwash tank and delivered when required by the backwash water pump, again via a manifold system (both shown in figure 4.5).

The plant control and monitoring system was based on a PLC with operator interface (keypad) and display. Operation of control valves and electrical drives from the PLC was via a panel which had isolators for each drive. Instantaneous values of process variables (such as temperature, pH, flow) could be viewed on the PLC display.

## 4.3 Operational procedure

This section describes how the various components of the pilot plant functioned.

### 4.3.1 Raw Water Delivery

The raw water pump was started by the PLC as pre-programmed on the PLC keypad.

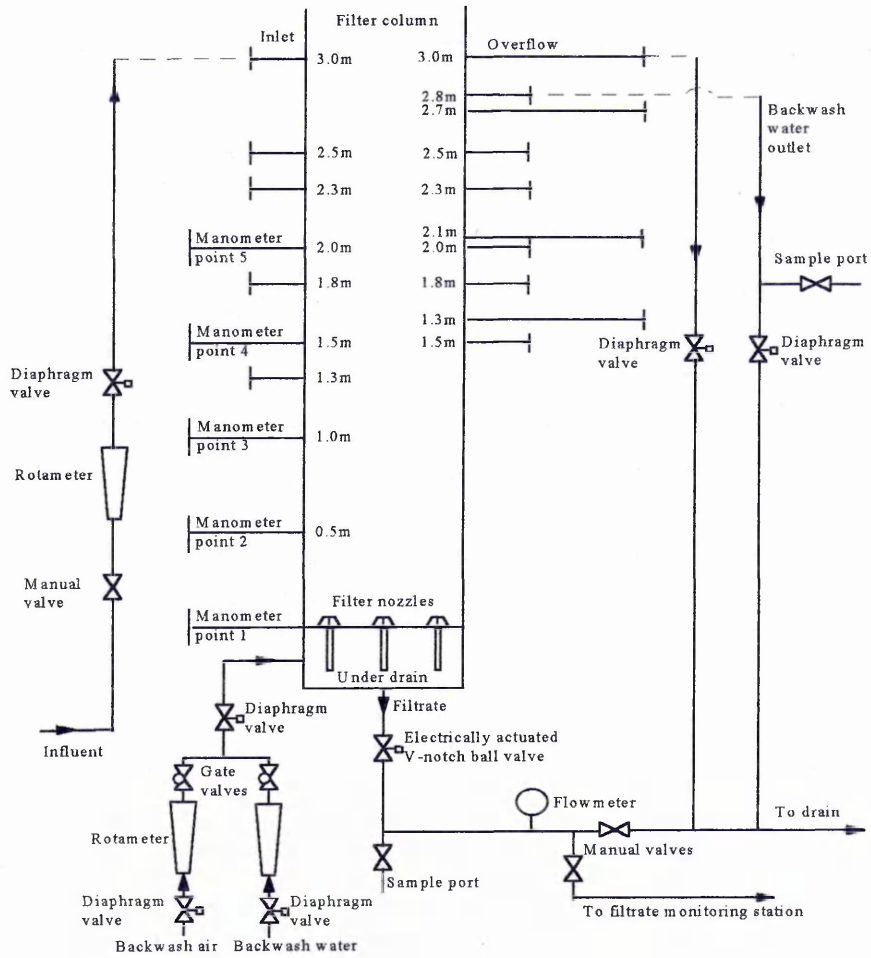


**Figure 4.3. Schematic diagram of a lostock pilot plant filter column (not to scale).**

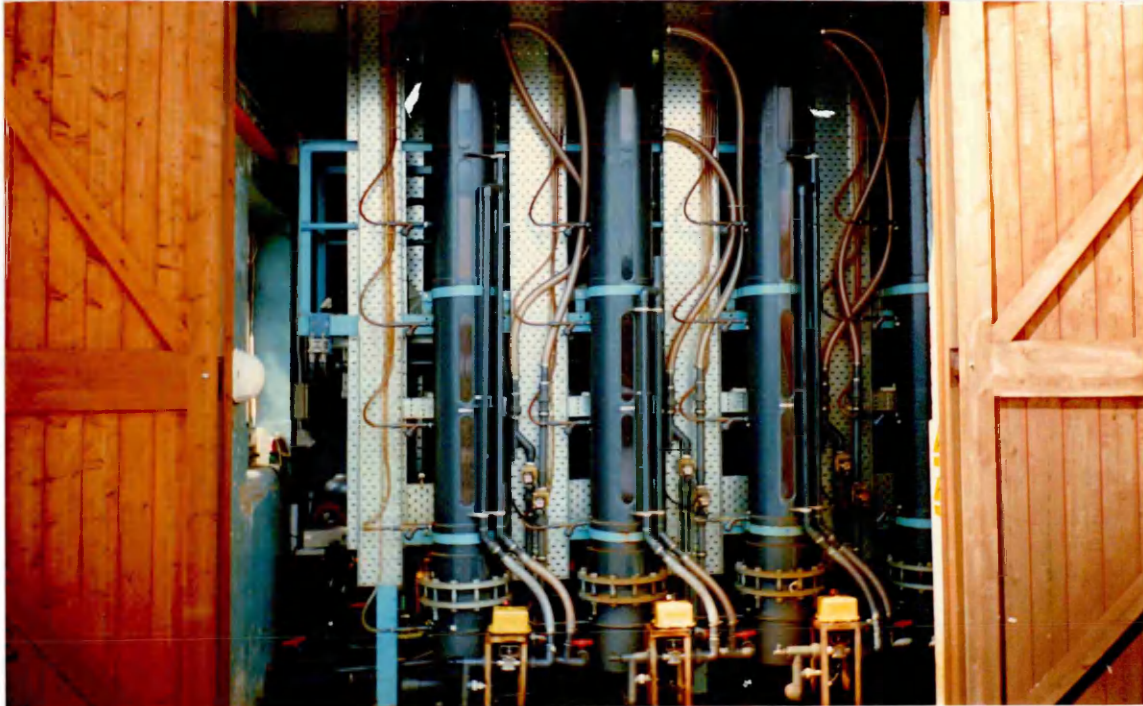


**Figure 4.4. Photograph showing four of the lostock pilot plant filter columns.**

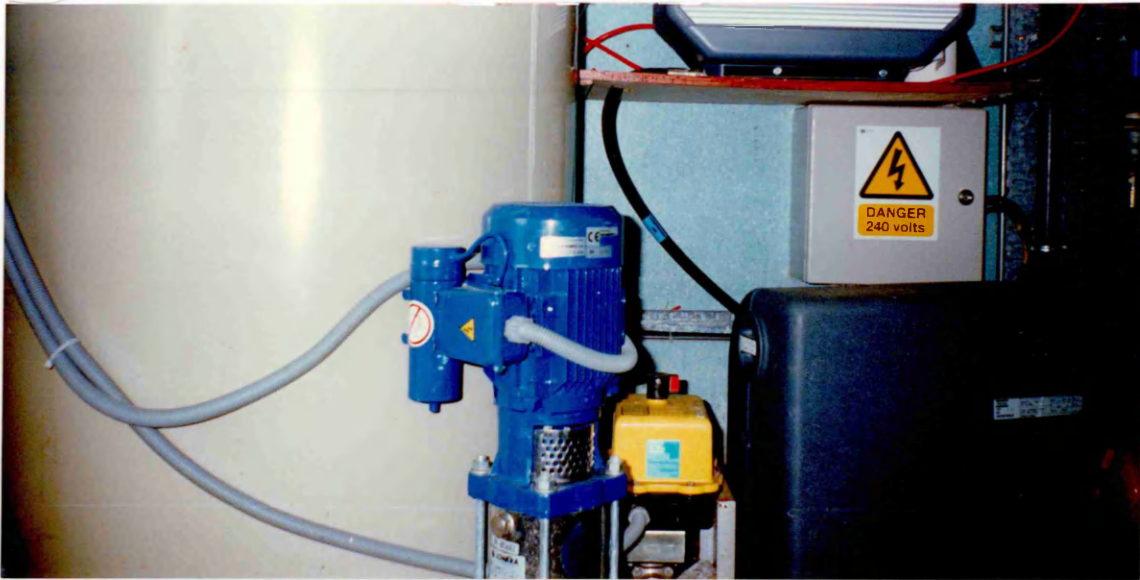


**Figure 4.5. Photograph showing backwash water tank, pump and compressors.**

#### 4.3.2 *pH Control*

The pH of treated water was sensed by the pH probe and the dosing rates of the sulphuric acid pump and sodium hydroxide pump were adjusted automatically by the PLC to achieve the desired pH ( which was entered on the PLC keypad). There was a manual override on the pH control loop.

#### 4.3.3 *Coagulation and Flocculation*

The pilot plant ran with low manganese ferric sulphate supplied by Industrial Alum, the optimum direct filtration coagulant dose was determined from the range 0.5mg/L to 2mg/L as  $\text{Fe}^{3+}$  at pH 5.5. This range had been pre-determined by jar testing (O'Neil, 1993). The optimum dose determination is shown in Figs 4.6 to 4.9 for two different media types. The dosing pump dosed the chemical into the raw water under manual control (the rate of addition was set on the dosing pump), the dosing apparatus are shown in Figures 4.10 and 4.11. The optimum flocculation time was determined using five delay loops, which allowed a flocculation time of 1 up to 20 minutes. Any combination of the delay loops could be put into service by operation of the appropriate 3-way valves. However only one delay loop could be selected for the control filter.

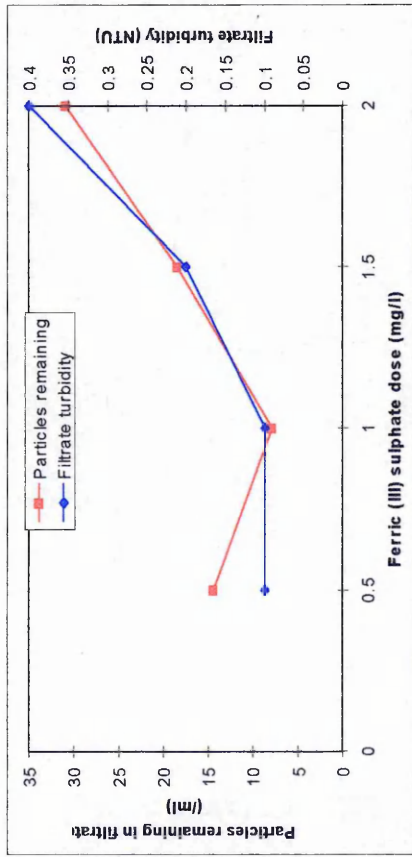


Figure 4.6 Coagulant optimisation using particle count and turbidity -1m deep 0.5-1.0mm sand filter.

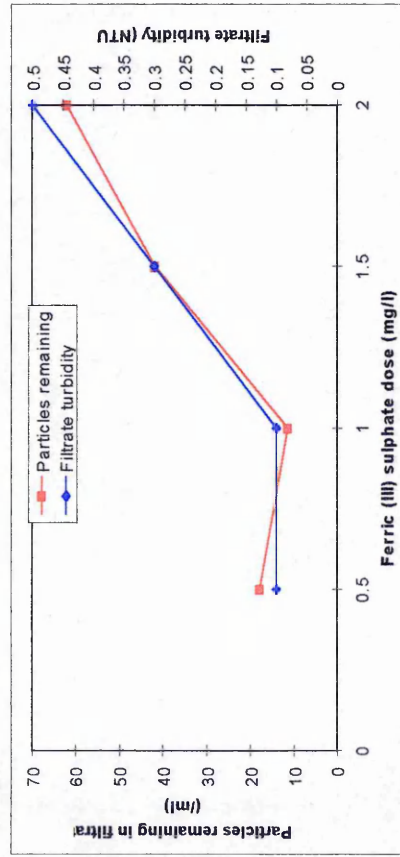


Figure 4.8 Coagulant optimisation using particle count and turbidity -2m deep 2.0-3.35 mm sand filter.

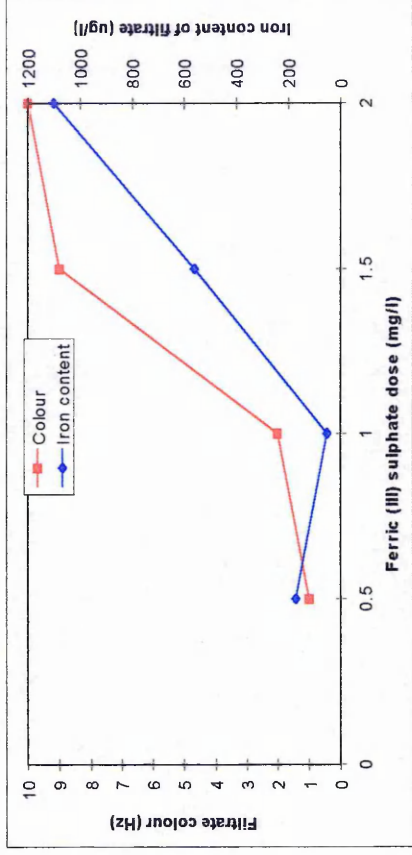


Figure 4.7 Coagulant optimisation using colour and iron content -1m deep 0.5-1.0mm sand filter.

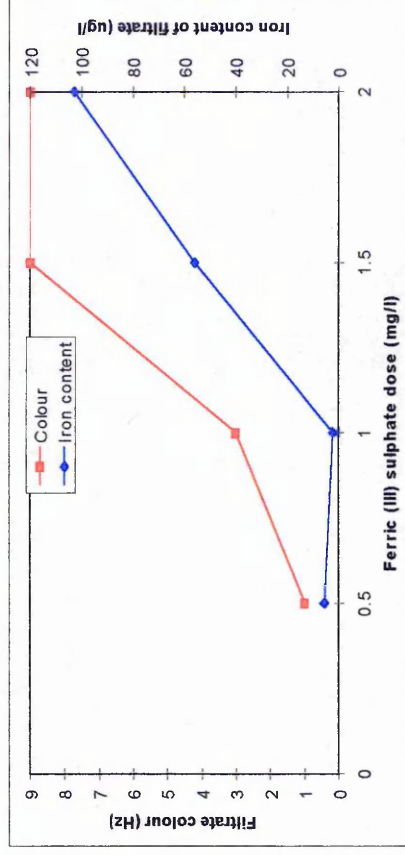


Figure 4.9 Coagulant optimisation using colour and iron content -2m deep 2.0-3.35 mm sand filter.

#### 4.3.4 Normal Operation

This section covers all eight filters, i.e. including the control filter.

The inlet valve was open and the feed was adjusted by the diaphragm valve upstream of the rotameter ( which gave the flow indication ). The bottom outlet was open. The outlet stream could be directed to drain or via the turbidity and particle size meters by positioning of the relevant manual valves. Only one filter at a time could be directed to the meters. The filters were operated in a declining rate mode, the overflow was normally open and allowed the filter to overflow as the medium became clogged, thereby reducing the bottom flow. The overflow level could be varied by moving a flexible hose on the outlet pipework. The backwash outlet valve would be closed.



Figure 4.10. Photograph showing pre-treatment chemicals and dosing pumps.



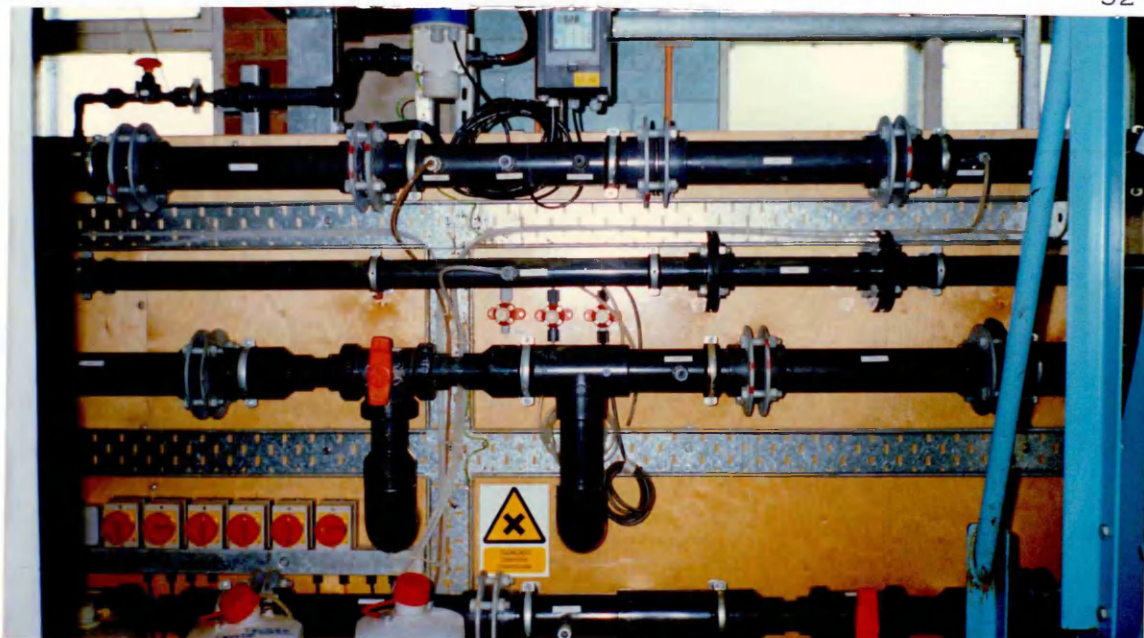


**Figure 4.11.** Pre-treatment system, showing dosing points, in-line mixers and pH control system.

#### 4.3.5 Backwash

When the bottom discharge of one of the filters fell to a pre-set value a backwash was initiated. The value was specified for each filter on the PLC. The following sequence would occur: The inlet valve and overflow closed simultaneously, followed by the bottom outlet valve after a pre-set time (allowing a drain down period). The backwash outlet valve opened as the bottom outlet closed. The backwash outlet level could be changed by moving a flexible hose on the outlet pipework. After a further pre-set time, adjustable for each filter, the following sequence was initiated - The backwash air compressor was started, the air line valve and the air inlet valve at the base of the filter were both opened. This admitted air to the filter base ( the flow of air to each filter was adjusted by the diaphragm valve on the individual air line into each filter, since there was only one rotameter).

After a further pre-set time, adjustable for each filter, the following sequence was initiated:

The backwash pump was started and the backwash water inlet valve was opened to its first position. This admitted water to the filter base. The position of this valve was selectable for each filter. It was held in the first position for a pre-set time before opening to its second position, which was again selectable. The backwash water flowrate was indicated on the backwash water rotameter. After a further pre-set time, adjustable for each filter, the air inlet valve closed and the

backwash air compressor stopped in sequence. After a further pre-set time, adjustable for each filter, the backwash water inlet valve closed, the backwash water pump stopped and the backwash outlet valve closed in sequence.

Immediately following backwash completion the filter was brought back onto line by the bottom outlet and overflow valves opening simultaneously, followed by the inlet valve. The outlet valves were segmented ball valves, which had 1000 positions. The valves could be programmed to open by linear stepping over a set duration. The adjustable parameters were therefore the final position (% open) and the time taken to reach that position. One of the outlet valves is shown in Figure 4.12.

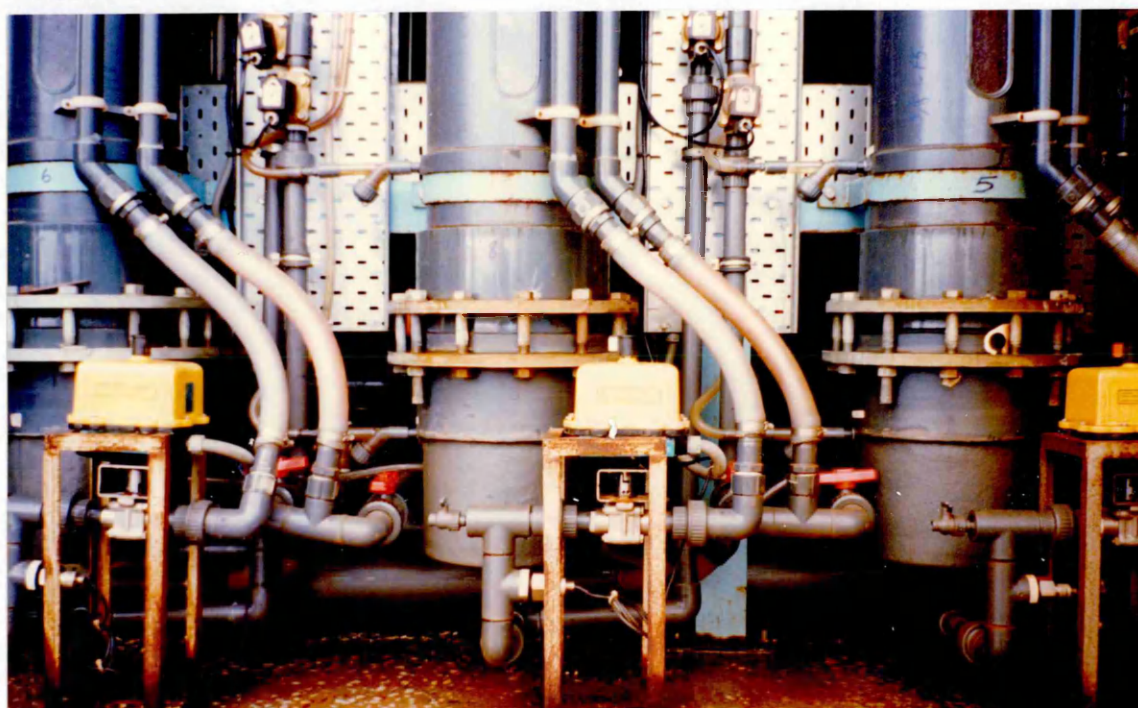


**Figure 4.12. Photograph showing electrically actuated v-notch ball valves on filter outlet.**

There were also a number of backwash manual options. Any filter backwash could be initiated manually by PLC keypad entry. In addition, automatic backwash initiation could be manually overridden, again by keypad entry. Any filter backwash could be initiated by time - If after a pre-set time for each filter, low outlet flowrate had not initiated a backwash, then a backwash would automatically be started.

There was a backwash queuing system to ensure that no two filters could backwash simultaneously.

## 4.4 Plant Monitoring

### 4.4.1 Influent Monitoring

The influent water quality was monitored in terms of temperature, turbidity, pH, particle size analysis, and Iron and Manganese content

The turbidity of the raw water was continuously monitored by a Endress and Hauser CUS1 turbidity probe and CUM 141S turbidity and temperature measuring transmitter. The turbidity and temperature data was fed back to the PLC and logged.

The pH of the treated water was sensed by an Endress and Hauser CPM 240 pH and Redox measuring instrument and controller. The measured value resolution was 0.01 pH. The error on the probe was 0.5%. The data was fed to the PLC and logged. The data also controlled the dosing rates of the sulphuric acid and hydrogen peroxide pumps, as explained previously.

The particle size distribution of the raw water was monitored every five minutes by a Hiac Royco Versacount LV model light obscuration particle counter. This model had eight size channels (>2um, >5um, >10um, >15um, >20um, >25um, >50um, and >100um ). The data was stored in the counters internal memory. The data would periodically be downloaded to a PC. The concentration limit of the counter was 12,000 particles/ml. The sample flow rate was 25ml / minute ( $\pm 5\%$ ). The particle counters were sent away for calibration every 3-4 months.

Duplicate 1litre samples of the influent were taken daily and sent off-site to NWW laboratories for: suspended solids, pH, Iron and Manganese content determination.

### 4.4.2 Effluent Monitoring

The effluent quality was monitored in terms of turbidity and particle size distribution. The bottom discharge from only one filter at a time could be monitored for treated water turbidity and

particle size distribution.

The turbidity probe used was an on-line Endress and Hauser CUS 1 turbidity sensor and CUM 141S turbidity and temperature measuring transmitter. The measured value resolution was < 0.5% of the upper range value. The error on the probes was a maximum of  $\pm 0.5\%$ . After installation calibration was carried out at regular intervals. Data was fed back to the PLC and logged.

The particle counter was a Hiac Royco Versacount LV model. This was the same model as that used on the influent.

The filtrate from individual filters was monitored for 10 minutes prior to and for up to 80 minutes after a backwash, at 1 minute intervals. A sampling rate of 25ml/minute was used.

#### *4.4.4 Headloss Monitoring*

Each filter had five tap points for headloss monitoring (refer to Fig 4.3 ). Each tap point was connected to manometer tubes mounted at the side on a graduated board. The headloss was recorded at regular times during the day on a log sheet . This data was then put into a PC.

#### *4.4.5 Backwash Water Monitoring*

Turbidity analysis of backwash water was performed by collecting samples of the backwash water from the filter backwash outlet sample tap. 0.5 l samples were taken continuously for the duration of the washout. These were then analysed on-site using a Hach Turbidity meter.

### **4.5 Appurtenances**

Table lists all of the appurtenances, utilised in the filter system, and their purposes and specifications, manufacturer, and model number of each appurtenance.

Table 4.1. Appurtenances used in the Lostock pilot plant.

ITEM	PURPOSE AND SPECIFICATION	MANUFACTURER
Raw water pump	Pumping raw water to pilot plant.	Lowara - Centrifugal close-coupled pump CN4
Backwash water pump	Pumping backwash water to filters.	Illawara
Backwash air compressor(s)	To supply backwash air to filters.	Atlas Copco
Sulphuric acid pump	To add H <sub>2</sub> SO <sub>4</sub> to raw water-pH correction.	ProMinent - Gamma G/4a
Sodium Hydroxide pump	To add NaOH to raw water-pH correction.	ProMinent - Gamma G/4a
Ferric sulphate pump	To add coagulant to raw water.	ProMinent - Gamma G/4a
In-line static mixers	To rapid mix chemicals into test flow	Chemineer - Kenics 5 filament helix flash mixers
Filter influent rotameters	To measure filter influent flowrate.	GeorgeFischer
Backwash water rotameter	To measure backwash water flowrate.	GeorgeFisher
Backwash air rotameter	To measure backwash air flowrate.	GeorgeFisher
PLC	To monitor and control pilot plant.	Texas Instruments

# *CHAPTER 5*

## **MEDIA TESTING**

### **5.1 Introduction**

The rapid gravity unit process contains filter media through which a suspension is passed. A variety of media types (e.g. sand, anthracite and garnet) and size ranges are available, a number of which were selected for use in the pilot trials. It was necessary to determine some physical properties of the media prior to the trials. The particle size distribution, settling velocities, fluidised bed behaviour, and the effect of varying combinations of air and water backwash were determined, and are reported.

### **5.2 Experimental Procedure**

#### *5.2.1 Media particle size distribution*

The size distributions of all the media as supplied were determined. The standard method for establishing the size distribution of filter media is sieve analysis (BEWA, 1993).

The apparatus consisted of a range of sieves manufactured to BS420: 1986, and an electric balance. The sieving procedure followed was the method for dry sieving given in BS812 section 103.1 (1985). The standard does not specify when sieving is complete and therefore the criterion given in BEWA (1993) was used. This states that sieving is complete when there is less than 1% change in any sieve fraction for each additional minute of shaking.

#### *5.2.2 Settling Velocity measurement*

For each medium, a sample of grains was taken from the intermediate sieve sizes, after sieve analysis was complete. The samples were pre-wetted by leaving them in water for 24 hours. From these samples, 20 individual grains were removed at random. The grains were released in the centre of a testing column (150mm I.D) below the water line. The settling velocity of each grain was individually

measured by timing its vertical fall in water through a distance of 1m. The water temperature was recorded to undertake viscosity adjustments. In order to ensure the terminal velocity of each grain had been reached, a freeboard water level of 500mm was used above the testing mark.

### 5.2.3 Fluidised bed behaviour assessment

The rig used in this assessment is shown in Fig 5.1. The procedure followed was that specified in the BEWA standard (1993). The column used had an internal diameter of 150mm, and a height of 2m. A media depth of 1m was employed. A point that needs to be stressed is how % bed expansion was determined: The depth of the bed was recorded for each flow rate and the expansion quoted as the % increase in depth over the residual bed depth after flow has ceased (not the initial depth).

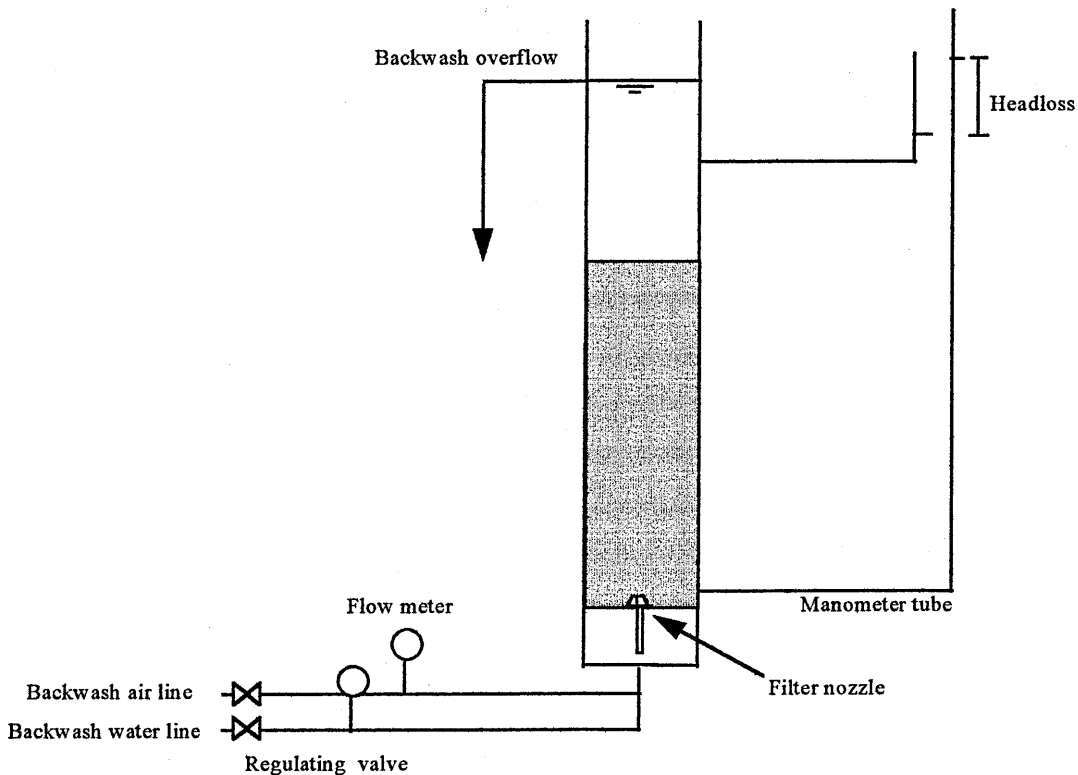


Figure 5.1. Schematic of testing apparatus used in media studies.



#### *5.2.4 Collapse-pulsing backwash determination*

After the conclusion of the water only backwash experiments a further set of qualitative observations were undertaken on combined air and water backwash flow regimes, using the same apparatus. The purpose of this was to determine different flow rate combinations that produced the fluid dynamic state of collapse-pulsing. The procedure used was described fully by Hewitt and Amirtharajah (1984).

#### *5.2.5 Scanning electron microscope examination*

A scanning electron micrograph (SEM) type 250 Mark 3 was used to observe the shape and surface microtopography of the media grains. Photographs were taken of a number of the media samples.

### **5.3 Results**

#### *5.3.1 Media particle size distribution*

The particle size distributions of four media samples were determined. Sand with size ranges specified by the supplier, Universal Mineral Supplies Ltd, as: 0.5-1.0mm, 1.18-2.8mm, and 2.0-3.35mm; and anthracite of size 2.5-5.0mm. Two other media, 0.3-0.6mm sand and 0.3-0.6mm garnet, were selected for use at Lostock at a later date. Sieve analysis was not performed on these additional media. The data is also summarised in Table 5.1, included is the  $d_{10}$  which is used as the effective size, the  $d_{60}$  and  $d_{90}$ , and also the uniformity coefficient (UC). Both the effective size and the UC (which is the ratio of  $d_{60}$  to  $d_{10}$ ) are widely used terms.

**Table 5.1 Sieve analysis results.**

Media type/size <sup>1</sup>	$d_{10}$ (mm)	$d_{60}$ (mm)	$d_{90}$ (mm)	Effective size	UC
16/30 sand 0.5-1.0mm	0.58	0.79	0.92	0.58	1.36
6/14 sand 1.18-2.8mm	1.59	2.21	2.6	1.59	1.39
5/8 sand 2.0-3.35mm	2.21	3.03	3.18	2.21	1.37
Anthracite No.3 2.5-5.0mm	2.62	3.81	4.86	2.62	1.45

1- as labelled by suppliers.

### 5.3.2 Settling Velocity measurement

The settling velocities of all of the size ranges of the 4 media that underwent sieve analysis were determined. As explained in the previous section 2 other media's that were to be used at Lostock that did not undergo sieve analysis. A representative sample of 20 grains was taken from these two media's and tested in the same manner. This then gave an average settling velocity ( $V_s$ ) for these two media. The data is plotted in Fig. 5.2 and listed in Table 5.2, the time taken to fall through 1m and the settling velocity are shown in Table 5.2.

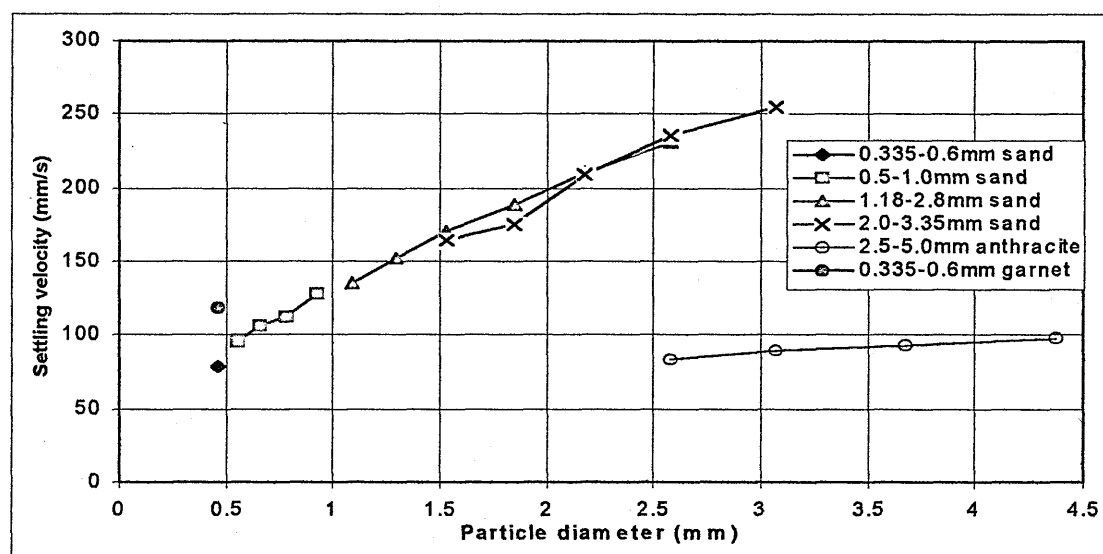


**Figure 5.2. Media Settling velocities at 10°C.**

The  $V_s$  values showed an expected trend. With reference to the sand media tested,  $V_s$  increased with particle size. The average  $V_s$  of the 0.3-0.6mm garnet sample illustrated how  $V_s$  increased with density

for a given size. This was confirmed by the anthracite, which has a lower density than sand, since the  $V_s$  of the anthracite was lower than that of the sand despite its larger size.

**Table 5.2. Media settling velocities at 10°C.**

Sieve <sup>1</sup> range (mm)	0.6-0.355mm sand		0.1-0.5mm sand		2.8-1.18mm sand		3.35-2.0mm sand		2.5-5.0mm anthracite		0.6-0.355mm garnet	
	Time (s)	$V_s^2$ (mm/ s)	Time (s)	$V_s$ (mm/ s)	Time (s)	$V_s$ (mm/ s)	Time (s)	$V_s$ (mm/ s)	Time (s)	$V_s$ (mm/ s)	Time (s)	$V_s$ (mm/ s)
4.75-4.0									10.2	98		
4.0-3.35									10.8	93		
3.35-2.8							3.95	253	11.1	90		
2.8-2.36					4.33	231	4.22	237	11.9	84		
2.36-2.0					4.73	212	4.77	210				
2.0-1.7					5.3	190	5.69	176				
1.7-1.4					5.8	171	6.08	164				
1.4-1.18					6.6	152						
1.18-1.0					7.4	136						
1.0-0.85			7.81	128								
0.85-0.71			8.93	112								
0.71-0.6			9.43	106								
0.6-0.5			10.4	96								
Average	12.7	79									8.47	118

1- BS420:1986; 2-settling velocity.

### 5.3.3 Fluidised bed behaviour assessment

The aim of the fluidised bed behaviour investigation was to determine the minimum fluidisation velocity ( $V_{mf}$ ) and the degree of bed expansion of the different media.

The headloss development and bed expansions over a range of backwash flowrates for the 6 media tested are shown in Figs. 5.3 to 5.8. A number of general observations can be made from these figures. As the sand size increases the backwash water velocity required to fluidise the media also increases.

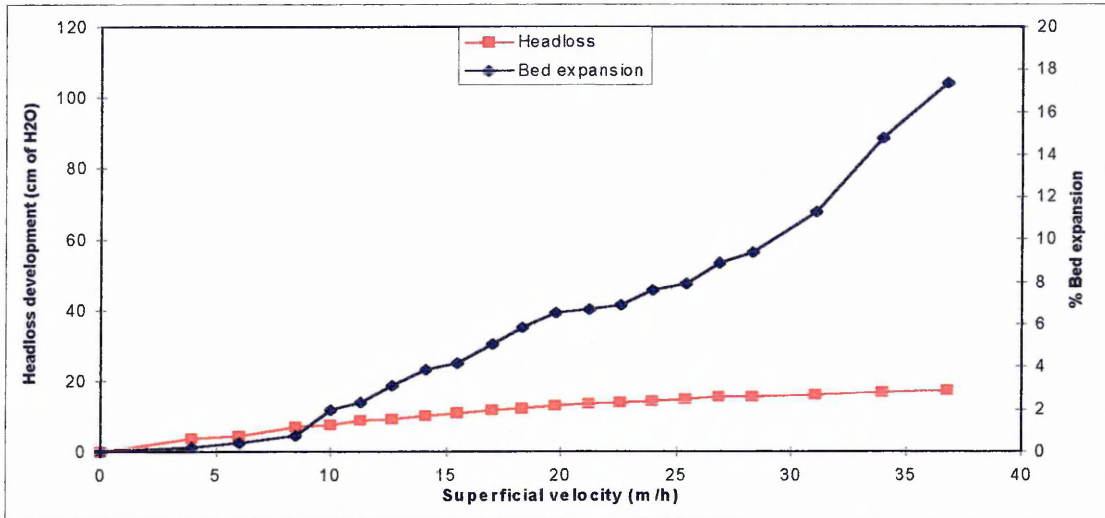


Figure 5.3 Headloss and bed expansion curves for water only backwash, 0.355-0.6mm sand.

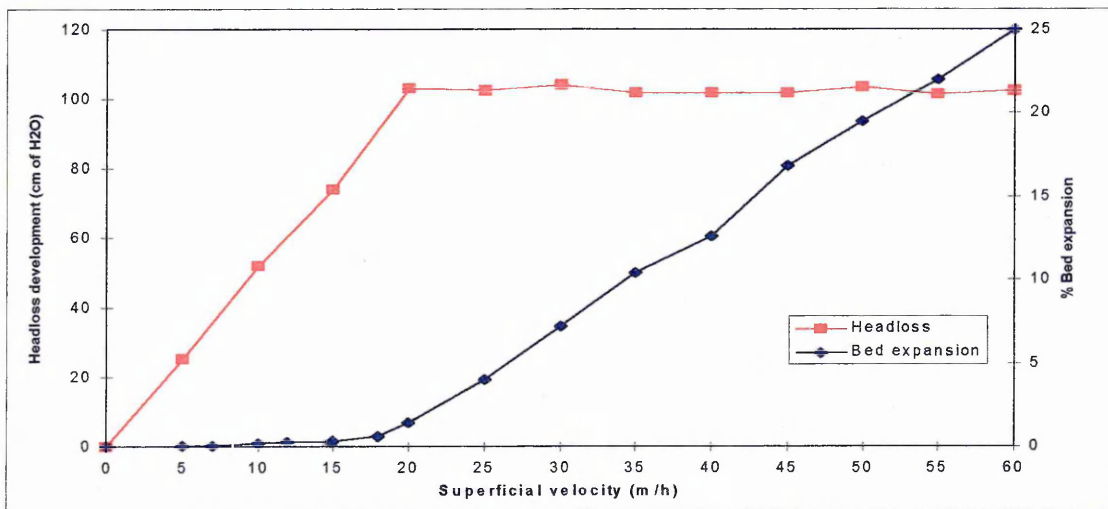


Figure 5.4 Headloss and bed expansion curves for water only backwash, 0.5-1.0mm sand

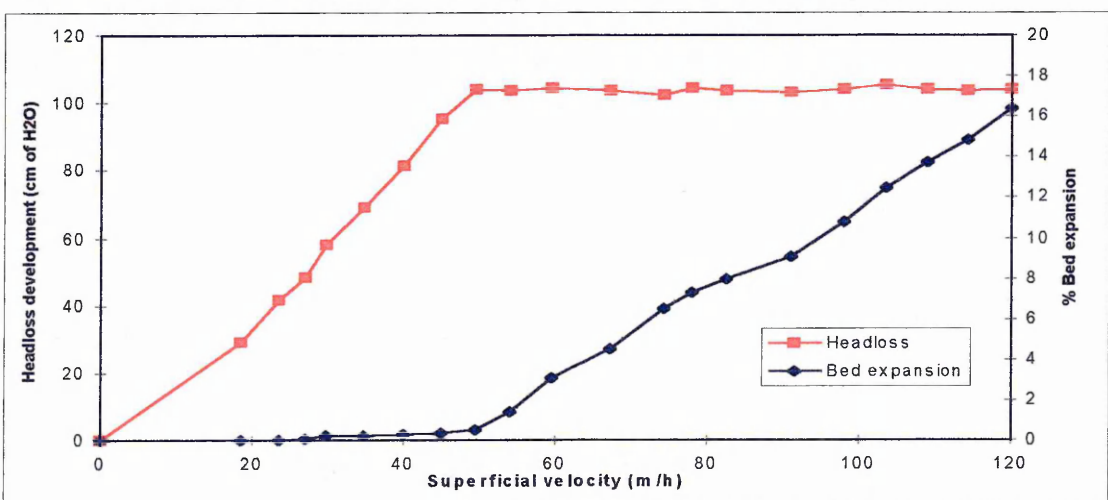


Figure 5.5 Headloss and bed expansion curves for water backwash, 1.18-2.8mm sand

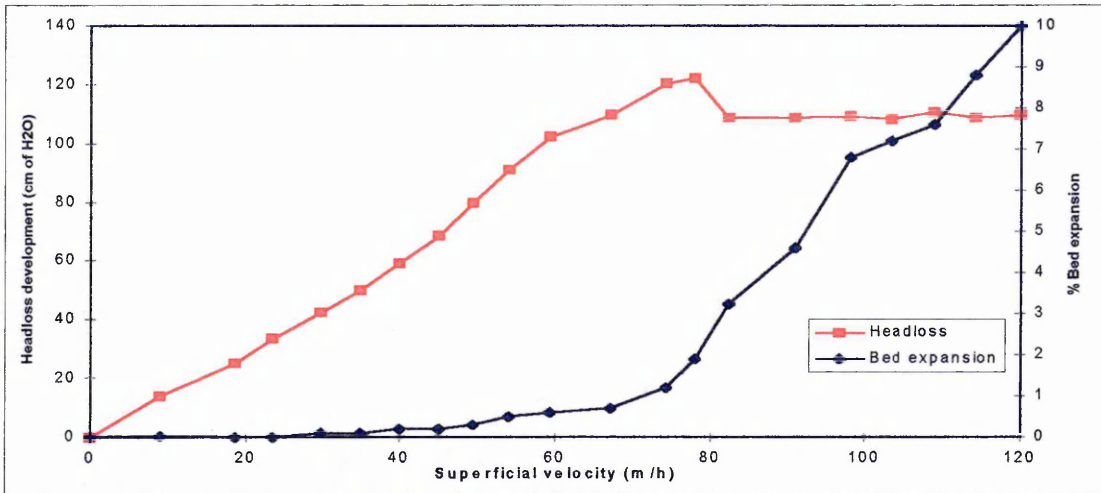


Figure 5.6 Headloss and bed expansion curves for water backwash, 2.0-3.35mm sand

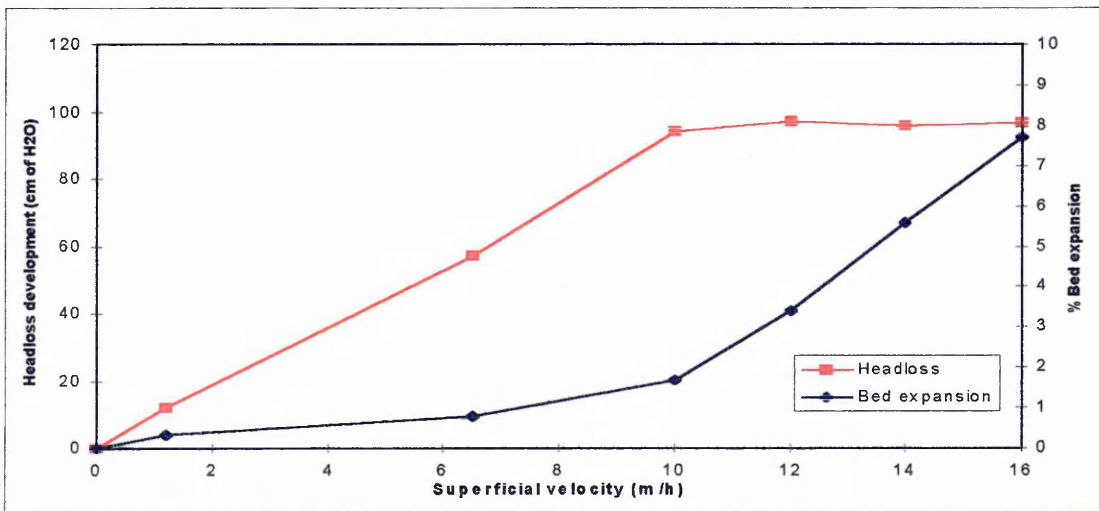


Figure 5.7 Headloss and bed expansion curves for water only backwash, 0.3-0.6mm garnet.

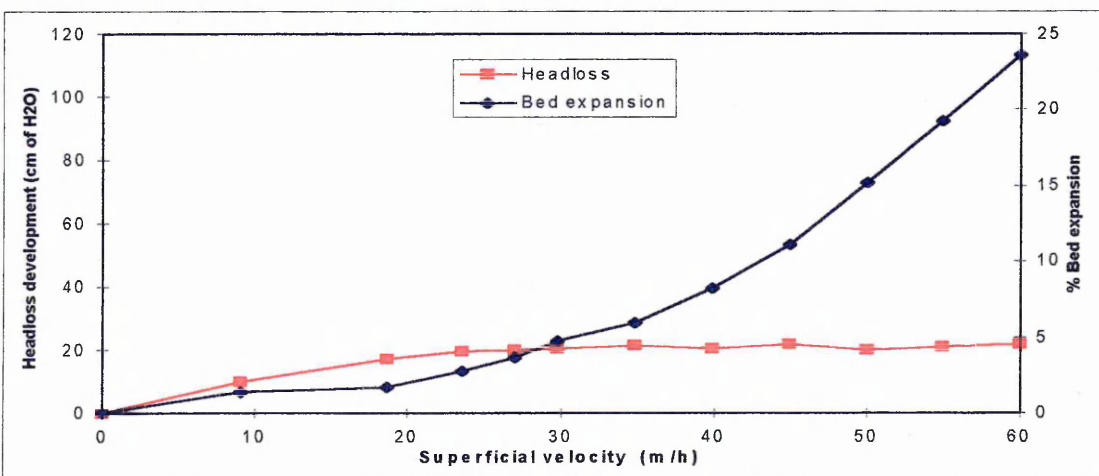


Figure 5.8 Headloss and bed expansion curves for water backwash, 2.5-5.0mm anthracite.

Take for example Fig. 5.4, at a backwash velocity of 60m/h the bed has expanded by 23%, at the same velocity the larger sand in Fig. 5.6 has not even fluidised. The density of the media can again be seen to have a significant effect, the large anthracite in Fig. 5.8 had expanded by 24% at the same backwash velocity.

The  $V_{mf}$  values of the media, as determined from Figs. 5.3 to 5.8 are shown in Table 5.3. Also shown are the theoretical values of  $V_{mf}$  calculated using the Wen and Yu (1966) equation. When the experimentally determined  $V_{mf}$  are compared to the calculated values some large discrepancies are apparent, especially for the larger media .

**Table 5.3 Experimentally and theoretically determined values of  $V_{mf}$ .**

Media type and size range	Experimental $V_{mf}$ (m/h)	Theoretical $V_{mf}$ (m/h)
0.6-0.355mm sand	10	8.82
0.1-0.5mm sand	17.5	24.10
2.8-1.18mm sand	52	104.04
3.35-2.0mm sand	68	126.67
2.5-5.0mm anthracite	10.5	76.94
0.6-0.355mm garnet	22	13.84

#### 5.3.4 Collapse-pulsing backwash determination

The combinations of air and water flowrates that achieved collapse-pulsing for the different media are shown in Fig. 5.9.

An observation made during this assessment was that the introduction of air at sub-fluidised backwash water rates was seen to cause bed contraction. Collapse-pulsing was not observed at air flowrates of below 30m/h, and at these rates bed movements were low. When collapse-pulsing was reached the movement of the media was extremely violent and significant bed contraction occurred.

The same data was plotted in the format seen in Fig. 5.10 to facilitate comparison with Amirtharajah's design graph (Fig. 3.9). It can be seen that the two graphs show good correlation.

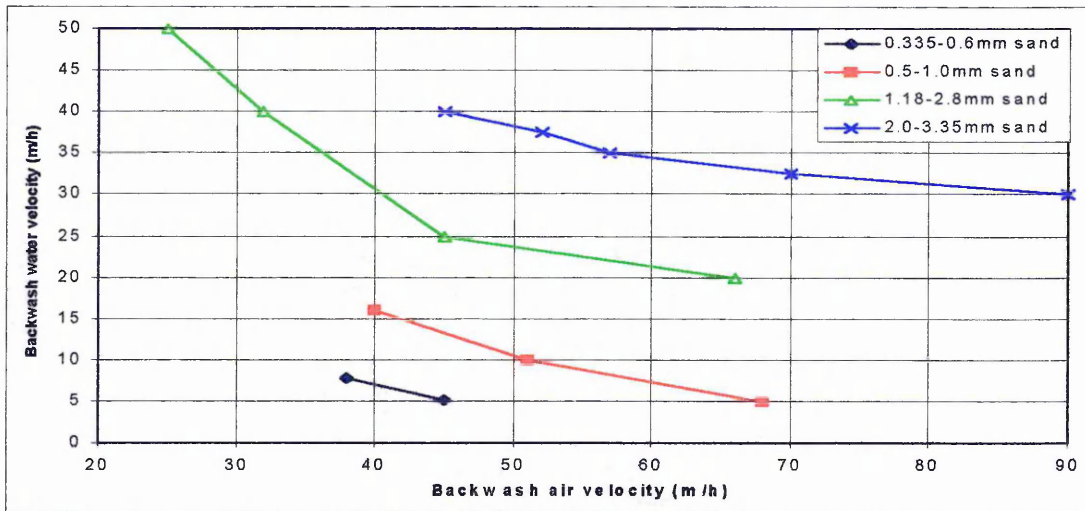


Figure 5.9 Air and water backwash rates that cause collapse-pulsing.

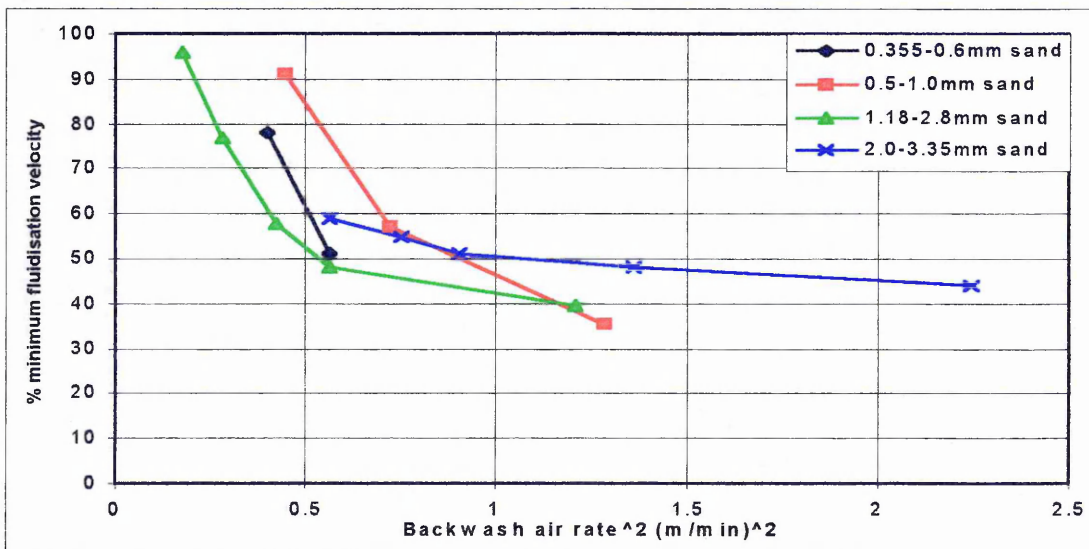


Figure 5.10 Air rates and %  $V_{mf}$  that cause collapse-pulsing.

### 5.3.5 Scanning electron microscope examination

The results from the SEM analysis are shown in Figs. 5.11 to 5.16. It was only possible to photograph the 0.5-1.0mm, 1.18-2.0mm, and 2.0-3.35mm sands. Two photographs of each media are shown, a shot of the whole grain (showing the sphericity) and a shot of the grain surface (showing the microtopography). The 0.5-1.0mm sand, shown in Figs. 5.11 and 5.12, can be seen to be rounded and have a smooth surface. The 1.18-2.8mm sand, Figs 5.13 and 5.14 had similar features.

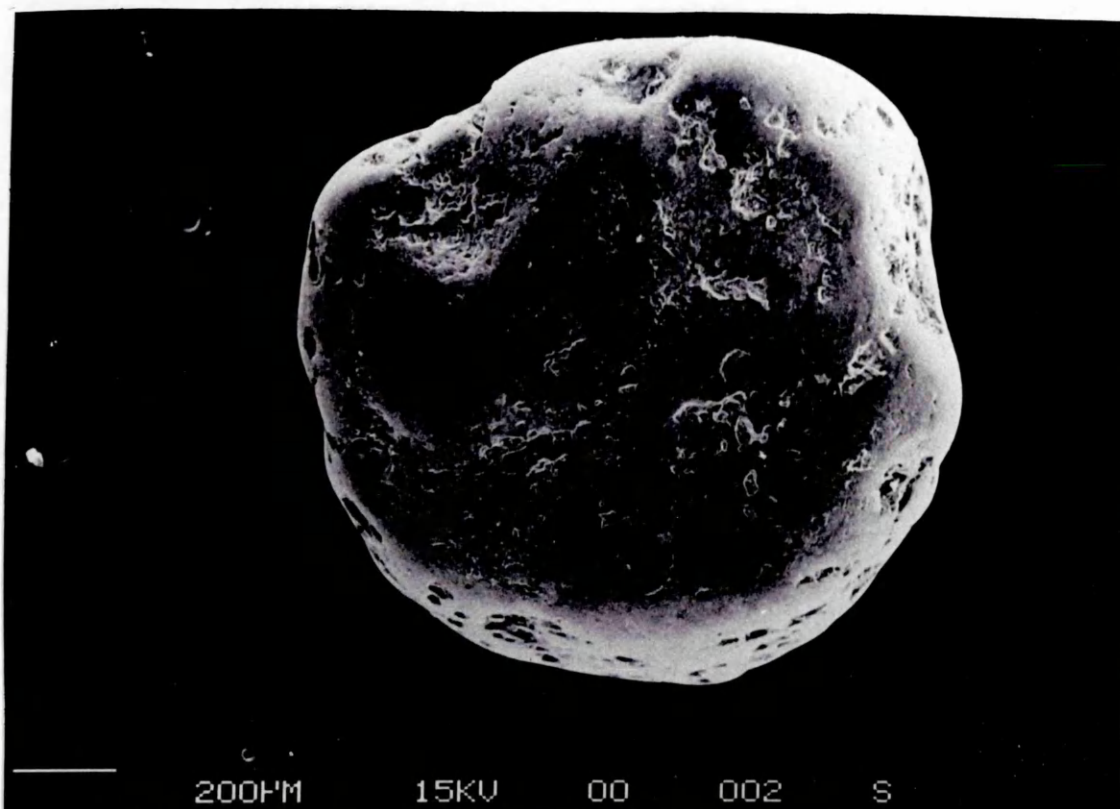


Figure 5.11 Scanning electron micrograph of 0.5-1.0mm sand, x 50 magnification.



Figure 5.12 Scanning electron micrograph of 0.5-1.0mm sand, x 500 magnification.



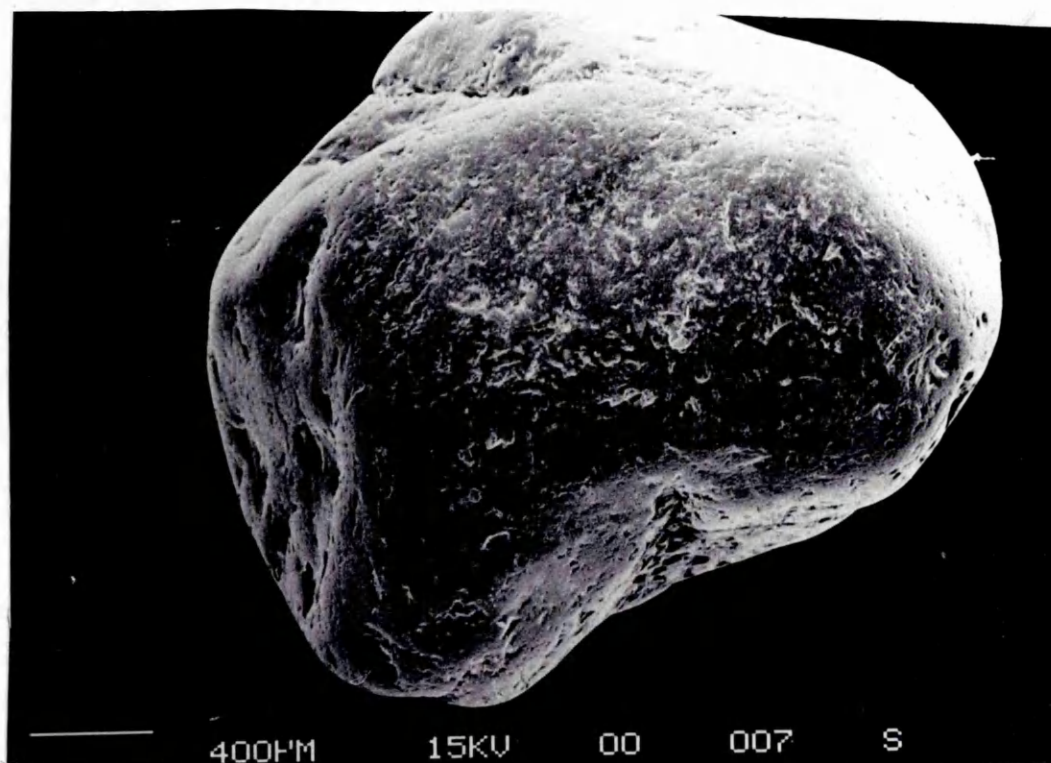


Figure 5.13 Scanning electron micrograph of 1.18-2.0mm sand, x 30 magnification.

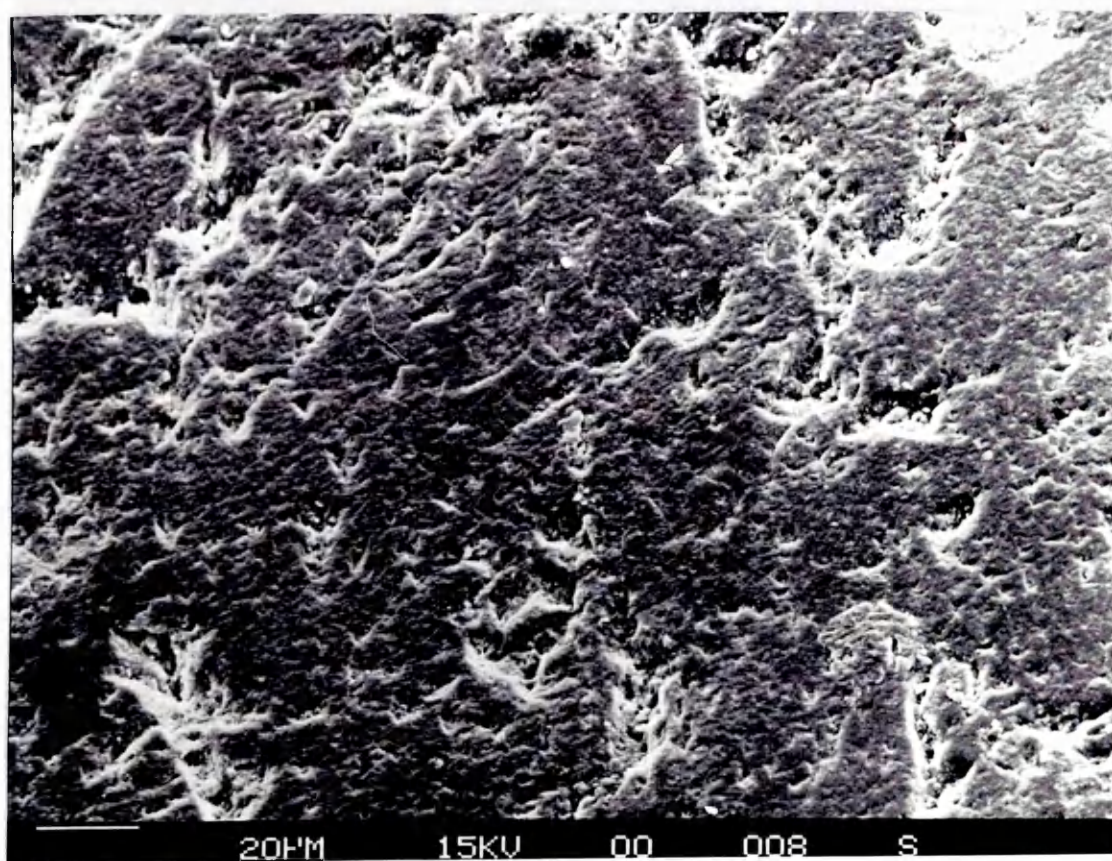


Figure 5.14 Scanning electron micrograph of 1.18-2.0mm sand, x 500 magnification.

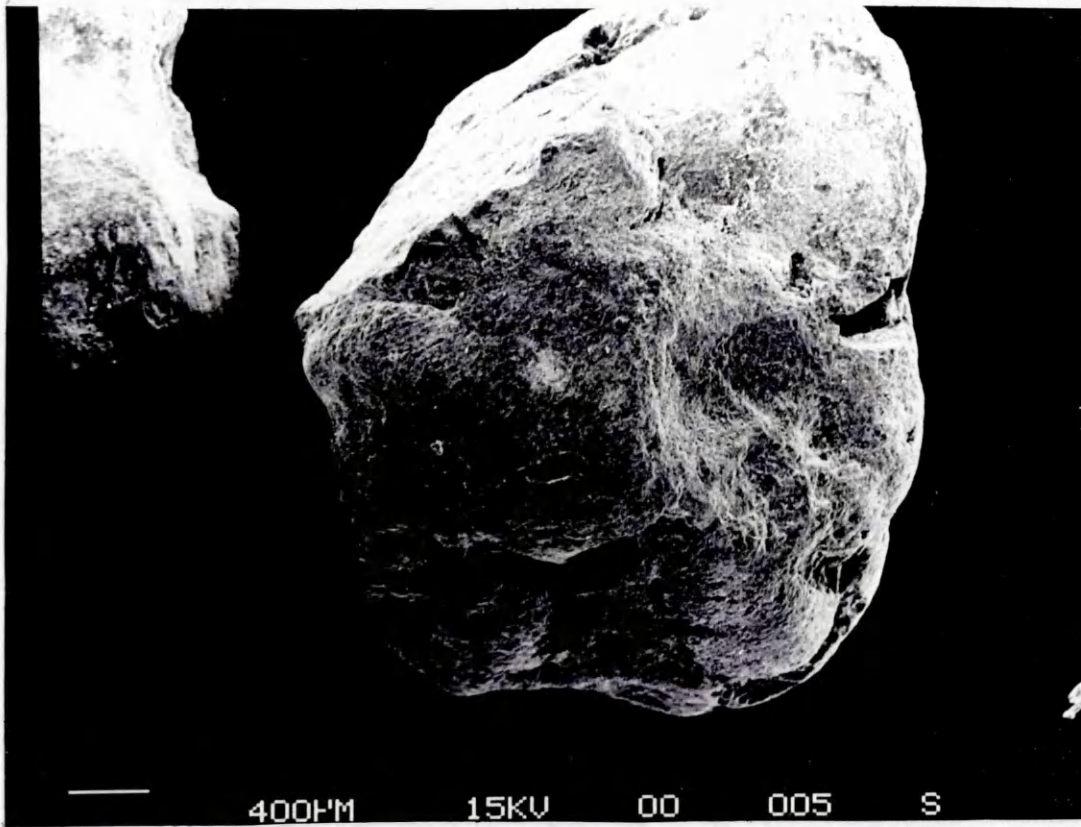


Figure 5.15 Scanning electron micrograph of 2.0-3.35mm sand, x 20 magnification.

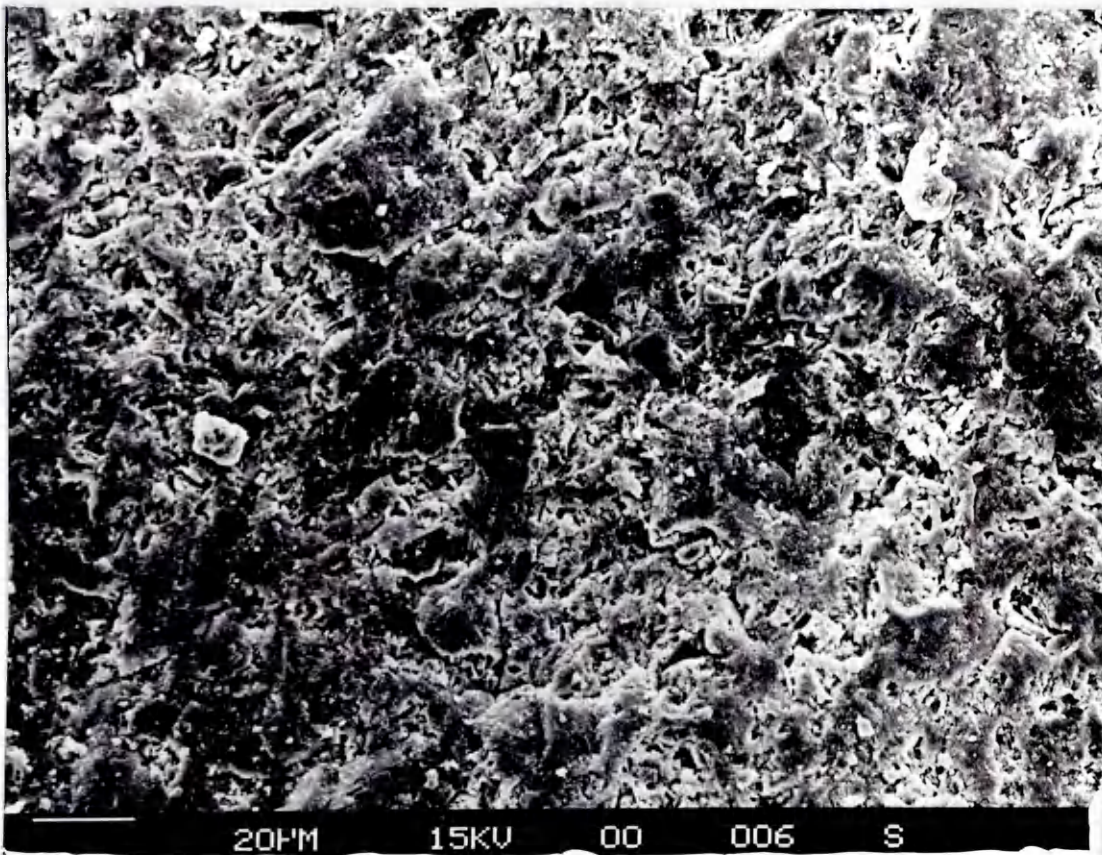


Figure 5.16 Scanning electron micrograph of 2.0-3.35mm sand, x 500 magnification.

The 2.0-3.35 mm sand (Figs. 5.15 and 5.16), however, could be seen to have some different features, the grain appears to be less rounded, with some planar surfaces. The surface microtopography appears to be much rougher than the other two sand samples.

## **5.4 Discussion**

### *5.4.1 Media particle size distribution*

The particle size distributions obtained for the media concurred with the suppliers data. The suppliers state that 90% of grains will be in the specified size range. The media tested generally showed a normal distribution; this is characterised by a linear plot. Some deviations from linearity were apparent, Humby (1994) attributed these deviations to methods used to manufacture the media, methods used to classify the media, and experimental error in the sieve analysis.

### *5.4.2 Settling Velocity measurement*

All the settling velocity ( $V_s$ ) experiments were carried out at a temperature of 10°C. The  $V_s$  is affected by water viscosity, so therefore it is temperature dependent. Historical data showed water from the Thirlmere aqueduct at Lostock has a temperature range of 3-15.5°C, with an average value close to 10°C.

The purpose of determining the settling velocity of media was to predict stratification behaviour during water only backwash of any dual media combinations selected for use at Lostock. The data in Fig 5.2 shows that intermixing should not occur after fluidisation, expansion and re-settling for certain combinations of media. For instance, a combination of the 2.0-3.35mm sand and 2.5-5.0mm anthracite should not display any significant degree of intermixing. A combination of the same anthracite and the 0.3-0.6mm garnet may facilitate a small degree of intermixing.

These examples illustrate once again how significant media size and density are,  $V_s$  increases with size for a specific media, and with density of the media..

### 5.4.3 Fluidised bed behaviour

The graphs obtained in the fluidised bed behaviour assessment show general accordance to published data (Bayfield, 1993; Humby, 1994), and indeed to "typical" curves. A number of interesting deviations occurred: the point of  $V_{mf}$  was very difficult to determine for the anthracite, and the 2.0-3.35mm sand exhibited a peak in headloss greater than the limiting headloss.

The anthracite used had a wide size range, 2.5-5.0mm, Humby (1994) stated that the smaller grains will become fluidised first, followed by larger grains, resulting in a graduated fluidisation of the bed. The  $V_{mf}$  is therefore hard to pinpoint for such a media. The sand used had smaller size ranges and this problem was not so apparent.

The headloss development seen prior to  $V_{mf}$  for the 2.0-3.35mm sand was most likely due to media interlocking, this has the effect of preventing significant expansion until the whole bed becomes fluidised.

The experimental and theoretical values of  $V_{mf}$  were in reasonably close agreement for the smaller media size ranges. However, the values for the larger media: 1.18-2.8mm sand, 2.0-3.35mm sand, and 2.5-5.0mm anthracite showed large differences. The reasons for such discrepancies have been discussed by other authors (Bayfield, 1993; Humby, 1994), they found that  $V_{mf}$  was highly dependant upon porosity. For instance, a 4% change in porosity was found to result in a 19% increase in  $V_{mf}$  for sand. Since the equation used for predicting  $V_{mf}$  doesn't take into account porosity, significant errors between the experimental and theoretical values can occur.

With this in mind, much care was taken over the backwash valve closure during the experiments, since the rate of backwash water valve closure will directly effect the bed porosity. The valve was always turned off rapidly because this was how the backwash valve at Lostock would behave. However, the discrepancies between observed and theoretical  $V_{mf}$  still occurred.

### 5.4.4 Collapse-pulsing backwash determination

The purpose of this investigation was to determine a number of combinations of air and sub-

fluidisation water rates that would cause collapse-pulsing (CP) in the media to be used at Lostock. This particular investigation was not meant to be a complete characterisation of CP. It was desirable to use the lower end of the  $\%V/V_{mf}$  because backwash water is more expensive than backwash air. Selection of CP rates for use at Lostock was therefore based on both this factor and accordance with Amirtharajah's design graph (shown in Fig 3.9).

# *CHAPTER 6*

## MEDIA PERFORMANCE ASSESSMENT

### 6.1 Introduction

For a valid assessment of the filtration performance of different filter media it is important to look at data points above and below the normal, in this case the normal was a 1m bed of 0.5 -1.0mm sand (standard NWW practice). From a similitude point it is important to use bed depths, media sizes and combinations that would be practical at full-scale. In the US current practice for dual media filters is for anthracite to make-up the majority of the media, with a small sand layer used for final polishing. U.K practice is for sand to form the bulk of the media with anthracite added as a retro-fit option usually to reduce headloss development. It was therefore decided to assess the performance of a range of sand sizes in single bed configurations, and a number of dual media combinations.

### 6.2 Experimental Procedures

The filter media that were used in the trial are listed below in Table 6.1. All the media selected were characterised previously, the details of which are in the previous chapter.

**Table 6.1. Media sizes and bed depths.**

Filter number	Filter media	Bed depth sand	Bed depth anthracite
1	0.5-1mm Sand	1.0m	-
2	2.0-3.35mm Sand	2.0m	-
3	1.18-2.8mm Sand	1.5m	-
4	0.35-0.6mm Sand	0.5m	-
5	2.0-3.35mm Sand, 2.5-5.0 mm Anthracite	1.5m	0.5m
6	2.0-3.35mm Sand, 2.5-5.0 mm Anthracite	0.5m	1.5m
7	0.35-0.6mm Garnet 2.5-5.0 mm Anthracite	0.3m	1.7m

The filtration velocity and filter run times were fixed at 6 m/h and 48 hours respectively for the duration of the programme. The run times were set at 48 hours to ensure that each filter washed whilst the pilot plant was staffed.

A fixed ferric (III) sulphate coagulant dose of 1.0 mg/l as  $\text{Fe}^{3+}$  was used at pH5.5.

The air and water velocities that produced collapse-pulsing in each of the filter media configurations were pre-determined (see previous chapter) and are shown in Table 6.2. Also shown in Table 6.2 are the backwash rinse velocities (designed to achieve 5-10% expansion). The final high velocity water rinse was of a fixed 5 minute duration (providing at least 2.7 bed volumes).

**Table 6.3. Collapse-pulsing and rinse flowrates for all media.**

Filter media /bed depth	V <sub>WATER</sub> (m/h)	V <sub>AIR</sub> (m/h)	V <sub>RINSE</sub> (m/h)
0.5-1.0mm Sand (1m)	10	50	30
2.0-3.35mm Sand (2m)	30	90	92
1.18-2.8mm Sand (1.5m)	20	66	68
0.35-0.6mm Sand (0.5m)	7.8	38	17
2.0-3.35mm Sand, (1.5m)	19	50	80
2.5-5.0 mm Anthracite (0.5m)			
2.0-3.35mm Sand, (0.5m)	17	54	59
2.5-5.0 mm Anthracite (1.5m)			
0.35-0.6mm Gamet (0.3m)	9	39	34
2.5-5.0 mm Anthracite (1.7m)			

The particle count in the filtrates from each filter was assessed using a Hiac Royco Versacount LV particle size analyser. The filtrate from individual filters was monitored for 15 minutes prior to and 60 minutes after backwash (the ripening period). Full details of the monitoring strategy to assess influent quality, filtrate quality and filter performance are shown in Chapter 4.

Headloss development was assessed using manometers, the positions of which are shown in Fig 4.3, readings were taken every 2 hours during the working day.



Backwash water was sampled every 15 seconds during the first 5 minutes of backwash, and every 30 seconds during the remaining 4 minutes of backwash. Turbidity analysis of samples was carried out on site using a Hach turbidimeter.

Detention times in all the filters were required for data interpretation, Fig. 6.1 illustrates how detention times were calculated. Plug flow with negligible axial dispersion was assumed. The theoretical detention times for all the filters are shown in Table 6.4.

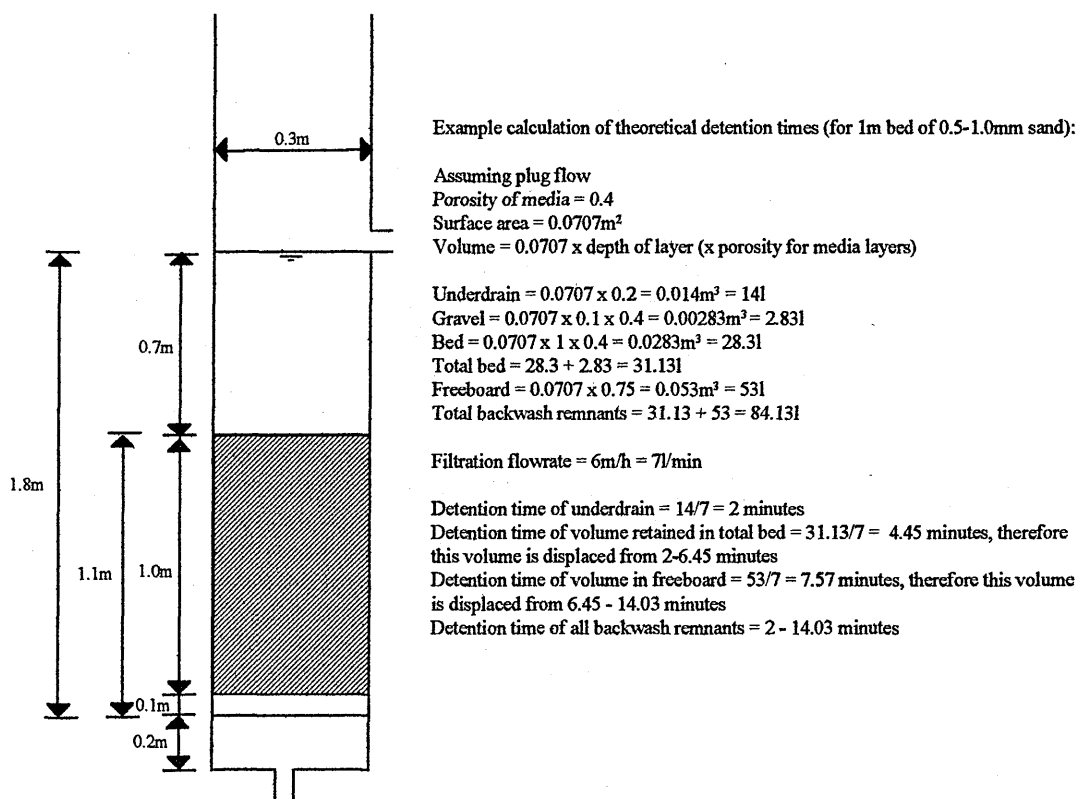


Figure 6.1. Illustration of how theoretical detention times were determined.

**Table 6.4 Theoretical detention times for all the filter media/configurations.**

Filter media	Detention times for the backwash remnants (in minutes)					
	Underdrain	Within lower bed	Within upper bed <sup>#</sup>	Total bed	Above bed	Total
0.5-1.0mm sand	0-2	2-6.45	-	-	6.45-14.03	2-14.03
2.0-3.35mm sand	0-2	2-10.66	-	-	10.66-18.23	2-18.23
1.18-2.8mm sand	0-2	2-8.70	-	-	8.7-16.27	2-16.27
0.35-0.6mm sand	0-2	2-4.62	-	-	4.62-12.19	2-12.19
2.0-3.35mm sand, 2.5-5.0mm anthracite	0-2	2-4.62	4.62-10.66	2-10.66	10.66-18.23	2-18.23
2.0-3.35mm sand, 2.5-5.0mm anthracite	0-2	2-8.70	8.70-10.66	2-10.66	10.66-18.23	2-18.23
0.35-0.6mm garnet 2.5-5.0mm anthracite	0-2	2-3.21	3.21-10.66	2-10.66	10.66-18.23	2-18.23

# - For dual media filters only.

### 6.3 Results

The influent conditions during the trial will be covered initially, the performance of the individual filters will then be assessed, the results for this trial will then be concluded with a summary analysis of all the filter media.

#### 6.3.1 Influent conditions

During this trial the influent quality was found to be very consistent in terms of both turbidity and particle counts. The mean influent turbidity was very low at 0.27 NTU and the mean total particle count was 1908 particles/ml for the period of work detailed below. The temperature dropped from a high of 15°C during August to a low of 11°C during October.

**Table 6.5 Summary of influent quality during trial.**

	pH	Turbidity (NTU)	Manganese (µg/l)	Iron (µg/l)	True colour (°Hazen)	Particle count (No./ml)
Mean	8.45	0.27	8.11	28.69	3.77	1908.4
Std. dev	0.25	0.15	3.76	9.64	0.67	153.9
Min	7.7	0.12	3	15	2	2183.0
Max	8.7	0.6	13	40	5	1644.2

#### 6.3.2 Filter performance

The data presented in this section was obtained over a period of two months. The mean filtrate particle counts have been plotted with the standard errors on the mean values at 95% confidence levels) displayed to illustrate the degree of reproducibility. The mean number of 2-5µm particles in the filtrate (NPF) as a function of the various components of the ripening period have been calculated (see Fig 2.11). The number of runs completed from which the mean values were obtained is expressed. Other performance indicators presented are: the rate of headloss development over the entire 48 hour run; and finally the amount of particulate matter (measured in terms of turbidity) removed from the filters during backwash

### 6.3.2.1. 1m bed of 0.5-1.0mm sand

The particle count data plotted in Fig. 6.2 is the mean values taken from 3 runs. Clearly, there was a high degree of reproducibility between runs. Some variability was, however, apparent in the magnitude of the initial peak. The peak appeared to be a function of the volume of backwash remnants contained within the filter bed; this component had a theoretical detention time of 6.45 minutes.

The variability in the next component, the volume of backwash water retained above the media, was much lower. It had a theoretical detention time of 14.03 minutes. The receding limb that follows was very reproducible and was a function of the influent, i.e. the removal efficiency of the filter improved until it had ripened. The time taken by this filter to ripen was very consistent at 41 minutes.

It is important to realise that the data in Fig 6.2, was for the 2-5 $\mu$ m particles, which were used as performance indicators. The larger particles measured by the particle counter (5-400 $\mu$ m) had an initial peak magnitude of approx. 300/ml, this was very much lower than the 2-5 $\mu$ m peak. It can be seen from Table 6.6 that the large particles reached a steady state value much more rapidly than the 2-5 $\mu$ m particles, 22 minutes compared to 41minutes.

The NPF data included in Table 6.6 was again for the indicator size range (2-5 $\mu$ m), it can be seen that large numbers of particles are in the filtrate during all three components of ripening. The backwash remnants displaced from within the filter bed contained  $4.28 \times 10^7$  2-5 $\mu$ m particles, the backwash remnants displaced from above the media contained  $5.97 \times 10^7$ , and  $4.69 \times 10^7$  were a function of the influent, i.e. classical ripening. An interesting observation is that the highest standard deviation was recorded for the backwash remnants within the bed; this corresponds with the variability shown in the particle count data plot (Fig 6.2).

The significance of the ripening period with respect to filter performance was well illustrated by the finding that 38.2% of all the 2-5 $\mu$ m particles that entered into supply during a 48 hour run for this media do so during the ripening period.

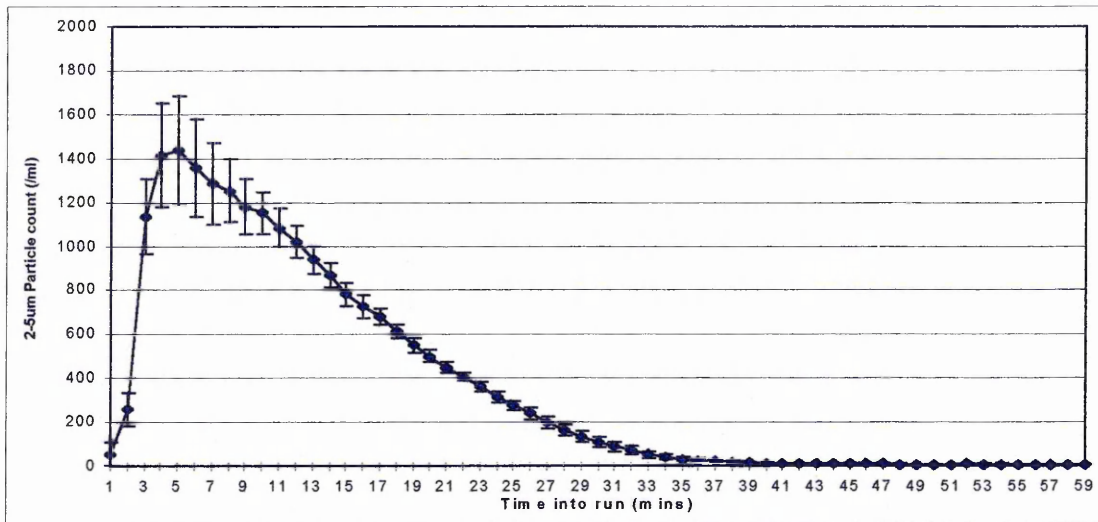


Figure 6.2 Mean filtrate 2-5µm particle count during ripening - 0.5-1.0mm sand.

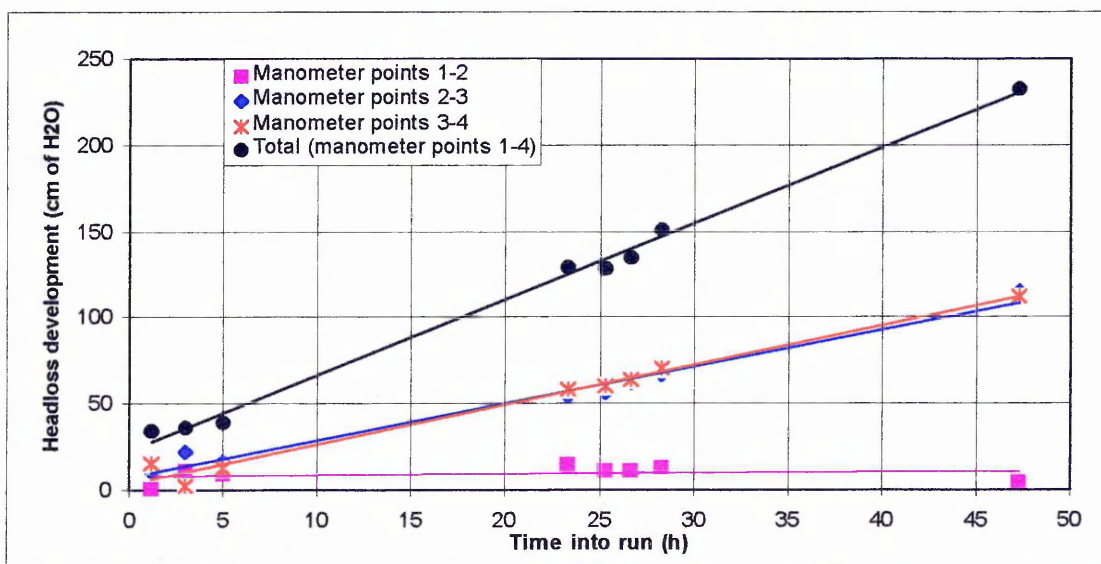


Figure 6.3. Headloss development during 48 hour run - 0.5-1.0mm sand.

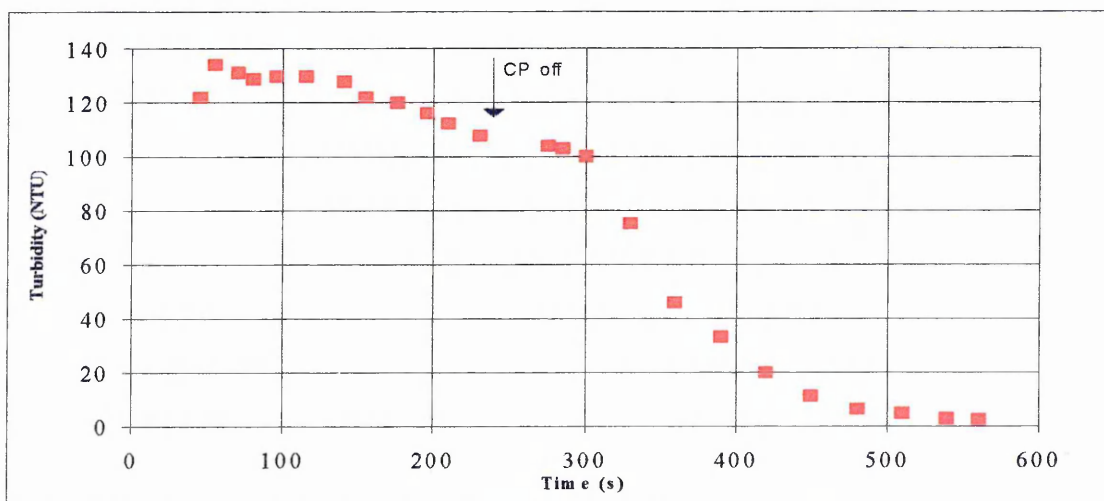


Figure 6.4. Backwash water turbidity during backwashing of 0.5-1.0mm sand filter.

Whilst the ripening period is the most significant part of a filter run, in terms of particulate passage into the filtrate, the performance over the whole run needs to be evaluated for design purposes. A number of parameters are therefore included in Table 6.6. Particulate breakthrough towards the end of a filter run can, as the term suggests, be a cause of large numbers of particles entering into supply. For this media/ bed configuration breakthrough was not reached by the end of the 48 hour run.

**Table 6.6. Summary performance data for 1m bed of 0.5-1.0mm sand.**

Filter performance parameter	Mean	Std deviation
Average runlength (time to reach 2m headloss)	38.1 hr	1.04
Breakthrough occurring at end of run ?	No	-
Time to reach steady state (2-5 $\mu$ m)	41.6 min	0.57
Steady state value (No. of 2-5 $\mu$ m/ml)	9.8	0.08
Time to reach steady state (5-400 $\mu$ m)	21.6 min	4.10
Steady state value (No. of 5-400 $\mu$ m/ml)	2.6	0.63
2-5 $\mu$ m NPF in backwash remnants within media	4.28 x10 <sup>7</sup>	1.15 x10 <sup>7</sup>
2-5 $\mu$ m NPF in backwash remnants above media	5.97 x10 <sup>7</sup>	9.12 x10 <sup>6</sup>
2-5 $\mu$ m NPF in all backwash remnants	1.04 x10 <sup>8</sup>	2.02 x10 <sup>6</sup>
2-5 $\mu$ m NPF as function of influent	4.69 x10 <sup>7</sup>	6.84 x10 <sup>6</sup>
Total 2-5 $\mu$ m NPF	1.51 x10 <sup>8</sup>	2.71 x10 <sup>6</sup>

A terminal headloss of 2m (exceeded in this case since the run continued for the full 48 hours) was reached after 38 hours. The rate of headloss development for the different sections of the bed are shown in Fig. 6.3. The headloss development can be seen to be predominantly in the top section of the bed, manometer points 3 to 4 cover the top 15cm of this media and 2 to 3 cover the next 50cm of bed, with little penetration into the lower half of the bed, this implies particulate removal occurred in the top layers of the filter. Indeed, visual inspection showed particulate matter in the top layers with a visible gradation (i.e. less visible particulate matter) down into the bed.

The particulate matter removal during backwash (in terms of turbidity) is shown in Fig.6.4. The arrow marks the point where the CP wash stops and the water rinse begins. For the first 2 minutes of CP wash a constant amount of particulate matter was been removed, for the next 2 minutes of CP wash a reduction can be seen, suggesting the media was becoming cleaner. The fixed rinse period of 5 minutes at 10 % expansion is shown to be effective at removing any particulate matter that has been dislodged from the filter media during the CP wash.

### 6.3.2.2 2m beds of 2.0-3.35mm sand.

The particle count data plotted in Fig. 6.5 are the mean values taken from 4 runs. The particle counts for this filter configuration exhibited a high degree of reproducibility over the 4 runs. There was, however, some variability in both the magnitude and timing of the initial peak. The initial peak again appeared to be a function of the volume of backwash remnants contained within the filter bed; the variability in the next two component was much lower. This filters ripening time was consistent at 52 minutes.

The removal efficiency of the filter improved more rapidly for the larger particles measured, 5-400 $\mu$ m, which reached steady state after 42 minutes. The initial peak for these larger particles was approximately 690/ ml, the particle count was almost down to steady state after the backwash remnants contained in the media had been displaced.

The 2-5 $\mu$ m NPF data included in Table 6.7 shows large numbers of particles in the filtrate as a result of all three backwash components. The most significant component, in terms of particulate passage into the filtrate, was the volume of backwash water retained in the bed. The figure was  $9.72 \times 10^7$ , almost half of the total NPF. This component also had the highest degree of variability, as shown by a standard deviation of  $1.63 \times 10^7$ . The component of ripening contributing the least was the volume of backwash water above the bed -  $5.14 \times 10^7$ .

The ripening period was again found to be the most significant stage of the filter run, in terms of particulate passage, since particulate breakthrough was not observed at the end of the 48 hour runs. The ripening period contributed on average 34.6% of the 2-5 $\mu$ m particles that entered into supply during an entire 48 hour run.

It can be seen from Table 6.7 that this filter media did not reach a terminal headloss of 2m in the course of a 48 hour run. A potential filter runlength - time to reach 2m headloss - was estimated from the headloss data available. The figure was a runlength of 200 hours. This is of course only taking into account headloss development, it is unlikely that such a runlength could be achieved without particulate breakthrough occurring first

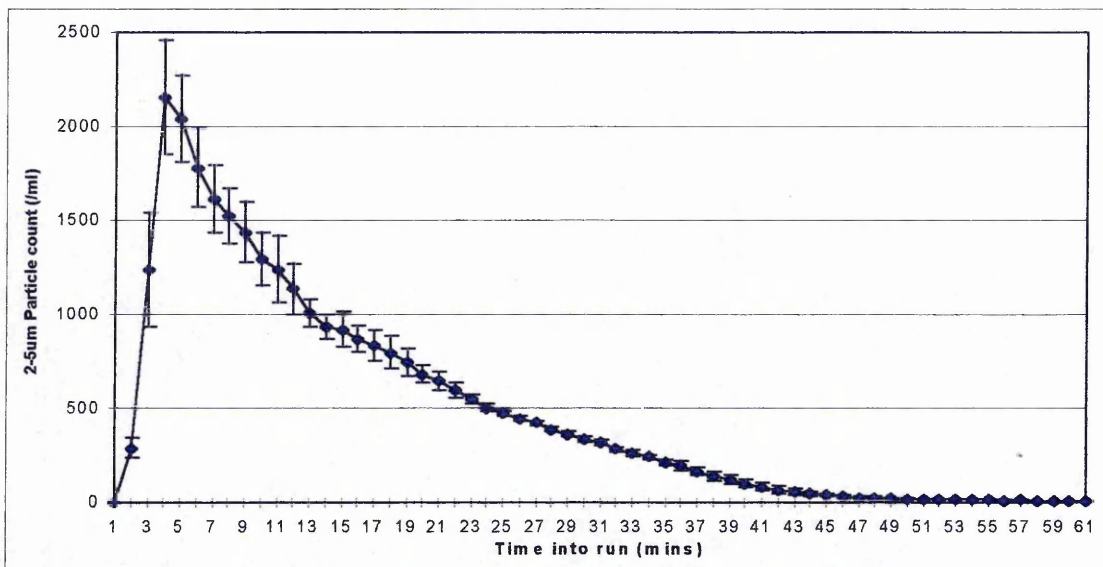


Figure 6.5 Mean filtrate 2-5µm particle count during ripening - 2.0-3.35mm sand.

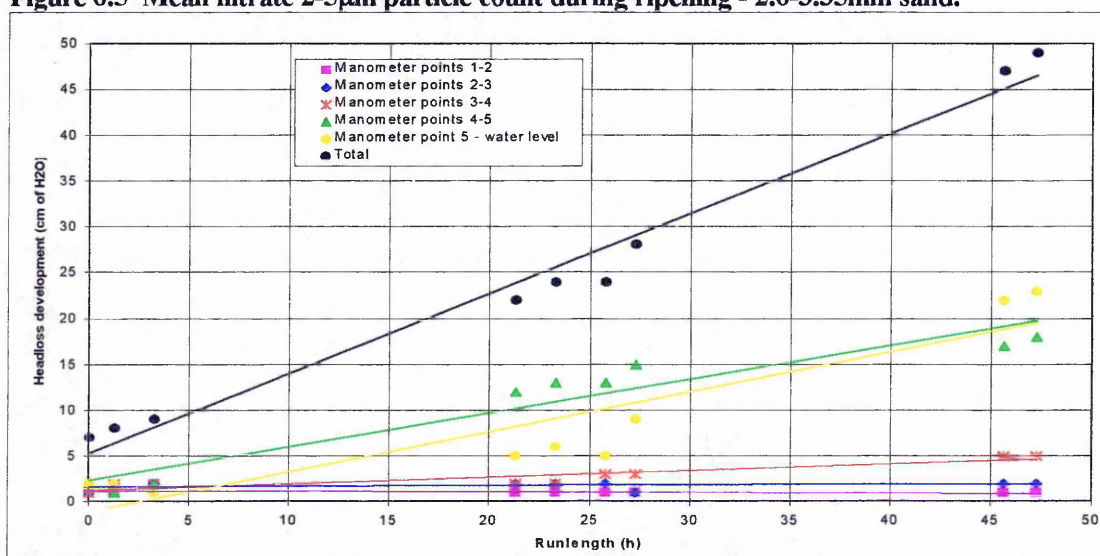


Figure 6.6. Headloss development during 48 hour run - 2.0-3.35mm sand.

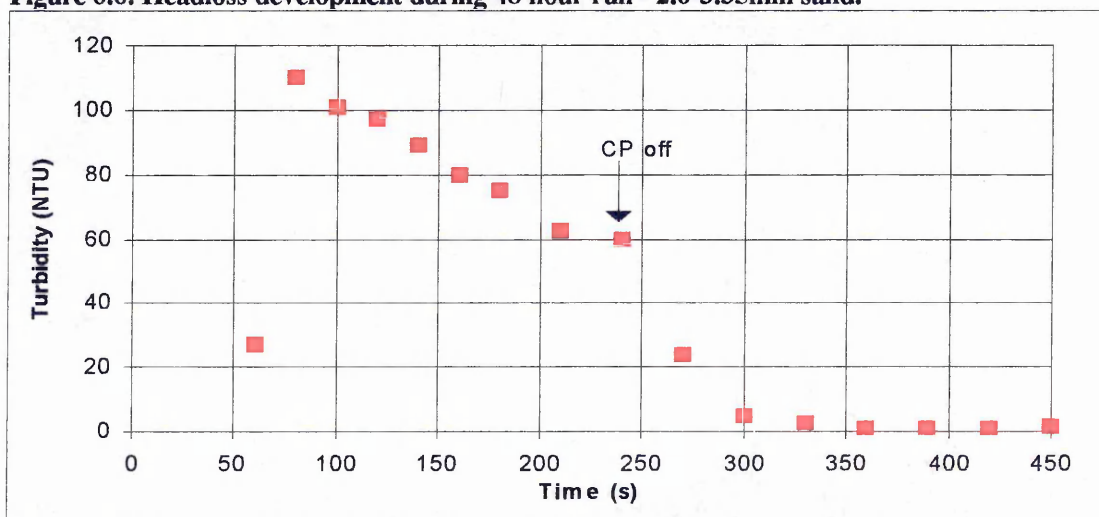


Figure 6.7. Backwash water turbidity during backwashing of 2.0-3.35mm sand filter.



The reason for the slow development of headloss in this filter was the coarseness of the sand grains. It can be seen from Fig. 6.6 that headloss development was occurring deep into the bed. The top 15cm of bed (5-wl) contributed the same, 20cm of headloss, as the next 50cm of bed (4-5), the next 50cm (3-4) also contributed 5cm to the total headloss at the end of the run. This implied removal of particulate matter was occurring deep into the bed. This was confirmed by visual observation of the filter bed, dirty orange coloured deposits could be seen in the bed down to a depth of approximately 1m .

**Table 6.7. Summary performance data for 2m bed of 2.0-3.35mm sand.**

Filter performance parameter	Mean	Std deviation
Average runlength (time to reach 2m headloss)	200 hr est.	-
Breakthrough occurring at end of run ?	No	-
Time to reach steady state (2-5 $\mu$ m)	52 min	1.0
Steady state value (No. of 2-5 $\mu$ m/ml)	15.38	1.24
Time to reach steady state (5-400 $\mu$ m)	42.3 min	2.31
Steady state value (No. of 5-400 $\mu$ m/ml)	4.53	0.34
2-5 $\mu$ m NPF in backwash remnants within media	$9.72 \times 10^7$	$1.63 \times 10^7$
2-5 $\mu$ m NPF in backwash remnants above media	$5.14 \times 10^7$	$9.90 \times 10^6$
2-5 $\mu$ m NPF in all backwash remnants	$1.48 \times 10^8$	$1.76 \times 10^7$
2-5 $\mu$ m NPF as function of influent	$5.74 \times 10^7$	$7.74 \times 10^6$
Total 2-5 $\mu$ m NPF	$2.08 \times 10^8$	$2.23 \times 10^7$

The particulate matter removed during a typical backwash, expressed in terms of turbidity, is shown in Fig 6.7. A high level of turbidity was recorded in the wash water initially, however, this was reduced quite rapidly, it appeared to remain relatively constant at 40 NTU from 2 to 4 minutes of the CP wash. Once the CP wash was completed and the higher rate rinse was initiated the remaining turbidity was fully rinsed out after 1.5 minutes.

### 6.3.2.3 1.5m bed of 1.18-2.8mm sand.

The particle count data plotted in Fig. 6.8 is the mean values taken from 3 runs. The particle counts for this filter configuration also exhibited a high degree of reproducibility between runs. Again there was some variability in both the magnitude and timing of the initial peak. The initial peak was very high, up to 4800 2-5 $\mu$ m particles/ml, but it was still a function of the volume of backwash remnants contained

within the filter bed. The variability in the subsequent components was much lower. This filter's ripening time was consistent at around 45 minutes.

The numbers of larger particles (5-400 $\mu$ m) reaching the filtrate were also high, the initial peak was approximately 1200/ml. All the backwash remnants entering the filtrate contained these larger particles, steady state for these particles was not reached until 37 minutes had passed. Interestingly, the steady state value for these particles was higher than that for the 2-5 $\mu$ m particles - 21.3 compared to 14.9.

The 2-5 $\mu$ m NPF data included in Table 6.8 again shows large numbers of particles in the filtrate as a function of all three backwash components. The most significant was the volume of backwash water retained in the bed. The figure was  $1.72 \times 10^8$ , greater than half of the total NPF. This component also had the highest degree of variability (std. dev =  $2.85 \times 10^7$ ). The component of ripening contributing the least was the one that was a function of the influent, only  $5.68 \times 10^7$ .

The ripening period was again found to be the most significant stage of the filter run, in terms of particulate passage, contributing on average 31.8% of the 2-5 $\mu$ m particles that entered into supply during an entire 48 hour run.

The time to reach 2m terminal headloss had to be estimated for this media. The estimated achievable runlength was 150 hours, as in the previous example this does not take into account particulate breakthrough which would probably occur long before 150 hours.

The headloss development as shown in Fig 6.9 was well spread throughout the top half of the bed. Somewhat unexpected was the fact that the top portion of the bed did not contribute the most to the headloss development. The upper 15cm of bed (4-5) caused about 20cm of headloss by the end of the run, whereas the next 50cm of bed caused about 35cm. Some degree of headloss development was also evident across the next 50cm of bed. This all suggests removal was occurring deep down into this filter bed. Visual observations again confirmed these findings, orange/brown deposits were evident at a depth of up to 1m.

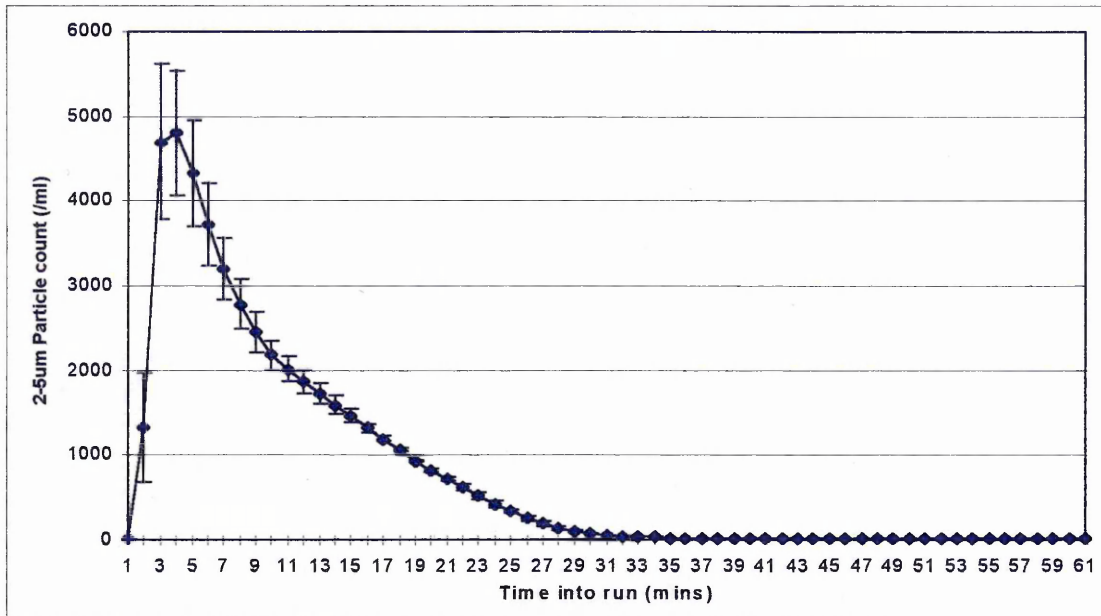


Figure 6.8 Mean filtrate 2-5µm particle count during ripening - 1.18-2.8mm sand.

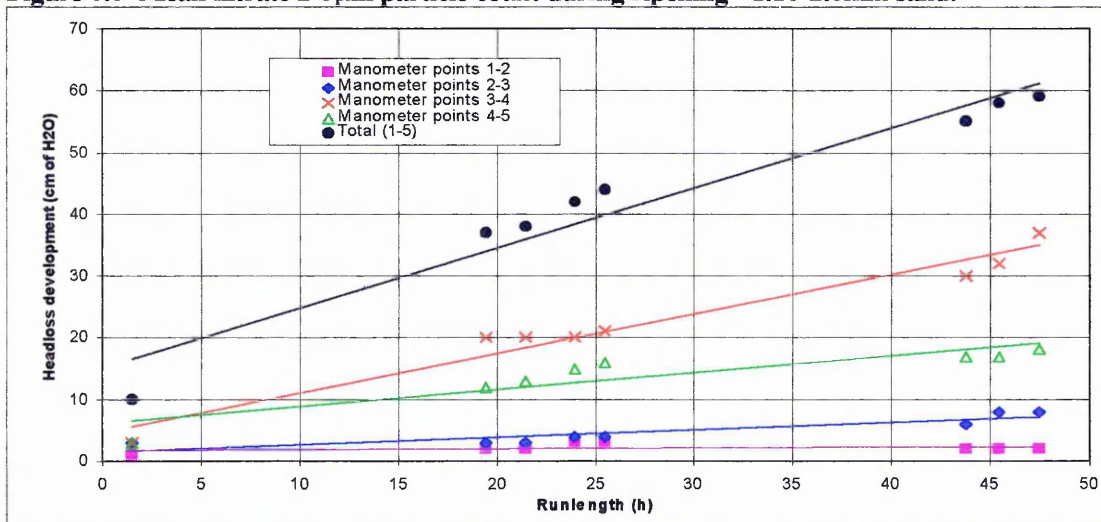


Figure 6.9. Headloss development during 48 hour run - 1.18-2.8mm sand filter.

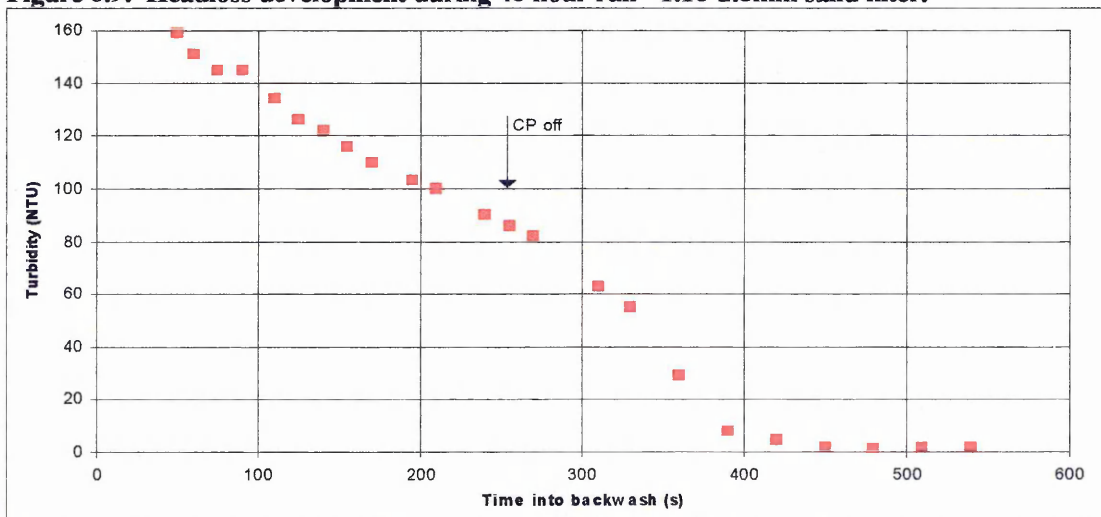


Figure 6.10. Backwash water turbidity during backwashing of 1.18-2.8mm sand filter.

**Table 6.8. Summary performance data for 1.5m bed of 1.18-2.8mm sand.**

Filter performance parameter	Mean	Std deviation
Average runlength (time to reach 2m headloss)	150 hr est.	-
Breakthrough occurring at end of run ?	No	-
Time to reach steady state (2-5 $\mu$ m)	45.5 min	2.12
Steady state value (No. of 2-5 $\mu$ m/ml)	14.8	2.74
Time to reach steady state (5-400 $\mu$ m)	37.5 min	2.13
Steady state value (No. of 5-400 $\mu$ m/ml)	21.28	4.02
2-5 $\mu$ m NPF in backwash remnants within media	$1.72 \times 10^8$	$2.85 \times 10^7$
2-5 $\mu$ m NPF in backwash remnants above media	$1.04 \times 10^8$	$1.73 \times 10^7$
2-5 $\mu$ m NPF in all backwash remnants	$2.76 \times 10^8$	$4.43 \times 10^7$
2-5 $\mu$ m NPF as function of influent	$5.68 \times 10^7$	$8.94 \times 10^6$
Total 2-5 $\mu$ m NPF	$3.33 \times 10^8$	$5.32 \times 10^7$

The particulate matter removed during a typical backwash is shown in Fig 6.10. A high level of turbidity was recorded initially, however, this was reduced at an apparently constant rate over the course of the 4 minute CP wash. Once the CP wash was completed and the higher rate rinse was initiated the remaining turbidity was fully rinsed out after about 3 minutes.

#### 6.3.2.4 0.5m bed of 0.35-0.6mm sand.

It can be seen from Fig. 6.11 that a high degree of variability was associated with the mean particle count (from 3 runs) for this filter. There was variability in both the magnitude and timing of the initial peak. The initial peak was quite low, only 1600 2-5 $\mu$ m particles/ml. The volume of backwash remnants contained within the filter bed had a theoretical retention time of 2.9 minutes, since the peak occurred after this, the volume of backwash water retained above the media must have been contributing to the numbers of particles in the filtrate. The receding limb that followed was also very variable. The ripening time was also inconsistent but had a mean duration of 40 minutes.

The numbers of larger particles (5-400 $\mu$ m) reaching the filtrate were much lower, the initial peak was approximately 500/ml. Both the backwash remnant components contained these larger particles that

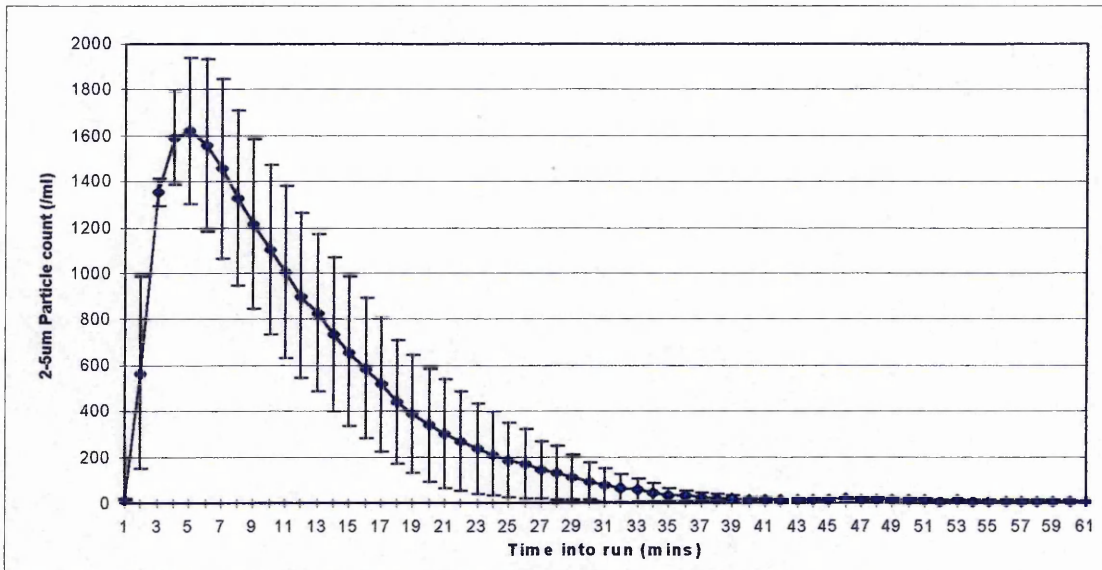


Figure 6.11 Mean filtrate 2-5 $\mu$ m particle count during ripening - 0.35-0.6mm sand.

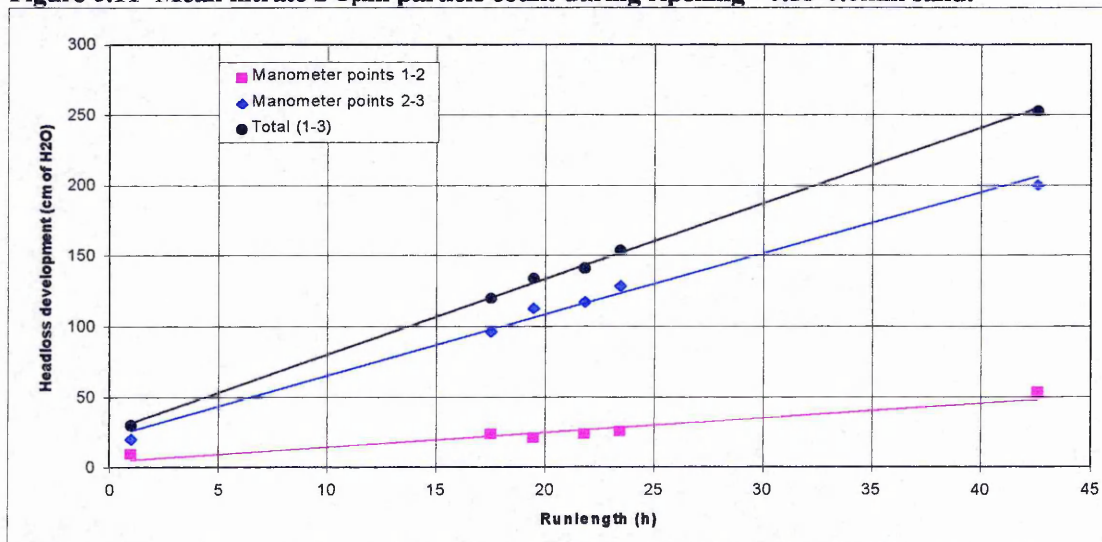


Figure 6.12. Headloss development during 48 hour run - 0.35-0.6mm sand filter.

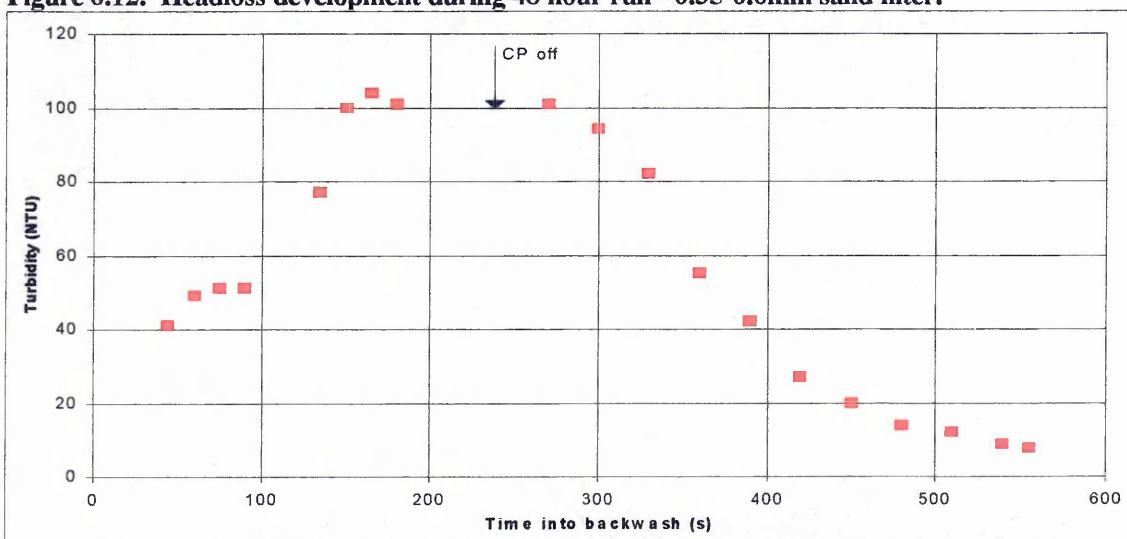


Figure 6.13. Backwash water turbidity during backwashing of 0.35-0.6mm sand filter.

reached the filtrate, the removal efficiency did not reach steady state for these particles until 31 minutes had passed.

The 2-5 $\mu\text{m}$  NPF data contained in Table 6.9 shows all three backwash components contributing. The most significant components, were the volume of backwash water retained above the bed, and the interface with the influent. The figures were  $6.72 \times 10^7$  and  $5.86 \times 10^7$  respectively. The component that was a function of the influent had a very high degree of variability, as shown by a standard deviation of  $4.93 \times 10^7$ . This had an effect on the reproducibility of the total NPF which was very poor.

The ripening period was again found to be the most significant stage of the filter run, in terms of particulate passage, contributing on average 54.9% of the 2-5 $\mu\text{m}$  particles that entered into supply during an entire 48 hour run.

**Table 6.9. Summary performance data for 0.5m bed of 0.35-0.6mm sand.**

Filter performance parameter	Mean	Std deviation
Average runlength (time to reach 2m headloss)	32.5 hr	1.84
Breakthrough occurring at end of run ?	No	-
Time to reach steady state (2-5 $\mu\text{m}$ )	40.0 min	4.22
Steady state value (No. of 2-5 $\mu\text{m}/\text{ml}$ )	7.08	5.16
Time to reach steady state (5-400 $\mu\text{m}$ )	31.5 min	7.78
Steady state value (No. of 5-400 $\mu\text{m}/\text{ml}$ )	6.02	4.76
2-5 $\mu\text{m}$ NPF in backwash remnants within media	$1.70 \times 10^7$	$1.67 \times 10^6$
2-5 $\mu\text{m}$ NPF in backwash remnants above media	$6.72 \times 10^7$	$2.46 \times 10^7$
2-5 $\mu\text{m}$ NPF in all backwash remnants	$8.64 \times 10^7$	$2.08 \times 10^7$
2-5 $\mu\text{m}$ NPF as function of influent	$5.87 \times 10^7$	$4.93 \times 10^7$
Total 2-5 $\mu\text{m}$ NPF	$1.45 \times 10^8$	$7.02 \times 10^7$

The time to reach 2m terminal headloss was 32.5 hours, however, the filter run continued for the full 48hours with overflow occurring. The headloss development as shown in Fig. 6.13 was concentrated in the top layer of 15cm. This layer had caused a 2m loss of head by the end of the run. Visual observations confirmed this, removal appeared to be in the very top layer, with a heavy build-up of orange/brown deposits on top of the media. This resulted in the formation of mudballs which could not be removed by backwashing.

The backwash water turbidity, as shown in Fig 6.14 suggested that deposits were been removed to a greater degree as the CP wash progressed. This implied that a lot of particulate matter was removed from this small bed. The rinse was sufficient to remove most of the deposits that had been dislodged out of the filter.

#### *6.3.2.5 1.5m 2.0-3.35mm sand and 0.5m 2.5-5.0mm anthracite*

The mean particle counts (from 4 runs) for this filter configuration showed that whilst the shape was consistent i.e. double-peaked, the magnitude of the two peaks was very variable. The initial peak appeared to be a function of the volume of backwash remnants contained within the 1.5m of sand. The start of the second peak corresponded to the detention time at the media interface. By the time the backwash remnants above the dual media bed had been displaced, 18.5 minutes, the particle count was well into the characteristic receding limb. The mean ripening time was 54 minutes. The filter ripened at the same rate for the larger particles measured (5-400 $\mu$ m), which reached steady state after 53.6 minutes. The initial peak for these larger particles was approximately 500/ml.

The 2-5 $\mu$ m NPF data is contained in Table 6.10. The most significant component, in terms of particulate passage into the filtrate, was the volume of backwash water retained in the bed. The NPF was  $1.27 \times 10^6$ . This component also had the highest degree of variability, as shown by a standard deviation of  $6.46 \times 10^5$ . The component of ripening contributing the least was the volume of backwash water above the bed -  $1.00 \times 10^6$ .

The ripening period was again found to be the most significant stage of the filter run, contributed on average 24.3% of the 2-5 $\mu$ m particles that entered into supply during an entire 48 hour run.

It can be seen from Table 6.10 that this filter configuration did not reach a terminal headloss of 2m in the course of a 48 hour run. A potential filter runlength of 220 hours was estimated from the headloss data available.

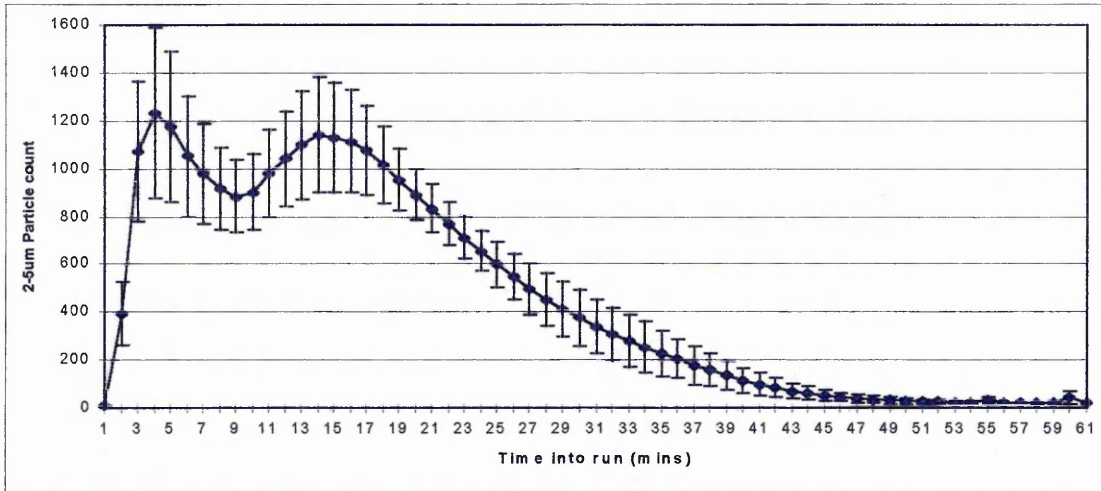


Figure 6.14 Mean filtrate 2-5µm particle count during ripening - 1.5m 2.0-3.35mm sand and 0.5m 2.5-5.0mm anthracite.

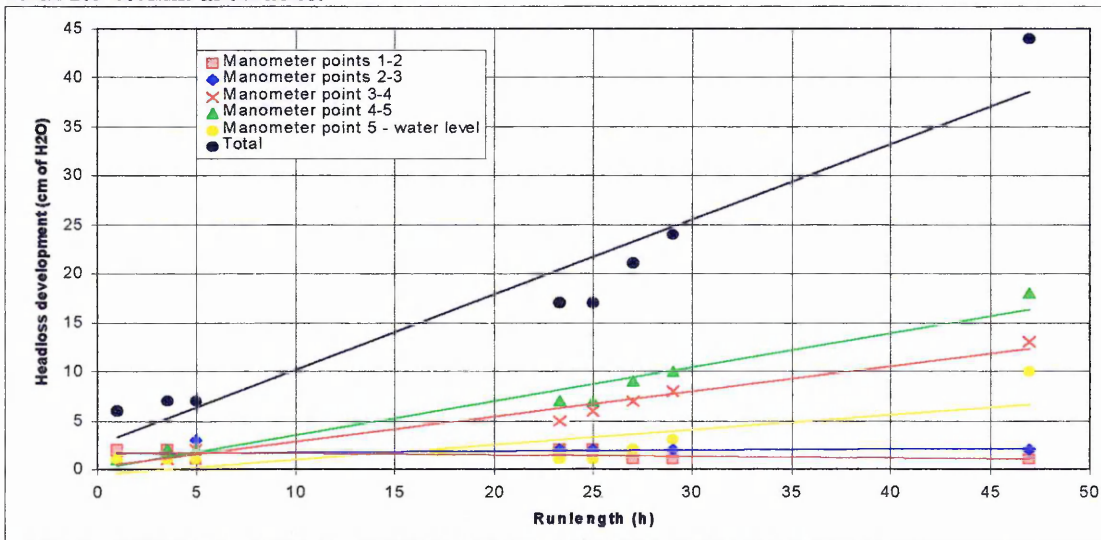


Figure 6.15. Headloss development during 48 hour run -1.5m 2.0-3.35mm sand and 0.5m 2.5-5.0mm anthracite filter.

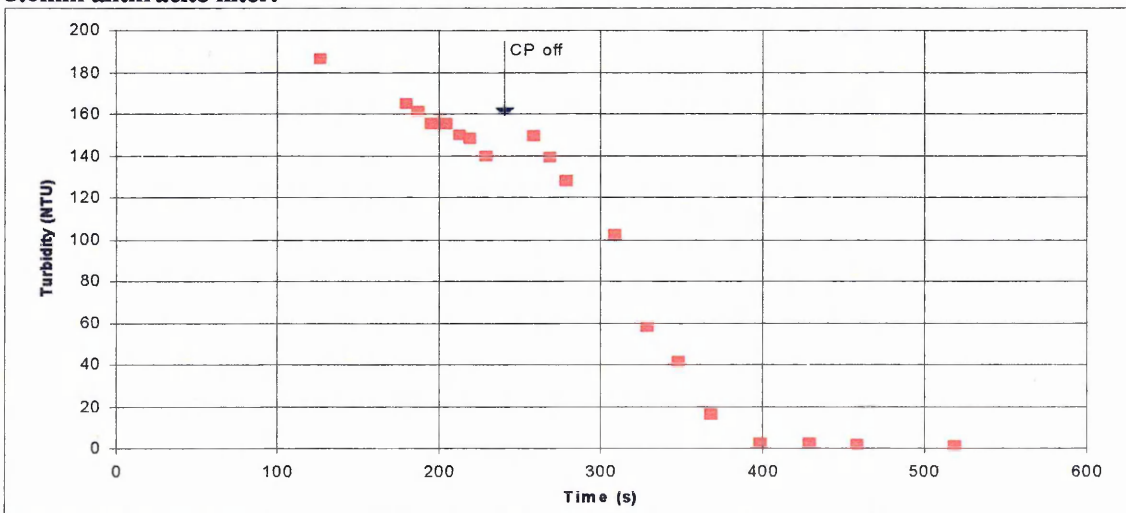


Figure 6.16. Backwash water turbidity during backwashing of 1.5m 2.0-3.35mm sand and 0.5m 2.5-5.0mm anthracite filter.



**Table 6.10. Summary performance data for 1.5m 2.0-3.35mm sand and 0.5m 2.5-5.0mm anthracite.**

Filter performance parameter	Mean	Std deviation
Average runlength (time to reach 2m headloss)	220 hr est.	-
Breakthrough occurring at end of run ?	No	-
Time to reach steady state (2-5 $\mu$ m)	54.0 min	3.60
Steady state value (No. of 2-5 $\mu$ m/ml)	18.9	6.11
Time to reach steady state (5-400 $\mu$ m)	53.6 min	2.08
Steady state value (No. of 5-400 $\mu$ m/ml)	11.9	1.52
2-5 $\mu$ m NPF in backwash remnants within media	$7.62 \times 10^7$	$3.88 \times 10^7$
2-5 $\mu$ m NPF in backwash remnants above media	$6.00 \times 10^7$	$1.89 \times 10^7$
2-5 $\mu$ m NPF in all backwash remnants	$1.24 \times 10^8$	$3.23 \times 10^7$
2-5 $\mu$ m NPF as function of influent	$7.14 \times 10^7$	$2.42 \times 10^7$
Total 2-5 $\mu$ m NPF	$1.96 \times 10^8$	$1.13 \times 10^7$

Some interesting observations can be made when looking at the headloss development for this filter, shown in Fig 6.15. The top 15cm of the anthracite layer contributed very little to the overall loss of head, the next 50cm, which included the interface between the two media contributed significantly, as did the next 50cm of sand bed. There was, therefore, very deep penetration occurring in this filter. Visual observations confirmed that orange/brown deposits were present on the sand media down to a depth of 1m. However, no deposits could be viewed on the anthracite due to its black colour.

The deposits removed from the filter media during a typical backwash is shown in Fig 6.16. High levels of turbidity were recorded in the wash water, however, these levels were reduced before the CP wash was completed. When the higher rate rinse was initiated the remaining turbidity was fully rinsed out after 2.5 minutes.

#### 6.3.2.6 0.5m of 2.0-3.35mm sand and 1.5m of 2.5-5.0mm anthracite.

The particle count data plotted in Fig 6.17 is the mean values taken from 3 runs. The particle counts for this filter configuration show that whilst the shape was consistent i.e. double-peaked, the magnitude of the two peaks was very variable, especially the initial one. The initial peak appeared to be a function of the volume of backwash remnants contained within the 0.5m of sand.

The peak rapidly tailed off, whilst the volume that was a function of the backwash remnants contained in the 1.5m of anthracite, was displaced. By the time the backwash remnants above the dual media bed had been displaced, 18.5 minutes elapsed, a second peak was apparent. The ripening time was very consistent at 54 minutes.

The removal improved at about the same rate for the larger particles measured, which reached steady state after 50.4 minutes. The initial peak for these larger particles was high at 1750/ml.

The 2-5 $\mu$ m NPF data, contained in Table 6.11, showed that the most significant component, in terms of particulate passage into the filtrate, was the volume of backwash water retained in the bed. The figure was a very high  $2.45 \times 10^8$ . This component also had the highest degree of variability, as shown by a standard deviation of  $9.18 \times 10^7$ . The component of ripening contributing the least was the volume of backwash water above the bed -  $9.06 \times 10^7$ .

The ripening period was again found to be the most significant stage of the filter run, contributing on average 38.2% of the 2-5 $\mu$ m particles that enter into supply during an entire 48 hour run.

It can be seen from data in Table 6.11 that this filter did not reach a terminal headloss of 2m in the course of a 48 hour run. A potential filter runlength was estimated at 300 hours.

The headloss development for this filter is shown in Fig 6.18. It can be seen that the rate of headloss development is very slow for this media. The top 15cm of the anthracite layer contributed very little to the overall loss of head, the next 50cm of anthracite contributed significantly. Visual observations did not show-up much orange/brown deposit in the 0.5m layer of sand and deposits could not be viewed on the anthracite due to its black colour.

The particulate matter removed during a typical backwash, expressed in terms of turbidity, is shown in Fig 6.19. The turbidity of the wash water increased throughout the duration of the CP wash. When the higher rate rinse was initiated the remaining turbidity required the full 5 minutes to be rinsed out of the filter.

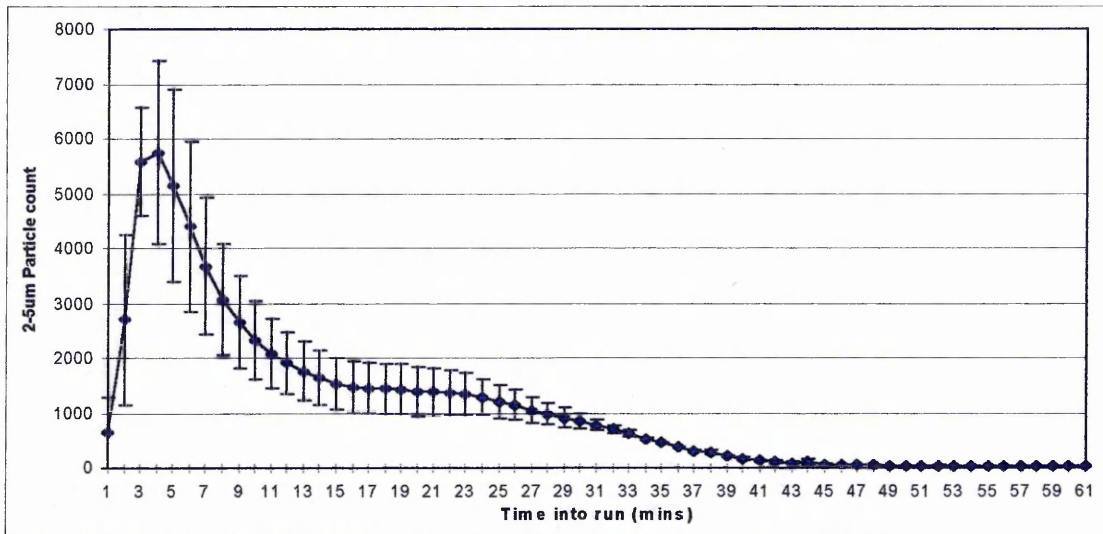


Figure 6.17 Mean filtrate 2-5µm particle count during ripening - 0.5m of 2.0-3.35mm sand and 1.5m of 2.5-5.0mm.

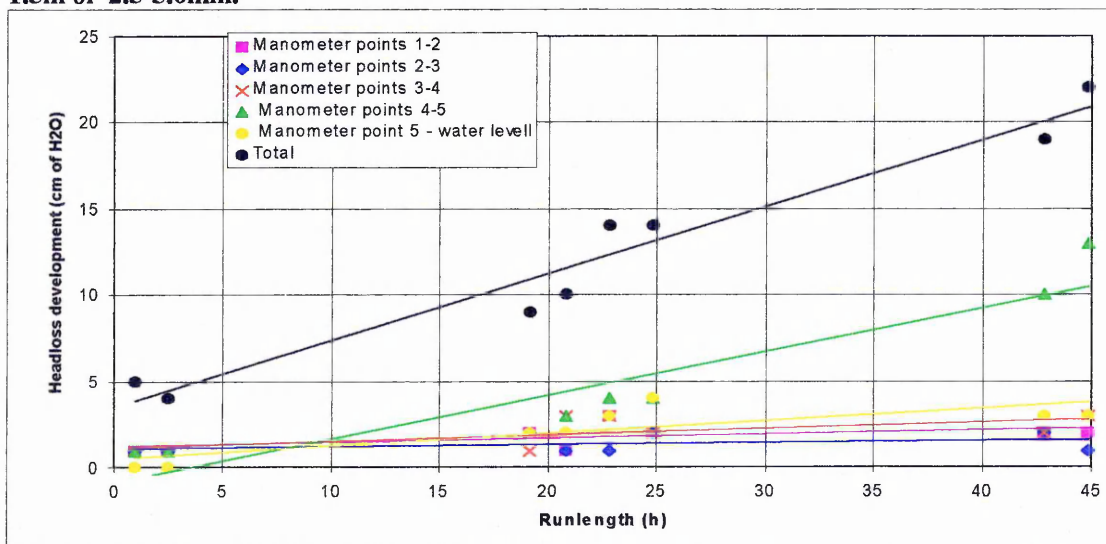


Figure 6.18. Headloss development during 48 hour run - 0.5m of 2.0-3.35mm sand and 1.5m of 2.5-5.0mm filter.

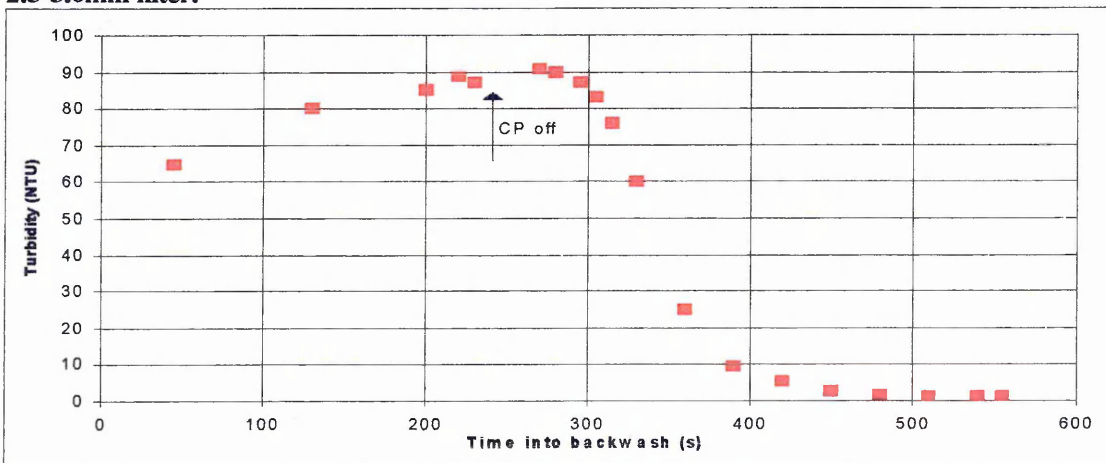


Figure 6.19. Backwash water turbidity during backwashing of 0.5m of 2.0-3.35mm sand and 1.5m of 2.5-5.0mm filter.

Table 6.11. Summary performance data for 0.5m 2.0-3.35mm sand and 1.5m 2.5-5.0mm anthracite.

Filter performance parameter	Mean	Std deviation
Average runlength (time to reach 2m headloss)	300 hr est.	-
Breakthrough occurring at end of run ?	No	-
Time to reach steady state (2-5 $\mu$ m)	54.2 min	0.71
Steady state value (No. of 2-5 $\mu$ m/ml)	23.98	2.63
Time to reach steady state (5-400 $\mu$ m)	50.4 min	0.98
Steady state value (No. of 5-400 $\mu$ m/ml)	15.4	1.58
2-5 $\mu$ m NPF in backwash remnants within media	$2.45 \times 10^8$	$9.18 \times 10^7$
2-5 $\mu$ m NPF in backwash remnants above media	$9.06 \times 10^8$	$3.87 \times 10^7$
2-5 $\mu$ m NPF in all backwash remnants	$3.47 \times 10^8$	$1.21 \times 10^8$
2-5 $\mu$ m NPF as function of influent	$1.33 \times 10^8$	$3.55 \times 10^7$
Total 2-5 $\mu$ m NPF	$4.81 \times 10^8$	$1.55 \times 10^8$

6.3.2.7 0.3m of 0.6-1.4mm garnet and 1.7m of 2.5-5.0mm anthracite.

The mean particle count data (from 3 runs) showed some degree of reproducibility, certainly in the initial peak and subsequent receding limb. The second peak and its associated receding limb displayed a greater degree of variability. The initial peak was a function of both the volume of backwash remnants contained within the 0.3m of garnet and contained in the 1.7m of anthracite. By the time this volume had been displaced the particle count had been greatly reduced. The backwash remnants above the dual media bed produced a slight peak in particle count as it was displaced. This filter's ripening time was very consistent at 50 minutes.

The 2-5 $\mu$ m NPF data in Table 6.12 shows the highest NPF was due to the volume of backwash water retained in the bed -  $1.97 \times 10^8$ . This component also had the highest degree of variability, as shown by a standard deviation of  $5.12 \times 10^7$ . The component of ripening contributing the least was the volume of backwash water above the bed -  $6.48 \times 10^7$ .

The ripening period was again found to be the most significant stage of the filter run contributing on average 28.6% of the 2-5 $\mu$ m particles that enter into supply during an entire 48 hour run.

The runlength for this filter was estimated as 400 hours since the rate of headloss development for this filter (Fig 6.21) was found to be very slow. The top 15cm of the anthracite had been lost over the backwash weir during previous washes, so there was no 5-wl value (top 15cm). The top 50cm of

anthracite contributed significantly to the overall loss of head. Although the values were very low the region that contained the interface between the media (1-2) had a higher headloss development than the 50cm of anthracite immediately above it (2-3). Visual observations did not show-up much due to the colour of the anthracite.

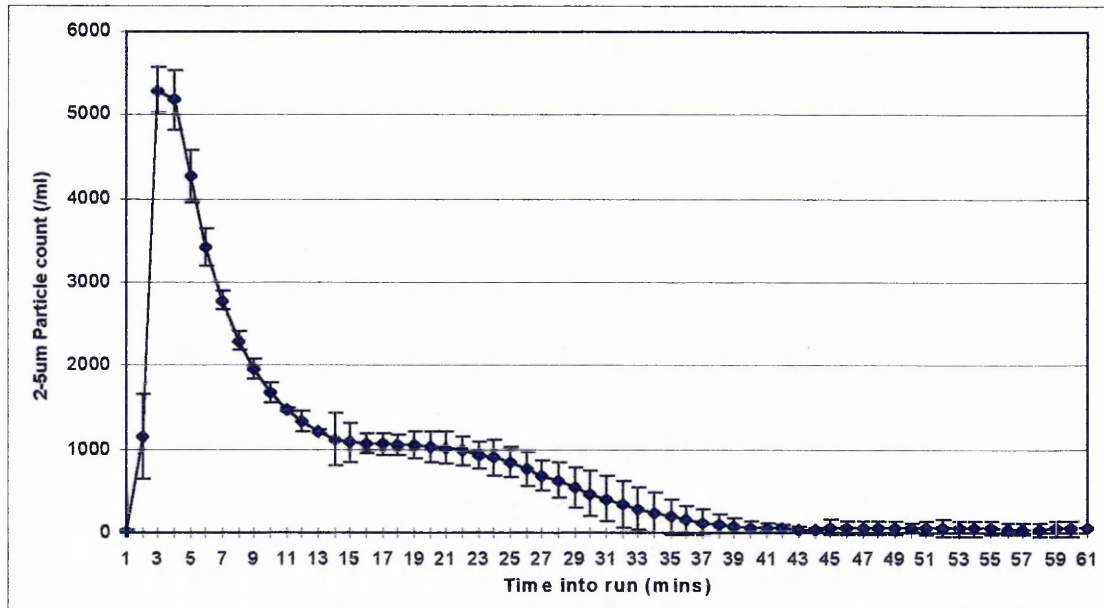


Figure 6.20 Mean filtrate 2-5µm particle count during ripening -0.3m of 0.6-1.4mm garnet and 1.7m of 2.5-5.0mm anthracite.

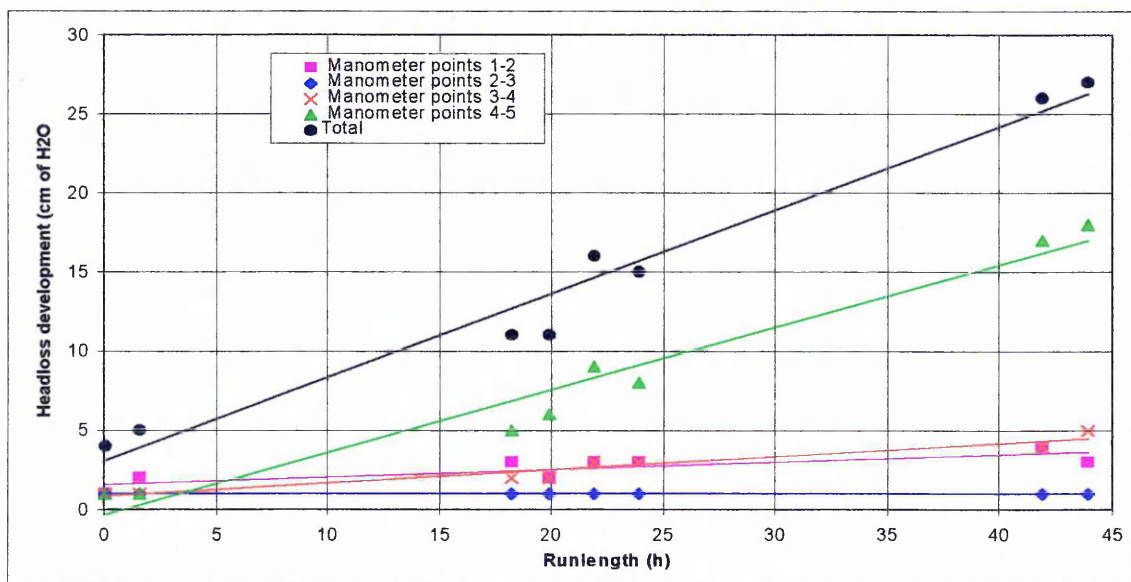
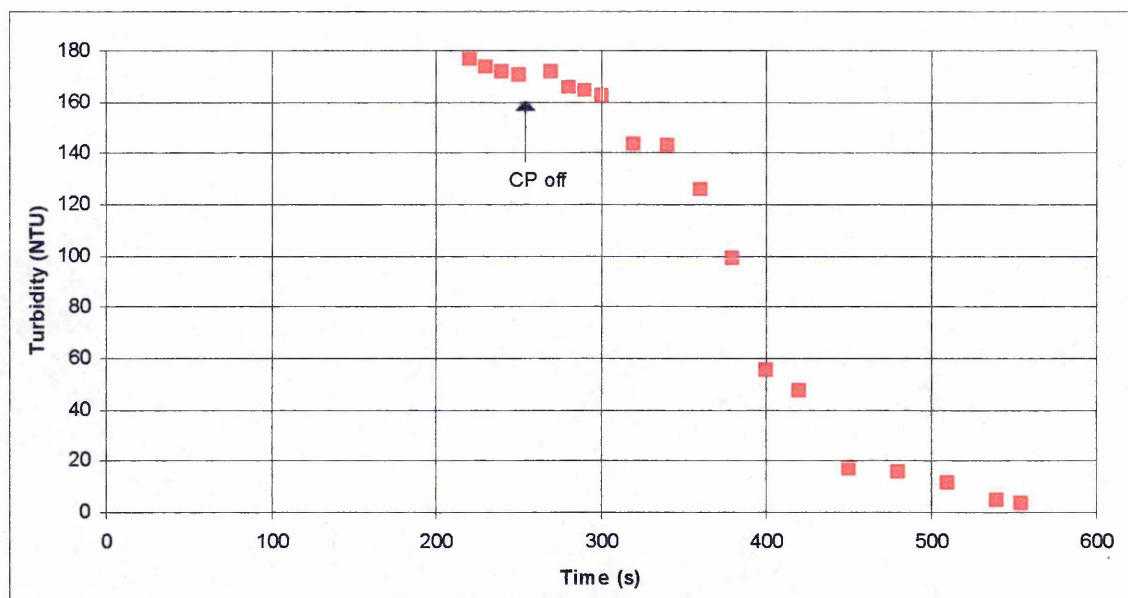


Figure 6.21. Headloss development during 48 hour run - 0.3m of 0.6-1.4mm garnet and 1.7m of 2.5-5.0mm anthracite filter.



**Figure 6.22. Backwash water turbidity during backwashing of 0.3m of 0.6-1.4mm garnet and 1.7m of 2.5-5.0mm anthracite filter.**

The turbidity of the wash water, shown in Fig. 6.22 peaked after about 1.5 minutes, thereafter it decreased prior to the rinse phase. When the higher rate rinse was initiated the remaining turbidity required the full 5 minutes to be rinsed out of the filter.

**Table 6.12. Summary performance data for 0.3m of 0.35-0.6mm garnet and 1.7m of 2.5-5.0mm anthracite.**

Filter performance parameter	Mean	Std deviation
Average runlength (time to reach 2m headloss)	400 hr est	-
Breakthrough occurring at end of run ?	No	-
Time to reach steady state (2-5 $\mu$ m)	50.1 min	2.12
Steady state value (No. of 2-5 $\mu$ m/ml)	25.6	5.49
Time to reach steady state (5-400 $\mu$ m)	43.3 min	1.53
Steady state value (No. of 5-400 $\mu$ m/ml)	18.9	3.39
2-5 $\mu$ m NPF in backwash remnants within media	$1.97 \times 10^8$	$5.12 \times 10^7$
2-5 $\mu$ m NPF in backwash remnants above media	$6.48 \times 10^7$	$3.88 \times 10^7$
2-5 $\mu$ m NPF in all backwash remnants	$2.66 \times 10^8$	$8.94 \times 10^7$
2-5 $\mu$ m NPF as function of influent	$8.76 \times 10^7$	$3.62 \times 10^7$
Total 2-5 $\mu$ m NPF	$3.53 \times 10^8$	$1.19 \times 10^8$

### 6.3.2.8 Filter performance summary.

When all the mean filtrate particle count data was plotted on the same graph, Fig 6.23, differences in performance between the different filter media/configurations became apparent. Three of the media clearly exhibited higher filtrate particle counts than the others: both the 2m deep filters that contained a majority of anthracite (1.5m anthracite, 0.5m 2.0-3.35mm sand; 1.7m anthracite, 0.3m 0.6-1.4mm gamet) and the 1.5m deep 1.18-2.8mm sand filter.

The filter media that exhibited the lowest particle counts in the filtrate during ripening were found to be the very fine 0.5m deep bed of 0.35-0.6mm sand and the 1m deep bed of 0.5-1.0mm sand. Only slightly worse, in terms of particulate passage, were the 2m deep beds of 2.0-3.35 media on its own and with 0.5m of anthracite.

Interestingly, the deep bed dual-media filters exhibited double peaks, conversely the single media tended to exhibit only single peaks. A possible exception was the 2m deep 2.0-3.35mm sand filter which had the suggestion of a double peak.

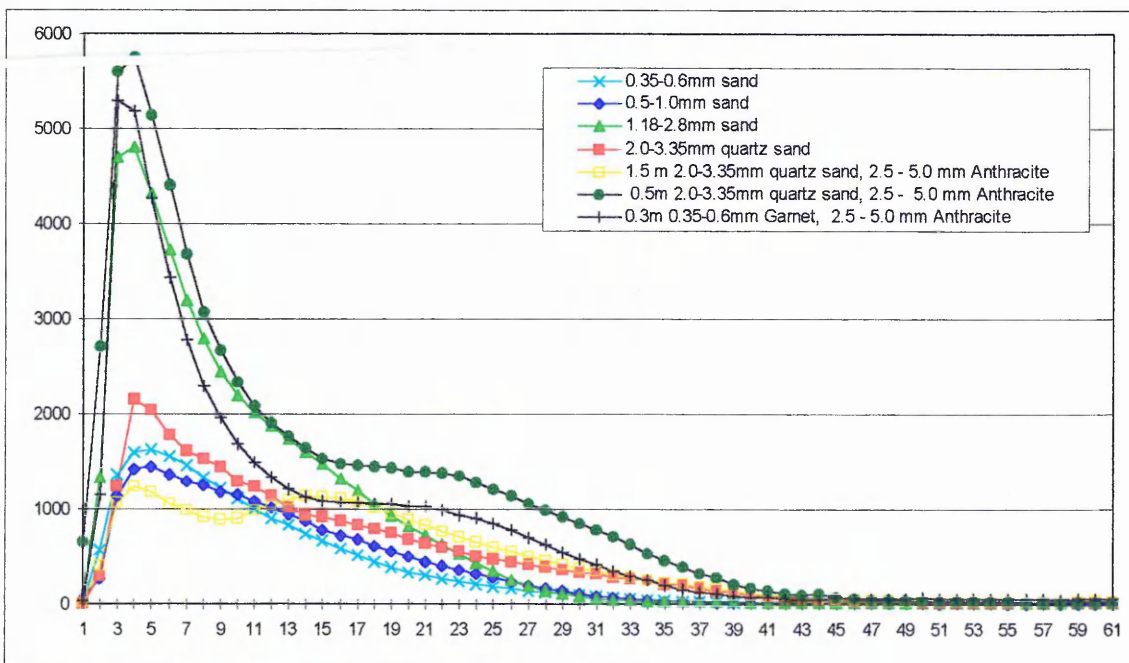


Figure 6.23. Comparison of mean filtrate particle counts.

The lowest initial peak was evident in the filtrate from the 2m deep bed of 2.0-3.35 sand with 0.5m of anthracite. However, it should be noted that this filter did display a high degree of variability.

The total 2-5 $\mu$ m NPF data has been plotted in Fig 6.24. The error bars show the standard error on the mean (95% confidence). The results reinforced the particle count plots, the filters that had the lowest numbers of 2-5 $\mu$ m particles in the filtrate during ripening were: 1m bed of 0.5-1.0mm sand, 2m bed of 2.0-3.35mm sand, 0.5m bed of 0.35-0.6mm sand, and also the 2m deep dual media filter containing 1.5m of 2.0-3.35mm sand and 0.5m of anthracite. The most reproducible were the same as above except for the 0.5m bed of .35-.6mm sand. The other filters had high NPF combined with high errors.

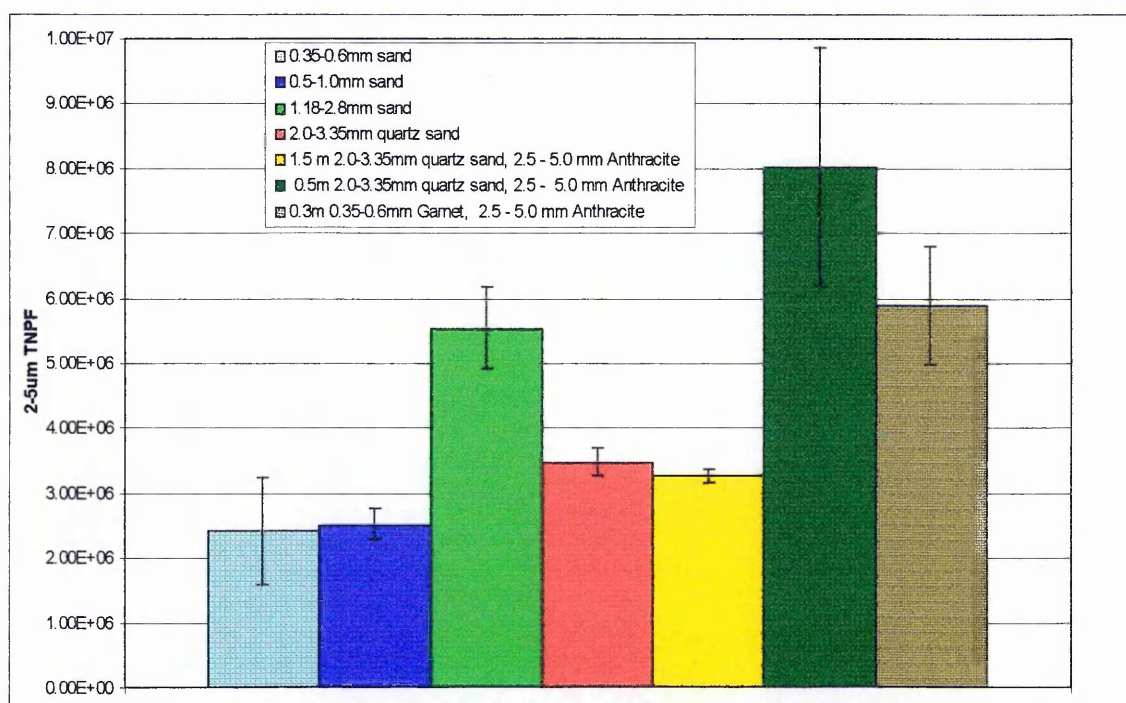


Figure 6.24. Comparison of total number of 2-5 $\mu$ m particles in first 420l of filtrate.

When the components of the NPF were compared it was found, as expected, that the deeper filters had more particles in the filtrate that were a function of the backwash remnants retained within the filter bed. For the shallower, finer beds the interface with the influent became more significant.

The runlengths achievable were a result of the headloss development that occurred in the filters during the course of a run. The headloss development for all the filters is shown in Fig. 625.



The rate of headloss development can be seen to be directly related to the media size, the rate of headloss development was found to decrease with increasing media size.

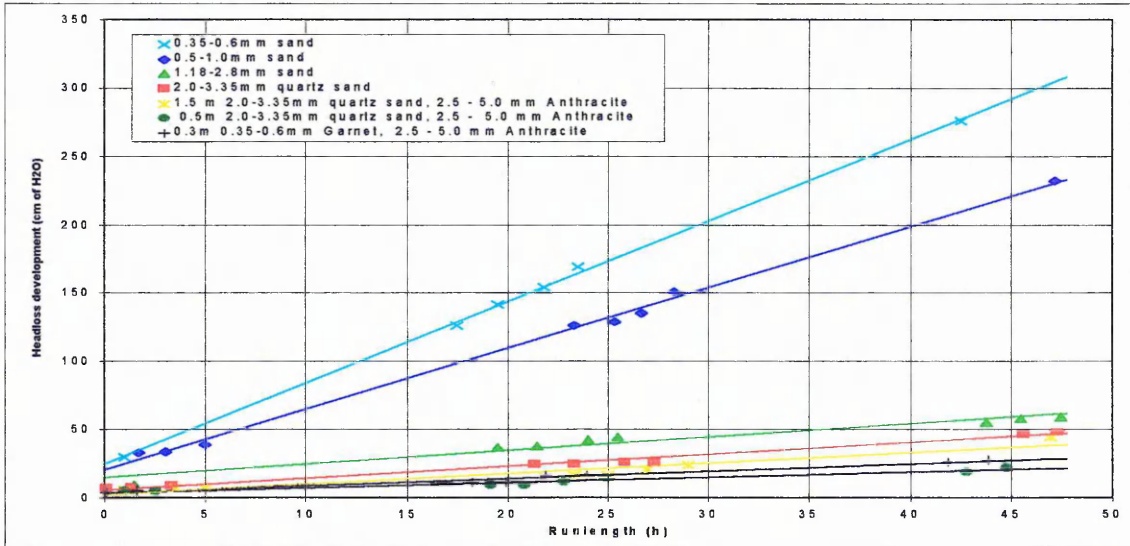


Figure 6.25. Comparison of headloss development during 48 hour run.

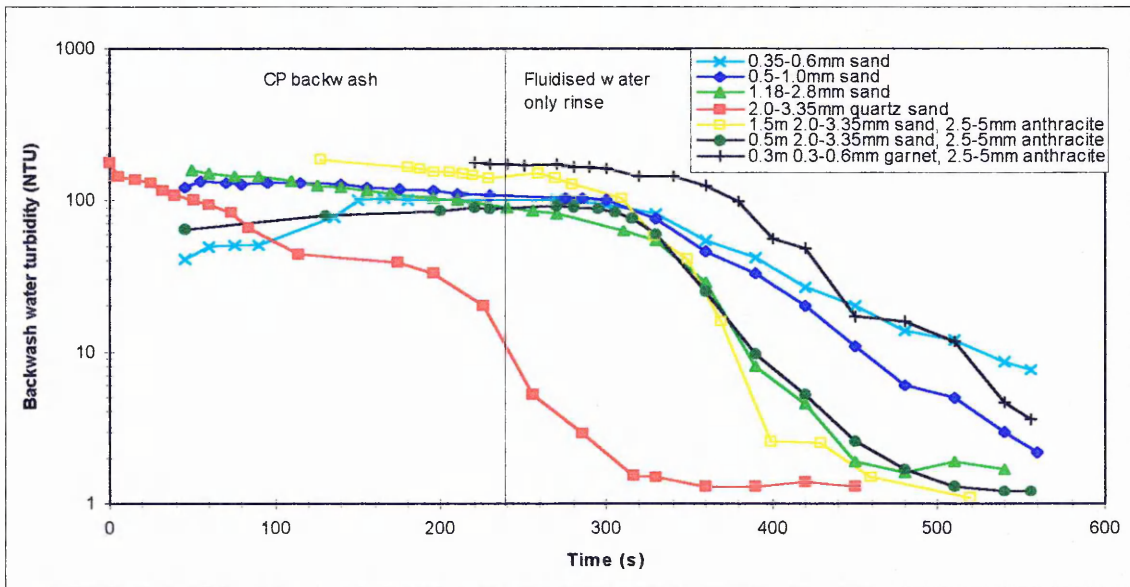


Figure 6.26. Comparison of backwash water turbidities.

## 6.4 Discussion

The monitoring procedures in the trial, in particular particle counting, will be discussed initially. Filtrate quality produced both during steady state operation and during filter ripening by the different filter media will then be discussed. The effectiveness of the backwash in terms of turbidity removal and the headloss developed by the different media during the entire run will then be covered. Finally, the two most effective media, taking all parameters into account, will be selected for use in subsequent trials.

### 6.4.1 Performance monitoring

The trials were designed such that on-line turbidity analysis of filtrate quality would occur in parallel to on-line particle counting. Unfortunately there were operational difficulties with both the turbidity probe itself and its installation. Thus, reliable data could not be provided.

The particle counter, however, proved to be very reliable and robust. The data supplied by the particle counter provided a more detailed analysis of filtrate quality during the ripening period than had previously been possible. The data once obtained from a particle counter can be presented in a number of ways. It was decided to present the information as real time particle counts and calculate the number of 2-5 $\mu\text{m}$  particles entering the filtrate during ripening. The rationale behind this decision is discussed below.

Real-time particle counts are informative and simple, providing valuable information that allows accurate monitoring of plant performance and early identification of problems. It is important to remember that this was an operational study. If particle counters are to be installed at works, operators will not have the time or possibly the expertise to convert or manipulate the data into formats other than real-time particle counts.

In a detailed study into interpretation of particle count data (Hargesheimer and Lewis, 1995) comparisons were made between particle counts and volume concentration. Volume concentration of particles in each size range is estimated by multiplying the particle count of that size range by the volume of the average diameter of particles in each size range. The example presented in the study

showed no additional information was found by converting data from particle count to volume concentration.

When particle counts are converted to volume concentration, the relative contribution of each size range is altered. Although there are more particles in the smaller size ranges, these particles contribute the lowest particle volume concentration. Hargesheimer and Lewis (1995) reported that data conversion to volume concentration could provide considerable benefit when many large particles are present in the water sample, such as a large algae species.

The filtrate particle count data (total count/ml) for a typical run of the 1m bed of 0.5-1.0mm sand filter is shown in Fig 6.27, also plotted is the volume concentration. It is clear that under the conditions of these trials that little or no additional information was supplied by converting particle counts to particle volume.

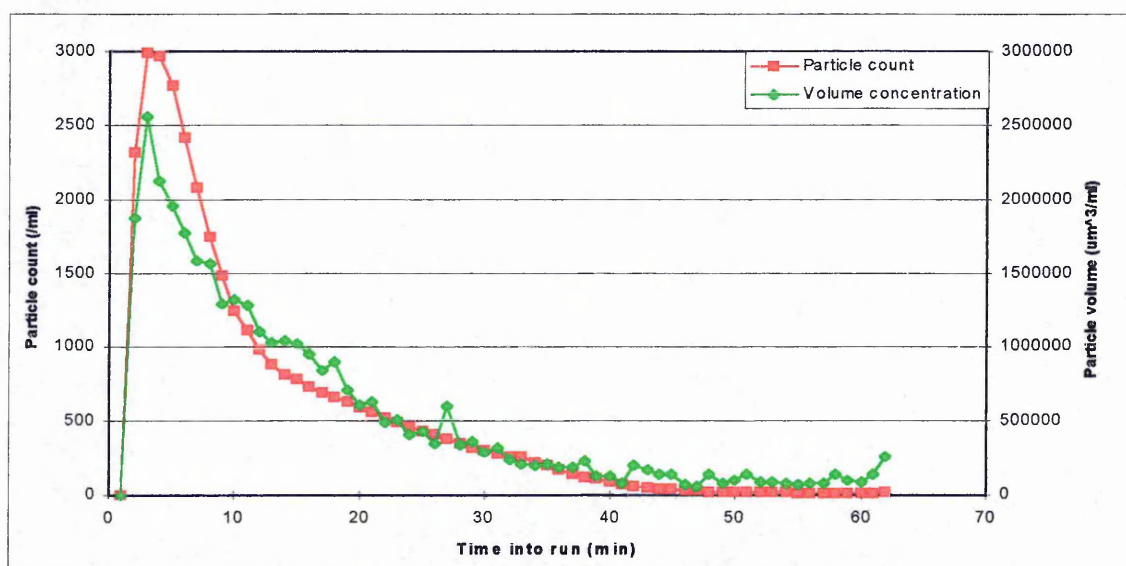


**Figure 6.27. Comparison of particle count and particle volume of filtrate during ripening - 2m 2.0-3.35mm sand filter.**

The size distribution of a water sample can be described by the power law slope coefficient, known as  $\beta$  (Kavanaugh *et al.*, 1980; Lawler and Caisson, 1990).  $\beta$  is the absolute value of the slope of a log-log plot (Fig 6.28) of differential number of particles divided by channel width against arithmetic mean particle diameter. For randomly distributed particles in water the slope is always negative.

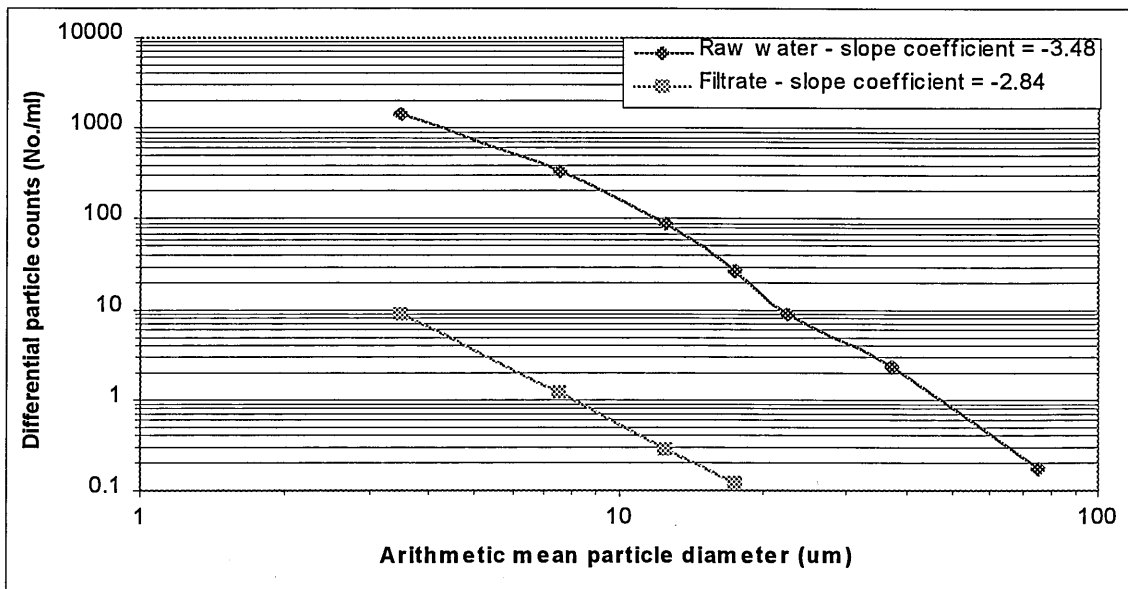


Figure 6.28. Particle size distribution of raw and filtered water (from 1m 0.5-1.0mm sand filter).

The particle size distribution data have been used with only limited success to compare the effects of water treatment processes on particle sizes (Hargeshimer *et al.*, 1991).  $\beta$  was found to be highly variable and influenced to a large extent by the small number of particles in the largest size channels. Reliable  $\beta$  values were obtained if samples had more than 10 particles /ml in each measured size band, which is not normally the case in filtered water. In this study  $\beta$  did not provide information that could be used as an operational tool to optimise treatment processes.

Log removal of particles by a treatment process, is frequently calculated and widely quoted. However as Ives (DoE/DoH, 1990) pointed out it is what is left in the filtrate that is important. By calculating the number of particles that enter into the filtrate during ripening (NPFR) a value is obtained that incorporates both the magnitude and duration of ripening. It is then possible to use this value to select and optimise processes. In these trials it was decided to calculate the number of 2-5 $\mu$ m particles entering the filtrate during ripening. This was mainly because this was the size range measured closest to the size of minimum removal efficiency (1 $\mu$ m), thus if the filter had the minimum number of these particles in the filtrate during ripening it would be operating at an optimum level. This size range also corresponded to that of *Cryptosporidium* oocysts, as sized by the particle counters used in this trial.

## 6.4.2 Filtrate quality

The filtrate quality needed to be evaluated during both steady state and during ripening. The filter operates at steady state for the vast majority of the filter run. However, the ripening period has been flagged in the Badenoch report (DoE/DoH, 1990) as the time during a filter run when *Cryptosporidium* oocysts are most likely to penetrate into supply, hence the performance measure of NPFR.

### 6.4.1.1 Filtrate quality during steady state operation.

According to filtration theory, smaller media should provide a higher degree of particulate removal from an influent suspension, since in the first order model (Iwasaki, 1935):  $\delta C / \delta L = -\lambda C$  the filter coefficient is inversely proportional to the filter media grain size.

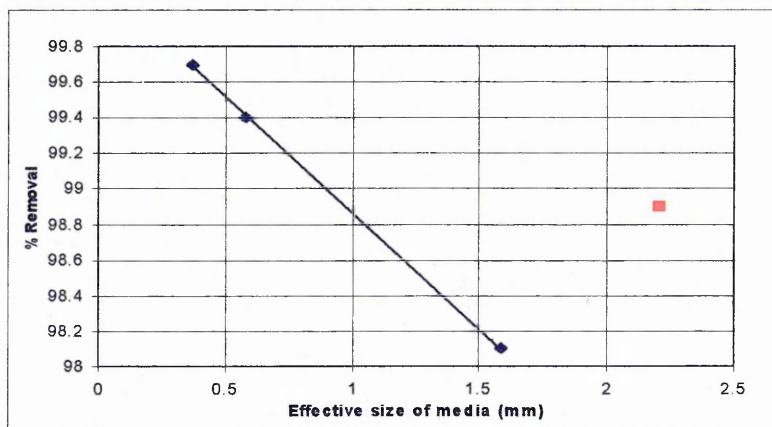
Media shape and surface characteristics play an important role because of both surface area and projections into the fluid stream lines. An illustration of this was a study by Ives and Sholji (1965), lab-scale filters of Anthracite, sand and glass beads, of the same size, were run under identical operating conditions. The best removals were found in the anthracite, followed by sand and then glass.

In the results section average steady state values were shown for all media. That data is summarised in Table 6.13, also shown is the percentage removal ( $C/C_0 \times 100$ ). It should be noted that the percentage removal figures are calculated from the average values and a degree of error is likely to be incurred. However, the figures provide a means of comparing performance at steady state.

It can be seen from Table 6.13 that percentage removals for the sand decreased as the size of media increased (99.7% removal for the 0.35-0.6mm sand, 98.1 % removal for the 1.18-2.8mm sand). These removal figures are plotted on Fig 6.29, to illustrate the linearity. Also shown on the graph is the removal shown by the 2.0-3.35 quartz sand (the red square).

**Table 6.13. Mean steady state particle counts and % removals.**

Filter media /bed depth	Particle count (No.s /ml)	% Removal (C/C <sub>0</sub> x100)	Log <sub>10</sub> removal
0.5-1.0mm Sand (1m)	12.40	99.4	2.19
2.0-3.35mm Sand (2m)	19.91	98.9	1.98
1.18-2.8mm Sand (1.5m)	36.08	98.1	1.72
0.35-0.6mm Sand (0.5m)	6.02	99.7	2.50
2.0-3.35mm Sand, (1.5m) 2.5-5.0 mm Anthracite (0.5m)	30.85	98.4	1.79
2.0-3.35mm Sand, (0.5m) 2.5-5.0 mm Anthracite (1.5m)	39.38	97.9	1.69
0.35-0.6mm Garnet (0.3m) 2.5-5.0 mm Anthracite (1.7m)	44.50	97.6	1.63

**Figure 6.29. Percentage removals at steady state for a range of sand sizes.**

The 2.0-3.35 media, whilst supplied as filtration sand, was actually quartz sand. In Chapter 5 SEM micro-graphs showed that not only was the sand more angular but it also had a much rougher surface topography. It was found that removals in the 2m bed of 2.0-3.35mm sand filter were higher than would be expected in an equivalent sized rounded sand. In fact, the removals were higher than a smaller rounded sand - 1.18 to 2.8mm sand.

A question therefore arises, as to whether the good removals shown by the 2.0-3.35mm sand filter were due to its surface characteristics or the extra bed depth i.e. 2m compared to 1.5 of the 1.18-2.8mm sand. Where good to moderate removal occurs published results (Ives and Sholji, 1965; Clark

*et al.*, 1992), have shown that, decreases in particle removal resulting from larger media may be offset with increased bed depth. However, in the study by Clark *et al.*, (1992), it was found that this was only true up to a certain size range. The performance of a sand of 1.85mm, which showed good to moderate removal, was improved with a greater bed depth but a 3.6mm sand showed very poor removals and increased depth had no effect. However, the bed depths used by Clark *et al.*, (1992) did not exceed 1.0m. The 2m bed of 2.0-3.35mm sand was not completely used in the 48 hour runs used in this trial; headloss measurements indicated some solids penetration up to 1.5m, and visual observations of deposits confirmed this. Therefore, under the conditions of the trial the extra bed depth was not utilised, and thus could not be contributing to the performance of the filter. This implies that it was the surface characteristics of the media responsible for the good removal.

A very recent study would seem to confirm the likelihood of surface characteristics being the significant factor. Suthaker *et al.*, (1995) carried-out pilot scale trials on filters containing equal sized grains (0.6mm) of sand, quartz, and sand anthracite dual media (anthracite slightly larger). At conditions most comparable to the trials detailed in this chapter the quartz media showed the best removals, followed by the sand and the dual media.

When the dual media filters were considered, it was found that performance generally concurred to published results (Conley, 1961 ). The filter with the most quartz sand and least anthracite (1.5m of 2.0-3.35mm sand and 2.5-5.0mm anthracite) performed better. The filter containing 1.7m of anthracite and 0.3m of fine garnet was expected to perform better than it did.

A number of possible reasons exist as to why this filter performed poorly. Firstly, 20cm of media were lost due to operational difficulties, these same difficulties resulted in some of the garnet being distributed throughout the bed (determined from visual observation). Therefore, the filter was no longer in the design configuration. The garnet layer was supposed to provide "polishing", if it had been diminished or entirely mixed with the anthracite this function would clearly not be occurring. The visual observation ports were above the expected interface and therefore this could not be confirmed. However, analysis of headloss data suggests at least some of the garnet was still in place.

Another reason may have been the better than expected performance of the 2.0-3.35mm quartz sand, reflecting badly on the anthracite/garnet filter when relative comparisons were made.

#### 6.4.1.2 Filtrate quality during the ripening period.

The reasons for using 2-5 $\mu$ m particle count as a performance measure has been explained in a previous

section (6.4.1). The 2-5 $\mu$ m particles are closest to the size of minimum removal efficiency (1 $\mu$ m) for sand filters. It would, therefore, be expected that the increase in removal efficiency for these particles will take longer. Figs 6.30 to 6.33 show the particle counts for a range of discrete size bands measured during a typical ripening period of 1m 0.5-1.0mm sand filter. Performance follows theoretical predictions, the closer the particle size is to that of minimum removal efficiency the longer it takes for removal to reach steady state (ripen). For instance, the filter ripens, for the 10-15 $\mu$ m size range, after approx. 20 minutes, for the 5-10 $\mu$ m size range after 30 minutes and for the 2-5 $\mu$ m size range after approx. 40 minutes. This trend was witnessed for all the filter media.

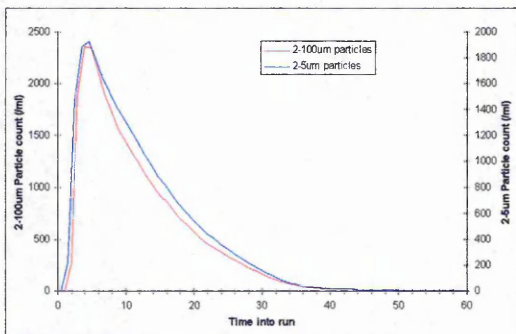


Figure 6.30. Filter ripening for 2-5 $\mu$ m and 2-200 $\mu$ m particles.

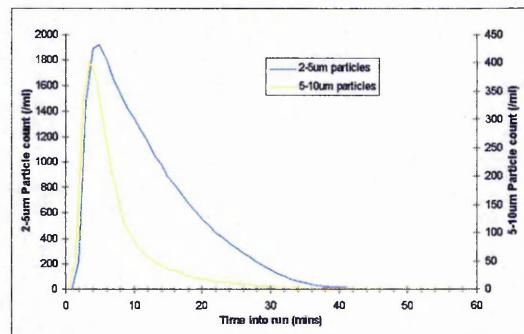


Figure 6.31. Filter ripening for 2-5 $\mu$ m and 5-10 $\mu$ m particles.

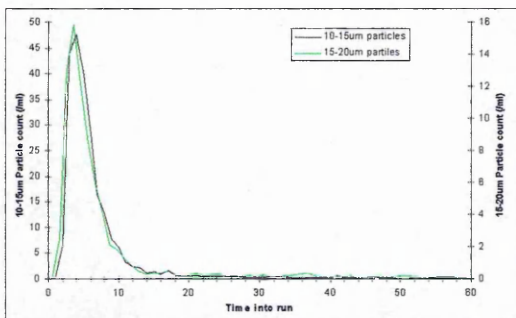


Figure 6.32. Filter ripening for 10-15 $\mu$ m and 15-20 $\mu$ m particles.

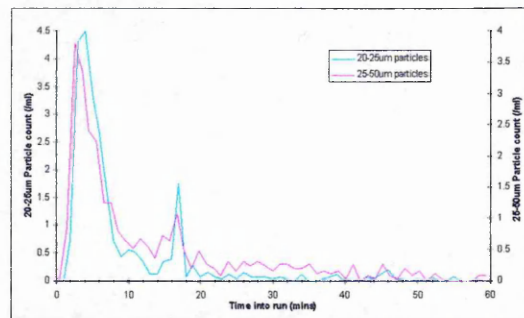


Figure 6.33. Filter ripening for 20-25 $\mu$ m and 25-50 $\mu$ m particles.

Differences were also seen in the time for 2-5 $\mu$ m particles, and the 5-200 $\mu$ m particles to ripen for the different filters. The time to ripen could be related to media size and thus removal efficiency. Generally, larger media sizes resulted in longer ripening, this trend appeared to be linear and is illustrated in fig. 6.34. Surprisingly, the 2.0-3.35mm quartz sand fitted into the linear trend, despite the fact that it had a relatively high removal efficiency at steady state. This media may require more additional collectors because of its size. There was virtually no difference between the ripening times of the two dual media



combinations containing the quartz sand; although they did take longer to ripen than the sand by itself, due to the low removal efficiency of the large anthracite. The remaining dual media filter - the 1.7m anthracite, 0.3m fine garnet - ripened more rapidly than the two dual media filters containing less anthracite. This has to be attributable to the fine garnet layer.

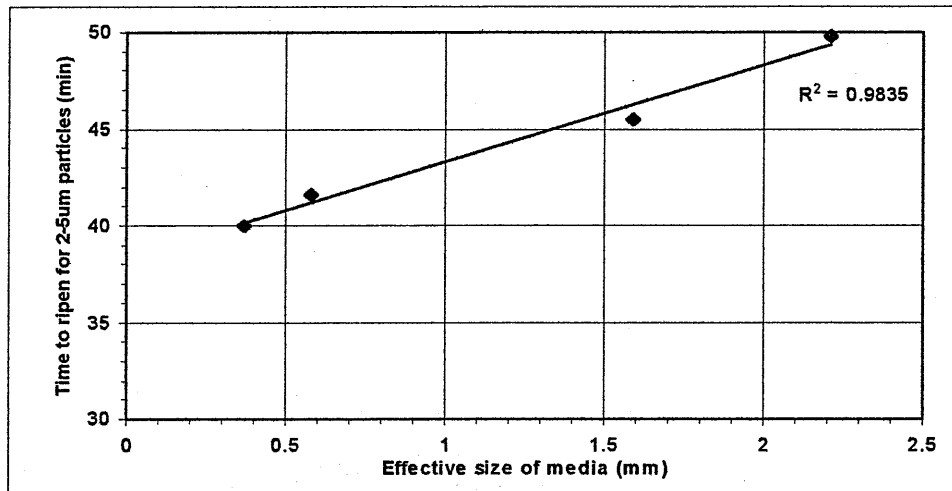


Figure 6.34. Relationship between media size and ripening time.

The real-time particle count summary, shown in fig 6.23, showed three filters with greater peak magnitudes. The 1.18-2.8mm sand and the 2 dual media filters that had the majority of anthracite. The filters with the lowest peaks were the fine sand media (0.33-0.6, 0.5-1.0mm) and the 2.0-3.35mm quartz sand filter on its own and with 1.5m of anthracite. This appears to be another example of the surface roughness of the quartz sand compensating for its size. The beneficial effects of quartz sand's roughness were also reported by Suthaker *et al.*, (1995). They also showed that the quartz sand produced a smaller peak, measured by turbidity, than sand and dual media combinations of similar size.

The shape of the filtrate quality plot, whether is it measured by turbidity or particle count, provides a great deal of information on what is occurring within the filter during ripening. In an original study, Amirtharajah and Wetstein (1980) drew attention to the fact that the period of poor quality following backwashing was caused by a combination of backwash remnants and low removal efficiency. This was shown in a schematic (Fig 3.11). The ripening period was normally overlooked because monitoring of filter performance was not normally frequent enough to highlight more than one or two data points during this period.

The study by Amirtharajah and Wetstein (1980) made some important findings, despite a number of shortcomings. The work was carried out on two different sized lab-scale filters, operating with different media, bed depths, and coagulation. Different results were obtained from the apparatus which

were not successfully accounted for. In Amirtharajah's rig ( 0.15m I.D, 0.3m media depth ) back calculation of the figures suggests a backwash weir height of a metre or more above the top of the bed. It is unlikely, therefore, that washout of material detached during backwash was effective.

When the filtrate quality during ripening of this filter is examined at the filtration rate closest to that used in this study - 8.6m/h - a very small initial peak associated with the backwash remnants occurs. A much larger second peak occurs after five minutes, four minutes before the interface with the influent. Amirtharajah and Wetstein (1980) concluded that the magnitude of the initial peak of poor filtrate quality was affected by the effectiveness and duration of backwash ( these observations are tested in the next trial). They also concluded that the second peak was larger and that it was principally caused by influent particles passing through the filter when filter efficiency is low. It is the writer's opinion that the results have been misinterpreted.

As mentioned the second peak in Amirtharajah's experiments occurs after 5 minutes, 4 minutes before the interface with the influent. It is the author's opinion that this second peak is mainly caused by particles in the backwash remnants above the media not successfully rinsed out in combination with a reduced filter efficiency. Amirtharajah and Wetstein (1980) carried out some tracer studies and demonstrated a degree of dispersion (which was probably exaggerated by wall effects), such that actual detention time was 84% of the theoretical detention time. Taking this account the second peak should occur after approx.7.5 minutes for Amirtharajah and Wetstein's hypothesis to be correct.

There is a large amount of evidence in the literature (e.g.Suthaker *er al.*, 1995, Hargesheimer and Lewis, 1995), including examples shown in Amirtharajah and Wetstein (1980) paper, that show the first peak is the largest and is a function of the backwash remnants within the media, and that the second peak if it does occur is a function of the backwash remnants above the media. There is also evidence (Mosher and Hendricks, 1986) from larger scale filter plants that dispersion effects are minimal during filter re-start.

The observations from these trials show that under the test conditions the first peak is always larger and is associated with the theoretical detention time of the backwash remnants in the bed, and the second peak, when it occurs is associated with the theoretical detention time of the backwash remnants above the bed. The second peak always occurred before the interface with the influent.

It should be noted that perfect plug flow will not occur in the filters and there will realistically be some overlap between components of ripening. The evidence suggests, that at the scale of plant used at Lostock, these effects will be minimal and that breaking down the ripening period into components based on theoretical detention times is a valid method of assessing filter performance.

The total number of 2-5 $\mu$ m particles in the filtrate during ripening (NPFR) value provides an easy way to assess the size of the filter ripening problem, because it gives one figure that encompasses the magnitude and length of the ripening period. This can then be compared when a process parameter is changed and hence optimisation of the process can take place. It also enables comparisons between different types and configurations of media. The effect of the ripening period on the filtrate quality over the whole run is shown when the NPFR is expressed as a percentage of the total number of 2-5 $\mu$ m particles entering the filtrate during a 48 hour run. For all the media tested the percentage value was on average 35.8 (min - 24.3%, max - 54.9%).

When the NPF figure is broken down into components - the backwash remnants both within and above media, and the function of the influent - a very detailed picture of what is occurring within the filter is obtained. This facilitates a far greater understanding of the start-up and filter ripening process than has previously been possible.

Amirtharajah and Wetstein (1980) reported that the amount of particulate matter that entered the filtrate in the backwash remnants from within the bed was affected by the effectiveness of the backwash, its duration and the rate of backwash valve closure (which causes bed contraction). The solids loading rate will also play a part. For each individual filter this variability in loading rate, albeit small, produced the variability seen in the numbers of particles in this component between runs, since all other variables were fixed. When numbers from different filters are compared differences must therefore be due to bed depth and/or backwash efficiency, since all other variable are fixed.

The media bed depth obviously affects the volume of backwash remnants in any one filter. Therefore, if the differences in NPF, for the backwash remnants within the bed component, was caused solely by bed depth the 0.5m deep 0.33-0.6mm sand filter would have the lowest NPF. Followed by the 1m deep 0.5-1.0mm sand filter, and then the 1.5m 1.18-2.8mm sand filter, followed by all the 2m deep filters. Clearly, this is not the case, the 1.5m deep 1.18-2.8mm sand filter has higher NPF than the 2m deep 2.0-3.35mm quartz sand filter and the 2m deep dual media filter containing 1.5m of 2.0-3.35mm quartz sand. Although each backwash is designed to achieve collapse-pulsing and give a rinse of between 5 and 10% bed expansion, flowrates are different for each media and hence different volumes of wash water are used (this is discussed in more detail in the next section). This will, therefore, have an effect on the numbers of particles in this volume.

In addition, the backwash rates for the dual media are not at optimum rates because a compromise has to be made for the two components. For instance the two 2m filters made up of different depths of 2.0-3.35mm sand and anthracite had very different NPFs. The filter that had 1.5m sand had its backwash rates more suited to the sand component because it made up  $\frac{3}{4}$  of the bed, and the NPF was  $7.62 \times 10^7$ . Whereas, the filter that had 1.5 m anthracite had much lower backwash rates and the 0.5m of sand was not effectively cleaned, the result was an NPF of  $2.45 \times 10^8$ .

The backwash overflow weir height and hence the volume of backwash remnants above the media in the filters was constant. This may not have employed the best similitude, since different media should have different weir heights, but by fixing the weir height at 75cm comparisons between filters could be made. That considered, there were large differences, in the numbers of particles in the filtrate that were present within this volume, between the different filters.

The lowest number of particles in the filtrate as a result of this component were found in the 2m bed of 2.0-3.35mm sand, the 1m bed of 0.5-1.0mm sand and the mixed media filter comprising 1.5m sand and 0.5m anthracite. The highest were in the 1.5m bed of 1.18-2.8mm sand and the dual media filter comprising 0.5m sand and 1.5m anthracite.

These trends can be related, with one or two exceptions to the removal efficiency of the media. The particles in this component pass through the filter bed and therefore some removal must occur, so those filters which show higher removal efficiencies such as the 1m bed of 0.5-1.0mm sand should have lower numbers in this component. However, this is compounded by the efficiency of the rinse phase of the backwash. For instance, the 0.5m bed of 0.335-0.6mm sand would be expected to have lower numbers in this component, but because of the relatively high backwash weir successful washout of detached solids did not occur (this is discussed further in the next section).

The particles in the backwash remnants above the media contribute to the improvement in removal efficiency that causes "classical ripening" but it is mostly the destabilised particles in the influent that bring about the improvement. The NPFs that are a function of the influent show that media type and size again play a significant role. Generally, as media size increases the NPF of this component increases. An exception is the 0.5m bed of 0.335-0.6mm sand, it is possible that the phenomenon of floc break-off (Clark *et al.*, 1990) is occurring in the very small pores of this media (this

is discussed further in section 8.4). All three of the dual media combinations had higher NPFs, for this component, than the single media filters. The 2m deep filter comprising 0.5m sand and 1.5m anthracite had an NPF far greater than any other filter (2-3 times greater). This particular filter performed poorly when all parameters are considered and is undoubtedly due to the inefficient cleaning of the sand layer.

When the NPFs from the components of filter ripening are added together a figure for the total number of particles in the first 420l of filtrate (TNPF) is obtained. The lowest TNPFs were found in the 0.5m bed of 0.335-0.6mm sand, the 1m bed of 0.5-1.0mm sand, the 2m bed of 2.0-3.35mm sand and the dual media filter comprising 1.5m sand and 0.5m anthracite. Of these the 0.5m sand filter had a high degree of variability. The remaining filters all performed significantly worse.

#### *6.4.2 Headloss development*

Theoretically the coarser the media the slower the headloss build-up. This is demonstrated very clearly by the filter media used in these trials. The finest media, the 0.335-0.6mm sand, had the quickest build-up of headloss, and the build-up took place in the very top part of the bed. The 0.5-1.0mm sand also has a rapid headloss development, but some deeper penetration of the bed occurred. There was then a significant difference to the 1.18-2.6mm sand and the 2.0-3.35mm sand. Therefore, for the single media the coarser the media grain size the greater the penetration of the filter bed, resulting in a greater portion of the bed removing particulates from the influent, thus producing slower headloss development.

When a coarse anthracite (2.5-5.0mm) was added to the 2.0-3.35mm sand, the headloss development would be expected to take longer. This was observed, the 0.5m of anthracite increased the estimated runlength by 10%, and the 1.5m anthracite by 50%. This relatively small increase for the 1.5m anthracite and 0.5m sand filter is likely to be due to the inefficient backwashing of the sand layer as discussed before. The filter containing 1.7m of anthracite and 0.3m of fine garnet had a greater headloss build-up and therefore shorter runlengths than the dual media filter containing 1.5m anthracite and 0.5m of 2.0-3.35mm sand). This implies the layer of garnet at the bottom of the filter was making a significant contribution to the headloss build-up, despite some dispersion. Indeed, when the headloss development in that section of the bed is referred to there was a higher level of headloss than in sections of bed above it.

### 6.4.3 Solids removal during backwash

There were two parameters measured that gave an indication of the effectiveness of the backwash in terms of solids removal from the filters: backwash water turbidity washout curves; and clean bed headloss.

#### 6.4.3.1 Turbidity washout curves

Backwash water turbidity profiles show the amount of solids that are being removed from the filter during backwashing. The backwashing regime used in this trial consisted of two phases, CP wash (4mins) followed by fluidisation rinse (5 mins), this was reflected in the general shape of the washout curves, shown in Fig 6.26. According to the literature (Amirtharajah, 1978,1979,1984 and 1993) CP is the most effective cleaning mechanism and water only wash is a weak cleaning mechanism. However, the water only phase is required to effectively rinse out the solids detached from the media during the CP phase since fluidisation essentially "unlocks" the media. In an extensive study, Moll (1986, 1990 and 1996), produced results that confirmed the importance of the fluidised water only rinse after CP. Performance, measured by clean bed headloss and runlength, was adversely affected when this stage was omitted. It is the writer's opinion, however, that Moll misinterpreted his data when formulating his conclusions, this will be discussed further in the next chapter.

If the turbidity of the washwater remained constant during the CP backwash then it would be likely that the media was been cleaned at a constant rate. That is significant amounts of deposit must still have been on the media. If turbidity declined during the CP backwash then it was likely the media was becoming clean. A decline in backwash water turbidity during the CP backwash was evident in all but one of the filters - the 0.5m bed of 0.35-0.6mm sand. In addition backwash water overflow was only just recorded, for the 2m deep bed of 2.5-5.0mm anthracite (1.7m) and 0.35-0.6mm garnet, during CP wash. These two filters had the lowest backwash water velocities during CP, however because of the small bed depth of the sand filter 1 bed volume (BV) was still used during the CP wash. Only 0.3BV was used in the CP wash for the anthracite filter. Since the different media required different water velocities, to achieve both CP and a 5-10% expansion, different volumes of washwater were used to clean the filters. The backwash water turbidities were plotted against volume of backwash water (Fig 6.34) to normalise the data.

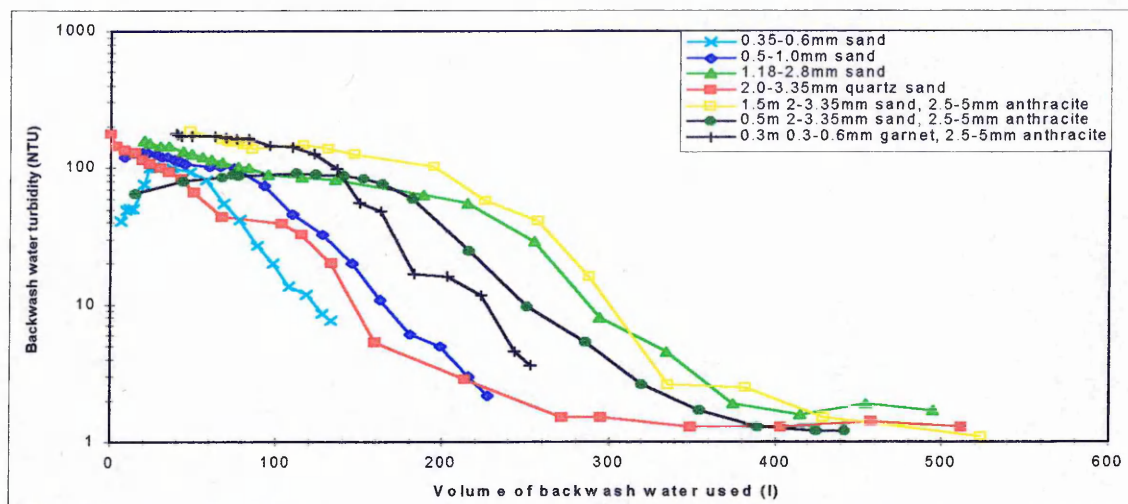


**Figure 6.34. Backwash water turbidities Vs. backwash water volume.**

The problems encountered in washing the 0.5m 0.35-0.6mm sand filter appeared to be with removing the detached deposits from the filter. 1BV was used during the CP wash but because the volume of water above the media bed up to the overflow weir was greater than 1BV solids carry-over was limited. It is only when the higher rate rinse started that deposits were successfully washed out. The fact that solids were so successfully rinsed out of the filters during the rinse phase, when fluidisation had occurred, in combination with Molls (1986, 1990 and 1996) results emphasise the importance of this phase. In addition the fluidised rinse releases air trapped in the bed from the CP wash. Air trapped in the bed can greatly reduce removal efficiency and increase headloss.

#### 6.4.3.2 Clean bed headloss

The clean bed headloss can give indications if a chronic problem in the backwashing regime employed to wash a filter. A chronic problem being one that gets worse over an extended period of time. If the clean bed headloss i.e. after backwash, increases over time the backwash is inefficient. Due to the time-scale of this trial long term trends could not be evaluated. It was decided to compare the clean bed headloss data to predicted levels (determined from Carmen-Kozeny equation (8)) in order to give an indication of backwash efficiency. Actual and predicted clean bed headloss is shown in Table 6.14.

**Table 6.14. Comparison of actual and predicted clean bed headloss.**

Filter media / bed depth	Actual clean bed headloss (cm of H <sub>2</sub> O)	Predicted clean bed headloss (cm of H <sub>2</sub> O)*
0.5-1.0mm Sand (1m)	23	29
2.0-3.35mm Sand (2m)	5	5
1.18-2.8mm Sand (1.5m)	15	6
0.35-0.6mm Sand (0.5m)	26	47
2.0-3.35mm Sand, (1.5m) 2.5-5.0 mm Anthracite (0.5m)	3	5
2.0-3.35mm Sand, (0.5m) 2.5-5.0 mm Anthracite (1.5m)	3	4
0.35-0.6mm Garnet (0.3m) 2.5-5.0 mm Anthracite (1.7m)	3	27

\* - As determined by Carman-Kozeny equation.

The actual clean bed headloss was only higher than the predicted value for the 1.5m of 1.18-2.8mm sand. The predicted value was very different to the actual value for the 2m deep bed of 2.5-5.0mm anthracite (1.7m) and 0.35-0.6mm garnet. This implies, as suggested earlier, that much of the garnet was dispersed throughout the bed.

#### 6.4.3.3 Problems with the backwashing process

Generally, the backwash process employed in this trial was very successful. A number of problems did result principally due to the placing of the backwash overflow weir. In order to reduce the variables a set weir height of 0.75m above the bed was selected, this did not however employ the best similitude. Problems were encountered in rinsing out the 0.5m bed of 0.35-0.6mm sand because the weir was too high. Other problems with media loss were encountered with the dual media filters because the weirs were too low. The worst case of media loss, due to weir height, occurred in the 2m bed consisting of 1.5m of sand and 0.5m anthracite. The backwash rates in this filter were more attuned to the sand which made up the bulk of the bed, as a result 21cm of anthracite were lost. This degree of media loss is clearly unacceptable, solutions would be to reduce backwash rates (this would affect performance), or install media retaining screens on the backwash overflow weir (this would incur capital cost), or assess different media combinations.



affect performance), or install media retaining screens on the backwash overflow weir (this would incur capital cost), or assess different media combinations.

Loss of anthracite, 0.3m also occurred in the 2m deep bed of 2.5-5.0mm anthracite (1.7m) and 0.35-0.6mm garnet. However, this was a result of PLC error and not the backwash regime itself.

### *6.5 Media selection*

Two of the filter media had to be selected for use in subsequent trials. The 1m bed of 0.5-1.0mm sand, the 0.5m bed of 0.335-0.6mm sand, the 2m bed of 2.0-3.35mm sand and the dual media filter comprising 1.5m sand and 0.5m anthracite all performed well in terms of the number of particles in the filtrate, both during ripening and at steady state. However, the performance of the 0.5m bed of 0.335-0.6mm sand was not very reproducible. That combined with the very short runlengths possible with this media rule it out. The performance of the 1m bed of 0.5-1.0mm sand was reproducible and runlengths of up to 44 hours were achievable. The 2m bed of 2.0-3.35mm sand and the dual media filter comprising 1.5m sand and 0.5m anthracite Filters 2 and 5 had greatly extended runlengths (estimated on headloss development), and were reproducible.

There would be a problem of media loss with the dual media combination in filter 5. Over extended periods (lost 21cm during 3.5months) the loss of anthracite from the top of the bed would be substantial, since the backwash flowrates are geared towards the 2.0-3.35mm sand which makes up most of the bed. This could be combated by installing screens on the backwash weir to retain the media. An easier solution would be to use the single media.

Using a single media allows the collapse-pulsing backwash and indeed the rinse flowrates to be optimal. Therefore the coarse 2.0-3.35mm quartz sand was selected. The other media selected was the 1m deep bed of 0.5-1.0mm silica sand. This was chosen, despite its relatively short runlengths, because it is a standard NWW sand and therefore commonly used. It would thus provide a valuable benchmark.

## 6.5 Conclusions

Under the operating conditions used in these trials and from the results obtained the following conclusions can be made:

Use of particle size analysis gave a more complete characterisation of the filter ripening period than had previously been possible. These investigations have confirmed that particle counters have much potential as a real time on-line monitor of filter performance and as an aid to improved filter operation and design.

Up to 54% of the total number of 2-5 $\mu$ m particles that enter the filtrate during a 48 hour run do so during the ripening period. Further a ripening period of one hour is only 2% of a 48 hour filter run. This clearly shows the ripening period is the critical part of the filtration cycle.

Generally, the larger the media the lower the removals at steady state (not compensated for by increased bed depth), the higher the NPF during ripening, the longer the ripening time, and the longer the time to reach a terminal headloss. An exception to this was the 2.0-3.35mm quartz sand.

The quartz sand media provided greater removals at steady state, and lower NPFs during ripening than silica sand of smaller size (1.18-2.8mm) due to its rough surface microtopography.

The dual media combinations used in this trial were found to be not operationally viable. The most operationally effective media were found to be 1m beds of 0.5-1.0mm sand, and 2m beds of 2.0-3.35mm quartz sand.

# *CHAPTER 7*

## THE EFFECT OF BACKWASH STRATEGY ON PERFORMANCE

### 7.1 Introduction

The fact that a combined air water backwash, at rates to achieve collapse-pulsing, is the most efficient backwash system available has long been acknowledged in the literature. However, little attention has been directed as to its effect on filtrate quality during the ripening period. It was therefore decided to compare the effect of the collapse-pulsing backwash, on filter performance during ripening, with that of more conventional backwash regimes.

The effect of the duration of the collapse-pulsing backwash upon filtrate quality during the ripening period was also unknown. Different durations of collapse-pulsing backwash were investigated in order to identify an optimum that minimised particulate passage into the filtrate during the ripening period.

### 7.2 Experimental Procedures

The two media that were selected from the previous trial (Chapter 6) were the 1m bed of 0.5-1.0mm sand, and the 2m bed of 2.0-3.35mm sand, details of which are shown in Table 7.1. The filters were run at a filtration rate of 6m/h, with a ferric (III) sulphate dose of 1.0mg/l as Fe<sup>3+</sup> at pH 5.5. The monitoring strategies employed were those described in Chapters 4 and 6.

**Table 7.1. Filter media and filter operating details**

Description	0.5-1.0mm rounded sand	2.0-3.35mm rounded sand
Effective size	0.52mm	2.21mm
Uniformity coefficient	1.37	1.37
Filter bed depth	1m	2m
Height of backwash overflow	0.75m	0.75m

#### 7.2.1 Backwash regime assessment

Three backwash regimes were assessed: water only fluidisation backwash, air scour followed by water fluidisation backwash, and collapse-pulsing (combined air/water wash) followed by water only rinse.

The flowrates used are shown in Table 7.2. At the time of this trial there were 3 columns of both 0.5-1.0mm sand, and 2.0-3.35mm sand. Therefore backwashing of the three filters, each with a different backwash regime occurred on the same day. Backwashing was carried out every 24 hours during this particular assessment.

**Table 7.2 Backwash flowrates and durations used in backwash regime assessment.**

Backwash regime	1m beds of 0.5-1.0mm sand		2m beds of 2.0-3.35mm sand	
	Backwash velocity (m/h)	Backwash duration (min)	Backwash velocity (m/h)	Backwash duration (min)
Fluidising water only	30	10	92	6
Air then fluidising water	V <sub>AIR</sub> - 50	5	V <sub>AIR</sub> - 90	5
	V <sub>WATER</sub> - 30	5	V <sub>WATER</sub> - 92	5
Collapse-pulsing	V <sub>AIR</sub> - 50	}4	V <sub>AIR</sub> - 90	}4
	V <sub>WATER</sub> - 10		V <sub>WATER</sub> - 30	
	V <sub>RINSE</sub> - 30	5	V <sub>RINSE</sub> - 92	5

### 7.2.2 Backwash duration assessment

The backwashing regime selected was a combined air/water wash at flowrates to achieve collapse-pulsing, followed by a higher velocity water rinse. Backwashing was carried out every 48 hours. The flow rates used are the same as those shown in Table 7.2. The collapse-pulsing backwash was assessed for wash durations ranging from 1- 5 minutes, the rinse was fixed at 5 minutes and designed to give 10% expansion.

## 7.3 Results

The performance of the two media selected - 1m beds of 0.5-1.0mm sand, and 2m beds of 2.0-3.35mm sand - under the different backwash regimes and then under different collapse-pulsing backwash durations are presented. Performance indicators used were: real-time filtrate particle counts; the numbers of 2-5 $\mu$ m particles in the filtrate during the components of the ripening period (see Fig 3.11); the rate of headloss development over the entire run; and finally the amount of particulate matter

(measured in terms of turbidity) removed from the filters during backwash.

### 7.3.1 Backwash regime assessment

The influent quality for the duration of the trial is initially presented. The performance of the 1m beds of 0.5-1.0mm sand and then the 2m beds of 2.0-3.35mm sand, after the different backwash regimes, is then presented. Finally the data obtained from both media is summarised.

#### 7.3.1.1 Influent quality

The influent quality during this trial is summarised in Table 7.3. Despite the short duration of this particular trial, only about 2 weeks (7/5/96 - 22/5/96), some rather large variations in quality were evident. This variability can be put down to the augmentation of Thirlmere water with water from other sources due to water demand and availability problems.

**Table 7.3 Summary of raw water conditions during backwash regime trial.**

	pH	Turbidity (NTU)	Manganese ( $\mu\text{g/l}$ )	Iron ( $\mu\text{g/l}$ )	Colour ( $^{\circ}\text{Hazen}$ )	Particle count (No./ml)
Mean	8.54	0.30	10.67	86.3	2	2214.9
Std. Dev	0.15	0.06	1.53	9.86	0	732.89
Min	8.35	0.40	9.55	75.19	2	1177
Max	8.7	0.20	12.14	93.47	2	3417

#### 7.3.1.2 1m beds of 0.5-1.0mm sand

The filtrate particle count data from filters with different backwash regimes is shown in Fig. 7.1. The fraction of 2-5 $\mu\text{m}$  particles remaining (concentration in filtrate/concentration in influent) was plotted against time into run. The data shown was the mean from four 24 hour runs. The water only backwash produced a sharp peak in filtrate quality, that receded rapidly. The peak was a function of the backwash remnants from within the filter bed. After 6.5 minutes, when this volume had been displaced, the quality was greatly improved. Removal efficiency continued to increase as the volume of the backwash remnants from above the bed was displaced. After this time, 14 minutes, the

filter had very nearly reached steady state, i.e. ripened.

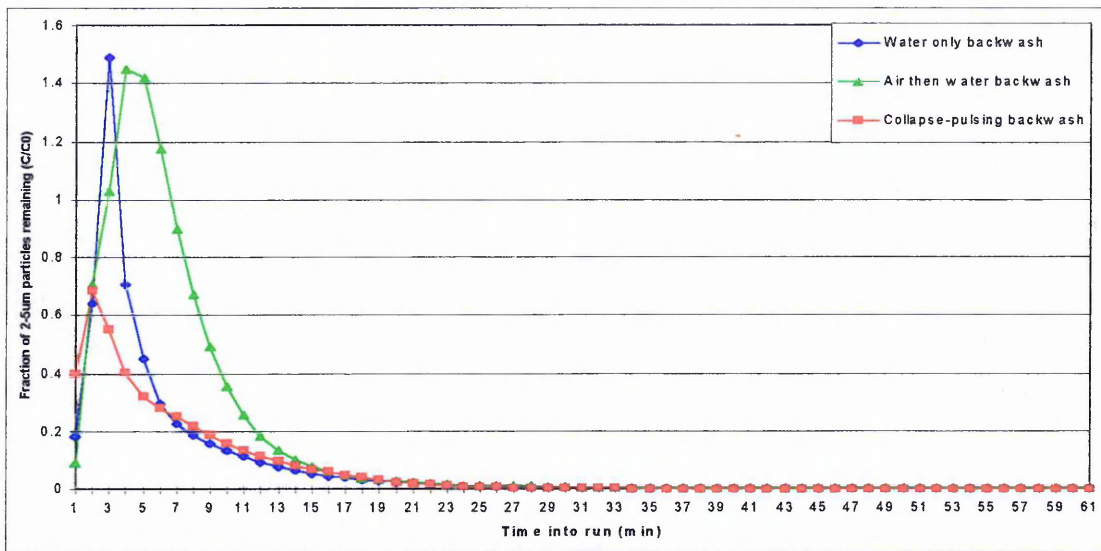


**Figure 7.1. Fraction of 2-5µm particles in filtrate after different backwash regimes.**

The air followed by water backwash resulted in a filtrate quality peak of similar magnitude but a longer duration. This peak was, therefore, a function of both of the backwash components. As the portion from above the bed was displaced the removal efficiency improved. The filter ripened after about the same time as the previous example.

The peak in filtrate quality after the CP backwash can be seen to be very much less than those produced after the other backwash regimes. However, the increase in removal efficiency appeared to be slightly slower, since the filter ripened after approximately the same time as the other filters.

The amount of particulate matter, measured by backwash water turbidity, that was washed out of the filters is illustrated in Fig. 7.2. This data was taken from one day, when all the filters washed within 5 hours. The raw water quality during the preceding 24 hours had been on average 2480/ml.

It is apparent that overflow occurred from the water only, and CP backwashed filters after about 30 seconds. Clearly, the backwash water from the water only backwashed filter was less turbid. The backwash water turbidity from this filter peaked after about 1 minute at 80 NTU, it was then reduced following the characteristic curve to a very low level. The CP washed filter's backwash water also peaked after about 1 minute but at 128 NTU. The decrease was also much slower. When the CP wash finished and the rinse started, after 240 seconds, the turbidity was still about 70 NTU. This was then successfully rinsed out over the next 5 minutes.

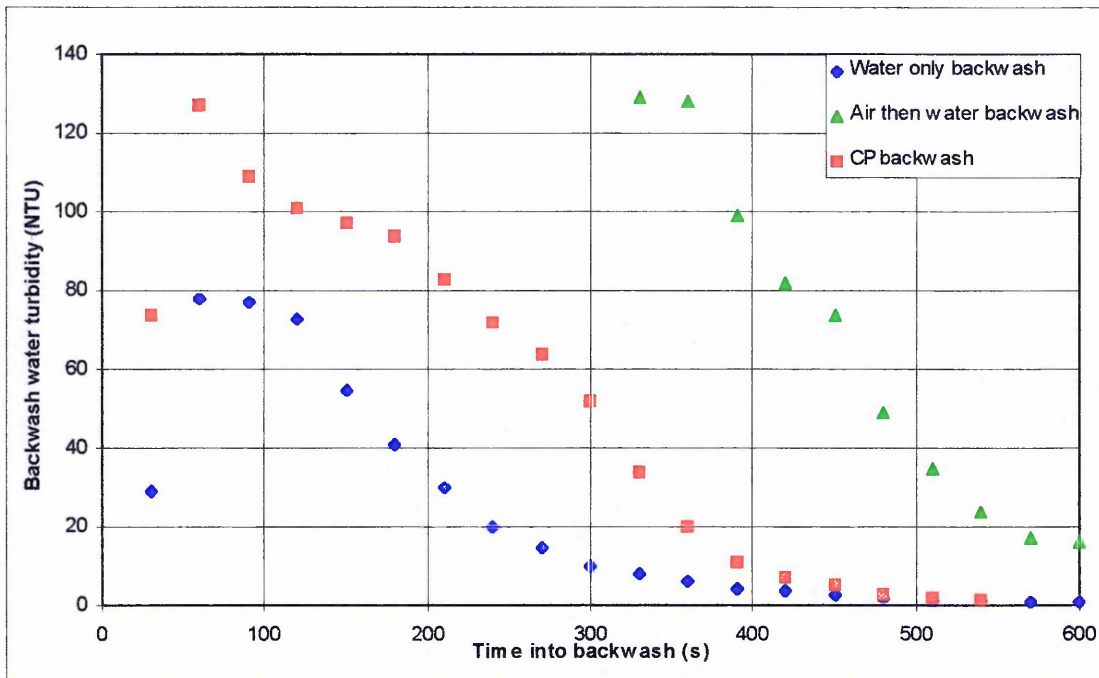


**Figure 7.2. Backwash water turbidities during different backwash regimes -0.5-1.0mm sand filters.**

The air followed by water backwashed filter obviously did not overflow for the first 5 minutes, during the air scour. It took a further 30 seconds into the water wash before overflow into the backwash weir/pipe occurred. The turbidity had a peak of equal magnitude to that from the CP washed filter. It was, however, reduced more rapidly. The level of turbidity at the end of the 5 minute water wash was still high, at 17 NTU, implying that all the particulate matter dislodged from the media during air scour was not successfully washed out. Less particulate matter, therefore, appeared to be removed from the water only washed filter. This observation was re-inforced when the headloss data for the filters was appraised (Fig. 7.3). Both the clean bed headloss, and the headloss development was greater for the water only washed filter. The clean bed headloss of the air followed by water and the CP backwashed filters was virtually the same. The rate of headloss development was slightly greater for the air followed by water washed filter. The runlengths, or time it would take to reach 2m headloss are shown in Table 7.4. The water only washed filter would reach terminal headloss 20 hours before the CP backwashed filter.



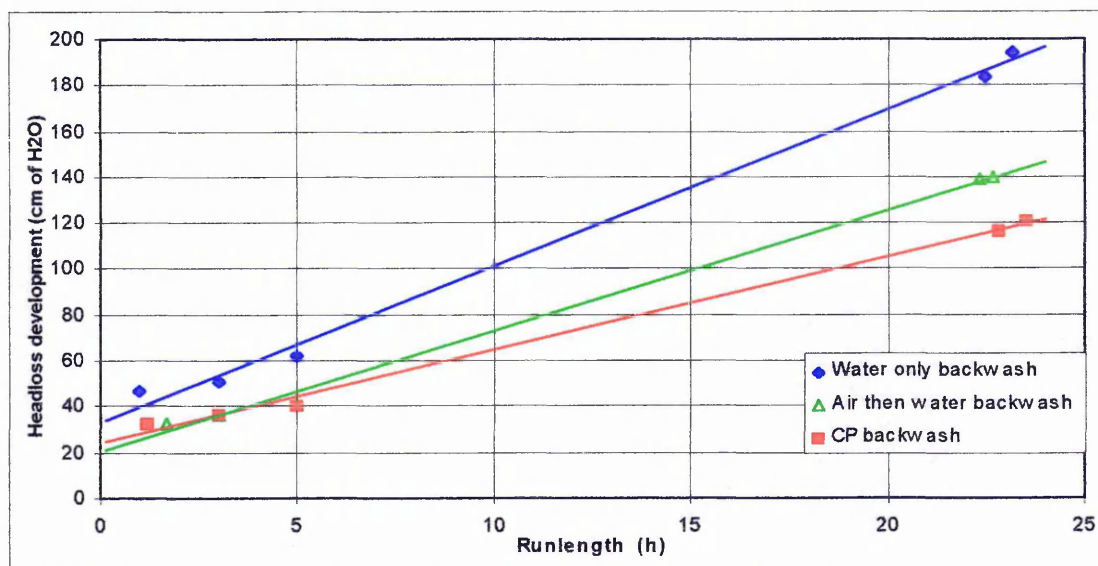


**Figure 7.3. Headloss development during filter run following different backwash regimes.**

### 7.3.1.3 2m beds of 2.0-3.35mm sand.

Similar trends were seen to occur when the performance of the 2m beds of 2.0-3.35mm sand was assessed. The water only backwash produced a large initial peak in filtrate quality, shown in Fig 7.4, which had virtually disappeared by the time the backwash remnants within the media had been displaced (10.6 minutes). A slight second peak was apparent which was a function of the backwash remnants above the bed. The removal efficiency then slowly increased until the filter had ripened after about 43 minutes.

The air followed by water backwashed filter had a lower initial peak, but a higher second peak. Therefore more particles from the backwash remnants above the bed were entering into the filtrate. The CP backwashed filter performed in a similar manner, the initial peak was greatly reduced but a large number of particles from the portion of backwash remnants above the media entered into supply. The removal efficiency increased slowly until the filters had ripened.

The backwash water turbidity, Fig 7.5, shows that a highly turbid backwash water overflowed from the water only washed filter after about 30 seconds. This initial high was rapidly reduced, indeed by 175 seconds into the backwash the turbidity was less than 5 NTU. The fact that material was still in the filter was illustrated when the turbidity of the backwash water from the CP washed filter was

examined. The first reading was taken after 80 seconds, and was lower than the water only wash. However, the levels were still high when the CP wash was completed and the rinse started (240 minutes). Any deposits that were dislodged by the CP wash were then successfully rinsed out. The air followed by water wash had an initial turbidity, when it started to overflow, as that of the CP filter. It was however, rapidly reduced, after only 2 minutes any deposits detached by the air scour had been rinsed out.

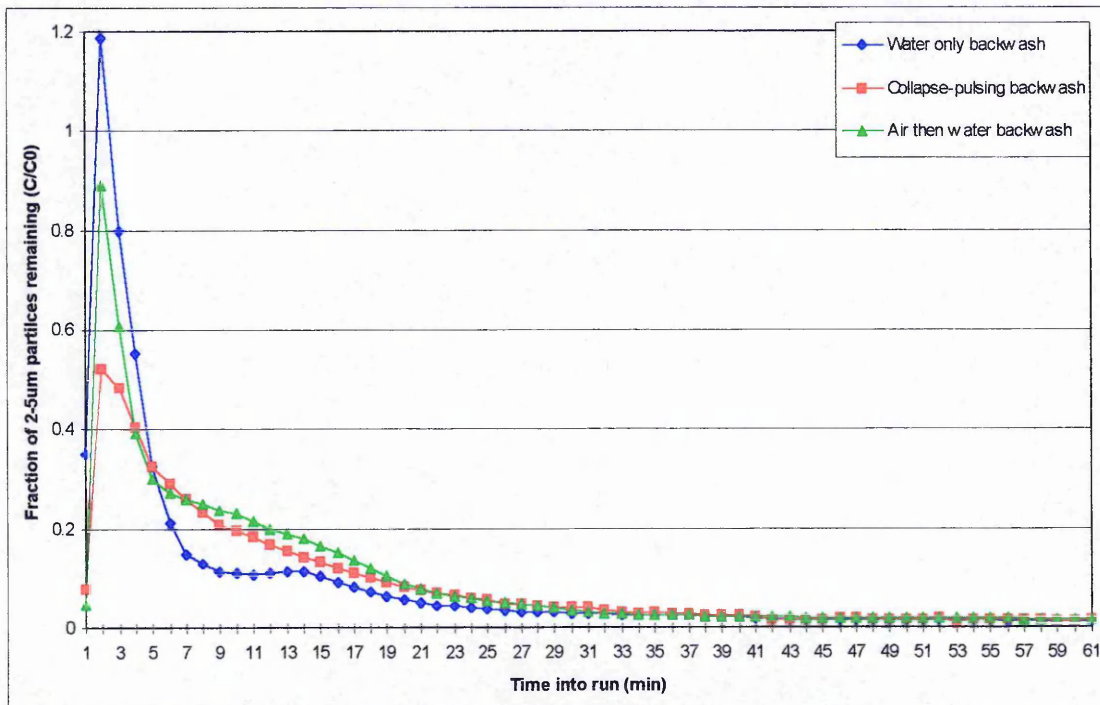


**Figure 7.4. Fraction of 2-5µm particles in filtrate after different backwash regimes.**

The headloss data, Fig 7.6, again reflects the amount of material left in the filter after backwash. The water only washed filter, which had the least particulate matter rinsed out had both a slightly higher clean bed headloss and a higher rate of headloss development. This filter had an estimated runlength of 160 hours. When this is compared with the CP washed filter it is obviously much lower, the CP filter had an estimated runlength of 230 hours. The air followed by water wash had a very similar clean bed headloss but a higher rate of headloss development compared to the CP washed filter.

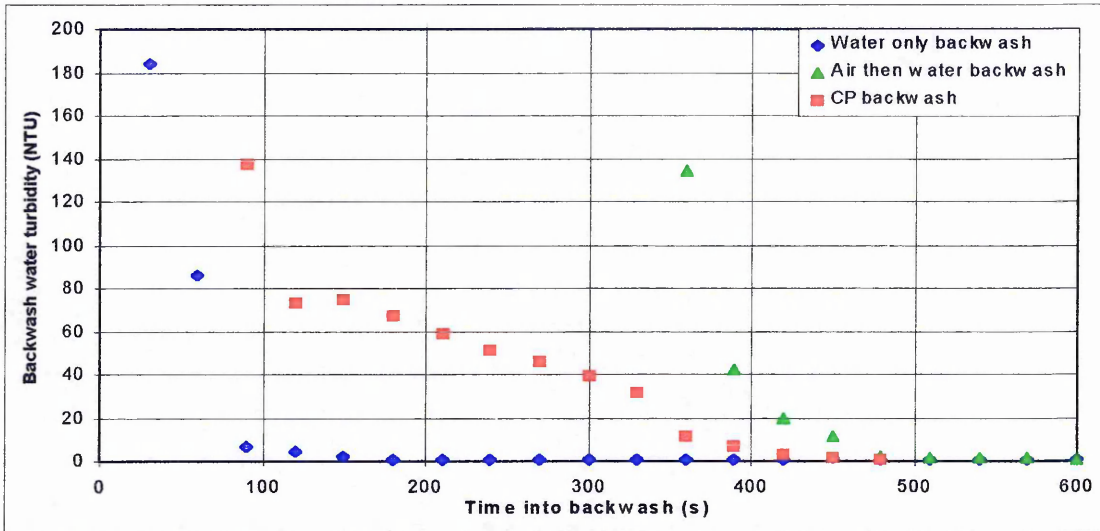


Figure 7.5. Backwash water turbidities during different backwash regimes.

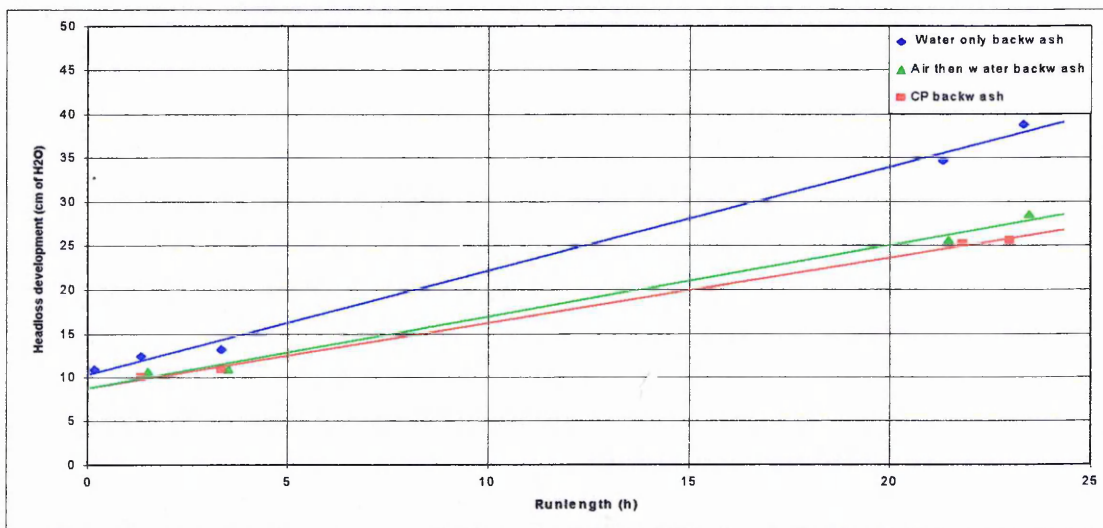


Figure 7.6. Headloss development during filter run following different backwash regimes.

### 7.3.1.3 Backwash regime summary

The results of the backwash regime assessment are summarised in Table 7.4. The estimated runlengths are shown, along with the average NPF values found in all the backwash components. It is apparent from Table 7.4 that the majority of the particles entering into the filtrate were a function of the backwash remnants within the media for the water only washed filters. The other two components contribute relatively little for these filters. The same can be said for the filters washed by air then water, although, more so for the 1m bed of 0.5-1.0mm sand. In addition, the filters cleaned by this backwash regime have the highest levels of particulates in the filtrate as a function of the backwash remnants

backwash remnants above the media. The filters cleaned by a CP backwash had a higher % contribution from those particles that were a function of the influent. Overall, the CP backwash resulted in the fewest particles in the filtrate during ripening.

**Table 7.4 Average NPF for backwash components after different backwashing regimes.**

Backwash regime → Performance parameter ↓	0.5-1.0mm sand			2.0-3.35mm sand		
	Water only	Air then water	CP	Water only	Air then water	CP
Average runlength (time to reach 2m headloss)	24.5	33 (est)	44 (est)	160 (est)	210 (est)	230 (est)
2-5µm NPF in backwash remnants within media	4.10 x 10 <sup>7</sup>	6.78 x 10 <sup>7</sup>	2.78 x 10 <sup>7</sup>	4.25 x 10 <sup>7</sup>	4.09 x 10 <sup>7</sup>	3.49 x 10 <sup>7</sup>
2-5µm NPF in backwash remnants above media	1.05 x 10 <sup>7</sup>	2.89 x 10 <sup>7</sup>	1.25 x 10 <sup>7</sup>	7.20 x 10 <sup>6</sup>	1.18 x 10 <sup>7</sup>	9.60 x 10 <sup>6</sup>
2-5µm NPF in all backwash remnants	5.15 x 10 <sup>7</sup>	9.72 x 10 <sup>7</sup>	4.04 x 10 <sup>7</sup>	4.97 x 10 <sup>7</sup>	5.27 x 10 <sup>7</sup>	4.46 x 10 <sup>7</sup>
2-5µm NPF as function of influent	4.42 x 10 <sup>6</sup>	5.47 x 10 <sup>6</sup>	4.12 x 10 <sup>6</sup>	1.13 x 10 <sup>7</sup>	1.45 x 10 <sup>7</sup>	1.43 x 10 <sup>7</sup>
Total 2-5µm NPF	5.59 x 10 <sup>7</sup>	1.02 x 10 <sup>8</sup>	4.45 x 10 <sup>7</sup>	6.12 x 10 <sup>7</sup>	6.72 x 10 <sup>7</sup>	5.89 x 10 <sup>7</sup>

### 7.3.2 Backwash duration assessment

#### 7.3.2.1 Influent conditions

During this trial the influent quality was found to be very consistent in terms of both turbidity and particle count. Quality was monitored continually by the SCADA system on site, and by random samples sent off-site for analysis (turbidity, pH, iron content). The influent quality during the trial is summarised in Table 7.5.

**Table 7.5. Summary of raw water conditions during trial.**

	pH	Turbidity (NTU)	Manganese (µg/l)	Iron (µg/l)	Colour (°Hazen)	Particle count (No./ml)
Mean	8.43	0.32	7.06	30.12	4.94	2002.2
Std. Dev	0.12	0.14	4.03	8.96	1.87	302.7
Min	7.8	0.23	3	15	3	1719.4
Max	8.7	0.6	19	48	12	2505.9

### 7.3.2.2 1m bed of 0.5-1.0mm sand

The data presented in this section (and in the following section) was obtained over a period of four months. Mean filtrate particle counts are shown, with data taken from at least 3 runs; error bars displaying the standard error associated with each mean value (95% confidence) are included in the graphs. The NPF data has also been averaged, and the means are plotted.

The particle count data for the 1 minute CP backwash duration is plotted in Fig 7.7. The data shown is the mean values taken from 5 runs. It can be seen that a high degree of variability was displayed in the particle counts recorded in the filtrate following the 1 minute CP wash. It was found that the filtrate particle count got successively greater after each run and backwash. The initial peak appeared to be a function of the volume of backwash remnants contained within the filter bed; this component had a theoretical retention time of 6.2 minutes. The variability in this component was high. The receding limb that followed was a function of both the volume of backwash water retained above the media, which had a theoretical retention time of 13.7 minutes, and the interface with the influent. A steady state value was reached after 57 minutes, however, it was very high (233 /ml) and unacceptable in terms of treatment objectives.

It is important to realise that the data in Fig. 7.7 and indeed for all the particle count data, was for the 2-5 $\mu$ m particles, which were used as performance indicators. The larger particles measured by the particle counter (5-400 $\mu$ m) had an initial peak magnitude of approx. 658/ml, this was much lower than the 2-5 $\mu$ m peak. From Table 7.6 it can be seen that the large particles reached a steady state value more rapidly than the 2-5 $\mu$ m particles, 39 minutes compared to 55 minutes, following the 1 minute CP backwash.

The mean filtrate particle count data (3 runs) from the filter after a 2 minute CP backwash is shown in Fig 7.8. The magnitude of the initial peak was reduced, relative to the previous example, as was the variability. The component with the most variability in this example was the volume corresponding to the interface with the influent. The ripening time for the filter following a 2 min CP backwash, was on average 54 minutes, the steady state value of 28.2/ml was much more acceptable. The removal efficiency of the filter for larger particles (5-400 $\mu$ m) improved more rapidly than that for the 2-5 $\mu$ m particles; 42 minutes compared to 54 minutes.

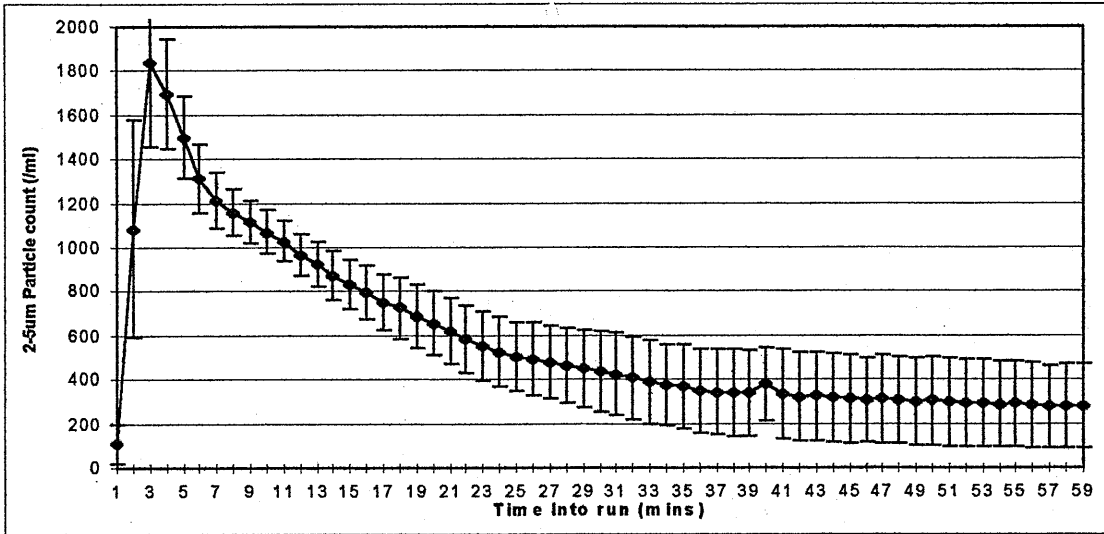


**Figure 7.7. Filtrate 2-5µm particle count following 1 minute CP backwash - 0.5-1.0mm sand.**

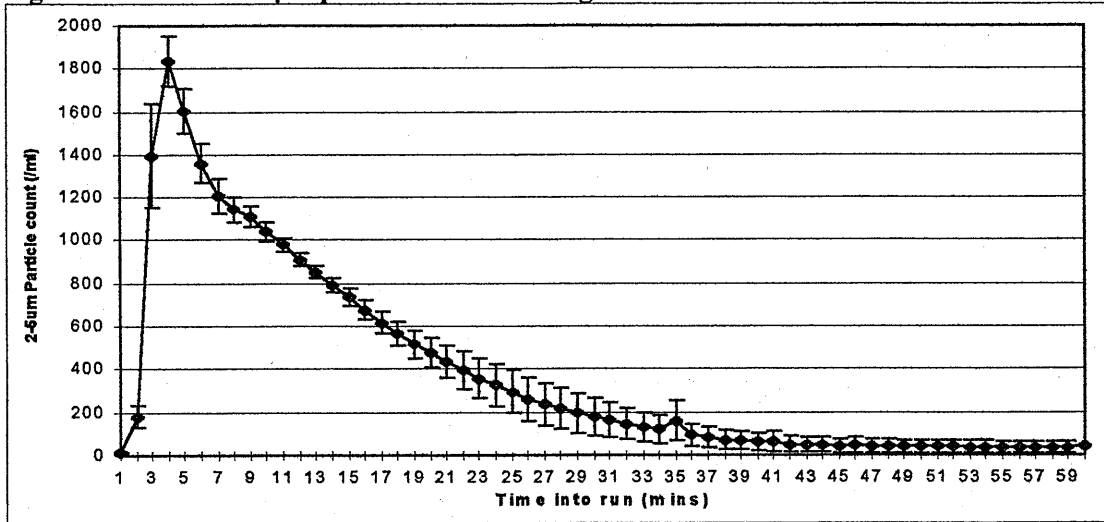


**Figure 7.8. Filtrate 2-5µm particle count following 2 minute CP backwash -0.5-1.0mm sand.**

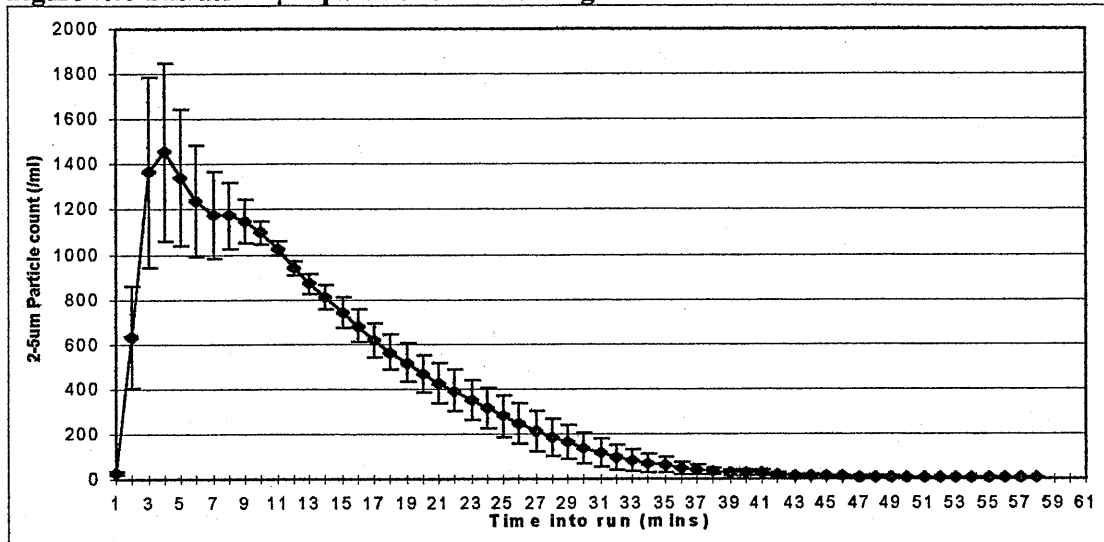


**Figure 7.9. Filtrate 2-5µm particle count following 3 min CP backwash-0.5-1.0mm sand.**

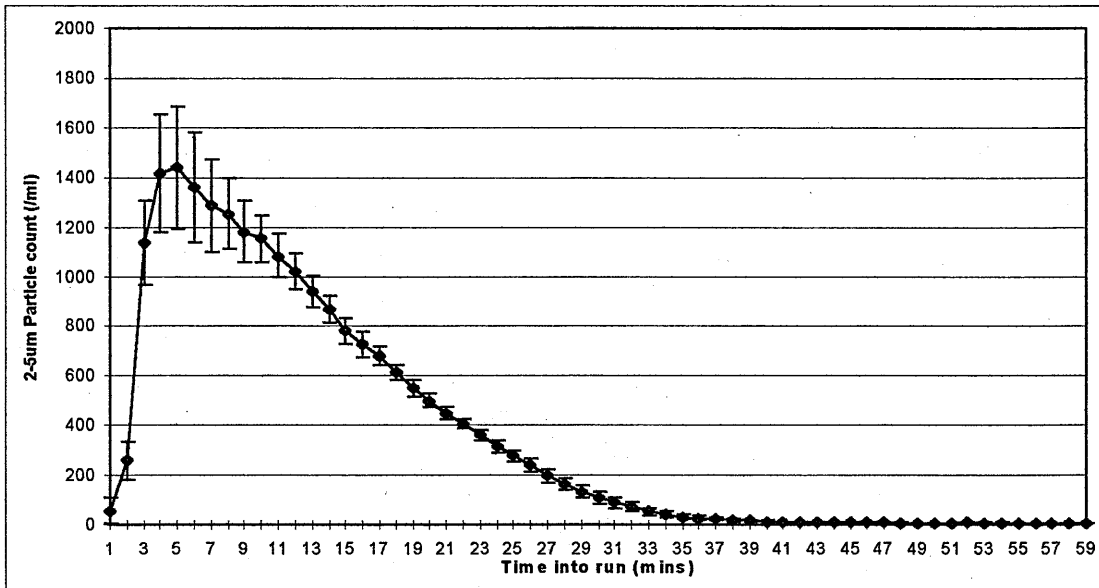


**Figure 7.10 Filtrate 2-5µm particle count following 4 minute CP backwash -0.5-1.0mm sand.**

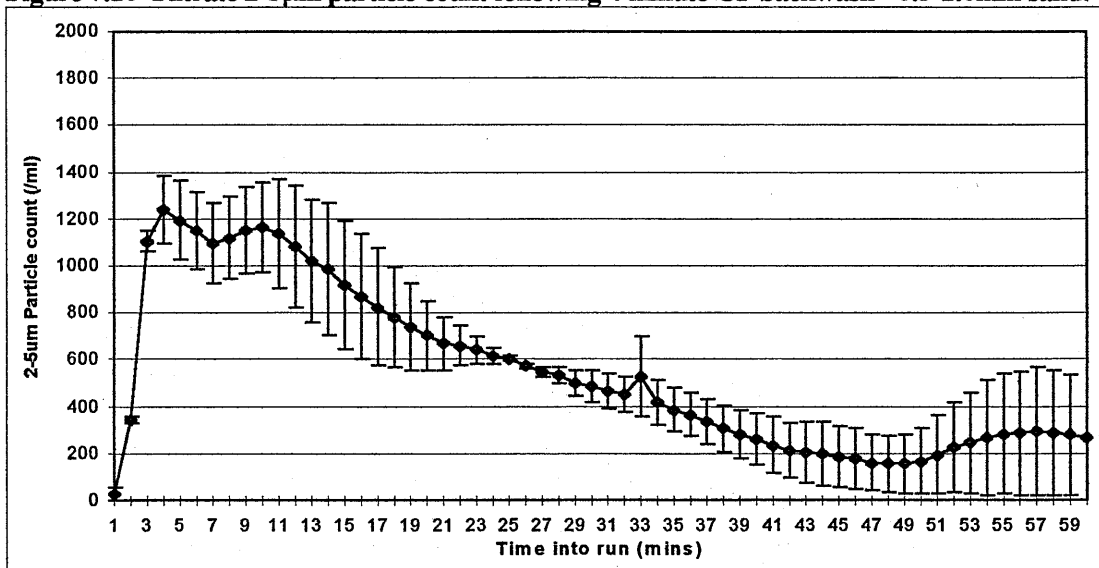


**Figure 7.11 Filtrate 2-5µm particle count following 5 minute CP backwash -0.5-1.0mm sand.**

Fig 7.9 shows the mean filtrate particle count after a 3 minute CP backwash (3 runs). The initial peak was reduced still further to 1460 2-5µm particles /ml. There was however, considerable variability associated with the volume of backwash water retained within the media. Interestingly, there was a double peak in the particle count, the second peak corresponded to the interface between the backwash remnants retained within the bed and the backwash remnants retained above the bed. The filter reached steady state, or ripened, more rapidly following the 3 minute CP backwash - 48 minutes.

**Table 7.7. Filter performance parameters for a range of CP backwash durations - 1m beds of 0.5-1.0mm sand.**

Filter performance parameter	Collapse-pulsing backwash duration (mins)				
	1	2	3	4	5
Average runlength (time to reach 2m headloss)	21	27	34	38	44
Breakthrough occurring at end of run ?	No	No	No	No	No
Time to reach steady state (2-5µm)	55mins (3.56)	54mins (3.61)	48mins (4.02)	42mins (0.57)	56mins (4.56)
Steady state value (No. of 2-5µm/ml)	233.1 (310.6)	28.2 (12.9)	20.59 (11.05)	9.8 (0.01)	125.6 (163.9)
Time to reach steady state (5-400µm)	38.8mins (3.59)	42.3mins (2.9)	40.0mins (3.44)	21.6mins (4.10)	35.7mins (4.04)
Steady state value (No. of 5-400µm/ml)	18.3 (14.90)	9.6 (3.74)	12.9 (8.61)	2.6 (0.63)	25.6 (13.6)
2-5µm NPF in backwash remnants within media	5.24 x 10 <sup>7</sup> (1.54 x 10 <sup>7</sup> )	4.40 x 10 <sup>7</sup> (1.90 x 10 <sup>7</sup> )	4.73 x 10 <sup>7</sup> (6.18 x 10 <sup>6</sup> )	4.28 x 10 <sup>7</sup> (1.15 x 10 <sup>7</sup> )	5.68 x 10 <sup>7</sup> (3.31 x 10 <sup>7</sup> )
2-5µm NPF in backwash remnants above media	5.71 x 10 <sup>7</sup> (9.78 x 10 <sup>6</sup> )	5.61 x 10 <sup>7</sup> (4.21 x 10 <sup>6</sup> )	5.49 x 10 <sup>7</sup> (4.99 x 10 <sup>6</sup> )	5.97 x 10 <sup>7</sup> (9.12 x 10 <sup>6</sup> )	6.06 x 10 <sup>7</sup> (2.74 x 10 <sup>7</sup> )
2-5µm NPF in all backwash remnants	1.13 x 10 <sup>8</sup> (2.71 x 10 <sup>7</sup> )	1.03 x 10 <sup>8</sup> (2.44 x 10 <sup>7</sup> )	1.03 x 10 <sup>8</sup> (9.48 x 10 <sup>6</sup> )	1.04 x 10 <sup>8</sup> (2.02 x 10 <sup>7</sup> )	9.96 x 10 <sup>7</sup> (1.63 x 10 <sup>7</sup> )
2-5µm NPF as function of influent	1.34 x 10 <sup>8</sup> (1.01 x 10 <sup>8</sup> )	9.18 x 10 <sup>7</sup> (6.90 x 10 <sup>7</sup> )	6.66 x 10 <sup>7</sup> (3.25 x 10 <sup>7</sup> )	4.69 x 10 <sup>7</sup> (6.84 x 10 <sup>6</sup> )	1.31 x 10 <sup>8</sup> (4.89 x 10 <sup>7</sup> )
Total 2-5µm NPF	2.48 x 10 <sup>8</sup> (1.19 x 10 <sup>8</sup> )	1.94 x 10 <sup>8</sup> (6.42 x 10 <sup>7</sup> )	1.69 x 10 <sup>8</sup> (2.93 x 10 <sup>7</sup> )	1.51 x 10 <sup>8</sup> (2.71 x 10 <sup>7</sup> )	2.31 x 10 <sup>8</sup> (1.71 x 10 <sup>7</sup> )

Figures in brackets are standard deviations.



The mean filtrate particle count following the 4 minute CP backwash is shown in Fig 7.10. It has a very similar magnitude and shape to the 3 minute CP backwash particle count. There was some variability in the initial peak, however, the receding limb was very reproducible as indicated by the very small error bars. The double peak apparent in the 3 minute CP data was not as obvious in this example. The filter had a shorter ripening time, of 42 minutes, after the 4 minute CP backwash. The ripening time for the larger particles following this backwash was also greatly reduced - 22minutes.

The mean filtrate particle count following a 5 minute CP backwash (Fig.7.11) has a number of differences to the preceding examples. The initial peak has a slightly lower magnitude - 1220/ml - it also showed less variability. However, the second peak and the receding limb that follows showed a high degree of variability. The receding limb itself indicated the filter was taking a longer time to ripen than expected following the 5 minute CP backwash. The average ripening time for the filter under these backwash conditions was 56 minutes, with a steady state of 125 2-5 $\mu$ m particles/ml.

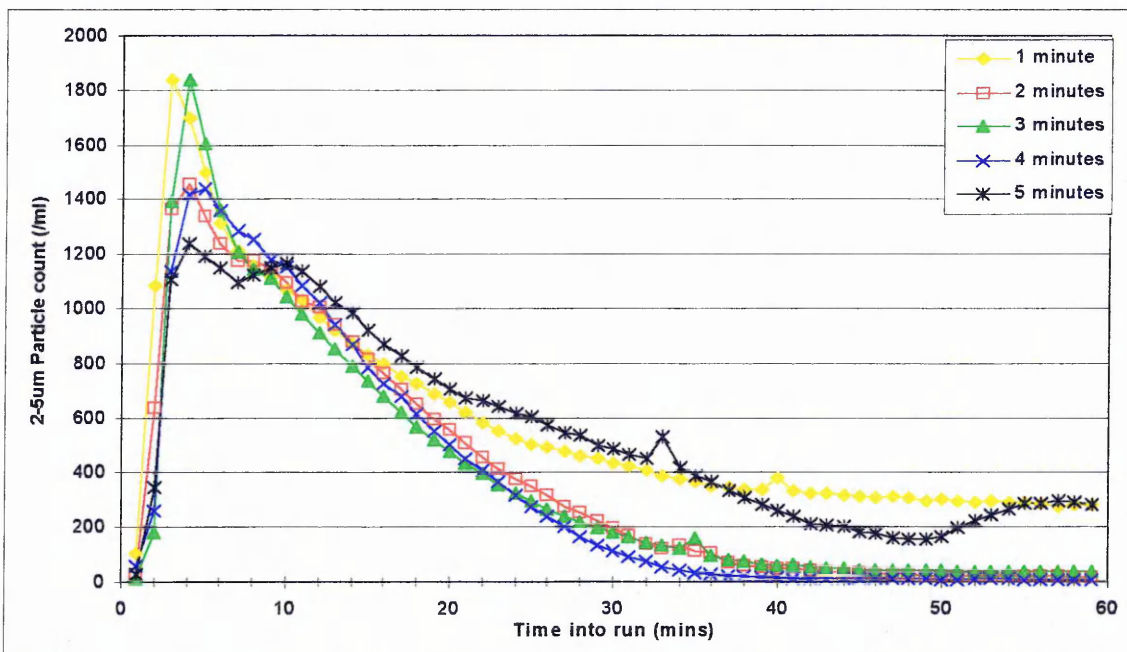


**Figure 7.12. Comparison of filtrate particles counts following a range of CP backwash durations - 0.5-1.0mm sand filter.**

When the mean particle counts from the filter under all the collapse-pulsing backwash durations are displayed on the same axis, as in Fig 7.12, the relative differences in performance become apparent. Both the 1 minute and 5 minute backwash durations produced a filtrate with higher particle counts. The counts from the 2, 3 and 4 minute backwash durations showed some similarities. When the numbers of

2-5 $\mu$ m particles reaching the filtrate were calculated and broken down into the components responsible for filter ripening as in Table 7.7, and plotted in Fig 7.13, a clearer picture of what was occurring emerged. The numbers of 2-5 $\mu$ m particles in the volume of backwash water retained both within and above the filter media were relatively constant. There was however a slight increase in numbers after the 5 minute duration.

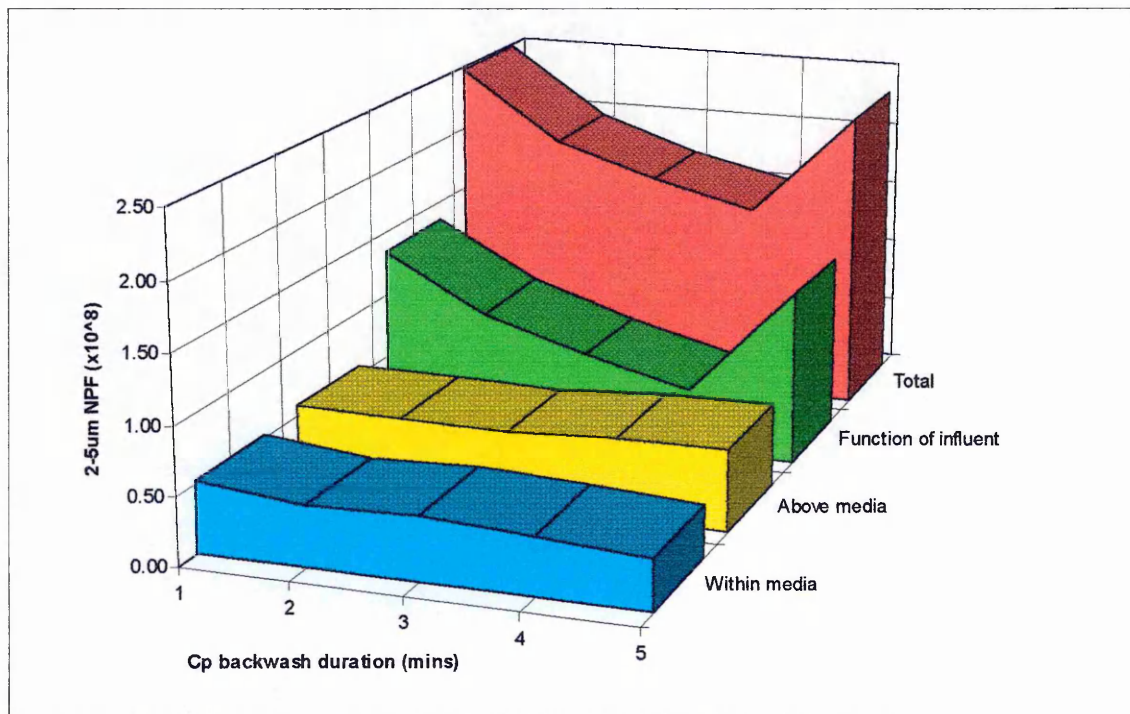


**Figure 7.13. Numbers of 2-5 $\mu$ m particles in the components of ripening following a range of CP backwash durations - 0.5-1.0mm sand filter.**

The effect of the different collapse-pulsing backwash durations appears to have been on the component that was a function of the influent, that is the time to ripen was affected. It was this component that influenced the total NPF and the two are plotted in Fig. 7.14 with associated errors displayed.

The NPF as a result of the influent and total NPF were high for the 1 minute duration, they were reduced as the backwash duration was increased until a minimum was reached after the 4 minute CP backwash. The NPF then increased for the 5 minute backwash duration.

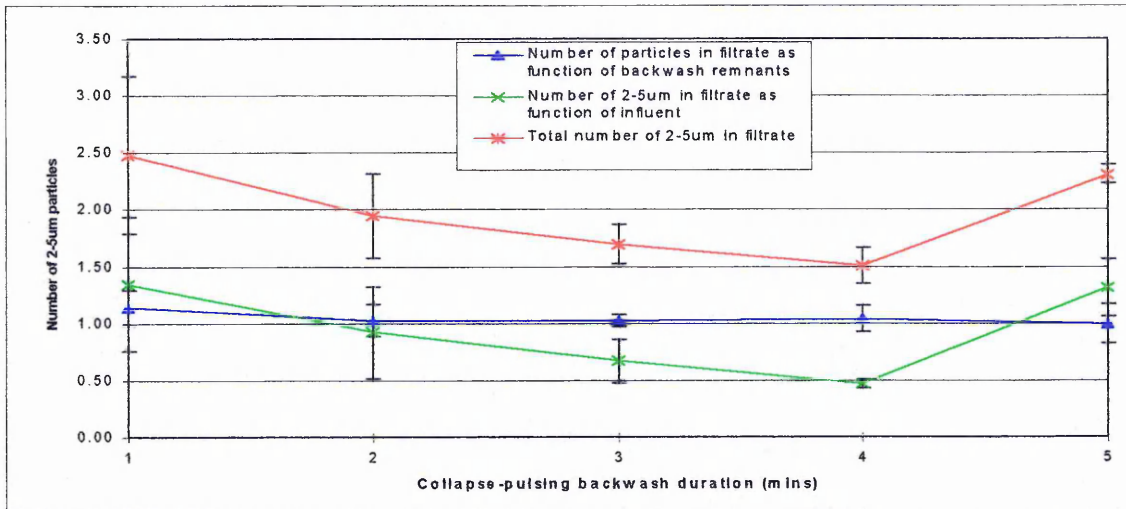


**Figure 7.14.** How the NPF following a range of CP backwash was affected by total backwash remnants and influent - 0.5-1.0mm sand.

The collapse-pulsing backwash duration had an effect upon other aspects of filter performance. The "cleaned" bed headloss, the rate of headloss development, and therefore, the runlength achievable were dependent upon the backwash duration. The time it took for the filter to reach 2m loss of head under the different durations is shown in Table 7.7. The rate of headloss development is shown in Fig 7.15. It can be seen that the longer the CP backwash the lower the headloss when the filter was returned to service, and also the lower the rate of headloss development. The result of this was a difference in runlength of 23 hours between a filter with a 1 minute and a filter with a 5 minute collapse-pulsing backwash.

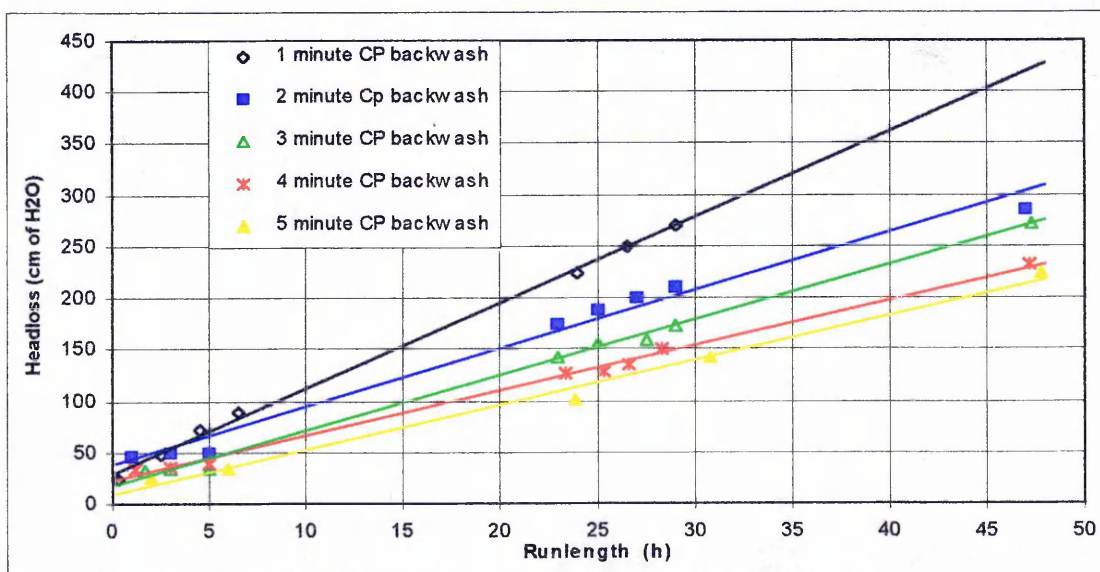


**Figure 7.15.** Headloss development following a range of CP backwash -0.5-1.0mm sand.

### 7.3.2.3 2m beds of 2.0-3.35mm sand

The particle count data for the 1 minute CP backwash duration (4 runs) is plotted in Fig. 7.16. It can be seen that a high degree of variability is displayed in the particle counts recorded in the filtrate following the 1 minute CP wash. It was found that the filtrate particle count got successively greater after each run and backwash. The initial peak appeared to be a function of the volume of backwash remnants contained within the filter bed; this component had a theoretical retention time of 10.2 minutes. The particle count decreased as this component was displaced. A very shallow second peak was evident, this peak corresponded to the interface between the volume of backwash water retained above the media, which had a theoretical retention time of 17.9 minutes, and the influent. A steady state value was reached after 58 minutes, however, it was very high (401 /ml), very variable and unacceptable in terms of treatment objectives.

The larger particles measured by the particle counter (5-400 $\mu$ m) had an initial peak magnitude of approx. 620/ml, this was much lower than the 2-5 $\mu$ m peak. From Table 7.8 it can be seen that the large particles reached a steady state value more rapidly than the 2-5 $\mu$ m particles, 45 minutes compared to 58 minutes, following the 1 minute CP backwash.

The mean filtrate particle count data (3 runs) from the filter after a 2 minute CP backwash is shown in Fig 7.17. The magnitude of the initial peak was somewhat reduced, relative to the previous example. The initial peak displayed some degree of variability, the particle counts from the backwash remnants from above the bed was found to be more consistent, as the interface with the influent was displaced the variability was further reduced. The ripening time for the filter following a 2 minute CP backwash, was on average 62 minutes, the steady state value of 152/ml was still too high to be acceptable. The removal efficiency of the filter for larger particles (5-400 $\mu$ m) improved more rapidly than that for the smaller particles - 48 minutes compared to 62 - and the steady state value was 11.6/ml.

Fig 7.18. shows the mean filtrate particle count after a 3 minute CP backwash (3 runs). The initial peak was slightly higher at 2200 2-5 $\mu$ m particles /ml. There was also considerable variability associated with the volume of backwash water retained within the media.

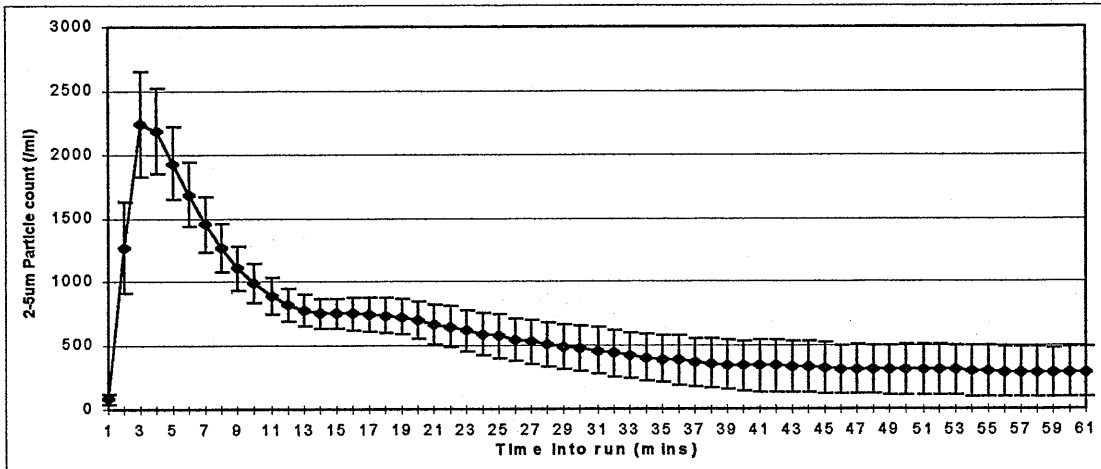


Figure 7.16 Filtrate 2-5µm particle count following 1 minute CP backwash -2.0-3.35mm sand.

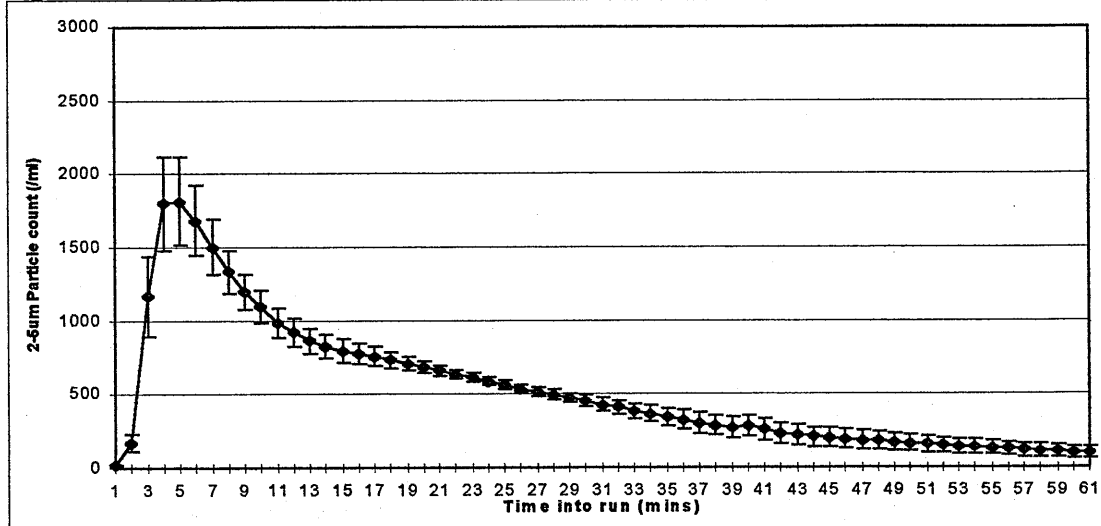


Figure 7.17 Filtrate 2-5µm particle count following 2 minute CP backwash -2.0-3.35mm sand.

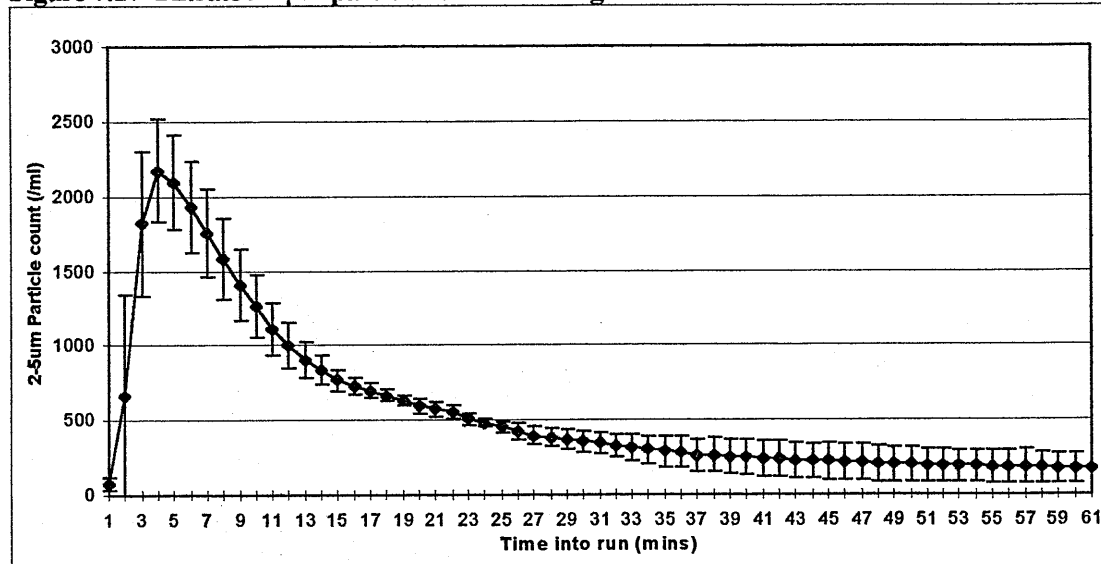


Figure 7.18 Filtrate 2-5µm particle count following 3 minute CP backwash -2.0-3.35mm sand.

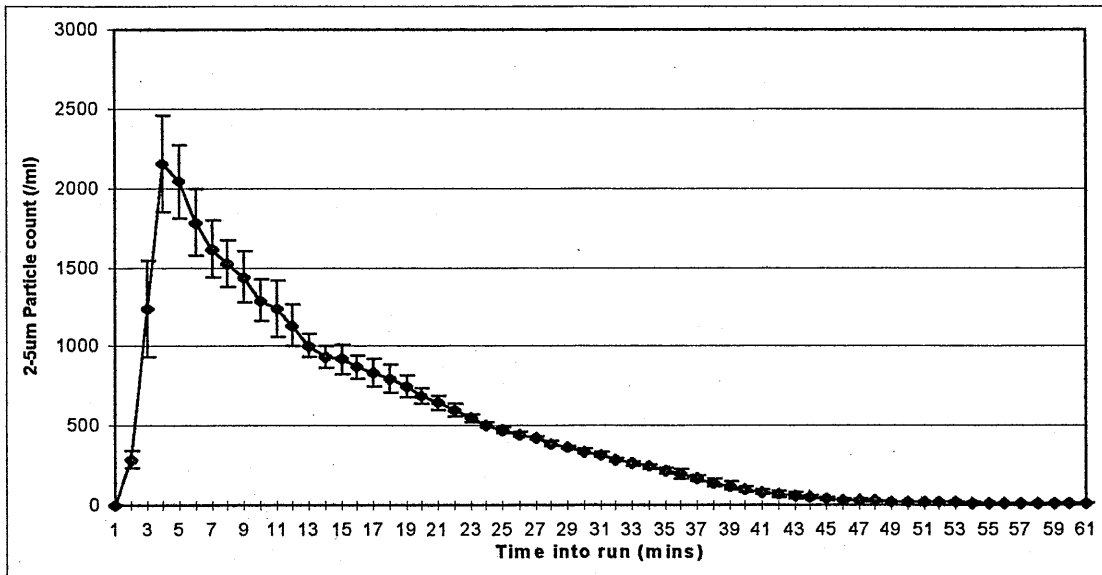


Figure 7.18 Filtrate 2-5µm particle count following 4 minute CP backwash -2.0-3.35mm sand.

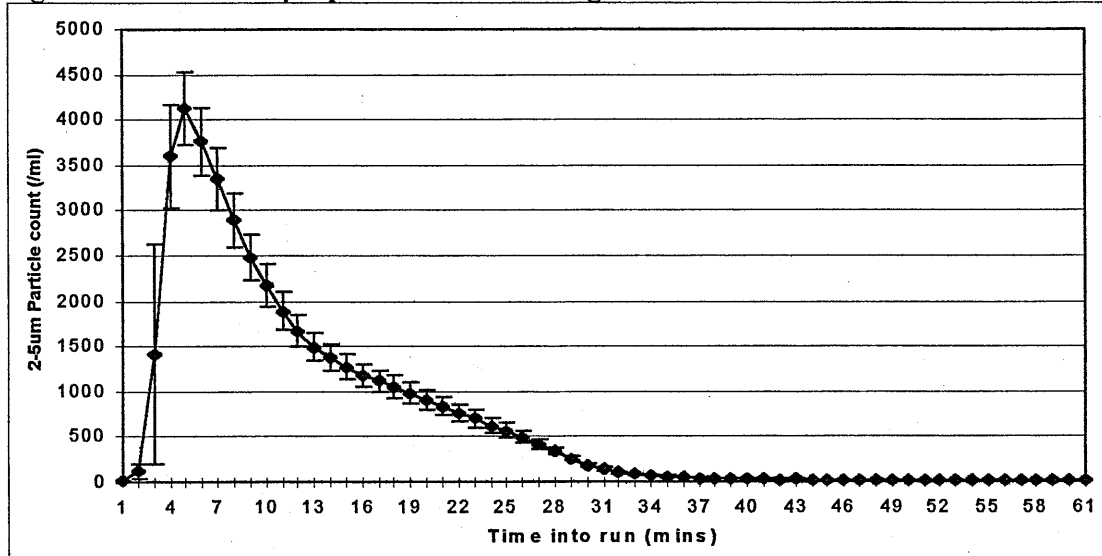


Figure 7.19 Filtrate 2-5µm particle count following 5 minute CP backwash -2.0-3.35mm sand.

The filter reached steady state, or ripened, after a similar time, on average 61 minutes following the 3 minute CP backwash. The steady state value was also lower at 130/ml, an improvement but still too high.

The mean filtrate particle count following the 4 minute CP backwash is shown in Fig 7.18. It had a very similar magnitude to the 3 minute CP backwash particle count. However, it was found to ripen more rapidly, in 49 minutes. There was some variability in the initial peak, however, the receding limb was very reproducible as indicated by the very small error bars.

**Table 7.8. Filter performance parameters for a range of CP backwash durations - 2m bed of 2.0-3.35mm sand**

Filter performance parameter	Collapse-pulsing backwash duration (mins)				
	1	2	3	4	5
Average runlength (time to reach 2m headloss)	110	160	200	250	330
Breakthrough occurring at end of run ?	No	No	No	No	No
Time to reach steady state (2-5µm)	58.3mins (3.2)	62.8mins (2.9)	61.3mins (4.8)	49.3mins (2.5)	48.0mins (1.7)
Steady state value (No. of 2-5µm/ml)	401.5 (449.3)	152 (95.5)	123.9 (159.1)	21.67 (2.8)	30.1 (6.1)
Time to reach steady state (5-400µm)	45.3mins (3.8)	48.0mins (1.73)	39.7mins (1.5)	42.3mins (1.53)	46.6mins (2.3)
Steady state value (No. of 5-400µm/ml)	23.9 (25.7)	11.6 (12.1)	10.7 (10.3)	4.9 (0.9)	10.6 (3.8)
2-5µm NPF in backwash remnants within media	1.01 x 10 <sup>8</sup> (3.65 x 10 <sup>7</sup> )	9.06 x 10 <sup>7</sup> (2.26 x 10 <sup>7</sup> )	1.01 x 10 <sup>8</sup> (8.22 x 10 <sup>6</sup> )	9.72 x 10 <sup>7</sup> (1.63 x 10 <sup>7</sup> )	1.73 x 10 <sup>8</sup> (3.19 x 10 <sup>7</sup> )
2-5µm NPF in backwash remnants above media	4.79 x 10 <sup>7</sup> (1.21 x 10 <sup>7</sup> )	4.46 x 10 <sup>7</sup> (1.05 x 10 <sup>7</sup> )	4.66 x 10 <sup>7</sup> (5.81 x 10 <sup>6</sup> )	5.14 x 10 <sup>7</sup> (9.90 x 10 <sup>6</sup> )	7.41 x 10 <sup>7</sup> (1.38 x 10 <sup>7</sup> )
2-5µm NPF in all backwash remnants	1.49 x 10 <sup>8</sup> (4.82 x 10 <sup>7</sup> )	1.35 x 10 <sup>8</sup> (3.24 x 10 <sup>7</sup> )	1.48 x 10 <sup>8</sup> (6.84 x 10 <sup>7</sup> )	1.48 x 10 <sup>8</sup> (1.76 x 10 <sup>7</sup> )	2.48 x 10 <sup>8</sup> (4.21 x 10 <sup>7</sup> )
2-5µm NPF as function of influent	1.53 x 10 <sup>8</sup> (1.09 x 10 <sup>8</sup> )	8.64 x 10 <sup>7</sup> (2.87 x 10 <sup>7</sup> )	5.69 x 10 <sup>7</sup> (2.41 x 10 <sup>7</sup> )	5.74 x 10 <sup>7</sup> (7.74 x 10 <sup>6</sup> )	5.35 x 10 <sup>7</sup> (1.09 x 10 <sup>7</sup> )
Total 2-5µm NPF	3.07 x 10 <sup>8</sup> (1.36 x 10 <sup>8</sup> )	2.23 x 10 <sup>8</sup> (4.03 x 10 <sup>7</sup> )	2.05 x 10 <sup>8</sup> (2.45 x 10 <sup>7</sup> )	2.08 x 10 <sup>8</sup> (2.23 x 10 <sup>7</sup> )	3.02 x 10 <sup>8</sup> (5.06 x 10 <sup>7</sup> )

The 2-5  $\mu\text{m}$  steady state value was much improved at 22/ml. The ripening time for the larger particles following this backwash showed no significant improvement.

The mean filtrate particle count following a 5 minute CP backwash (Fig.7.19) has a number of differences to the previous examples. The initial peak had a much greater magnitude -4150/ml - it also showed a high degree of variability. However, the receding limb that follows showed very good reproducibility. The receding limb itself indicated the filter was taking a shorter time to ripen following the 5 minute CP backwash. The average ripening time for the filter under these backwash conditions was 48 minutes, with a steady state of 30.1 2-5 $\mu\text{m}$  particles/ml.

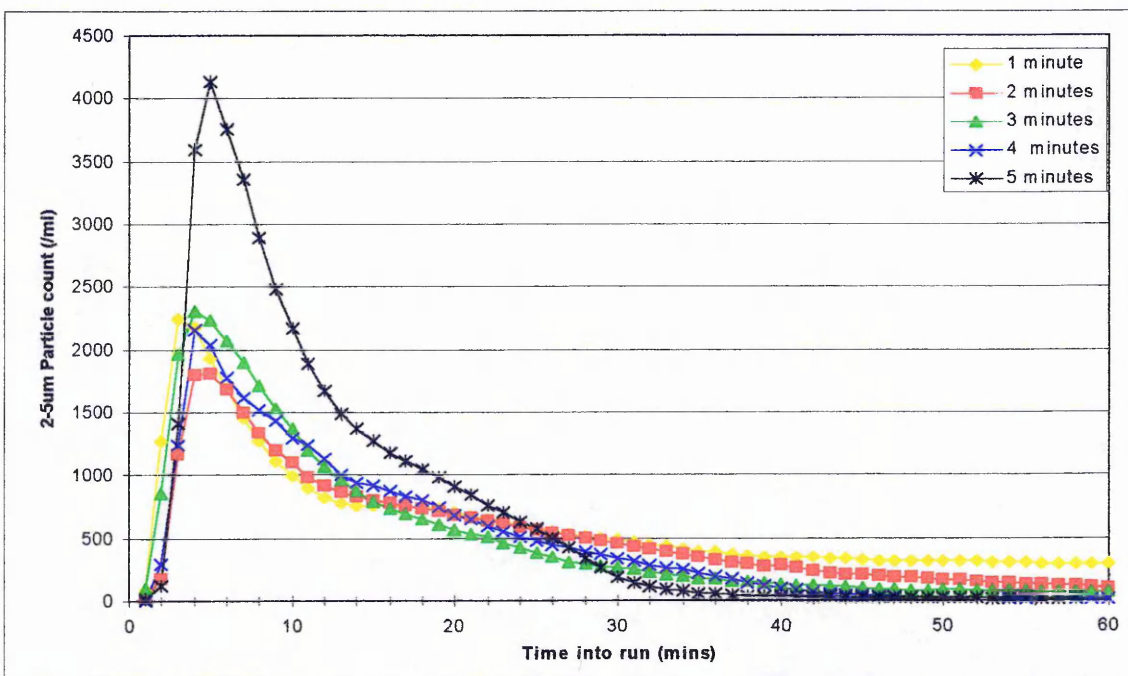


Figure 7.20. Comparison of filtrate particles counts following a range of CP backwash durations - 2.0-3.35mm sand filter.

When the mean particle counts from the filter under all the collapse-pulsing backwash durations are displayed on the same axis, as in Fig.7.20, the relative differences in performance become apparent. The 5 minute backwash duration produces a filtrate with higher particle counts, but ripens more rapidly. The counts from the 1 and 2 minute backwash durations both take a longer time to ripen and have lower removals.

When the numbers of 2-5 $\mu\text{m}$  particles reaching the filtrate are calculated and broken down into the



components responsible for filter ripening as in Table 7.8, and plotted in Fig.7.21, a clearer picture of what was occurring emerged. The numbers of 2-5 $\mu$ m particles in the volume of backwash water retained within the filter media were very much higher than for the other filter configuration. For the 1-4 minute CP durations the numbers were of a similar magnitude, after 5 minutes, however, there was a significant increase. The numbers of 2-5 $\mu$ m particles in the volume of backwash water retained above the filter media showed a similar trend but the increase after 5 minutes CP backwash was less significant. The numbers of particles in the filtrate as a function of the influent were reduced as the CP backwash duration increased.

What was occurring within the filter appeared to be different for this filter configuration compared to the previous example. However, when the total numbers of particles entering the filtrate during ripening are considered the same trend emerges, that is a clear optimum of between 2-4 minutes CP backwash.

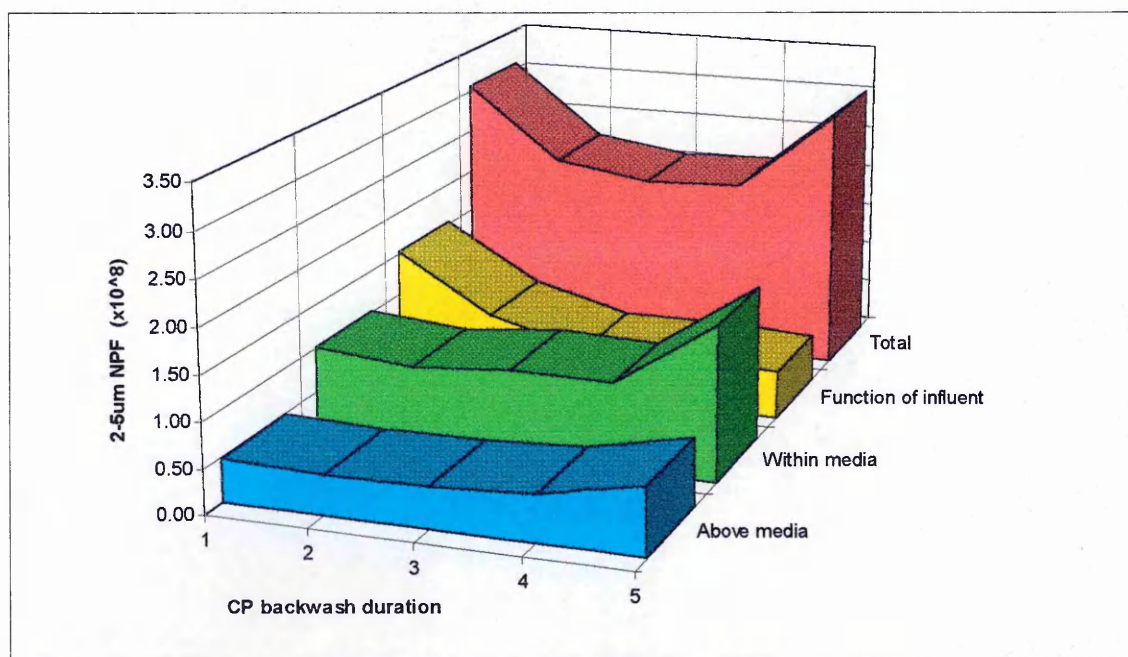


**Figure 7.21. Numbers of 2-5 $\mu$ m particles in the components of ripening following a range of CP backwash durations - 2.0-3.35mm sand filter.**

The total NPFs and the factors that influenced it are further displayed in Fig.7.22. The NPFs as a function of the total backwash remnants, and of the influent are shown with associated error bars to illustrate the reproducibility.

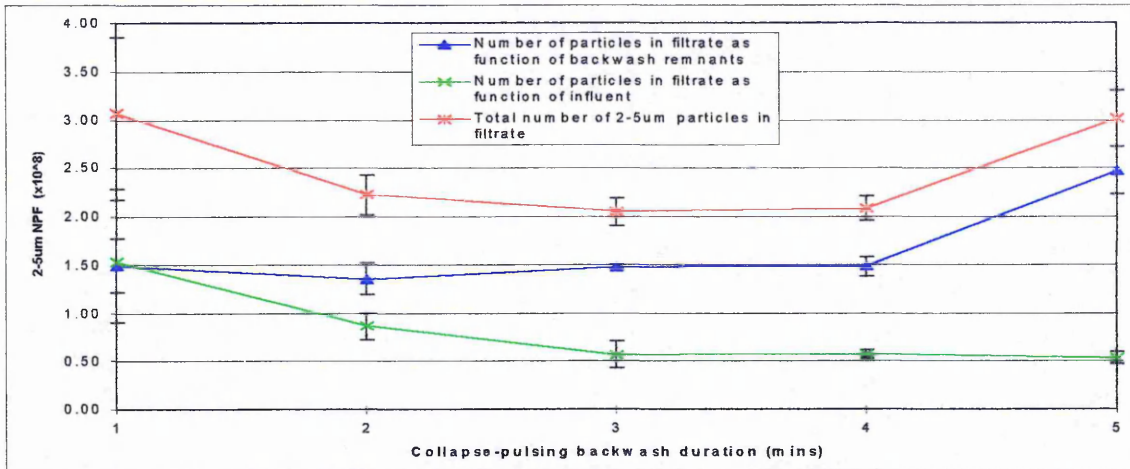


**Figure 7.22.** How the NPF following a range of CP backwash was affected by total backwash remnants and influent - 2.0-3.35mm sand.

The collapse-pulsing backwash duration had an effect upon other aspects of filter performance. The "cleaned" bed headloss, the rate of headloss development and therefore the runlength achievable were found to be dependent upon the backwash duration for this media configuration also. The time it took for the filter to reach 2m loss of head under the different durations was much greater than the 48 hours used as a runlength in this trial. It was therefore estimated from the available data and is shown in Table 7.8. The rate of headloss development is shown in Fig 7.23. It can be seen that the CP backwash had no obvious effect on the headloss when the filter was returned to service. However, the lower the rate of headloss development was affected by the CP backwash duration - the longer the backwash the lower the rate of headloss development. The result of this was a potential difference in runlength of greater than 200 hours between a filter with a 1 minute and a filter with a 5 minute collapse-pulsing backwash.

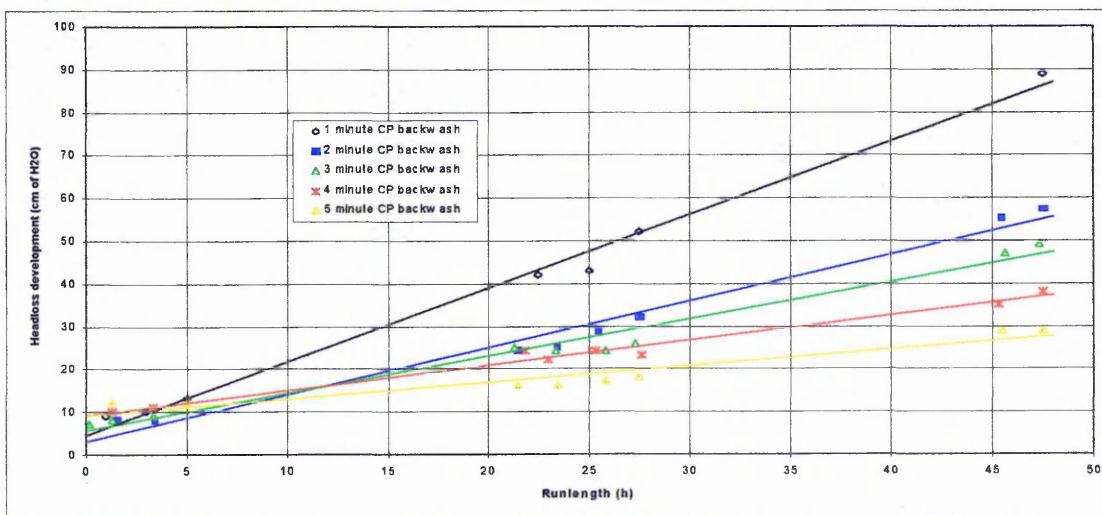


**Figure 7.23** Headloss development following a range of CP backwash - 2.0-3.35mm sand.

## 7.4 Discussion

The effectiveness of the different backwash regimes and the different backwash durations are discussed initially. The performance of the 1m beds of 0.5-1.0mm sand and the 2m beds of the 2.0-3.35mm sand following the different backwash regimes will then be discussed. The effect of the collapse-pulsing backwash duration, on filter performance will then be covered.

### 7.4.1 Backwash effectiveness

In the previous trial (chapter 6), it was suggested that the NPF, in the backwash remnants retained within the bed, was affected by the effectiveness of the backwash. In this trial three different backwash regimes of differing effectiveness were used. Water only wash is reported to be inefficient, in terms of solids detachment because of the limited amount of media collisions and abrasions that occur. Air followed by water wash is reported to be more effective than water only wash because abrasions occur in the bed during air scour. Collapse-pulsing is widely reported to be the most effective and efficient backwash regime because of the violent bed agitation that occurs.

#### 7.4.1.1 Backwash regime

The effectiveness of a backwash can be determined from the backwash water turbidity and the clean bed headloss when the filter is returned to service. The results showed that water only wash was indeed less effective than the other backwash regimes, for both filter configurations. The backwash water turbidity was lower and was reduced rapidly suggesting little in the way of solids was washed out of the filter. The clean bed headloss was greater following this backwash regime, also suggesting deposits remaining in the bed. Solids removal during an air then water backwash was less than that during the CP wash followed by a high velocity rinse, especially for the coarse 2.0-3.35mm sand filters. The clean bed headloss following these two types of backwash was, however, very similar suggesting that similar amounts of solids had been dislodged during backwash, this was better removed from the filter during the CP backwash regime. These findings are in contradiction to work published by Moll (1986, 1993, and 1996). Moll carried-out extensive trials on backwashing of a model filter, looking at the effectiveness of different water wash rates, the use of air scour, and in the final study the effectiveness of collapse-pulsing. In the early work (1986, 1993) Moll found that air scour followed by combined

air and water (not CP) made no difference to filter performance, as measured by clean bed headloss and runlength, when compared to water only wash. He concluded that volume flow of the water wash was the critical factor. When the data is closely observed it can be seen that for most of the study the water wash was at rates well below  $V_{mf}$ . Therefore deposits that had been detached from the media would not have been successfully rinsed out of the filter, in addition air would probably remain trapped in the media causing the clean bed headlosses seen in his data. When the wash rate was greater than  $V_{mf}$  successful rinsing out of the deposits and air seems to have occurred. However, the water only wash, which was Moll's control, had a longer duration and thus a greater amount of backwash water was used compared to the air and water wash (1.96 compared to 1.60 bed volumes).

The volume of backwash water used in these trials was different between regimes, and the backwash water turbidity during backwash is plotted against backwash water volume in Figs 7.25 and 7.26. Despite larger volumes of backwash water the water only wash removes far less solids from the filter. It is therefore less efficient as a cleaning wash, however, it is vital as a rinse following a CP wash in order to flush out detached deposits and air.

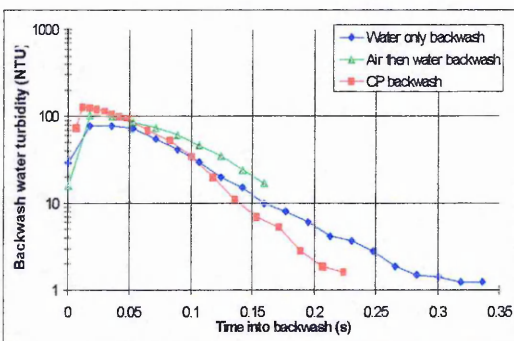


**Figure 7.25** Backwash water turbidity profiles following different backwashing regimes - 1m 0.5-1.0mm sand filter.

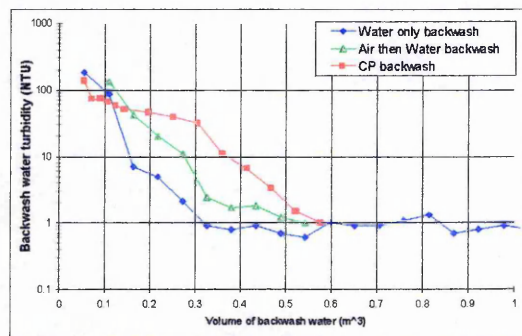


**Figure 7.26** Backwash water turbidity profiles following different backwashing regimes - 2m 2.0-3.35mm sand filter.

#### 7.4.1.2 CP backwash duration

With the rinse flowrate and duration fixed it was found that the duration of the CP backwash had a clear effect on the efficiency of the cleaning process. The clean bed headloss increased and the filter run time decreased as the CP duration decreased for both filter configurations. Thus the filter becomes cleaner the longer the CP duration. This is seen clearly in the backwash water turbidity profiles, Figs

7.27 and 7.28. The effect of the CP duration appears to be greater for the larger 2.0-3.35mm sand, this may be due to the relatively large volume flows employed.

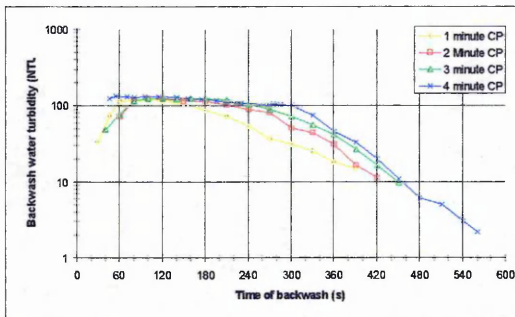


**Figure 7.27** Backwash water turbidity profiles following range of CP backwash durations - 1m 0.5-1.0mm sand filter.

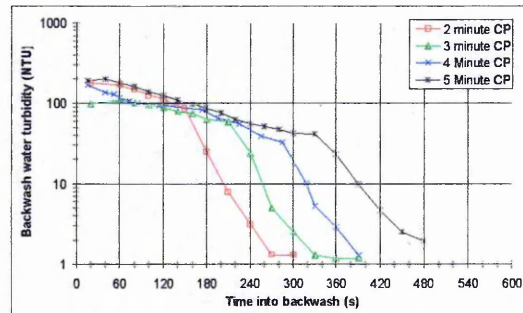


**Figure 7.28** Backwash water turbidity profiles following range of CP backwash durations - 2m 2.0-3.35mm sand filter.

In Moll's latest work (1996) the effectiveness of combined air water backwash, including collapse-pulsing backwash, with a variable rinse duration and flowrate was assessed. It is the writer's opinion that Moll misinterpreted his results. From his experimental matrix he concluded that CP was of secondary importance to the water wash. Indeed, he stated that CP during the air-water backwashing stage only had an effect on the overall result of the backwashing operation when water volume flow in the subsequent water wash was sufficient to fluidise and expand the filter media. It is the author's opinion that CP is of primary importance in terms of cleaning but the higher velocity is necessary to "unlock" the media and rinse out the detached deposits. Moll only used a fixed CP duration, and did not compare CP to combined air water wash when the rinse was sufficient to expand the media. He simply showed that after CP wash a water wash that expands the bed is necessary.

#### 7.4.2 Filter performance during ripening

Collapse-pulsing backwash was confirmed as the most effective cleaning regime and its duration was found to have an effect on the state of the bed when it was returned to service. The effect of these findings on filter performance during ripening in terms of the number of particles in the filtrate, especially as a function of the backwash remnants is discussed.

#### 7.4.2.1 Backwash regime

When backwash effectiveness was discussed it was stated that the air then water wash and the CP wash removed similar amounts of deposits because the clean bed headlosses were the same. However, less turbidity was washed out of the air then water washed filter, especially for the 0.5-1.0mm sand, which implies more particulate matter was contained in the backwash remnants retained in the filter.

When the particle counts were observed (Figs 7.1 and 7.4) large peaks were found in the filtrate particle count from the air then water washed filters, especially for the 0.5-1.0mm sand filter. The NPFs in the total backwash remnants were 1.9 times and 1.1 times greater than the water only wash for the 0.5-1.0mm sand and 2.0-3.35mm sand filters respectively. When the total NPFs were examined (Table 7.4) it was found that the highest were from the air then water washed filters. This is likely due to the fact that the duration of the water rinse was too short.

The NPF in the backwash remnants retained within the filter beds, identified as the component of highest risk, was lowest in the filtrate of the CP washed filters, as was the total NPF. Therefore CP backwash regime was the most effective in cleaning and in minimising the NPF. This is in agreement with results published by Hall and Pressdee (1995) from trials carried out on a pilot filter containing 0.5-1.0mm sand. The limited data set presented showed that CP backwash resulted in a lower NPF when compared to air then water and water only wash.

It is interesting to note that the CP washed filters have relatively high NPF as a function of the influent and despite lower peaks, they take as long, if not longer to ripen. This is likely to be due to the fact that fewer additional collectors remain on the media after CP backwashing so that the improvement in removal efficiency takes longer. It was for this reason that the duration of the CP backwash was investigated, the CP backwash already gave the lowest NPF in both the backwash remnants in the bed and the total ripening period. If additional collectors could be left on the media by reducing the backwash duration, the ripening period could be further reduced.

#### 7.4.2.2 Backwash duration

The CP duration clearly had an effect on the filtrate particle counts, the behaviour of the two filter configurations showed some differences. The CP duration had little effect on the NPF from the backwash remnants in the bed and above the bed because the rinse was of a fixed volume and therefore

rinsed out detached particles to the same degree. One exception to this was after 5 minutes of CP wash for the 2.0-3.35mm sand filter. The capacity of the backwash water tank did not allow a rinse of the same duration as for the other runs. The result was that the backwash water had a higher turbidity at the end of the backwash and therefore a higher initial peak during ripening.

The CP duration did affect the NPF that was a function of the influent. In the 0.5-1.0mm sand filters the NPF of this component was reduced as the CP increased from 1 to 4 minutes, however, after 5 minutes a significant increase occurred. After a 1 minute CP backwash many deposits were obviously left on and/or within the media. The filter might reasonably be expected to ripen more rapidly and thus have a lower NPF in this component. Clearly, this does not happen and it is possible the phenomenon of floc break-off was occurring, this is a phenomenon where individual particles are captured and then help to capture other particles; a group of captured particles would then break-off as a floc as the attachment mechanisms were overcome by increasing hydraulic shear forces (Clark *et al.*, 1990). This is covered in detail in section 8.4. As the CP duration is increased the media becomes cleaner, thus the pores are less clogged on re-start and localised shear forces are lower negating the effect of floc break-off. After 4 minutes CP an optimum appeared to have been reached where a number of deposits remained on the media acting as additional collectors facilitating a faster ripening. A further minute of CP seemed to remove these and thus ripening took longer resulting in a higher NPF. In effect the media had been over cleaned.

Something similar occurred on the 2.0-3.35mm sand media, the NPF as a function of the influent was reduced as the CP backwash duration increased. However, no corresponding increase was found after 5 minutes. It is possible one would have been seen if the CP duration had been increased further, however this was beyond the capabilities of the plant. It is likely that the shape and micro-topography, as illustrated in the micro-graphs in Chapter 4, made it more difficult to clean the coarse quartz sand when compared to the smooth rounded 0.5-1.0mm sand.

The result of combining the NPFs from the components into the total NPF produced U-shapes for both media. Therefore under the conditions of these trials both showed clear optimums. For the 0.5-1.0mm sand filter the 4 minutes CP wash showed the lowest TPNF,  $1.51 \times 10^8$ , and was found to be reproducible ( $\pm 10\%$ ). When this is compared to the TPNF after 1 and 5 minutes CP wash  $2.48 \times 10^8$  and  $2.31 \times 10^8$  respectively, it becomes apparent what a significant reduction optimisation of backwash duration can provide.

The 2.0-3.35mm quartz sand had TNPFs higher than the 0.5-1.0mm sand as expected. There was little to choose in terms of TNPF between 2, 3 and 4 minutes of CP backwash,  $2.03 \times 10^8$ ,  $2.04 \times 10^8$  and  $2.08 \times 10^8$  respectively. There was again a significant reduction by optimising the CP backwash.

The scale of the pilot plant means that these findings should be confidently applied to full-scale plant. This belief is reinforced by a recent paper by Chipps *et al.*, (1995) which reviewed the performance of collapse-pulsing backwash on a number of full-scale plants. They also found that over cleaning the media resulted in poor filtrate quality, and that an optimum CP duration existed that produced the highest quality filtrate during ripening.

#### 7.4.3 Backwash selection

It was necessary to select the optimum backwash regime for subsequent trials. This had to be done mainly on the performance, i.e. minimising particulate passage during ripening, but consideration also had to be given to process economics. There was no point choosing a backwash duration that resulted in short runlengths because this would result in more frequent backwashing and thus more ripening periods. Such an option would not be viable for an operational plant. Fortunately, the optimum for the 1m beds of 0.5-1.0mm sand occurred after a 4 minute CP backwash, this gave a 38 hour runlength. The 5 minute CP gave a runlength was 44 but the NPF was 1.5 times higher. Therefore 4 minutes was selected for this filter. With the 2m beds of 2.0-3.35mm quartz sand the achievable runlengths were so long in terms of headloss development that the optimum could be chosen purely in terms of minimum TNPF. Therefore the optimum CP backwash duration was 3 minutes.



## 7.5 Conclusions

For the conditions experienced in this trial and from the results obtained the following conclusions can be made:

The duration of the collapse-pulsing backwash had a significant effect on the TNPF. Generally, very short backwash durations (1 minute) resulted in high TNPFs due to inefficient cleaning, and longer durations (5 minutes) resulted in high TNPFs due to over efficient cleaning. This effect was, however, influenced by media size.

The duration of the collapse-pulsing backwash also had a significant effect on the headloss development of the media. The longer the CP backwash, the lower the clean bed headloss and the slower the rate of headloss development.

The ripening period has two main components: backwash remnants and the interface with the influent. It was the interface with the influent component that was affected by the CP backwash duration.

Optimum backwash regimes, in order to minimise the TNPF, for each media were identified: 4 minutes of CP followed by a 5 minute rinse for the 1m beds of 0.5-1.0mm sand; and 3 minutes of CP followed by a 5 minute rinse for the 2m beds of 2.0-3.35mm sand.

# *CHAPTER 8*

## START-UP STRATEGY ASSESSMENT

### 8.1 Introduction

Two possible methods of reducing the passage of particulates into supply during the ripening period were presented in the Badenoch report (DoE/DoH, 1990). The first was filter to waste, which is rarely an option when retro-fitting old plants. The second was slow start - gradual opening of the filter inlet/outlet valves so as to avoid any surges in flow. Slow start has been taken up in some parts of the UK water industry with some plants being retro-fitted. However, the effect of slow start on performance during the ripening period is still largely unknown. An alternative start-up strategy was found to be delayed start. This is achieved by retaining the backwash remnants in the filter for a period of time before starting the filter run.

It was the aim of this trial to assess the effect of both slow start and delayed start on the degree of particulate passage during the ripening period.

### 8.2 Experimental methods

The filters were operated at a filtration rate of 6 m/h with a ferric (III) sulphate dose of 1 mg/l as  $\text{Fe}^{3+}$  (the ferric sulphate dose was increased to 1.5mg/l as  $\text{Fe}^{3+}$  about halfway through the trial due to deteriorating raw water quality, under drought conditions). Backwashing was carried out every 48 hours. The backwashing regime employed was a combined air/water wash at flowrates to achieve collapse-pulsing, followed by a higher velocity water rinse fixed at 5 minutes and designed to give 10% expansion. The optimum backwash times determined in Chapter 7 were used in the assessment of start-up strategies. The flow rates used are shown in Table 6.2.

A segmented ball valve with 1000 positions was used to provide the slow start. The valve could be programmed to open by linear stepping over a set duration, providing a rate of change of velocity within the range 0.08 to 0.3m/h./m<sup>2</sup>. A 1/2 hour and 1 hour slow start duration were assessed i.e. from zero to full flow over a 1/2 hour and 1 hour period. Fig 8.1 shows the flowrates (recorded by digital flowmeters at the base of the columns) for 1/2 and 1 hour slow start. The delayed start was provided by retaining the backwash remnants in the filter for 1/2 hour and 1 hour before opening the outlet valve in the normal manner.

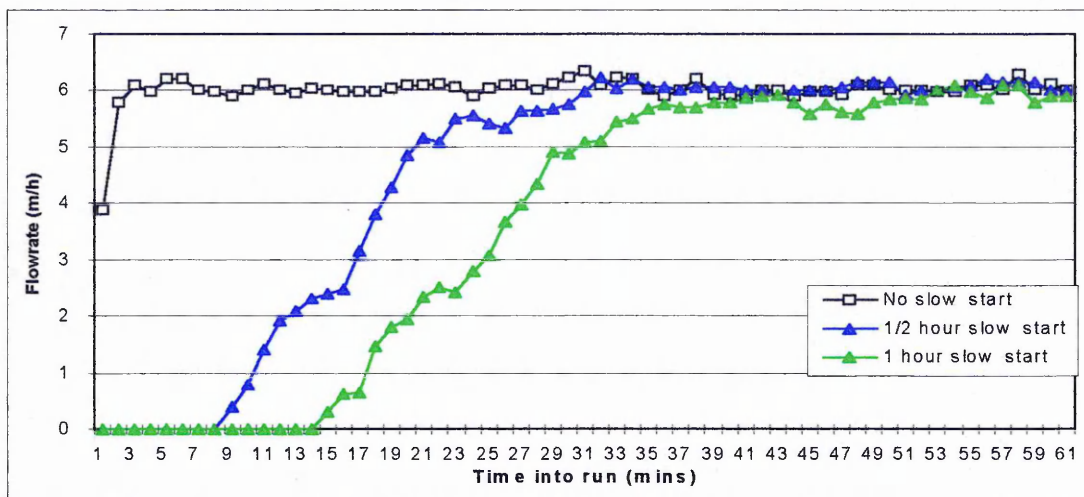


**Figure 8.1. Filtration flowrates (measured by digital flowmeters) for slow start strategies.**

Monitoring was carried out in the manner described in section 6.2.

### 8.3 Results

The results section will cover the influent conditions, the filter performance in terms of particle counts and numbers of particles in the influent during ripening (NPFR), the filter performance in terms of headloss development, and finally, the relationship between raw water quality and NPFR.

#### 8.3.1 Influent quality

During the course of this trial the raw water quality was very variable. Drought conditions meant that water taken from wherever possible was used to augment and maintain the supply from lake Thirlmere to the 22 Thirlmere aqueduct take-offs, which included Lostock. As a result of the deterioration in raw water quality, treatment goals were not being met. A steady state value not greater than 30 2-5 $\mu$ m particles per ml was desired, whereas, a steady state value of approx. 180/ml was being achieved. It was therefore decided to increase the ferric (III) sulphate dose by the smallest step possible (with the dosing pumps being used), from 1.0 mg/l as  $\text{Fe}^{3+}$  to 1.5 mg/l. The effect of this variable supply on the raw water quality parameters can be seen by looking at the data in Tables 8.1 and 8.2. Table 8.1 contains the raw water quality data prior to the time of

ferric dose change (from 1.0-1.5 mg/l as  $\text{Fe}^{3+}$ ), Table 8.2 contains the raw water quality data after the ferric dose increase. It is interesting to note, that despite the increase in both turbidity and particle count, the colour, and therefore the organic content of the water was particularly low throughout the trial.

**Table 8.1 A summary of the raw water quality during the trial (before ferric dose increase).**

Raw water quality parameter	Mean	Maximum	Minimum	Std Deviation
Turbidity (NTU)	0.5	1.0	0.3	0.24
Colour (Hazen)	2.76	5	1.3	0.99
pH	8.5	8.8	8.2	0.1
Manganese ( $\mu\text{g/l}$ )	16.3	25	11	5.0
Iron ( $\mu\text{g/l}$ )	29.9	41	24	6.4
Particle count (/ml)	2044	2736	1122	254

**Table 8.2. A summary of the raw water quality during the trial (after ferric dose increase).**

Raw water quality parameter	Mean	Maximum	Minimum	Std Deviation
Turbidity (NTU)	0.8	1.7	0.4	0.45
Colour (Hazen)	3.09	5	2	1.14
pH	8.33	8.73	8.1	0.16
Manganese ( $\mu\text{g/l}$ )	16.6	31	6	6.6
Iron ( $\mu\text{g/l}$ )	40.04	65	23	11.7
Particle count (/ml)	3302	6956	2219	844

This change in ferric dose had an effect on the numbers of particles going on to the filter but little effect on the particle size distribution. This is illustrated in Fig 8.2, the graph shows the effect of ferric addition and flash mixing on the particle size distribution of a good quality raw water (means from 20 samples). Both ferric doses are shown; the effect of adding the ferric and flash mixing is to increase the number of particles across all the measured discrete size bands as floc is formed from sub- $2\mu\text{m}$  colloidal matter. The higher dose further increases the number of particles in all size bands.

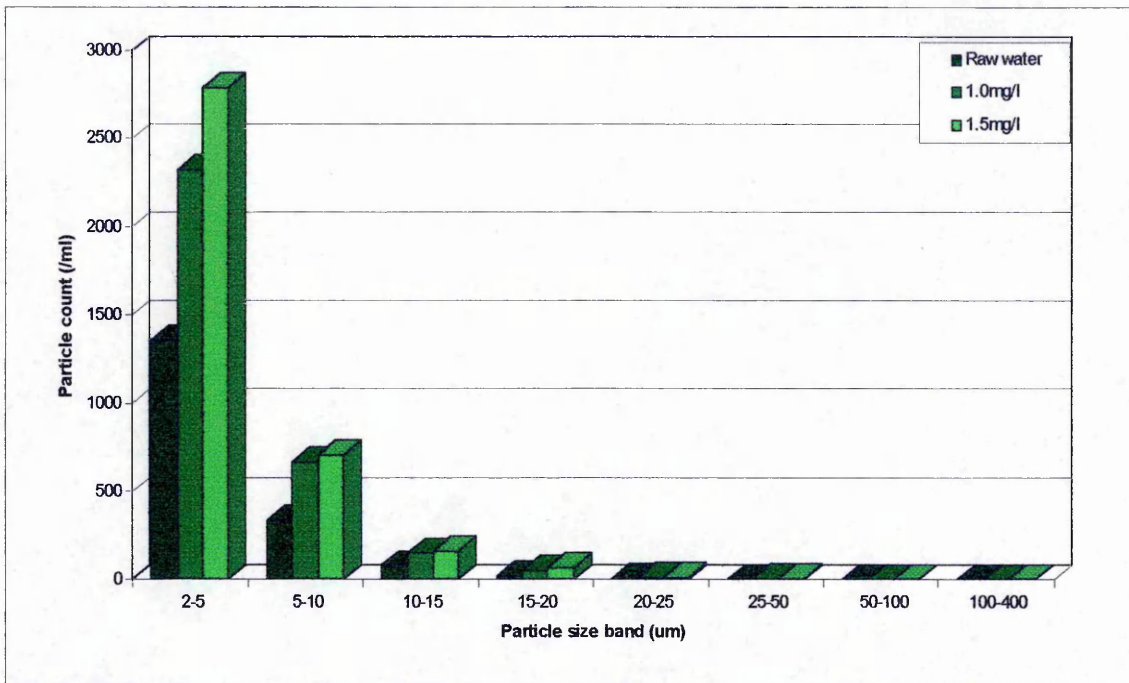


**Figure 8.2.** The effect of ferric (III) sulphate coagulation and flash mixing on the particle size distribution of high quality raw water (mean of 20 samples).

The same data is shown in Fig 8.3, with the arithmetic mean particle diameter plotted on the x-axis. This shows that the mean particle size has not actually been increased by the higher ferric dose, the effect was to flocculate more colloidal sub-2µm particles, or possibly precipitate out hydroxide floc. The power law slope coefficient ( $\beta$ ) for the raw and flocculated water (derived from Fig 8.4) reinforces the observation of little change in the particle size distribution, with only a slight increase from 2.84 to 2.92 and 2.93 for the 1.0mg/l and 1.5mg/l doses respectively. Figure 8.5 shows the effect the higher dose of ferric had at the time of poor quality, the  $\beta$  values were 3.06, and 3.1. Overall, it appeared that despite the apparent variability in particle count of the raw water the particle size distribution was quite consistent (min  $\beta$  - 2.82, max.  $\beta$  - 3.13), i.e. most of the particles were small. Even after flocculation most of the particles were located in the smaller sizes, and the 1.0mg/l and 1.5mg/l ferric increased particles in all size bands by approx. 40% and 55% respectively.

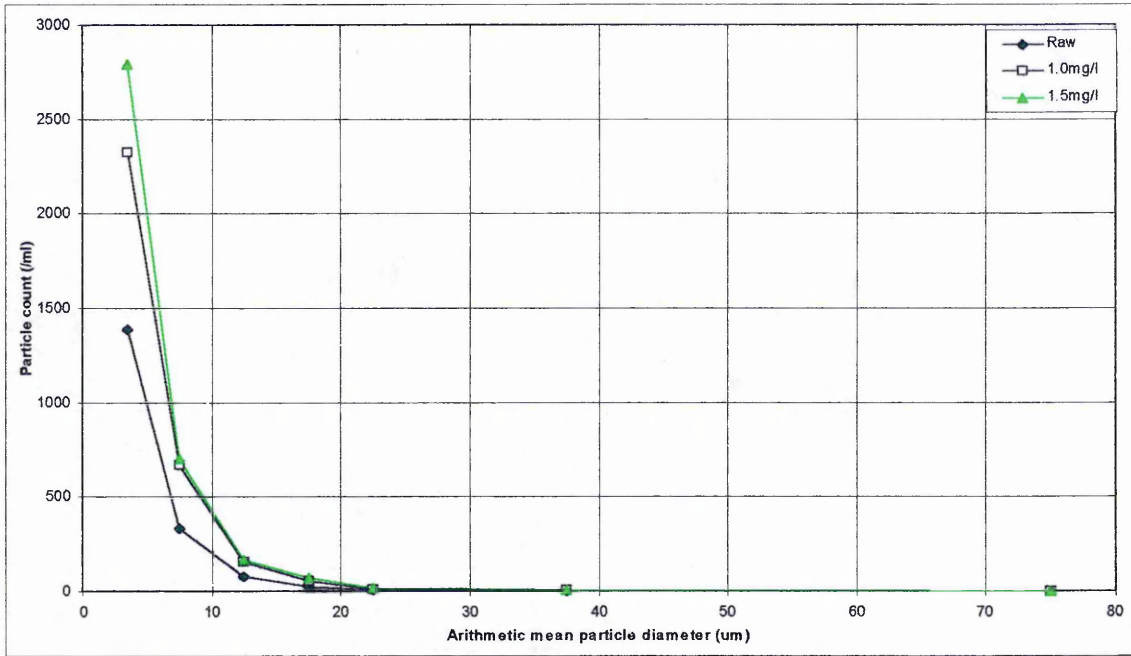


Figure 8.3. The effect of ferric (III) sulphate flocculation and flash mixing on the particle diameter of high quality raw water (mean of 20 samples).

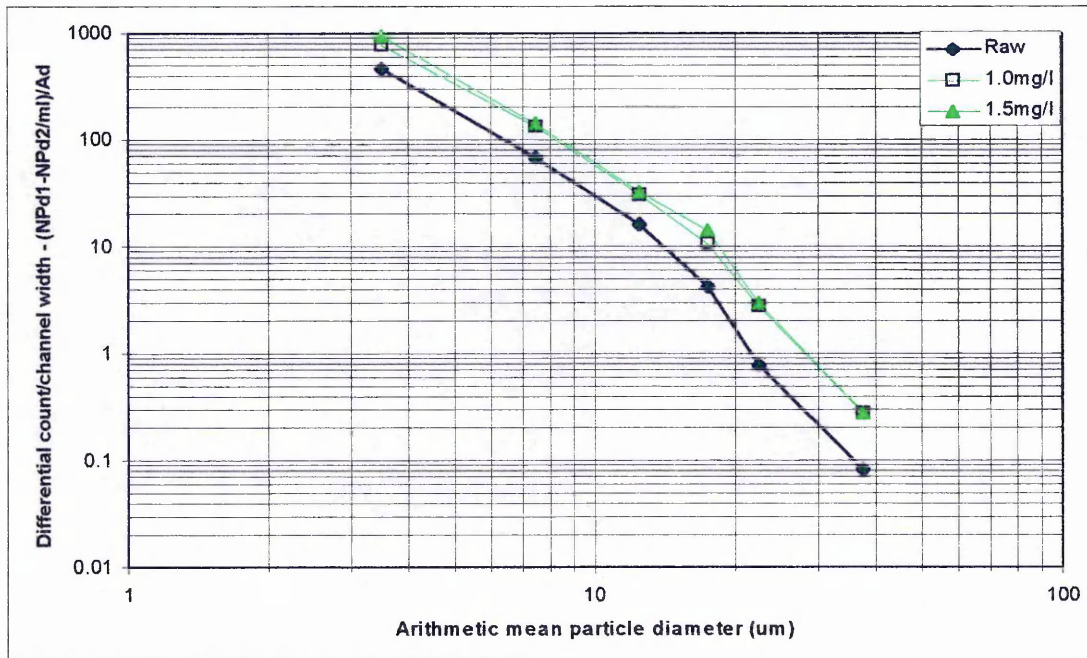
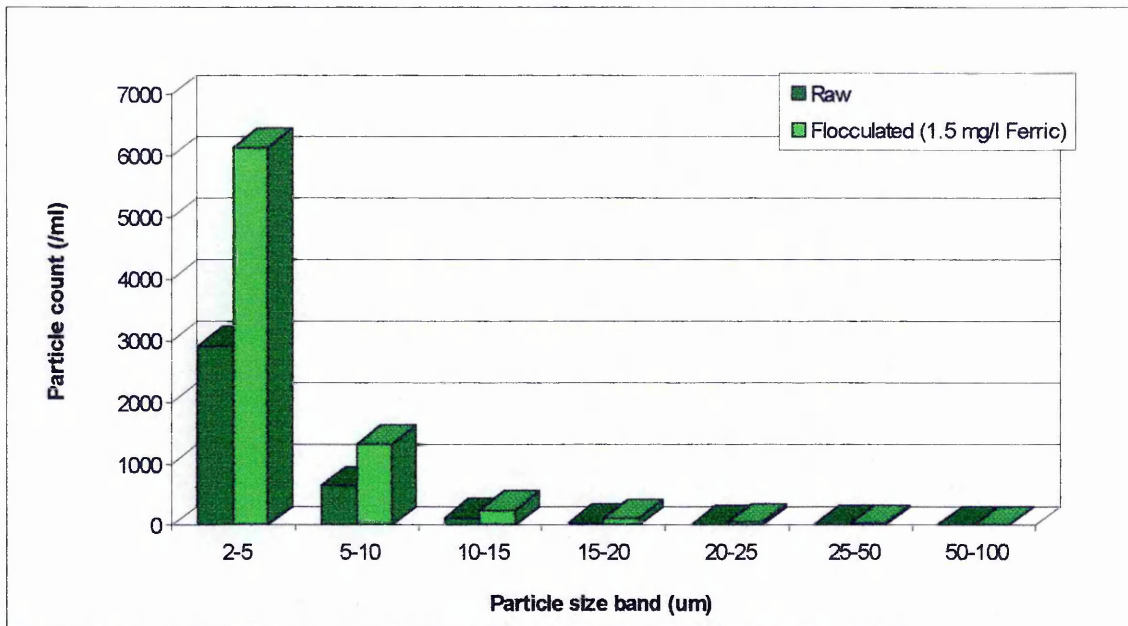


Figure 8.4. The effect of ferric (III) sulphate flocculation and flash mixing on the power law slope coefficient ( $\beta$ ).



**Figure 8.5.** The effect of ferric (III) sulphate flocculation and flash mixing on the particle size distribution of low quality raw water (mean of 8 samples).

### 8.3.2 Filter performance

This section will cover the affect of deteriorating raw water quality on performance of the control filters and the implications this had on the trials. The performance of the filters under the various start-up strategies, as assessed using particle count data, will then be covered. Examples of runs under a range of conditions, for both filter media are included in the main text. The data is presented as particle count vs. time (i.e. real time data); particle count vs. volume of filtrate produced; and finally as cumulative number of 2-5µm particles in the filtrate vs. volume of filtrate produced. The headloss data is also presented. The data is summarised in tabular form showing the total number of 2-5µm particles in the first 420l of start -up filters filtrate as a % of the control filters NPFR.

#### 8.3.2.1 The effect of poor raw water quality and increased ferric on filtrate quality

Under “normal” raw water conditions (particle counts from 1000-2000/ml) experienced at



Lostock, a ferric (III) sulphate dose of 1.0mg/l as  $\text{Fe}^{3+}$  was sufficient to produce a filtrate steady state value of approx. 30/ml for both filters, with a mean Iron content of 53 $\mu\text{g}$ . The total number of 2-5 $\mu\text{m}$  particles in the filtrate during ripening (NPF) for both the 1m beds of 0.5-1.0mm sand and 2m beds of 2.0-3.35mm sand control filters from the runs immediately before and after the increase in ferric were as follows: 0.5-1.0mm sand control filter -  $1.07 \times 10^8$  and  $5.63 \times 10^7$ ; 2.0-3.35mm sand control filter -  $2.33 \times 10^8$  and  $2.18 \times 10^8$ . A number of observations may be made from these figures, firstly the 0.5-1.0mm sand filters perform better than the 2.0-3.35mm sand filters for this parameter; secondly performance of both types of filters improved slightly with the higher ferric dose, despite the deteriorating raw water quality.

#### 8.3.2.2 1m beds of 0.5 -1.0mm sand

The first example, Fig 8.6a, b and c, shows a 1 hour slow start, 1/2 hour delayed start and the control (no start strategy). The raw water particle count was approx. 1600 and the ferric dose was 1.0mg/l as  $\text{Fe}^{3+}$ . Fig 8.6a shows particle count vs. time, it is immediately obvious that the peak in filtrate particle count from the slow start filter occurred much later, this was due to the valve characteristics i.e. very slow initial flow. It can also be seen that the peak is smaller in magnitude. The delayed start filters filtrate particle count more closely resembles that of the control, the ripening time was almost identical. However, it had two peaks in the particle count, the first of which was lower than the control.

When the data is viewed in terms of particle count vs. volume of filtrate produced (Fig 8.6b) it can be seen that the slow start filter required a smaller volume to be filtered in order to ripen. Indeed, by the time the volume of backwash water that was retained within the filter bed had been displaced (39.5 l) the filter had nearly ripened. It can be seen that the second peak in the delayed start filtrate particle count corresponded to the interface between the volume of backwash water retained within the media and that above the media; this implies the effect of the delayed start was to reduce the particle count of the volume of backwash water that was retained in the bed.

The cumulative number of 2-5 $\mu\text{m}$  particles in the filtrate (NPF) data is plotted in Fig 8.6c, this illustrated how significant the ripening period is, in terms of NPF. It also clearly shows the effect

of the 1 hour slow start (under these conditions), that is that because the initial particle count peak was lower and the filter ripened more rapidly the NPF was always lower than the control. The effect of the 1/2 hour delayed start could be seen as a reduction in NPF for the first 40 l, relative to the control, but after that the increase in NPF was identical to the control.

The second example (Fig 8.7 a, b and c) shows the performance of the same start-up conditions but under different conditions. The raw water particle count was much higher (approx. 2900/ml), and the ferric (III) sulphate dose had been increased to 1.5mg/l as  $\text{Fe}^{3+}$ . It can be seen from Fig 8.7a that despite the poor raw water quality, the increase in ferric resulted in what appeared to be lower particle counts. However, the steady state values achieved by the filters under these conditions were not as low. A number of observations can be made: The peaks appeared to be more "rounded" and lower than in the first example; the slow start filter took a lot longer to ripen; and the particle count from the delayed start filter was greatly reduced relative to the control filter.

When the same data was plotted against volume of filtrate produced (Fig 8.7b) these observations were reinforced. The 1 hour slow start filter required about 275 l of filtrate to be passed in order to ripen, this means a significant amount of influent was required to be filtered before the filter ripened. The filtrate particle count from the 1/2 hour delayed start filter only just shows a second peak which occurred at the interface between the two components of the backwash remnants, this filter still required the same volume of filtrate as the control to be ripened.

The cumulative NPF data (Fig 8.7c) showed that despite lower numbers of particles in the filtrate from the 1 hour slow start filter initially, the numbers increased more rapidly than that from the delayed start filter. As a result after about 35 l the NPFs were similar, after a further 100 l the 1 hour slow start NPF was greater than that of the 1/2 hour delayed start. The NPFs of both the slow start and delayed start filters were less than that of the control filter at all stages of ripening, with the delayed start showing a slightly greater improvement.

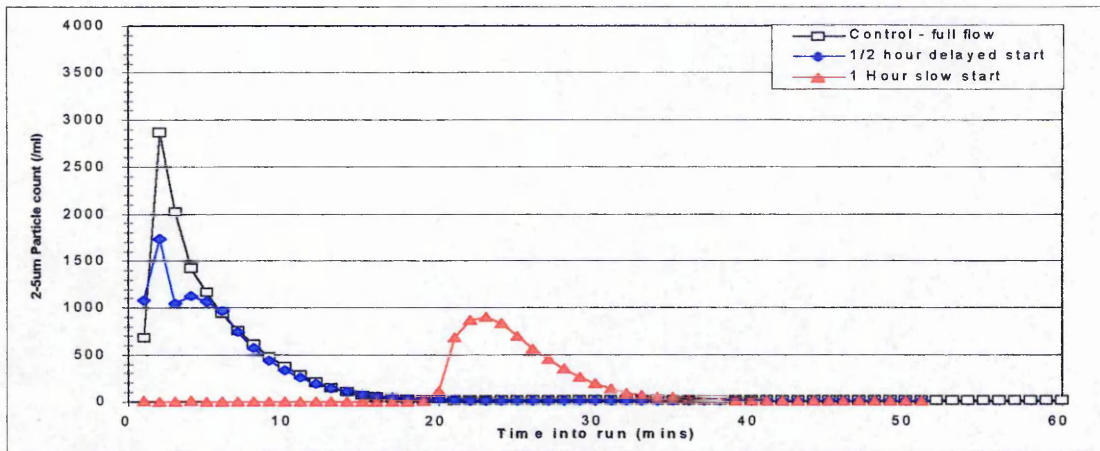


Figure 8.6a. Filtrate particle count vs. time - 1m beds of 0.5-1.0mm sand, 1.0mg/l ferric sulphate, 1 hour slow start, 1/2 hour delayed start.

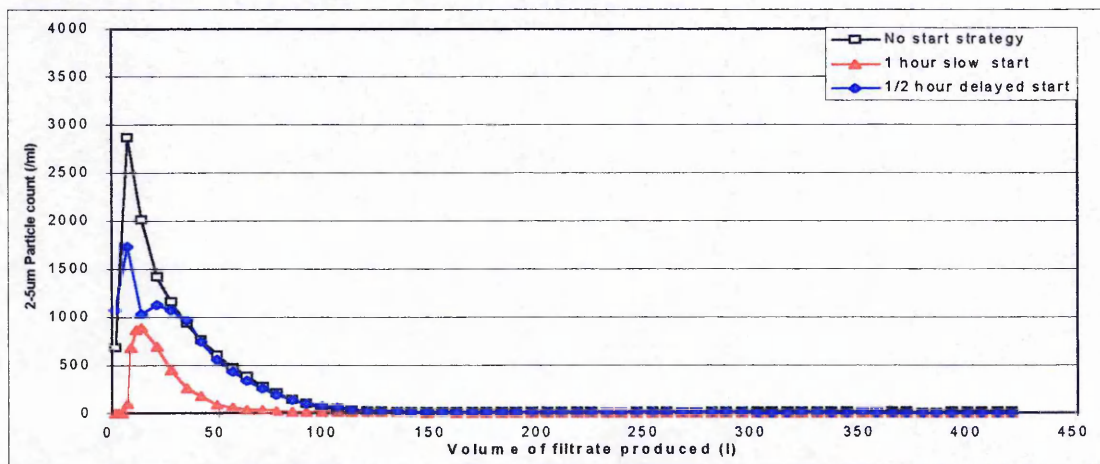


Figure 8.6b. Filtrate particle count vs. volume of filtrate produced - 1m beds of 0.5-1.0mm sand, 1.0mg/l ferric sulphate, 1 hour slow start, 1/2 hour delayed start.

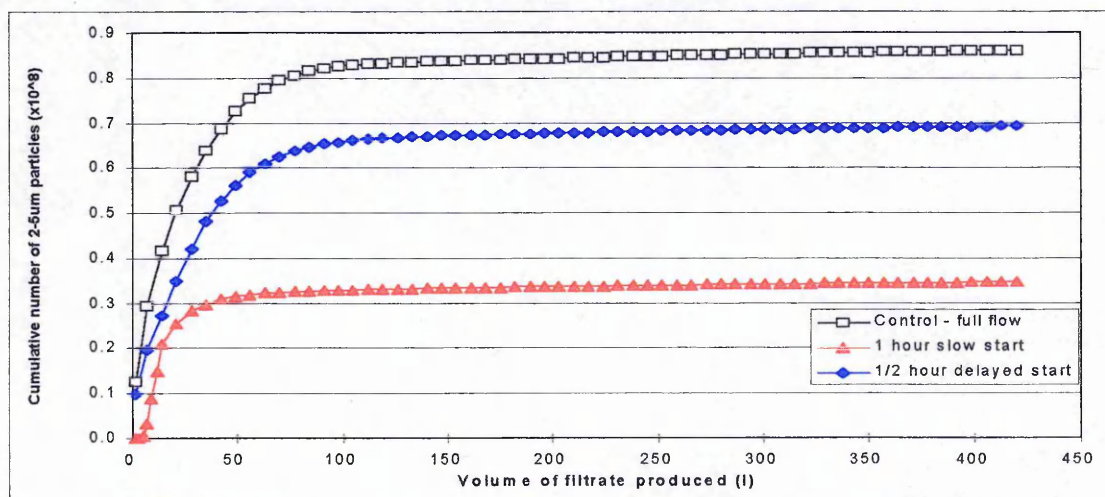


Figure 8.6c Cumulative number of 2-5µm particles in filtrate vs. volume filtrate produced - 1m beds of 0.5-1.0mm sand, 1.0mg/l ferric sulphate, 1 hour slow , 1/2 hour delayed start

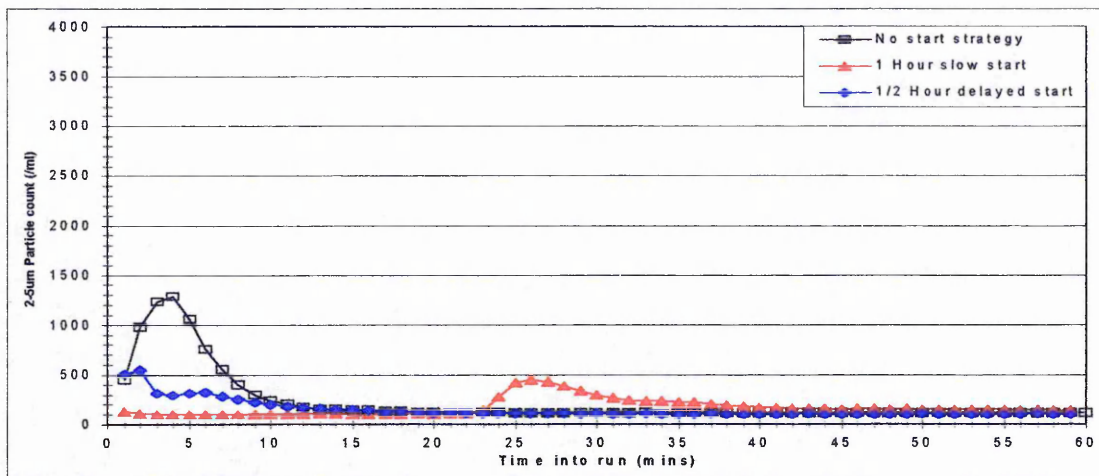


Figure 8.7a. Filtrate particle count vs. time - 1m beds of 0.5-1.0mm sand, 1.5mg/l ferric sulphate, 1 hour slow start, 1/2 hour delayed start.

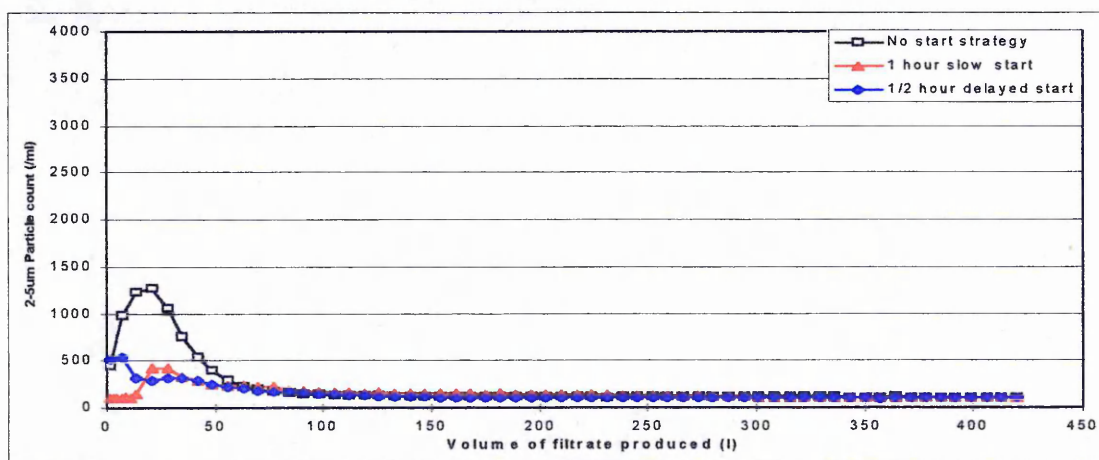


Figure 8.7b. Filtrate particle count vs. volume of filtrate produced - 1m beds of 0.5-1.0mm sand, 1.5mg/l ferric sulphate, 1 hour slow start, 1/2 hour delayed start.

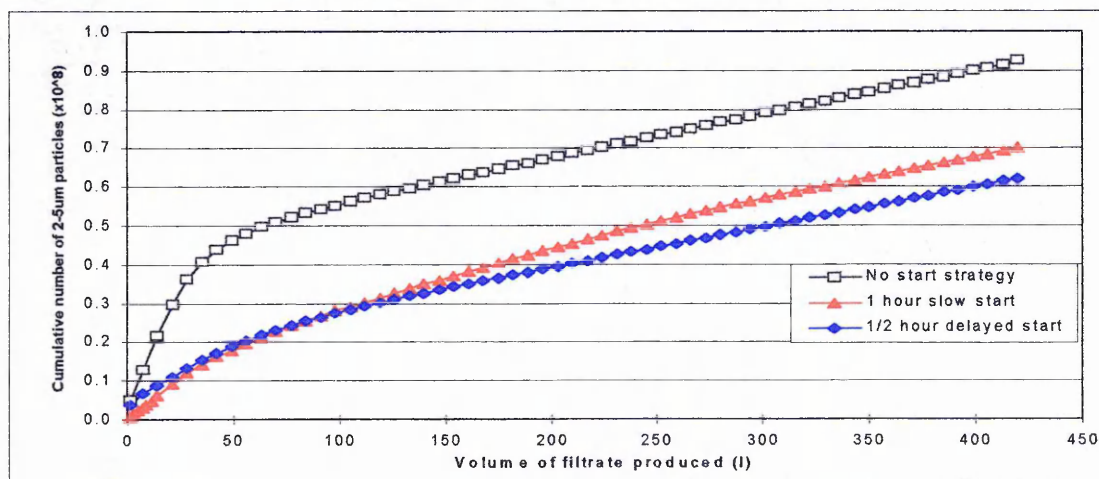


Figure 8.8c Cumulative number of 2-5µm particles in filtrate vs. volume filtrate produced - 1m beds of 0.5-1.0mm sand, 1.5mg/l ferric sulphate, 1 hour slow , 1/2 hour delayed start.

The third example (Fig 8.8a, b and c) shows the performance of different start-up durations, a 1/2 hour slow start and a 1 hour delayed start. The raw water was of poor quality (approx. 2700/ml) and the ferric dose was 1.0mg/l as  $\text{Fe}^{3+}$ . It is immediately evident from Fig.8.8a that performance of all the filters was poor. The particle counts were high, and there was an unsatisfactory filtrate steady state value of approx. 210/ml. It can be seen that the filtrate particle count peak from the 1/2 hour slow start occurred earlier, after 9 minutes, than that of the 1hour slow start from the previous examples. The 1hour delayed start filter produced the characteristic double peak, however this filter took longer to ripen than the control filter.

When particle count plotted against volume (Fig 8.8b) is considered it can be seen that the slow start filter required a much smaller volume to be passed before it ripened, about 65-70 l, than both the control and delayed start filters. The delayed start filters' double peak corresponded to the interface between the components of backwash remnants (39.5 l), the filter required about 160 l to be passed, which included a large amount of influent, about 75 l.

Fig 8.8 c shows that the slow start filter starts initially had an NPF equal to that of the control and greater than the delayed start filters. The NPF from the delayed start filter was significantly lower during the first 40l of filtration, after this it increases and becomes greater than that of the slow start filter, due to the faster ripening of the slow start filter. The NPF from the delayed start filter then closely resembles that from the control filter, whereas the NPF from the slow start filter remains lower than that of the control.

The fourth example (Fig. 8.9a, b and c) shows the performance of the filters under the same start-up conditions as the previous example, but with a better quality raw water ( 2500 /ml). However, the ferric dose had been increased from 1.0 to 1.5mg/l as  $\text{Fe}^{3+}$  . The effect of this change is clearly seen in Fig 8.9a, the particle count peaks were much lower and a steady state value of 30/ml was achieved. The slow start appears quite similar to the control, although the peak was slightly lower and it took longer to ripen. The delayed start filter did not have a clear double peak such as in the previous example, but the particle count was very much lower than the control.

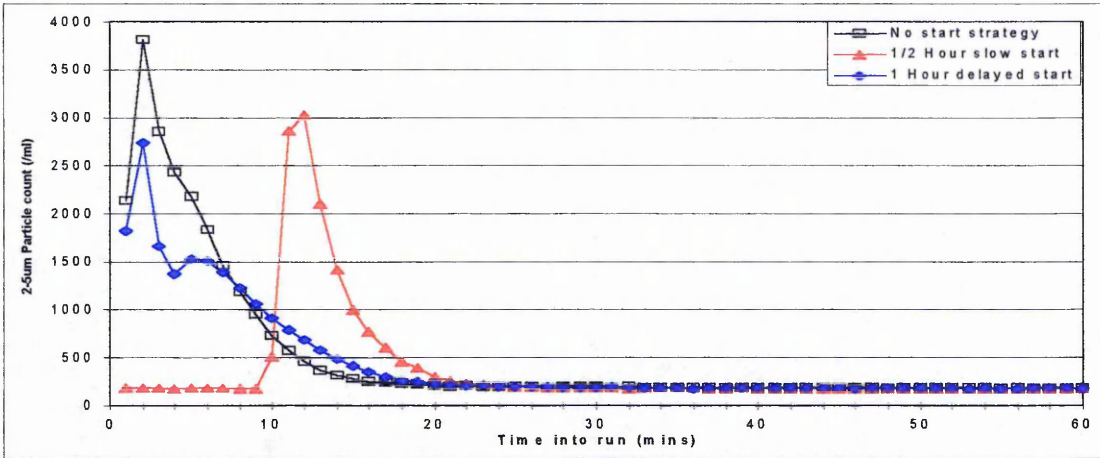


Figure 8.8a. Filtrate particle count vs. time - 1m beds of 0.5-1.0mm sand, 1.0mg/l ferric sulphate, 1/2 hour slow start, 1 hour delayed start.

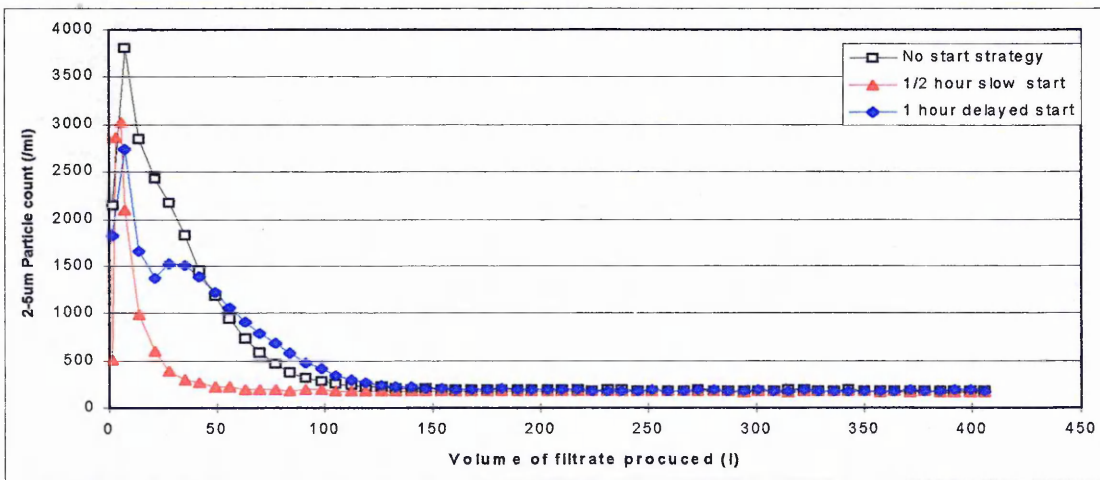


Figure 8.8b. Filtrate particle count vs. volume of filtrate produced - 1m beds of 0.5-1.0mm sand, 1.0mg/l ferric sulphate, 1/2 hour slow start, 1 hour delayed start.

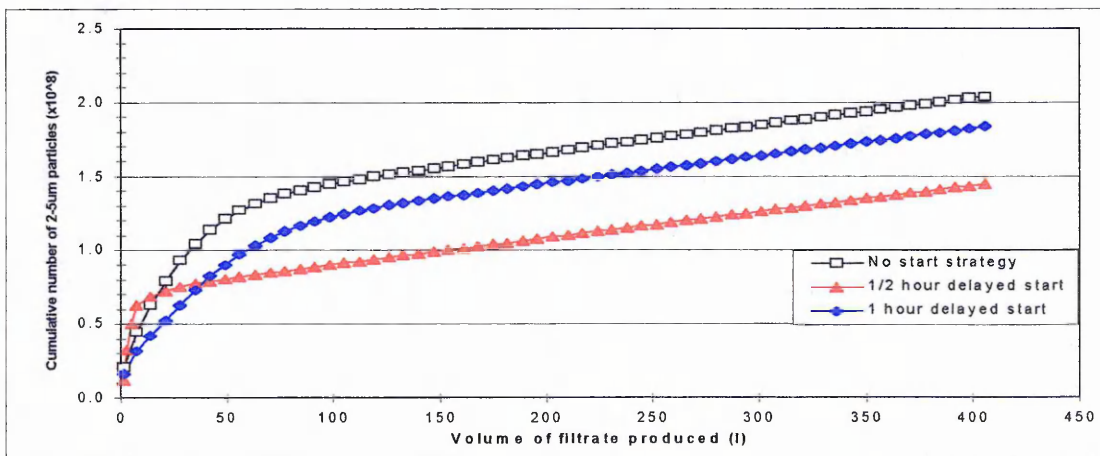
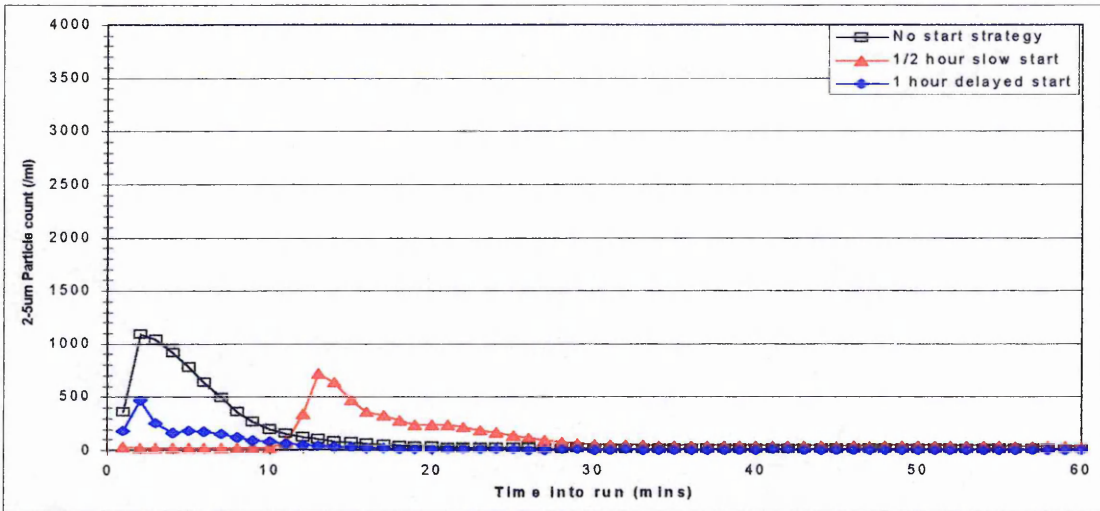
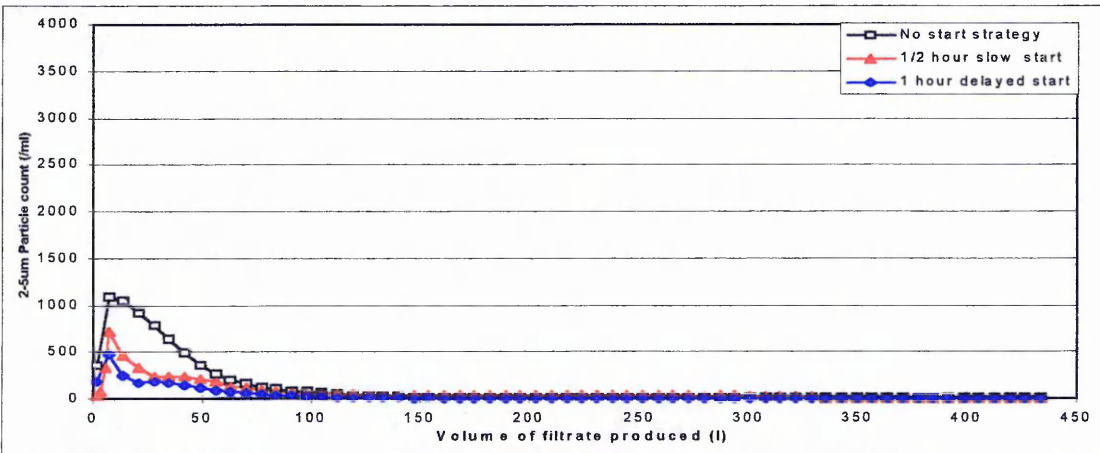


Figure 8.8c. Cumulative number of 2-5µm particles in filtrate vs. vol filtrate produced - 1m beds of 0.5-1.0mm sand, 1.0mg/l ferric sulphate, 1/2 hour slow, 1 hour delayed start.



**Figure 8.9a. Filtrate particle count vs. time - 1m beds of 0.5-1.0mm sand, 1.5mg/l ferric sulphate, 1/2 hour slow start, 1 hour delayed start.**



**Figure 8.9b. Filtrate particle count vs. volume of filtrate produced - 1m beds of 0.5-1.0mm sand, 1.5mg/l ferric sulphate, 1/2 hour slow start, 1 hour delayed start.**

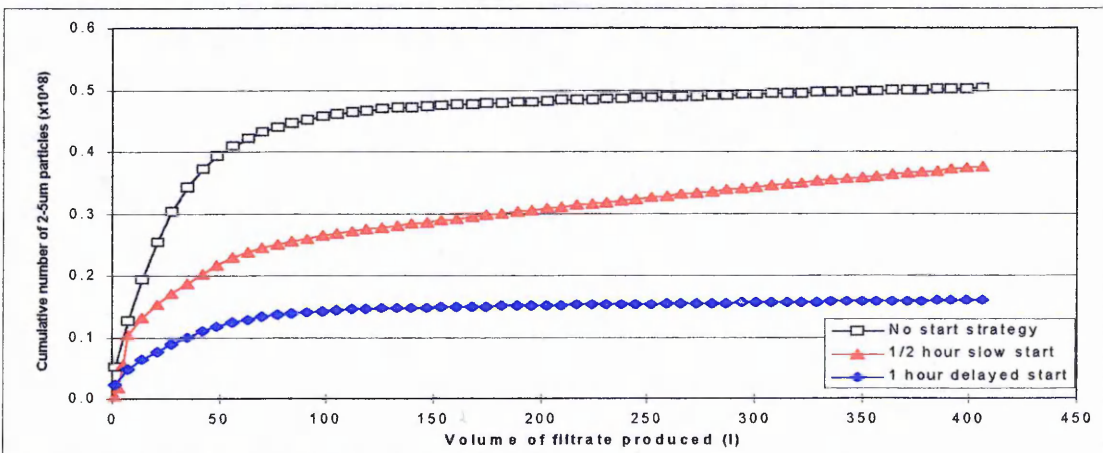


**Figure 8.9c Cumulative number of 2-5µm particles in filtrate vs. volume filtrate produced - 1m beds of 0.5-1.0mm sand, 1.5mg/l ferric sulphate, 1/2 hour slow, 1 hour delayed start.**

It can be seen from Fig 8.9b that the 1 hour delayed start filter required a smaller volume to ripen, only about 80l. Not only is this lower than the 1/2 hour slow start and control, but also the same filter in the previous example. When the cumulative NPF is examined (Fig 8.9c) the NPF from the delayed start filter was clearly much lower than the other filters.

The information in Table 8.2 summarises the performance of the start-up strategies relative to the control filters for the whole trial. The runs up to and including the 15/9/95 had the 1mg/l as  $\text{Fe}^{3+}$  ferric dose, the runs after this date had a dose of 1.5mg/l. The data is expressed as start-up strategy NPFR as a percentage of the control (i.e. no start strategy) NPFR.

**Table 8.3. The effect of start-up strategy on daily performance in terms of NPF.**

Date of run	Start-up strategy NPF as % of control (no start strategy) NPF			
	1/2 hour delayed start	1 hour delayed start	1/2 hour slow start	1 hour slow start
08/08/95	80.4			40.2
10/08/95	80.6			34.0
16/08/95	76.4			46.2
24/08/95		102	75.5	
30/08/95		90.3	71.4	
01/09/95		86.1	63.5	
15/09/95		84.9	69.1	
27/09/95		51.6	63.0	
05/10/95	66.6			75.0
23/10/95		41.7	62.9	
25/10/95		31.7	75.4	
27/10/95		33.9	140.9	
04/12/95	58.0			81.0
06/12/95	60.8			70.7

### 8.3.2.3 2m beds of 2.0-3.35mm sand

The first example for the 2.0-3.35mm sand filters shows the results from a run carried-out with 1 hour slow start and 1/2 hour delayed start. The particle count was moderate approx. 1650/ml. The ferric (III) sulphate dose was 1.0mg/l as  $\text{Fe}^{3+}$ . A number of observations can be made from the real-time particle count data (Fig 8.10a). The delayed start filter produced a large single peak which ripened at the same time as the control. The slow start peak was much smaller than both the delayed start filter and the control.



When the data is viewed in terms of particle count vs. Volume of filtrate produced (Fig 8.10b), it can be seen that the slow start filter required a smaller volume to ripen. There also appeared to be a small lag period not apparent in the particle count from the other two filters. It took 67.8 l to displace the backwash remnants retained within the bed, there didn't appear to be a double peak in the control or delayed start. The particle count was higher in the delayed start filter during this phase than the control and remained high until the backwash remnants from above the bed (up to the backwash weir) had been displaced (106.8 l). The filters are ripened after about 160l. The cumulative NPF seen in Fig. 8.10c. confirms these observations. The delayed start NPF was higher than the control at all times, and the slow start filter NPF was lower.

The second example, Fig (8.11a, b and c) shows the performance of the same start-up conditions, under worse conditions (particle count was approx. 2300/ml). The ferric dose had been increased up to 1.5mg/l as  $Fe^{3+}$ . From the filtrate particle count of the control filter (Fig8.11a) it can be seen that the filters were performing better, with lower peaks and a quicker ripening period. A reversal in performance of the slow start filter was immediately apparent, the peak occurred at the same time as in the previous example but it was much larger than the control. The delayed start showed an obvious double peak and it too was higher than the control.

When Fig 8.11b is looked at the double peak can be seen to occur prior to the interface between the backwash remnants (which occurs after 67.8 l). The second peak which didn't occur in the control filter filtrate lasted for up to 150 l of filtrate production. The slow start exhibited the same lag as seen in the previous example, and the peak in particle count was clearly larger. The cumulative NPF (Fig 8.11c) shows that both the delayed start and slow start, after its initial lag performed worse than the control.

The third example (Figs 8.12a, b, and c) shows the performance of 1/2 hour slow start and 1 hour delayed start under poor influent conditions. The raw water particle count was 2690/ml, and with a ferric dose of 1.0mg/l as  $Fe^{3+}$  a satisfactory steady state filtrate particle count could not be achieved. It can be seen from Fig 8.12a that the peaks were relatively low but all the filters took a long time to ripen. The filters all showed a double peak but at different times and to different degrees.

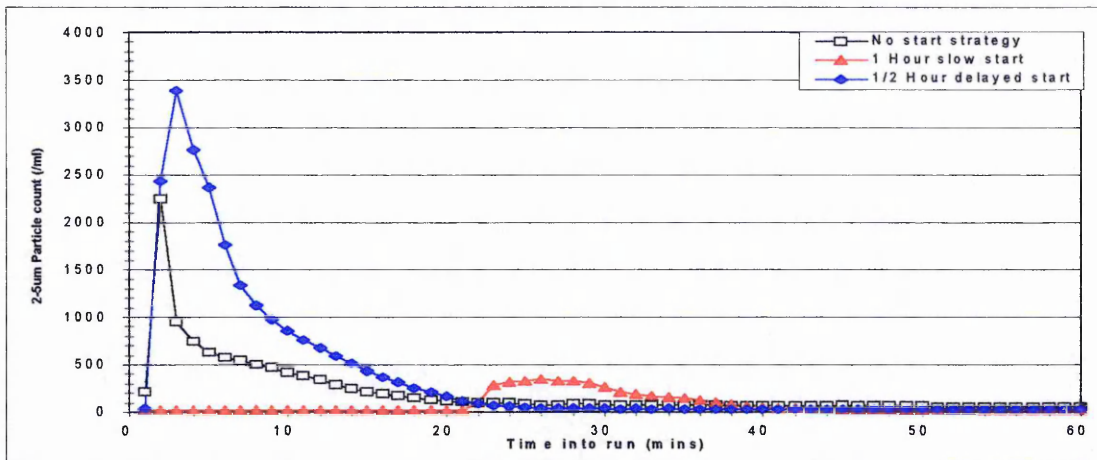


Figure 8.10a. Filtrate particle count vs. time - 2m beds of 2.0-3.35 sand, 1.0mg/l ferric sulphate, 1 hour slow start, 1/2 hour delayed start.

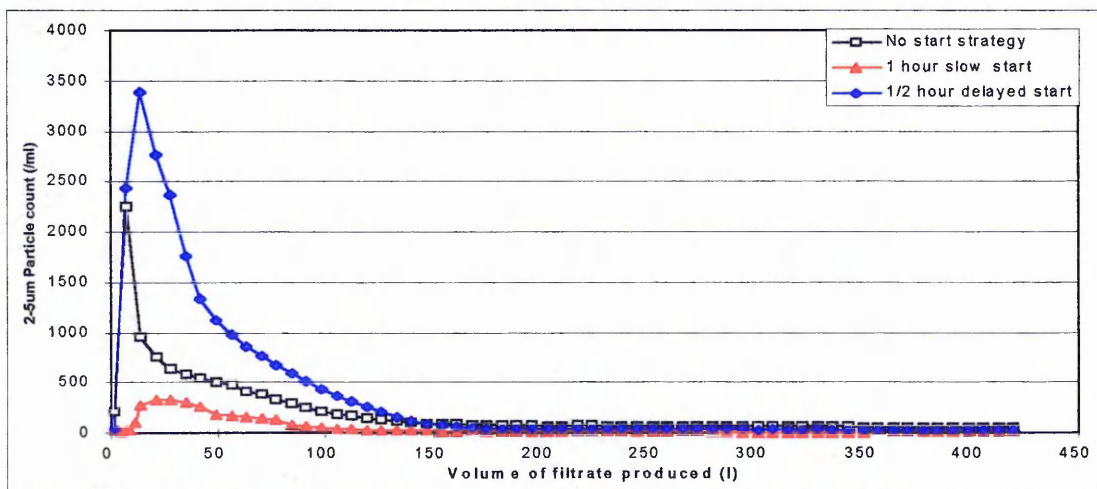


Figure 8.10b. Filtrate particle count vs. volume of filtrate produced - 2m beds of 2.0-3.35mm sand, 1.0mg/l ferric sulphate, 1 hour slow start, 1/2 hour delayed start.

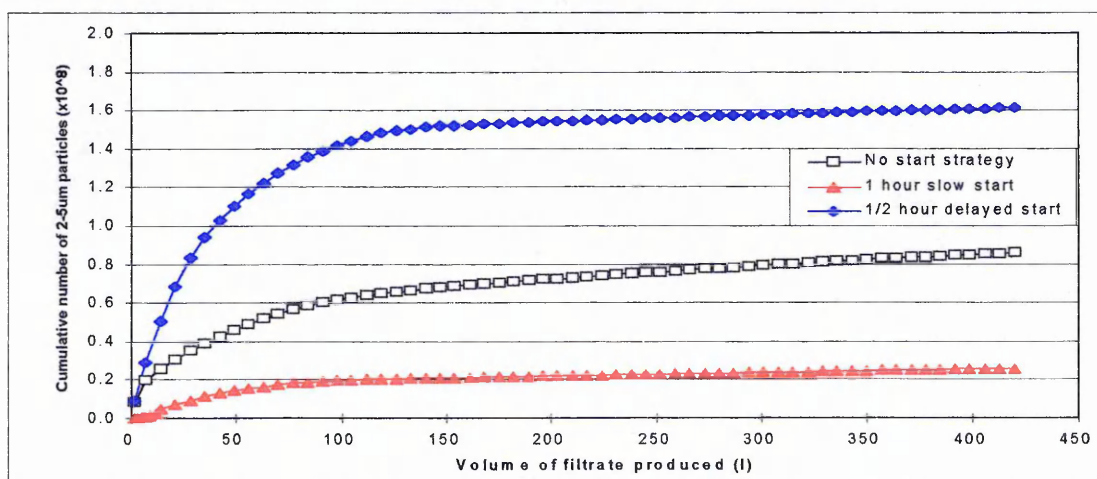
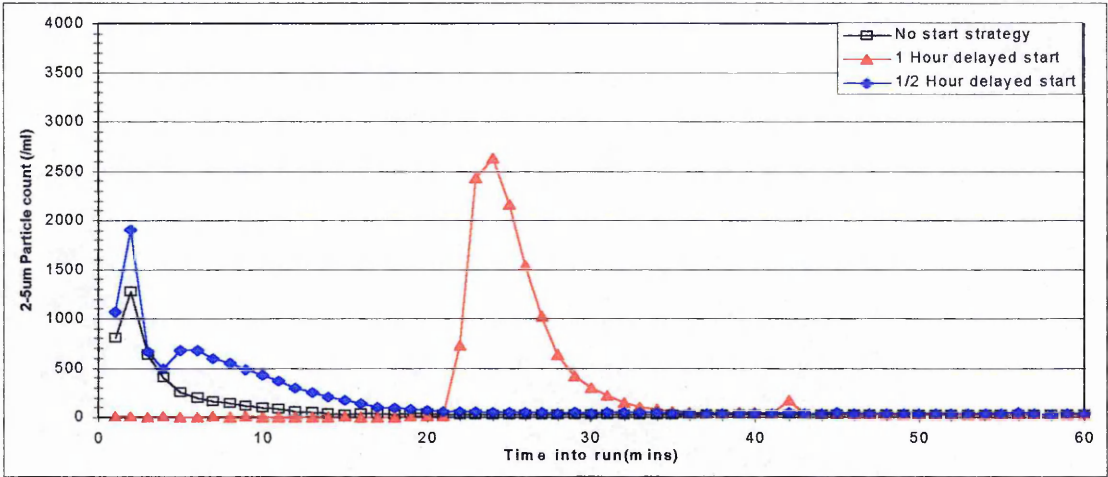
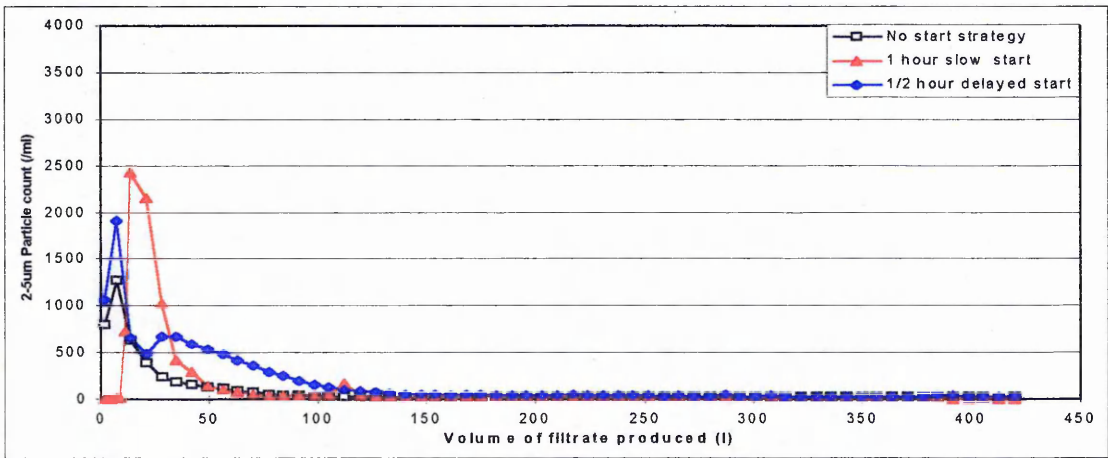


Figure 8.10c Cumulative number of 2-5µm particles in filtrate vs. volume of filtrate - 2m of 2.0-3.35mm sand, 1.0mg/l ferric sulphate, 1 hour slow start, 1/2 hour delayed start.



**Figure 8.11a Filtrate particle count vs. time - 2m beds of 2.0-3.35mm sand, 1.5mg/l ferric sulphate, 1 hour slow start, 1/2 hour delayed start.**



**Figure 8.11b. Filtrate particle count vs. volume of filtrate produced - 2m beds of 2.0-3.35mm sand, 1.5mg/l ferric sulphate, 1 hour slow start, 1/2 hour delayed start.**

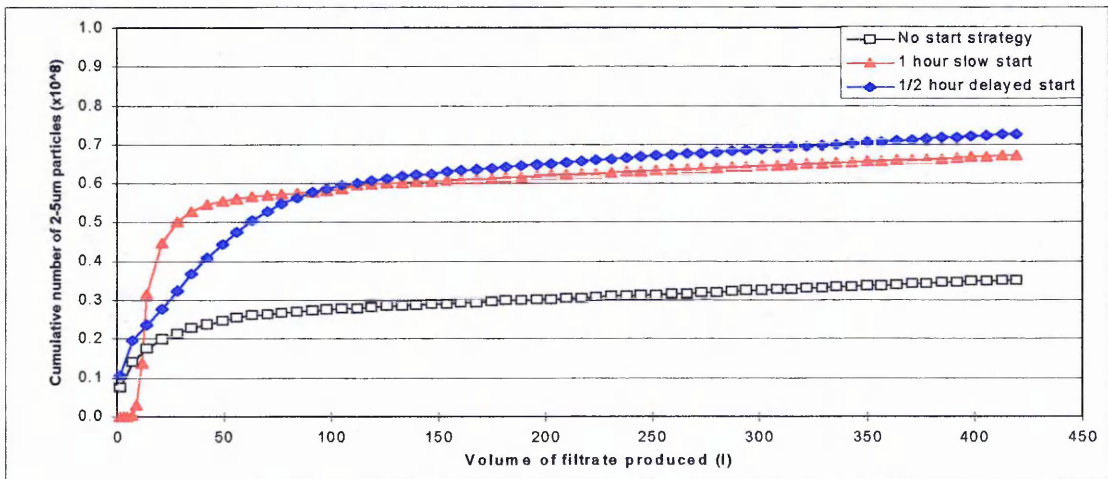


**Figure 8.11c Cumulative number of 2-5µm particles in filtrate vs. vol of filtrate - 2m of 2.0-3.35mm sand, 1.5mg/l ferric sulphate, 1 hour slow start, 1/2 hour delayed start.**

When the double peaks are looked at in terms of volume of filtrate passed (Fig. 8.12b), it can be seen that both the slow start and delayed start filter produced a second peak after about 25-30l, these peaks occurred a little before the interface between the backwash remnants (60.8 l). The slow start filter ripened the quickest, the control and delayed start filters required a large volume to ripen - between 250 and 300 l.

The cumulative number of particles in the filtrate (Fig 8.12c) show that during the first 20 l of filtrate the numbers from the three filters are similar. However, the numbers in the filtrate from the control filter were always higher. The numbers in the filtrate from the 1 hour delayed start filter were slightly less than the control throughout and became greater than the numbers in the filtrate from the 1/2 hour slow start filter after the first 50 l, due to slower ripening.

The fourth example (Fig 8.13a, b, and c) shows the performance of the same filters operating with the same start-up conditions to the previous example. However, the raw water particle count was slightly higher (3000/ml) and the ferric dose had been increased to 1.5mg/l as  $\text{Fe}^{3+}$ . It can be seen in the particle counts (Fig 8.13a) that the peaks, of the control and slow start filters, were higher than in the previous example. However, the filters ripened more rapidly, and the steady state values were lower. The biggest difference was the delayed start particle count, which had been greatly reduced relative to the control filter.

When the particle count is viewed plotted against volume of filtrate it can be seen that the control filter had ripened after 150 l had been filtered. The slow start filter ripened very rapidly, after only 60 l; and the delayed start filter ripened after 120 l. There was no clear double peaks, as in the previous example

When the cumulative number of particles is plotted against the volume of filtrate (Fig 8.13c) it becomes clear how low the numbers in the filtrate from the 1 hour delayed start filter were under these conditions. The slow start filter can be seen to perform similar to the control filter initially, but after 40 l the numbers in NPF is lower than the control.

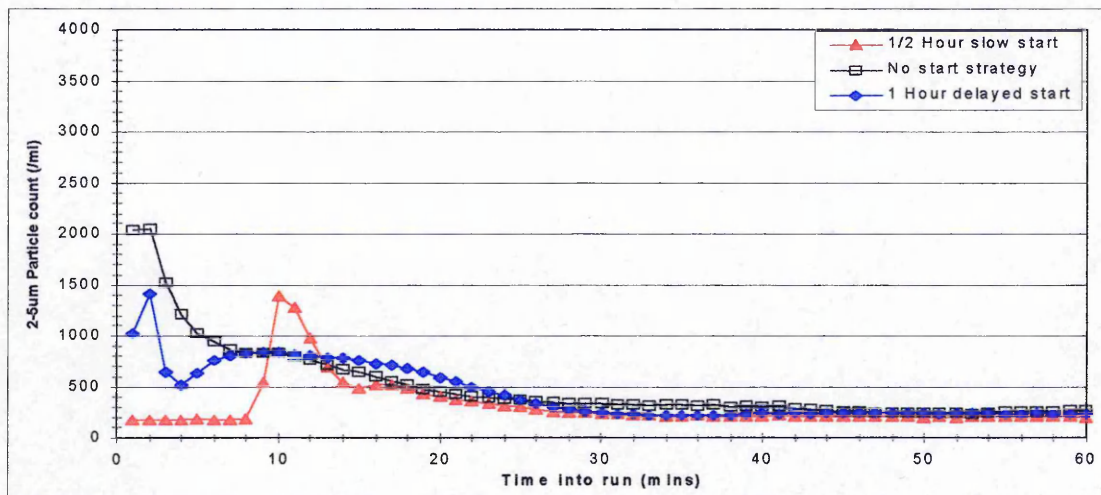


**Figure 8.12a** Filtrate particle count vs. time - 2m beds of 2.0-3.35mm sand, 1.0mg/l ferric sulphate, 1/2 hour slow start, 1 hour delayed start.

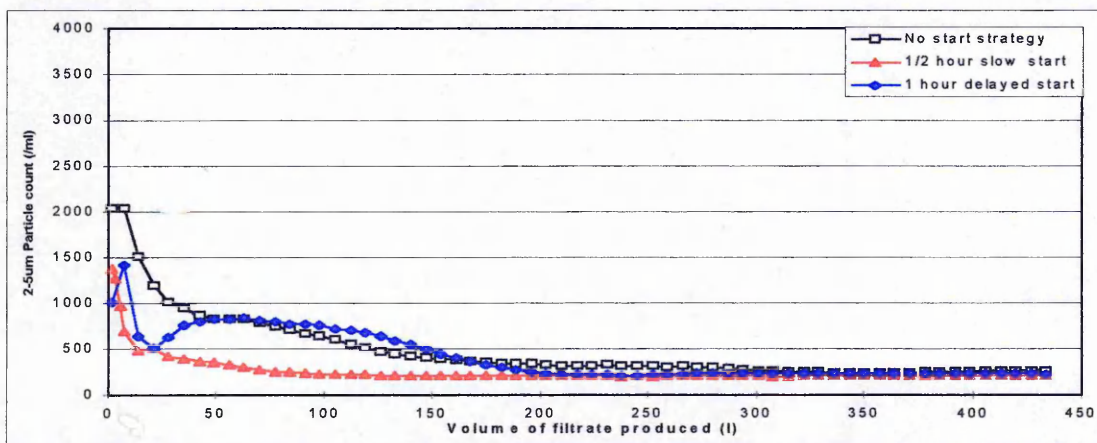


**Figure 8.12b** Filtrate particle count vs. volume of filtrate produced - 2m beds of 2.0-3.35mm sand, 1.0mg/l ferric sulphate, 1/2 hour slow start, 1 hour delayed start.

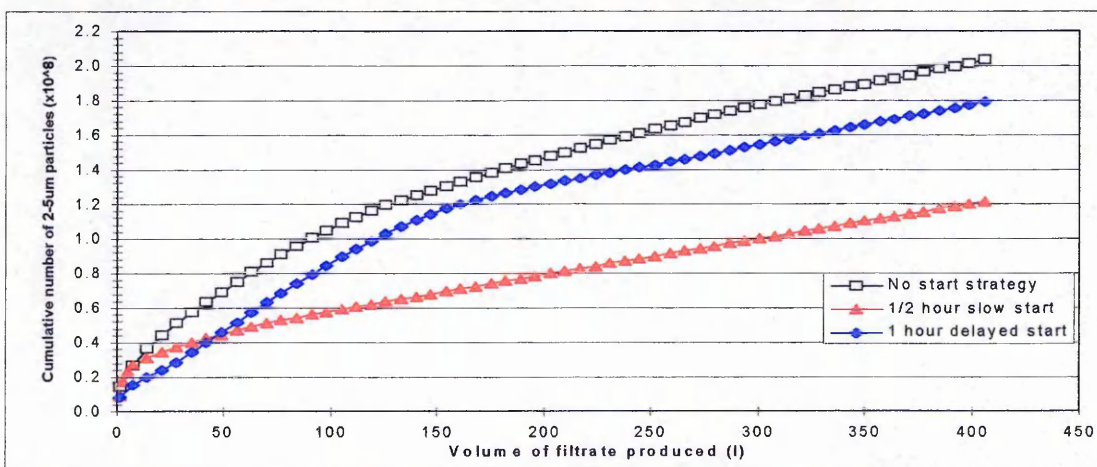


**Figure 8.12c.** Cumulative number of 2-5µm particles in filtrate vs. vol of filtrate produced - 2m of 2.0-3.35 sand, 1.0mg/l ferric sulphate, 1/2 hour slow start, 1 hour delayed start.

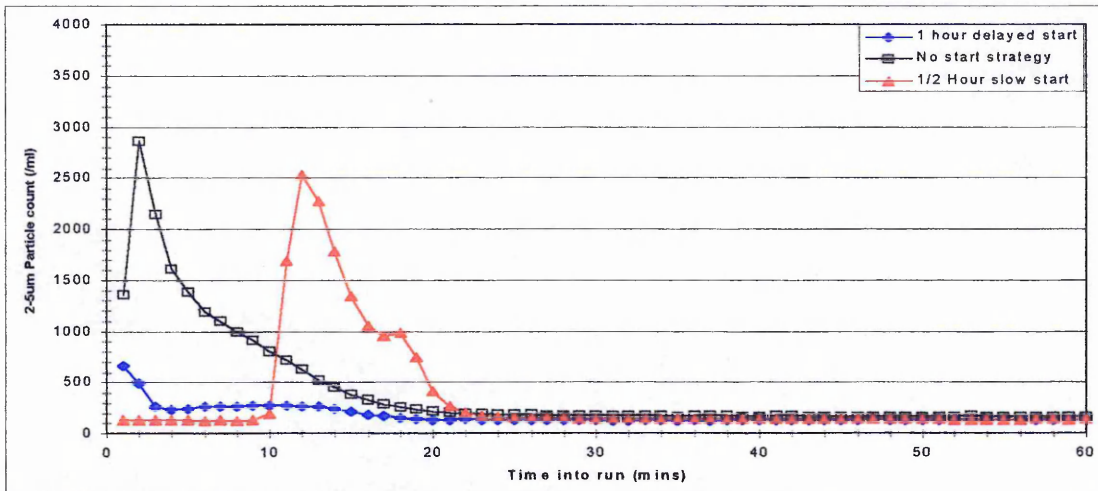


Figure 8.13a Filtrate particle count vs. time - 2m beds of 2.0-3.35mm sand, 1.5mg/l ferric sulphate, 1/2 hour slow start, 1 hour delayed start.

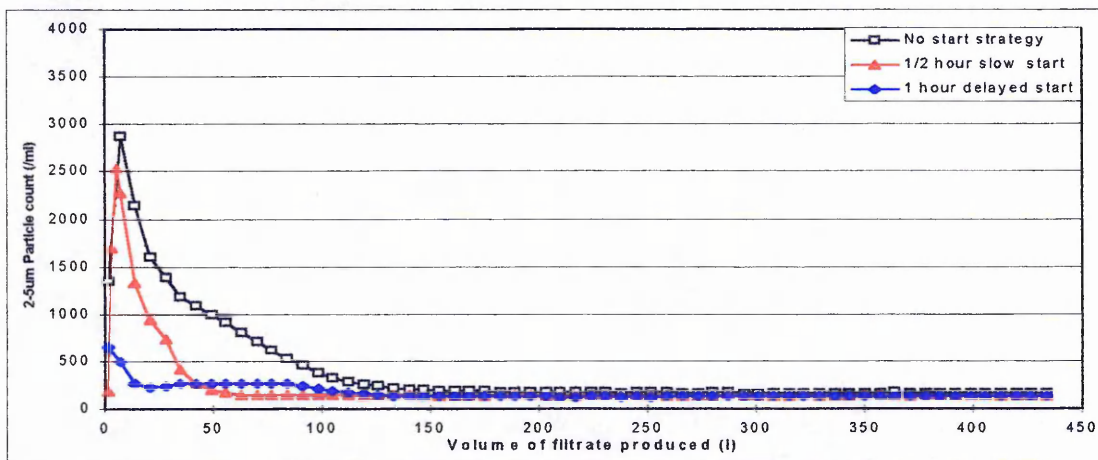


Figure 8.13b Filtrate particle count vs. volume of filtrate produced - 2m beds of 2.0-3.35mm sand, 1.5mg/l ferric sulphate, 1 hour slow start, 1/2 hour delayed start.

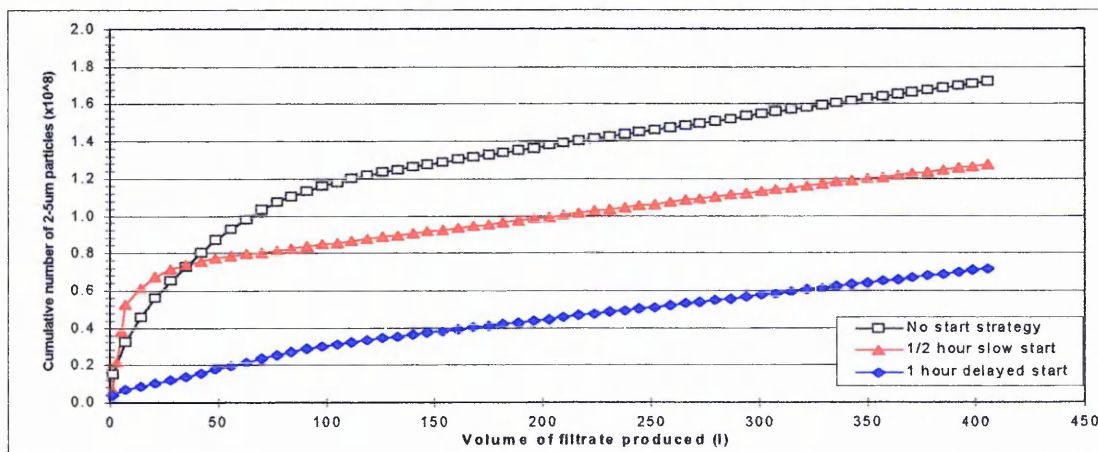


Figure 8.13c Cumulative number of 2-5µm particles in filtrate vs. vol of filtrate - 2m beds of 2.0-3.35mm sand, 1.0mg/l ferric sulphate, 1/2 hour slow start, 1 hour delayed start.

The information in Table 8.4 summarises the performance of the start-up strategies relative to the control filters for the whole trial. The runs up to and including the 31/8/95 had the 1mg/l as  $\text{Fe}^{3+}$  ferric dose, the runs after this date had a dose of 1.5mg/l. The data is expressed as start-up strategy NPF as a percentage of the control (i.e. no start strategy) NPF.

**Table 8.4. The effect of start-up strategy on daily performance in terms of NPF for 2m beds of 2.0-3.35mm sand.**

Date of run	Start-up strategy NPF as % of control (no start strategy) NPF			
	1/2 hour delayed start	1 hour delayed start	1/2 hour slow start	1 hour slow start
7/8/95	188.3			30.2
9/8/95	158.2			38.2
11/8/95	181.9			44.6
15/8/95		90.7	53.0	
17/8/95		85.4	61.0	
25/8/95		88.1	59.8	
31/8/95		82.8	48.2	
18/9/95		36.5	84.3	
20/9/95		42.2	74.4	
22/9/95		26.8	102.6	
20/10/95			121.7	
15/11/95	157.2			161.8
23/11/95	148.8			96.7
29/11/95	144.3			129.5
7/12/95	145.7			94.3

### 8.3.3 Filter headloss development

The following section details the effects of start-up strategies on the headloss development, especially during the start of the run, for the two types of filter.

#### 8.3.3.1 1m beds of 0.5-1.0mm sand

Figures 8.14 a-d show the headloss development under different start-up strategies, and ferric doses, for the 0.5-1.0mm sand filters. The headloss development is shown plotted against volume of filtrate produced in order to normalise the slow start; 2500l of filtrate equates to approximately 6 hours of filter run. It can be seen that the headloss development under all conditions was linear.

With a ferric dose of 1.0mg/l as  $\text{Fe}^{3+}$  the 1 hour slow start headloss development was greater and the 1/2 hour delayed start filters headloss development was less than that of the control (Fig 8.14a). According to the Carmen Kozeny equation the clean bed headloss of the filters should be 31cm; the initial headloss of all the filter was actually about 20cm under these conditions. The gradient of the 1 hour slow start filter can be seen to be slightly greater than that of the control, which means a shorter filter runlength can be achieved.

When the ferric was increased to 1.5mg/l (Fig 8.14b) the initial headloss (35cm) and indeed the headloss development of the control was slightly higher. The initial headloss of the 1 hour slow start was 38cm and of the 1/2 hour delayed start was the same as the control. The 1/2 hour delayed start filter was not performing as well, relative to the control, under these conditions.

Similar trends can be seen when looking at 1/2 hour slow start and 1 hour delayed start at both the 1.0 and 1.5mg/l ferric doses (Figs 8.14c and d). These particular start-up strategies seem to more closely resemble the control.

A number of general observations can be made: The control filters headloss development at the same ferric doses (i.e. figs 8.14a and c; b and d) were similar, with any slight differences due to variability of the raw water; and the duration of the start-up strategies did not seem to be significant in terms of headloss development.

#### 8.3.3.2 2m beds of 2.0-3.35mm sand

Figures 8.15a-d show the headloss development under different start-up strategies, and ferric doses, for the 2.0-3.35mm sand filters. The headloss development is shown plotted against volume of filtrate produced in order to normalise the slow start; 12000l of filtrate equates to approximately 28 hours of filter run. It can be seen that the headloss development under all conditions was linear.



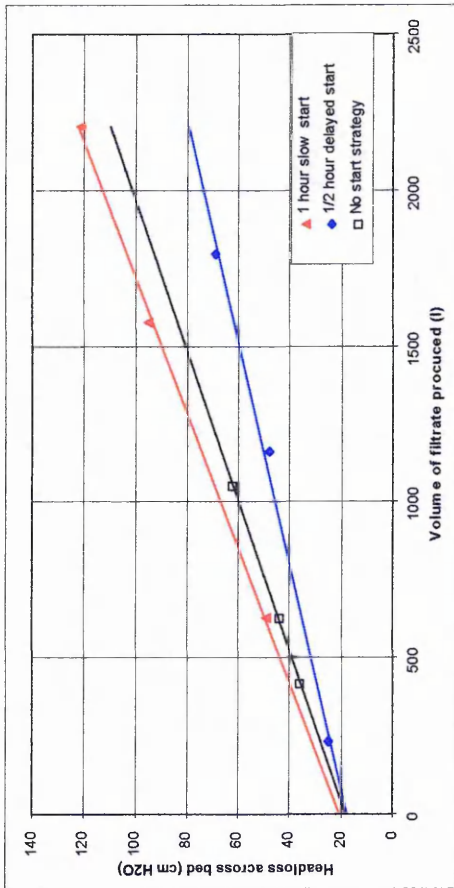


Figure 8.14a.  $\Delta H$  -1m beds 0.5-1.0mmsand, 1.0mg/l ferric.

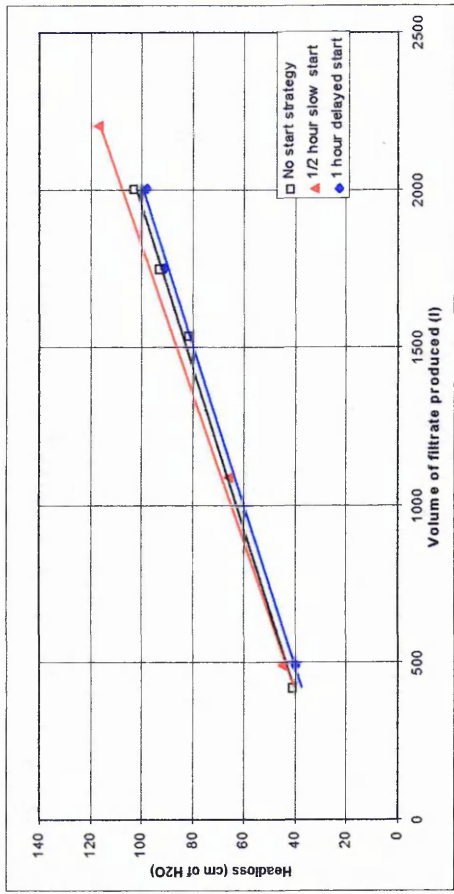


Figure 8.14c.  $\Delta H$  -1m beds of 0.5-1.0mm sand,1.0mg/l ferric

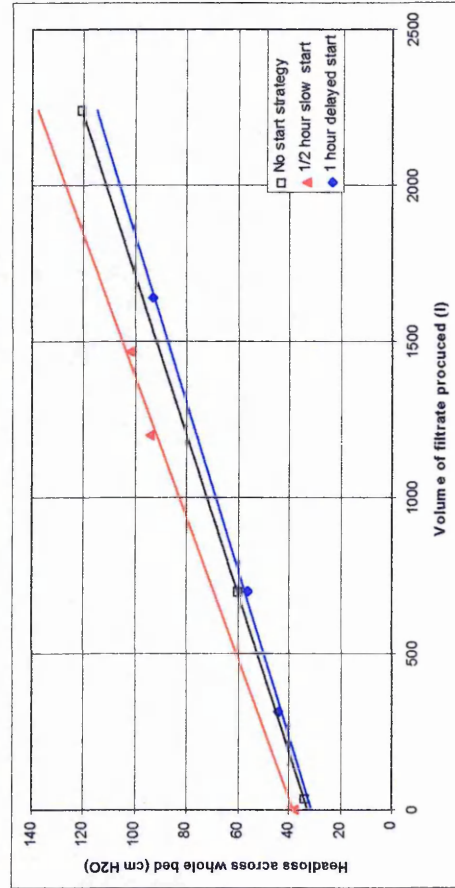


Figure 8.14b.  $\Delta H$  -1m beds of 0.5-1.0mm sand,1.5mg/l ferric.

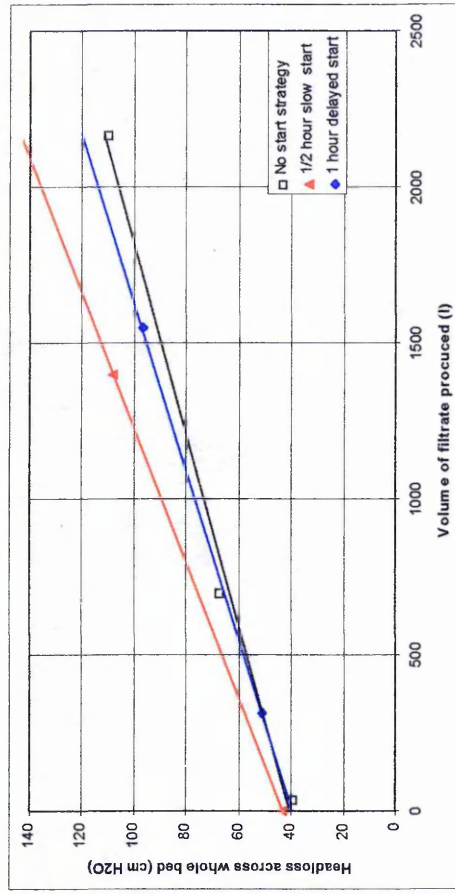


Figure 8.14d.  $\Delta H$  -1m beds of 0.5-1.0mm sand,1.5mg/l ferric

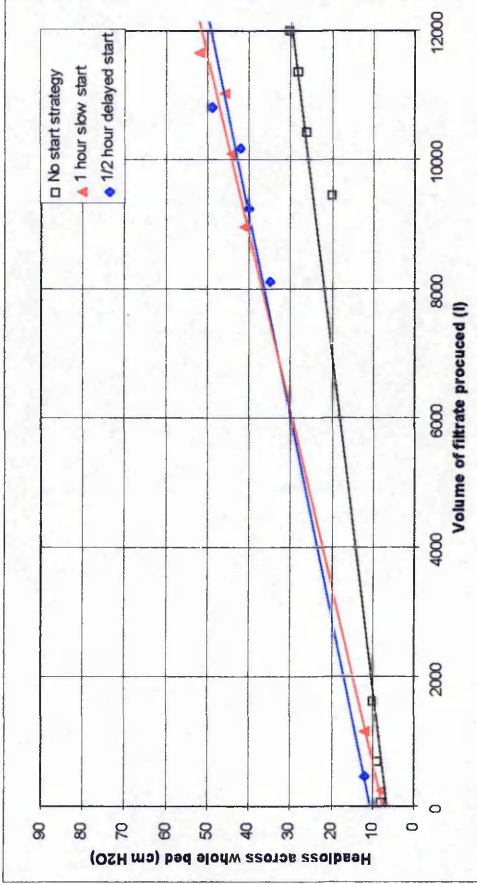


Figure 8.15a.  $\Delta H$  -2m beds of 2.0-3.35mm sand, 1.0mg/l ferric.

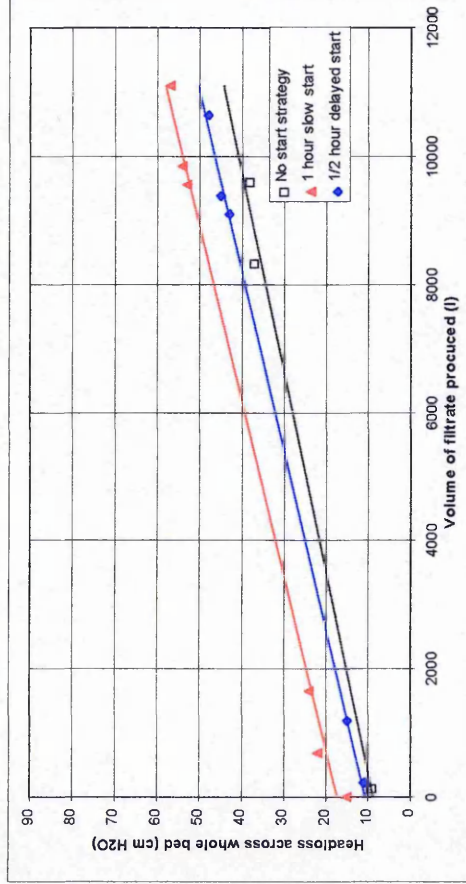


Figure 8.15b.  $\Delta H$  -2m beds of 2.0-3.35mm sand, 1.5mg/l ferric.

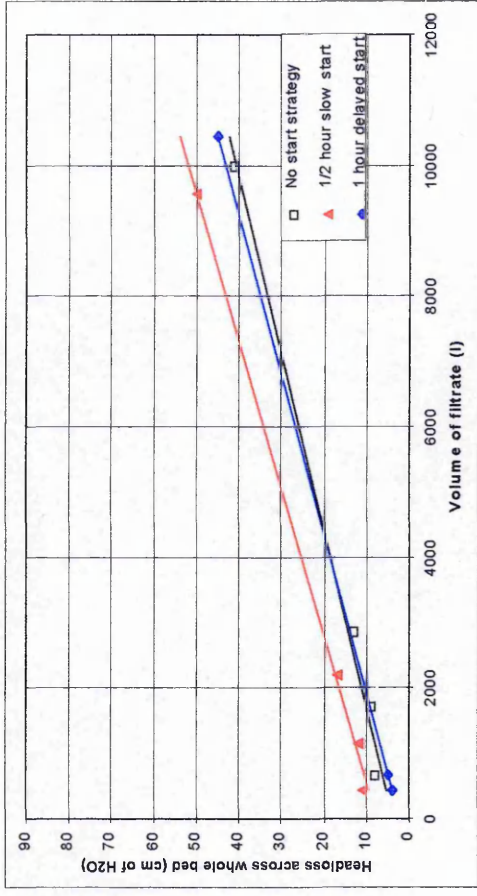


Figure 8.15c.  $\Delta H$  -2m beds of 2.0-3.35mm sand, 1.0 mg/l ferric.

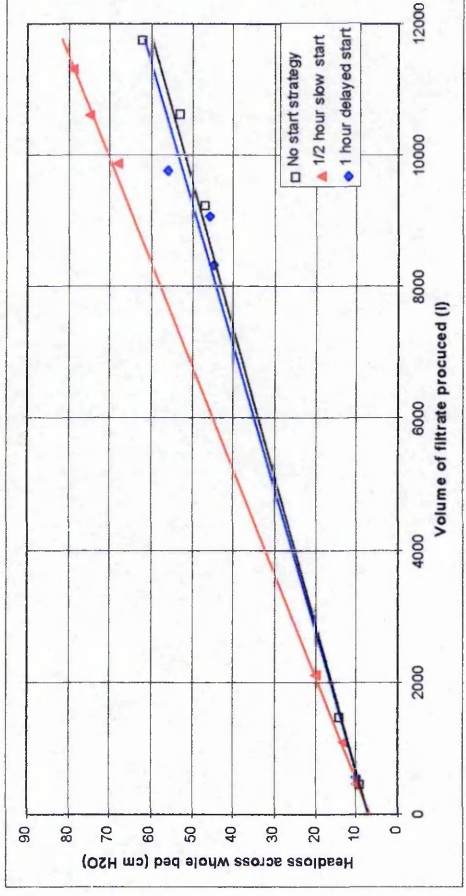


Figure 8.15d.  $\Delta H$  -2m beds of 2.0-3.35mm sand, 1.5mg/l ferric.

With a ferric dose of 1.0mg/l as  $\text{Fe}^{3+}$  both the 1 hour slow start and 1/2 hour delayed start filters headloss development was greater than that of the control (Fig 8.15a). According to the Carmen Kozeny the clean bed headloss of the filters should be 5cm; the initial headloss of the control filter was actually 8cm, as was that of the 1 hour slow start filter, whereas the initial headloss of the 1/2 hour delayed start filter was 11cm. The gradients of both the start-up strategy filters can be seen to be greater than that of the control, which means a shorter filter runlength can be achieved.

By increasing the ferric dose to 1.5mg/l the initial headloss of the 1hour slow start was increased from 8cm to 17cm (Fig 8.15b), The headloss development of all the filters was then fairly equal, however, it was higher than in the previous example - approx. 20cm greater after half the filter run. The 1/2 hour delayed start had improved slightly relative to the control.

Similar trends can be seen when looking at 1/2 hour slow start and 1 hour delayed start at both the 1.0 and 1.5mg/l ferric doses (Figs 8.15c and d). The 1 hour delayed start performs almost identically to the control. The initial headloss of the 1/2 hour slow start was slightly higher (5cm) at 1.0mg/l ferric. The gradients, or headloss development, was equal for all the filters at this ferric dose. The 1.5mg/l ferric dose increased the rate of headloss development for all the filters, by about 10cm at the half run stage.

Generally, the start-up strategies had the effect of slightly increasing the rate of headloss development. The biggest increase was caused by 1 hour slow start. However, this filter configuration could still produce very long runlengths - up to 100 hours.

#### *8.3.4 Relationship between raw water quality and NPFR*

When all the NPFR data is plotted against the NP in an equivalent volume of raw water at the time of ripening an interesting trend appears. Figures 8.16 and 8.17 show this relationship for the 1m beds of 0.5-1.0mm sand and 2m beds of 2.0-3.35mm sand respectively.

The best fit line in Fig 8.18 is a polynomial and is for the control filter only. The start-up NPFR data is included to show the relative improvements. It is interesting to note that, although not plotted, the start-up strategies display a similar pattern.

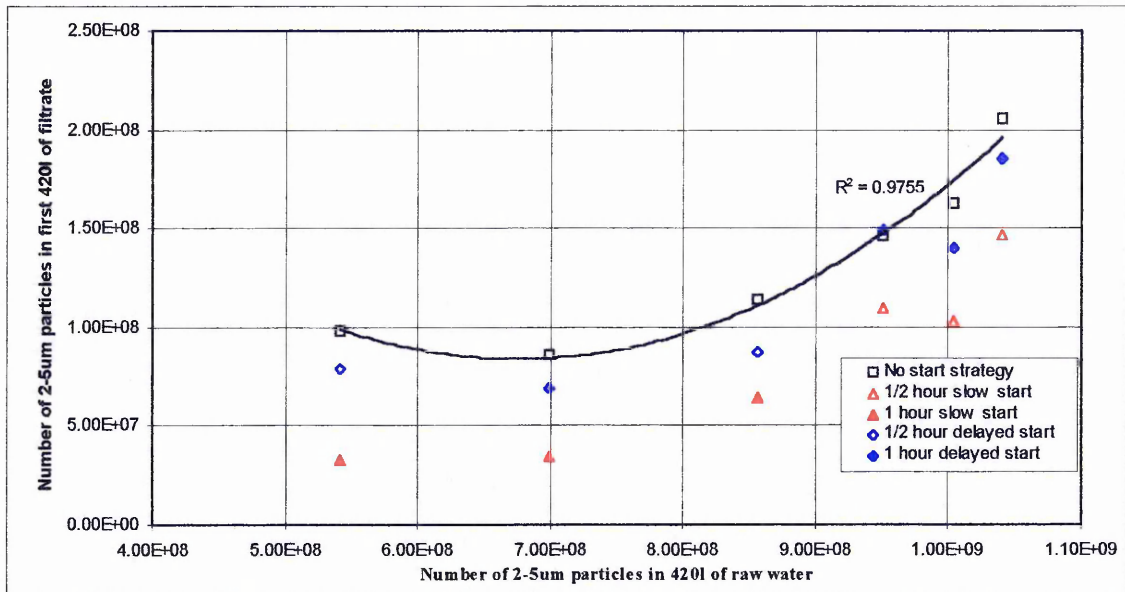


**Figure 8.16. Relationship between NPFR from 1m beds of 0.5-1.0mm sand (1.0mg/l ferric) and raw water quality. \*Polynomial best fit line is for control only.**

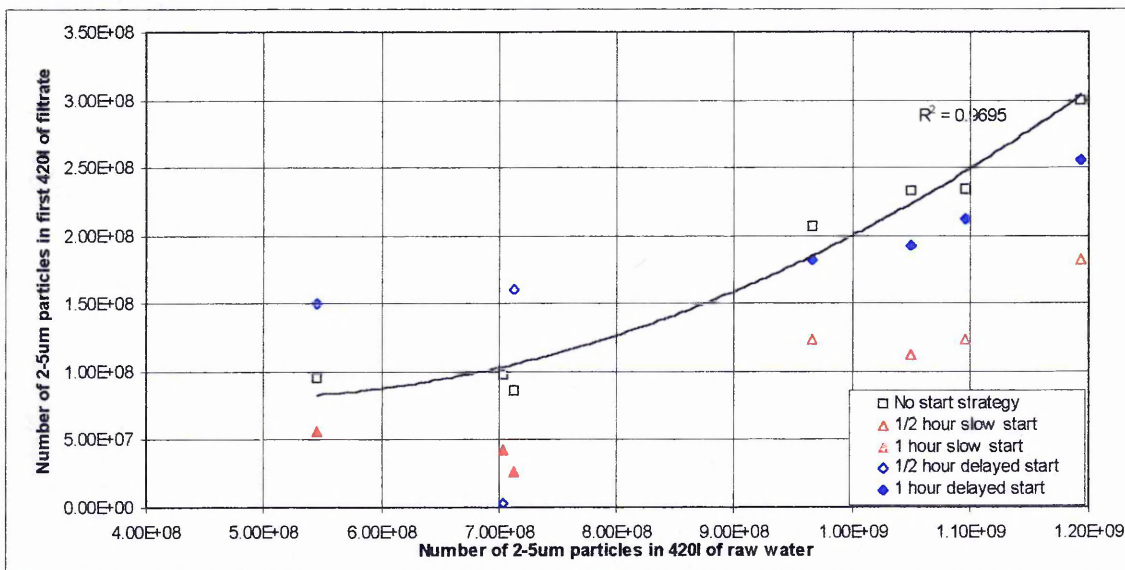


**Figure 8.17. Relationship between NPFR from 2m beds of 2.0-3.35mm sand (1.0mg/l ferric) and raw water quality. \*Polynomial best fit line is for control only.**

A comparison of the control NPFRs from the two types of filter is shown in Fig 8.18. Despite the differences in media size and bed depth, the polynomial plots are remarkably similar.

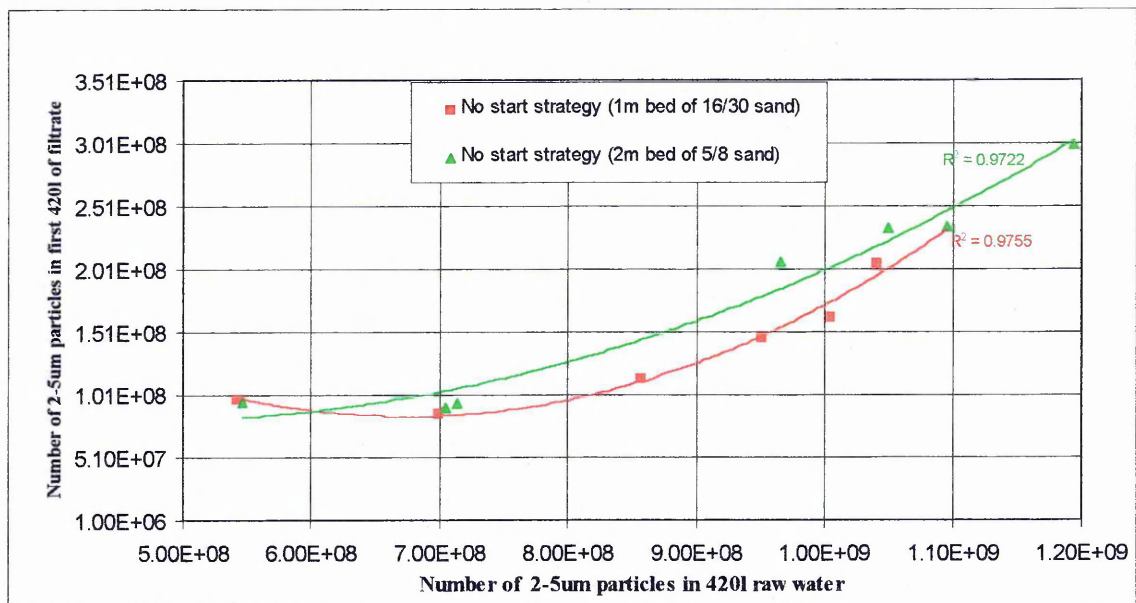


Figure 8.18. Comparison of relationships between NPFR and raw water quality.

## 8.4 Discussion

This section will discuss the effects of start-up strategies, under all operating conditions, on filter performance in terms of numbers of 2-5 $\mu$ m particles in the filtrate, and headloss development.

### 8.4.1 The effect of start-up strategies on filter performance

The overall effect of the start-up strategies on the filter performance relative to the control filters is summarised in Tables 8.5 and 8.6 for the 1m beds of 0.5-1.0mm sand and 2m beds of 2.0-3.35mm sand respectively.

**Table 8.5. The overall effect of start-up strategies on performance of 1m beds of 0.5-1.0mm sand.**

Start-up strategy → Coagulant dose ↓	Start-up strategy NPFR as % of control NPFR			
	1/2 hour delayed start	1 hour delayed start	1/2 hour slow start	1 hour slow start
1.0 mg/l Ferric (III) sulphate	79.1 (2.4) [3]	90.8 (7.8) [4]	69.9 (5.0) [4]	40.1 (6.1) [3]
1.5 mg/l Ferric (III) sulphate	61.8 (4.4) [3]	39.8 (9.0) [4]	85.5 (37.4) [4]	75.6 (5.2) [3]

Figures are start-up strategy NPFR as % of control NPFR. ( ) - standard deviations, [ ] - number of runs assessed.

**Table 8.6. The overall effect of start-up strategies on performance of 2m beds of 2.0-3.35mm sand.**

Start-up strategy → Coagulant dose ↓	Start-up strategy NPFR as % of control NPFR			
	1/2 hour delayed start	1 hour delayed start	1/2 hour slow start	1 hour slow start
1.0 mg/l Ferric (III) sulphate	176.1 (15.8) [3]	86.8 (3.4) [4]	55.7 (6.3) [4]	37.4 (7.2) [3]
1.5 mg/l Ferric (III) sulphate	149.5 (5.8) [4]	35.2 (7.7) [4]	95.8 (20.8) [4]	120.5 (31.8) [4]

Figures are start-up strategy NPFR as % of control NPFR. ( ) - standard deviations, [ ] - number of runs assessed.

#### 8.4.1.1 Performance under "normal conditions" with 1.0mg/l ferric dose.

The performance of the filters under "normal conditions" with a 1.0mg/l ferric dose will be discussed first.

Amirthirajah and Wetstein (1980) hypothesised that once a fluidised bed is brought back to the fixed bed state after backwashing, the collisions between the particles will cause some solids from the surface of the media grains to be dislodged into the backwash water remnants within the pores. The fraction of the backwash water above the media is not subjected to this mechanism and will exhibit characteristic unlike the other backwash component

The hypothesis behind delayed start was that the detached particles present in the interstitial spaces of the filter bed would be able to settle under gravity (without fluid streamlines) transporting them to the media surfaces, with which they may be able to re-attach to. Not only would these particles be removed and therefore not be present in the filtrate during ripening but they may act as additional collectors; going one step further than retaining some particles on the media after backwash (previous chapter).

Delayed start is therefore dependant upon the settling velocities of the particles present in the interstitial spaces. From particle count data of the ripening, corresponding to the detention time of the backwash remnants from within the bed (37.5 l for 0.5-1.0mm sand; 60.8 l for 2.0-3.35mm sand), it is known that the majority of the particles in this component that reach the filtrate are 2-5µm in diameter. The following calculations (adapted from Ives, 1995) show the settling velocity of a *Cryptosporidium* oocyst and of a ferric hydroxide floc of the same diameter.

For a free oocyst the settling velocity in water is defined by Stokes' Law as:

$$v_t = \frac{g (\rho_s - \rho)}{18 \mu} d^2$$

where  $v_t$  = terminal settling velocity (m/s)

$g$  = gravitational acceleration (9.81 m/s<sup>2</sup>)

$\rho_s$  = density of oocysts / particles? (1050 kg/m<sup>3</sup>)

$\rho$  = density of water (998 kg/m<sup>3</sup> at 20°C)

$\mu$  = viscosity of water (1.01 x 10<sup>-3</sup> kg/m s at 20°C)

$d$  = oocyst diameter (4 x 10<sup>-6</sup> m)

$$v_t = \frac{9.81 (1050 - 998)}{18 \cdot 1.01 \times 10^{-3}} (4 \times 10^{-6})^2$$

$$v_t = 0.5 \times 10^{-6} \text{ ms}^{-1}$$

$$v_t = 0.5 \times 10^{-3} \text{ mms}^{-1}$$

In half an hour the single oocyst will therefore settle 0.9mm and in one hour will settle 1.8mm

Average pore size of 0.5-1.0 sand = 6.9 x 10<sup>-5</sup> m = 0.69mm

Average pore size of 2.0-3.35 sand = 2.3 x 10<sup>-4</sup> m = 2.3mm

The calculations show that it would take approx. 23 minutes for a single oocyst to settle from the centre of an average sized pore in the 0.5-1.0mm sand bed, and 76 mins in the 2.0-3.35mm sand bed. These figures show that it is theoretically possible for many of the smallest particles to settle under gravity from within the interstitial spaces to interact with the media.

The setting velocity of hydroxide floc of the same particle diameter and density ( $\rho_s$ ) 1107 kg/m<sup>3</sup> (since  $\rho_s$  of hydroxide floc = 1180 kg/m<sup>3</sup>, but assuming 40% water  $\rho_{floc} = 1107 \text{ kg/m}^3$ )

$$v_t = \frac{9.81 (1107 - 998)}{18 \cdot 1.01 \times 10^{-3}} (4 \times 10^{-6})^2$$

$$v_t = 0.9 \times 10^{-6} \text{ ms}^{-1}$$

$$v_t = 0.9 \times 10^{-3} \text{ mms}^{-1}$$

The calculations show that it would take approx. 13 minutes for such a floc to settle from the centre of an average sized pore in the 0.5-1.0mm bed, and 43 minutes in the 2.0-3.35mm sand bed. The calculations show that a 1/2 hour delay would be long enough for such flocs to settle from the centre of pores in the 0.5-1.0mm sand beds, and therefore interact with the media. The



calculations also show that a 1/2 hour delay would be insufficient for such a floc to settle from the centre of a pore in the 2.0-3.35mm sand bed. Conversely, a 1 hour delay would be sufficient.

The nature of the attachments should be considered, since the deposit morphology is likely to be different due to the absence of fluid streamlines and the associated shear forces, the attachments will also occur throughout the depth of the bed as opposed to the top layers. There is also some recent evidence (Pugh, 1995) that attachment forces between particles and media surfaces may increase with time. This suggests a longer delay may be beneficial

The experimental evidence seems to validate the delayed start hypothesis. When the filtrate particle count data was plotted against volume of filtrate produced it could be seen that the reduction facilitated by delayed start corresponded to the component of the backwash retained within the media. When the data was summarised it was found that for the 1m 0.5-1.0mm sand filter, with a 1/2 hour delay this component was reduced relative to the control, and contributed 36.4% of the NPFR; compared to 41.1% contributed by the control filter. For a 1hour delay the contribution of this component to the total NPFR was 20.4 and 24.9% for the delayed start and control filters respectively.

For the 2m 2.0-3.35mm sand filters a somewhat different picture emerged, the 1/2 hour delay provided a greater contribution to the NPFR than the control (54.3 compared to 47.1%). Conversely, the backwash remnants retained within the bed contribute less to the NPFR for a 1 hour delay 24.7% compared to the control value of 30.5%.

It was noticeable that delayed start did not facilitate faster ripening, and that the backwash component from above the media was not reduced relative to the control. This was most likely due to the widespread distribution of the re-attached particles, that is they were not just in the very top layers acting as additional collectors.

The delayed start provided improvement in performance (measured in terms of NPFR) when compared to the control. However, as expected the duration of the delayed start had a significant affect upon filter performance. When the 0.5-1.0mm sand is considered, the 1/2 hour delay was more effective, and for the 2.0-3.35mm sand the 1 hour was effective, yet the 1/2 hour delay was not.

The 1/2 hour delayed start was detrimental to performance of the 2.0-3.35mm sand filter under these conditions. Indeed, the overall NPFR was 161% that of the control filter NPFR. When the particle data was examined it could be seen that the backwash remnants from within the media contained more particles compared to the control (contributed 54.3% to the NPFR, control was 42.1) as did the backwash remnants from above the bed. If it was simply that particles were failing to reattach in the delay period the filter should perform the same as the control filter, yet it performs worse. Therefore some other phenomenon is occurring, it is likely that some particles do re-attach, the attractive forces may not be strong enough to overcome the initial hydraulic shear when the filter is returned to service. It is possible that other particles/flocs are pulled off the media grains, or that an avalanche effect occurs due to the different deposit morphology. Whatever is occurring it is plainly overcome when the delay is increased to 1 hour, after an hour the attachments may be sufficiently strong to overcome the initial hydraulic shear.

The slow start procedure has been used in one form or another in the U.K for a number of years, however, there has been very little literature published relating its performance. It has, however, become in vogue in the last few years due to the publication of the original Report of the group of experts on *Cryptosporidium* in water (DoE/DoH, 1992). In this report slow start was suggested as a way to reduce the passage of particulates into supply during the ripening period.

It was believed that slow start would work because the lower hydraulic shear forces present during the initial stages of re-start would mean build-up of additional collectors in the very top layers would be more rapid and hence the improvement in removal efficiency would also be more rapid.

In normal ripening, i.e. not under slow start, the additional collectors are thought to form chain like deposits or dendrites (Tien *et al.*, 1977; O'Melia and Ali, 1978) such deposits then act as preferential sites for particle deposition since they project into the fluid streamlines, interception is the most likely mechanism. Mackie and Bai (1992) concluded that the effect of deposit morphology is most significant in the top layers of the bed.

Therefore, under slow start, there will be very little penetration into the bed so formation of

dendrites will occur in the very top layers and these particle chains will not initially be subjected to high hydraulic shear and hence their formation should be that much more rapid.

The experimental evidence showed that under a range of "normal" conditions the 1/2 hour slow start provided an average improvement in performance of 30% for the 0.5-1.0mm sands filters and 45% for the 2.0-3.35mm sand filters. The 1/2 hour slow start was therefore more effective for the coarse 2.0-3.35mm media. This is most likely due to its larger pores, as the calculations below show larger pores mean lower shear forces.

In order to estimate the hydraulic shear stresses at the media boundary a number of assumptions have to be made (Fitzpatrick, 1991):

- 1) Average interstitial flow velocity
- 2) Local pore dimensions are uniform
- 3) There is a paraboloid velocity distribution (Poiseuille flow) in the pores

For a paraboloid velocity distribution:

$$v_i(\text{max}) = 2v_i(\text{mean})$$

Mean interstitial velocity  $v_i(\text{mean}) = \frac{Q}{A\varepsilon} \quad (\text{m s}^{-1})$

At the boundary, velocity gradient  $\frac{dv_i}{dr}$  is a maximum and  $v_i = 0$

$$\frac{dv_i}{dr(\text{max})} = \frac{4v_i(\text{max})}{d} (\text{s}^{-1}) = 4 \times \frac{2Q}{A\varepsilon d} (\text{s}^{-1})$$

Maximum shear stress  $\tau(\text{max}) = \frac{\mu dv_i}{dr(\text{max})} = \frac{8\mu Q}{A\varepsilon d} (\text{Nm}^{-2})$

Where:

$\mu$  = Absolute viscosity -  $1.18 \times 10^{-3} \text{ Nsm}^{-2} @ 14^\circ\text{C}$

$Q$  = Filtration flowrate -  $1.17 \times 10^{-4} \text{ m}^3 \text{ s}^{-1}$

$A$  = Surface area of filter -  $0.0707 \text{ m}^2$

$d$  = Filter pore diameter (m)

$\varepsilon$  = Porosity - 0.39

Average pore size of 0.5-1.0mm sand =  $6.9 \times 10^{-5} \text{ m}$

Average pore size of 2.0-3.35mm sand =  $2.3 \times 10^{-4} \text{ m}$

$$\text{Mean shear stress} \quad \tau (\text{mean}) = \frac{2}{3} \times \tau (\text{max})$$

$$\text{For 0.5-1.0mm sand:} \quad \tau (\text{max}) = \frac{8 \times 1.18 \times 10^{-3} \times 1.17 \times 10^{-4}}{0.0707 \times 0.39 \times 6.9 \times 10^{-5}}$$

$$\Rightarrow \tau (\text{max}) = 0.58 \text{ Nm}^{-2}$$

$$\tau (\text{mean}) = \frac{2}{3} \times 0.58 = 0.39 \text{ Nm}^{-2}$$

$$\text{For 2.0-3.35mm sand:} \quad \tau (\text{max}) = \frac{8 \times 1.18 \times 10^{-3} \times 1.17 \times 10^{-4}}{0.0707 \times 0.39 \times 2.3 \times 10^{-4}}$$

$$\Rightarrow \tau (\text{max}) = 0.17 \text{ Nm}^{-2}$$

$$\tau (\text{mean}) = \frac{2}{3} \times 0.17 = 0.11 \text{ Nm}^{-2}$$

The maximum shear force is found at the media surfaces, and the increase in media size from 0.5-1.0mm to 2.0-3.35mm can be seen to reduce the shear force from 0.58 to  $0.17 \text{ Nm}^{-2}$ . These rough calculations illustrate the differences in hydraulic shear that occur upon the media surfaces in "average" sized pores of the two types of filter bed.

The experimental evidence suggests that the particles that form these dendrites and improve removal in the slow start filters do not come from the influent as expected (Amirthirajah and Wetstein, 1980) but instead come from the backwash remnant above the media. The slow start filters ripen before the backwash remnants have been displaced. In fact the backwash remnants from above the media contribute 11.9% and 12.2% to the total NPFR for the 0.5-1.0mm sand 1/2 hour and 1 hour respectively ( control values- 24.9 and 24.8%). For the 2.0-3.35mm sand this component contributes 7.6% and 11.5% to the total NPFR for the 1/2 hour and 1 hour respectively ( control values- 13.2 and 15.7%).

These findings are well illustrated in Fig 8.19, the run was carried out during a time of very good raw water quality on 1m bed of 0.5-1.0mm sand employing a 1/2 hour slow start. It shows that the backwash remnant from above the media contains many more particles, in the 2-15 $\mu$ m size ranges, than even the flocculated raw water.

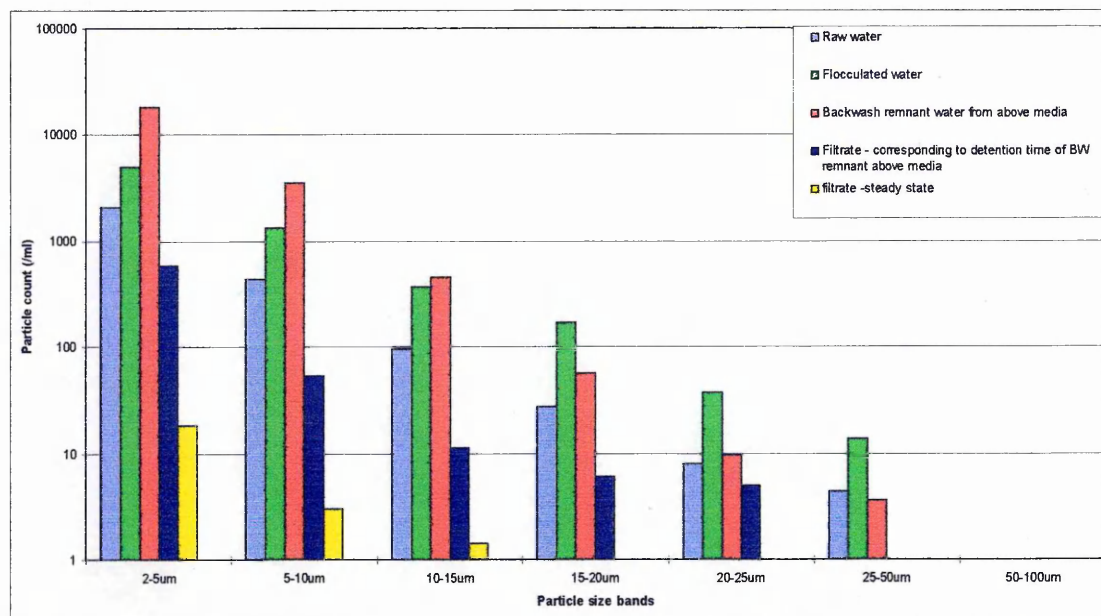


**Figure 8.19 Particle size distribution data for 1m 0.5-1.0mm sand filter, 1/2 hour slow start.**

This in itself is not too unexpected, what is unexpected is the numbers of particles in the same volume once it reaches the filtrate. The majority of these particles have been removed. It is likely that particle chains are forming rapidly in the very top layers from particles in the first part of this component (just above the bed) and therefore removing many of the remaining particles in this component.

It is especially interesting that the 5-15 $\mu$ m particles are being so well removed since a study by Clark *et al* (1992) reported poor removal of 6-13 $\mu$ m particles (without slow start), they attributed the poor removal to either floc break off or surface chemistry. It can be concluded that under these conditions floc break off is not occurring in the filter, nor was it occurring in the control filter under these conditions.

When the 1 hour slow start duration is considered it can be seen that the performance of the 0.5-1.0mm sand filters improves by a further 45% (total of 65% relative to control), whereas, the 2.0-3.35mm sand filter only improves a further 16%. The further reduced hydraulic shear during the 1 hour slow start means that dendrites will have more chance to form upon the smaller 0.5-1.0mm media with its associated smaller pores and higher shear forces (compared to the 2.0-3.35mm sand).

#### *8.4.1.2 Performance under "extreme conditions" with 1.5mg/l ferric dose.*

From Tables 6.1 and 6.2 it can be seen that very different results were obtained when the ferric (III) sulphate dose was increased from 1.0 to 1.5mg/l as Fe<sup>3+</sup>. This increase in ferric dose - which came into effect for a range of poor quality raw water - apparently caused the performance shift. Other factors that may have had an affect have been considered such as: temperature, organic content, algae content, raw water particle size distributions.

The colour of the water, and therefore its humic content, was very low and showed little variability throughout the entire trial and no significant change was observed immediately before, during or after the ferric increase ( mean = 2.3 Hazen; s.d = 0.71).

The temperature range across the duration of the trial was 15°C to 5.5°C and this at first glance may appear significant since the effect of temperature on filter performance is well documented. However, there are two reasons as to why temperature change was not a significant factor. Firstly, the performance of all start-up strategies is assessed relative to a control which backwashed and therefore ripened within hours of the others. Secondly, around the time of the ferric dose change the affect on performance was immediately obvious. Indeed, if the results are

looked at for 2 weeks either side of the increase, there are at least 2 readings for both types of filter (temp range 13°C to 12°C) that confirm the change in performance.

It has been shown how the increased ferric dose had little effect on the particle size distribution of the raw water, however, it did have an effect on the overall numbers of particles going onto the filters. The 1.0mg/l ferric (as  $\text{Fe}^{3+}$ ) did not appear to be sufficient to satisfy the chemical demand of the raw water under the deteriorating conditions and hence fully destabilise the particles, since the filters were not ripening to the same degree. It has been widely reported that such poor performance is indeed attributable to surface chemistry (Tobiason and O'Melia, 1988; Graham, 1988). By increasing the ferric dose to 1.5mg/l much more colloidal matter appeared to be flocculated, or it may be that the chemical demand was satisfied and precipitate was being formed. Performance of the filters did improve under the increased dose, so the surface chemistry appeared to be more favourable.

The effect of start-up procedures on filter performance under these conditions was dramatic. The delayed start shows an overall improvement: for the 0.5-1.0mm sand the 1/2 hour delayed start improves performance on average by 40% (20% more than the 1.0mg/l ferric dose) and the 1 hour delayed start by 60% (50% more than the 1.0mg/l ferric dose). When the results from the coarse 2.0-3.35mm sand filters are examined a similar trend is seen. The 1/2 hour delayed start improves compared to the 1.0mg/l ferric dose performance, but is still greater than the control (149%). The 1 hour gives an improvement in performance of 65% (50% improvement from 1.0mg/l ferric dose).

Under these more extreme drought conditions many more particles had to be filtered so the beds became more clogged. However, the backwash regime was not changed (to alter another variable mid trial was undesirable). Therefore, after a 48 hour run more material would be contained within the filter bed, the backwash would not be as efficient and more material would be left on the media grains (it has already been shown that this can improve performance). It follows that there would have been more particles released into the interstitial spaces upon bed contraction. The backwash component may also contain more particles. Fig. 8.20 shows backwash water turbidity curves for the 2 ferric doses on a 1m 0.5-1.0mm sand filter. It can be seen more solids are removed from the filter at the higher ferric dose, however as stated more material will also remain.

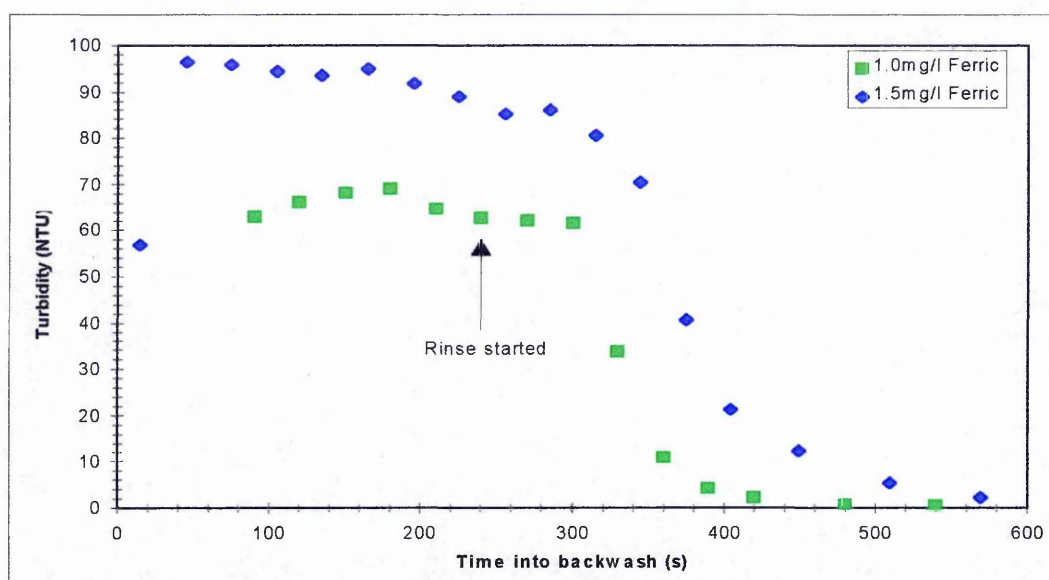


**Figure 8.20. Backwash water turbidities under different raw water and pre-treatment conditions - 1m 0.5-1.0mm sand filter.**

Under these conditions the delayed start data suggests that many more particles are re-attaching and if not actually forming dendrites (the deposit morphology will be different due to the lack of fluid streamlines) providing sites that they are more likely to form on. Under the 1.0mg/l ferric dose these were dispersed throughout the bed and didn't actually speed-up ripening. Under the 1.5mg/l ferric dose the greater numbers of re-attached particles meant they were speeding up the ripening process.

Interestingly, the 1/2 hour delayed start still performed poorly in the 2m 2.0-3.35mm sand filter, probably for the same reasons.

The performance of the slow start relative to the control under these conditions was also significantly affected by the change in ferric dose. For the 0.5-1.0mm sand filters 1/2 hour slow start still provided a 23% improvement relative to the control, this is almost identical to the improvement at 1.0mg/l ferric (there was however greater variability in performance). However, the 1 hour slow start gives no benefit under these conditions.

When the coarse media is considered the reversal in performance relative to the control is more



severe. The 1/2 hour slow start was 95% of the control, only 5% improvement; the 1 hour slow start was 120% of the control.

The reversal in performance of slow start in some cases, relative to the control is most likely due to the phenomenon of floc break off. A number of researchers have provided evidence of floc break off and re-attachment during ripening (Darby and Lawler, 1989, 1990; Clark *et al.*, 1992). In these well controlled lab-scale experiments individual particles were apparently captured and then helped to capture other particles; a group of captured particles would then break off as a floc. This phenomenon was seen to occur for both types of filter. Figs 8.21 and 8.22 show examples of 10-20 $\mu$ m particle counts during the ripening period of a 0.5-1.0mm sand filter with a 1/2 hour slow start. Fig 8.21 is under the better quality raw water and 1.0mg/l ferric dose, and Fig 8.22 is for the deteriorated raw water conditions and 1.5mg/l ferric dose.

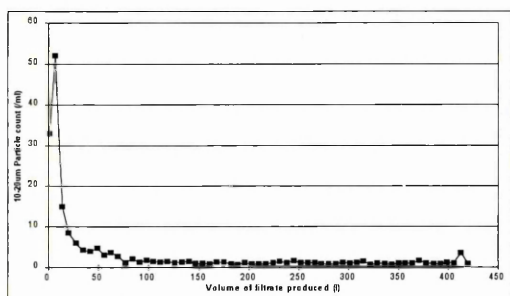


**Figure 8.21.** Ripening of 10-20 $\mu$ m particles - 1m 0.5-1.0mm sand, 1.0mg/l ferric.

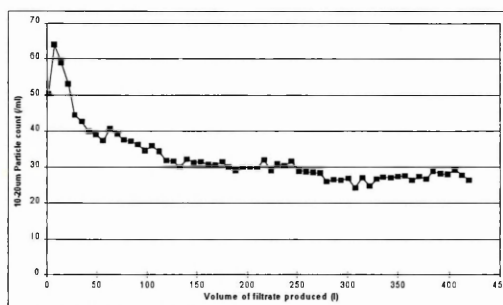


**Figure 8.22.** Ripening of 10-20 $\mu$ m particles - 1m 0.5-1.0mm sand, 1.5mg/l ferric.

The effects of floc break off were more likely to be observed in the slow start filters under these conditions since particle dendrites or flocs upon the media surface were likely to be formed in the very top layers, projecting into the streamlines, so when the flow approached the filtration rate they may have been too large to overcome the hydraulic shear and hence break off occurred. This had the effect of lengthening the ripening periods for the slow start filter, indeed particles from the influent were required in order for the filter to fully ripen. The effect may have been more severe on the 2.0-3.35mm sand filter because re-attachment deeper in the bed was more unlikely than for the 0.5-1.0mm sand filter.

#### 8.4.1.3 Summary of start-up strategy performance

Under normal raw water conditions which, landslides and drought apart, are usually very consistent a 1.0 mg/l ferric dose would provide the best removals and thus meet treatment goals of log removal. Under such conditions a 1 hour slow start would provide the most benefit, in terms of minimising particulate passage into supply, for both filter media/configurations (60% for 1m beds of 0.5-1.0mm sand; 65% for 2m beds of 2.0-3.35mm sand). However, a worse case scenario has to be considered, especially since drought conditions are likely to be the norm for a few summers to come. Under "extreme" conditions (high particle counts >3000, 1.5mg/l ferric dose) a plant such as Lostock is under more threat of a *Cryptosporidium* problem (HMSO, 1991). This work has shown slow start would be unsuitable under such conditions. Delayed start, however, can provide a significant improvement under such conditions (60% for 1m beds of 0.5-1.0mm sand; 65% for 2m beds of 2.0-3.35mm sand).

These improvements can sound impressive, but as has been stated (HMSO, 1995) its not removals or reductions that are important but what is left that is the danger. When numbers are considered even with the best performance (1 hour delay, 1.5mg/l ferric, 2.0-3.35mm sand) the NPFR of the control was  $1.87 \times 10^8$ , the NPFR of the delayed start filter was still  $5.01 \times 10^7$ ; and (1 hour slow start, 1.0mg/l ferric, 0.5-1.0mm sand) control NPFR was  $9.84 \times 10^7$ , the slow start NPFR was still  $3.33 \times 10^7$ . If these numbers were scaled-up to a 200 MLD plant the NPFS would be in the order of  $1.0 \times 10^{11}$ .

As reported in the Badenoch Expert Groups second report (into which this work had an input) this improvement in performance may not justify the expense of retro-fitting existing plant to provide a slow start procedure. However, delayed start would be relatively inexpensive in terms of retro-fitting, since valves and actuators don't have to be fitted; money would, however, be lost in production. Therefore delayed start may be a more attractive option, certainly a delayed start capability which could operate under "extreme conditions" should be strongly considered at high risk sites.

#### *8.4.2 The effect of start-up strategies on headloss development*

The effect of start-up strategies on headloss development appeared to be slight, the slow start had more of an effect than the delayed start. This was as expected since any additional collectors facilitated by the delayed start would be distributed throughout the bed, whereas those facilitated by slow start would be in the upper layers having a greater impact on headloss development.

An interesting observation was the degree of headloss build-up in the 0.5-1.0mm sand filters (overall), with terminal headloss reached after just 26 hours. As seen in previous chapters it can take as long as 44 hours under the same backwash conditions. The higher headloss development is due to the poor raw water conditions, obviously the more particulate matter in the raw water the greater the headloss development. The headloss development for the 2.0-3.35mm sand filters, which was much lower, again illustrates how this media and filter configuration can offer greatly extended runlengths.

The effect of larger particles and/or a higher coagulant on headloss development is well documented; the effect is an increase in headloss development, especially in the top layers of the bed. This was seen to have occurred, the headloss development of the control filters, for both media, did increase with the higher ferric dose. It was also seen to affect the start-up strategy headloss development in the same way.

The effect of the ferric dose increase on the headloss development of the start-up strategies relative to the controls was to reduce the differences, that is, under these conditions the headloss development of the start-up strategies filters and control filters was very similar.

#### *8.4.3 Relationship between raw water quality and NPFR*

The performance measure of the number of 2-5 $\mu$ m particles in the filtrate during ripening (NPFR) may be only an approximation but it addresses the most important issue, which is not what has been removed by the filters but what is left in the filtrate. This is especially critical during the ripening period since it is the time when oocysts are most likely to enter supply. By relating this parameter to influent conditions, particularly numbers of particles, it gives the possibility of

predicting filter performance under different influent conditions. With all the NPFRs from the start-up strategy filters included it helps identify the most suitable start-up option to use under a given set of conditions. The high degree of correlation between two very different types of filter implies that this method may well be a useful predictive tool. The fact that the relationship seems to be a polynomial suggests that the raw water quality that gives the best filtrate quality, is not simply the lowest.

This information from this trial illustrates the need for a flexible start-up strategy at a filter plant treating "high *Cryptosporidium* risk" water. Under such a flexible system the optimum option could be used whatever the raw water conditions. However, in reality a strategy that provides benefit under all conditions is required because operators will either not be able to or not want to make decisions on what start-up strategy to use when. Thus, a 1 hour delayed start should be considered since it provided benefit under all conditions tested.

## 8.5 Conclusions

Under the operating conditions used in these experiments and from the results obtained the following conclusions can be made:

Start-up strategies can provide considerable improvements in filter performance during the ripening period (up to 65%).

The performance of the start-up strategies was variable, dependent upon: the duration, the raw water particle count (and consequent coagulant dose), and media size.

A 1 hour slow start was the most effective strategy for both media tested at lower raw water particle counts (approx. 1500/ml).

Slow start performance deteriorated under increased raw water particle counts.

Slow start caused increased headloss development, under all conditions tested.

A 1 hour delayed start was the most effective strategy for both media tested at higher raw water particle counts (approx. 3000/ml).

Adoption of a 1 hour delayed start would provide improved performance under all conditions tested for both media.

# *CHAPTER 9*

## THE EFFECT OF FILTRATION RATE ON FILTER PERFORMANCE

### 9.1 Introduction

Particle removal efficiency in filtration is higher at lower filtration rates. However, economic pressures require that higher filtration rates are employed, thus reducing the size of the plant and the capital investment.

There are many published studies on the effect of higher filtration rates on runlength, filtrate quality during the run and water production (e.g. Brown, 1955; Bayliss 1956; Robeck *et al.*, 1964; and Mosher and Hendrick, 1986). Few, if any, of these studies have examined the effect of increased filtration rate on the degree of particulate passage into the filtrate during filter ripening.

Recently, so-called "fast-start" has been mooted as a possible start-up strategy. This is where a very high flow rate is passed through the filter initially in order to facilitate rapid ripening, after which the flow is ramped down.

It was the aim of this trial to assess the effect of higher filtration rates on the numbers of particles entering the filtrate during a fixed volume ripening period. In addition, the effect on performance in terms of headloss development was ascertained in order to work out unit filter run volumes (UFRV) and production efficiency.

### 9.2 Experimental procedure

There were three columns of the two previously selected media types/configurations: 1m beds of 0.5-1.0mm sand; and 2m beds of 2.0-3.35mm sand. Details of the media are included in section 7.2. One of the columns for each type of media was used as a control running at 6m/h. Higher filtration rates of 10 and 20m/h were investigated, full flow was reached after 1 minute i.e. no delayed or slow start was used. Pre-treatment was kept constant with ferric (III) sulphate dose of 1mg/l as  $\text{Fe}^{3+}$  at a fixed pH of 5.5.

Backwashing was carried out according to previously determined optimums: 4 minutes of CP followed by 5 minute rinse for the 0.5-1.0mm sand; and 3 minutes CP followed by a 5 minute rinse for the 2.0-3.35mm sand. The run lengths and hence frequency of backwashing are shown in Table 9.1.

**Table 9.1 Operational filter run lengths for a range of filtration rates.**

Filtration rate (m/h)	Operational run length	
	0.5-1.0mm sand	2.0-3.35 mm sand
10	24	24
20	8	24

The control filters ran for the same duration as the test filters, so that backwashing and ripening of the test and control filters would occur within a couple of hours of each other.

The monitoring strategy was the same as has been detailed in previous sections (section 6.2).

### 9.3 Results

The effect of the 10m/h and 20m/h filtration velocities upon filter performance, in terms of both filtrate quality and headloss development was assessed. The data obtained in this trial was collected over a period of 3 months.

#### 6.3.1 Influent quality

The influent quality for the duration of the trial is summarised in Table 9.2. A wide range of influent quality was experienced. Particle count was particularly varied, at times the count was extremely low. There was also a higher degree of variability seen in iron and colour content of the raw water than in previous trials, for which no explanation could be found.



**Table 9.2 Summary of influent conditions during backwash regime trial.**

	pH	Turbidity (NTU)	Manganese (µg/l)	Iron (µg/l)	True colour (°H)	Particle count (No./ml)
Mean	8.44	0.37	11.06	44.3	2.53	879.5
Std. Dev	0.16	0.21	5.11	27.6	0.9	529.5
Min	8.08	0.1	5	17.0	1	216.6
Max	8.7	1	23	134	5	2764.3

### 9.3.2 Filter performance

Since a control filter (6m/h) was operating in parallel to the test filter (10 or 20 m/h) the data was not grouped (as in chapters 6 and 7). Representative examples of filtrate particle counts are shown in the main text, as particle count vs. time, particle count vs. volume of filtrate produced, and as NPF vs. Volume of filtrate produced. The total NPF and headloss development has been summarised.

#### 9.3.2.1 1m beds of 0.5-1.0mm sand

The filters were run for 24 hours as opposed to 48 hours in the previous trials. The filtrate particle count of the control filter (Fig 9.1) had a peak of 1170 2-5µm particles /ml which occurred after 4 minutes, and ripened after 49 minutes. The filter running at 10m/h had a higher filtrate particle count peak (1962/ml) after 3 minutes. It also ripened more rapidly, reaching a steady state value similar to the control filter, 15.9/ml, after 26 minutes.

However, when the volume of filtrate that had to be passed in order for the filters to ripen is examined (Fig 9.2) it can be seen that the peak occurred as a function of the same volume of filtrate. This volume corresponded to the backwash remnants in the bed, the filters also ripened after the same amount of filtrate had been produced. When the numbers of 2-5µm particles in the filtrate was considered (Fig 9.3), it could be seen that the numbers in the filtrate from the filter operating at 10m/h were higher at all times, the total NPF for the example shown was  $1.25 \times 10^8$  and  $1.38 \times 10^8$  for the 6m/h and 10m/h respectively. The filter operating at 10m/h therefore had a total NPF 110% that of the control filters total NPF.

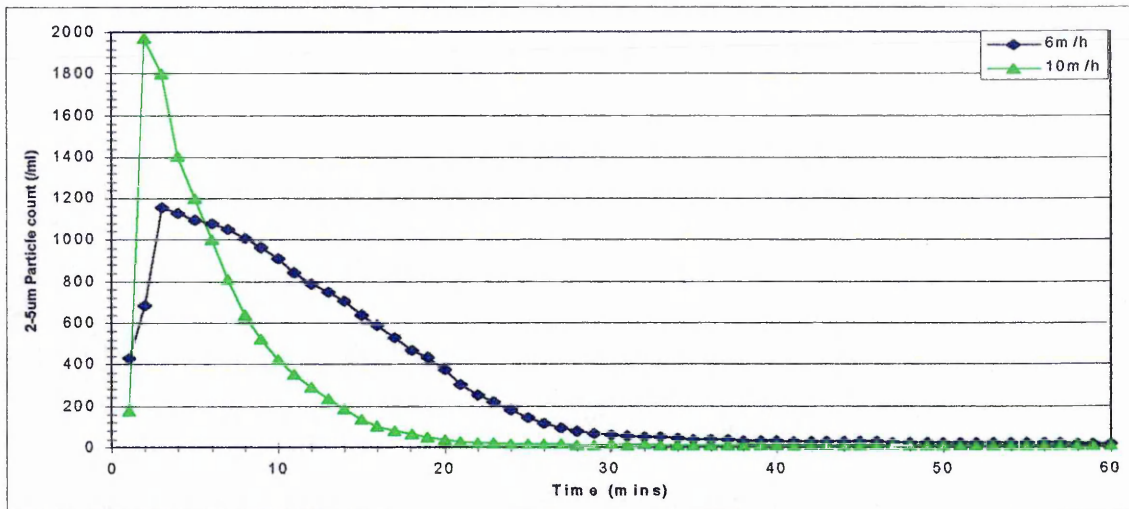


Figure 9.1 Real time filtrate particle count data at 6 and 10m/h (0.5-1.0mm sand).

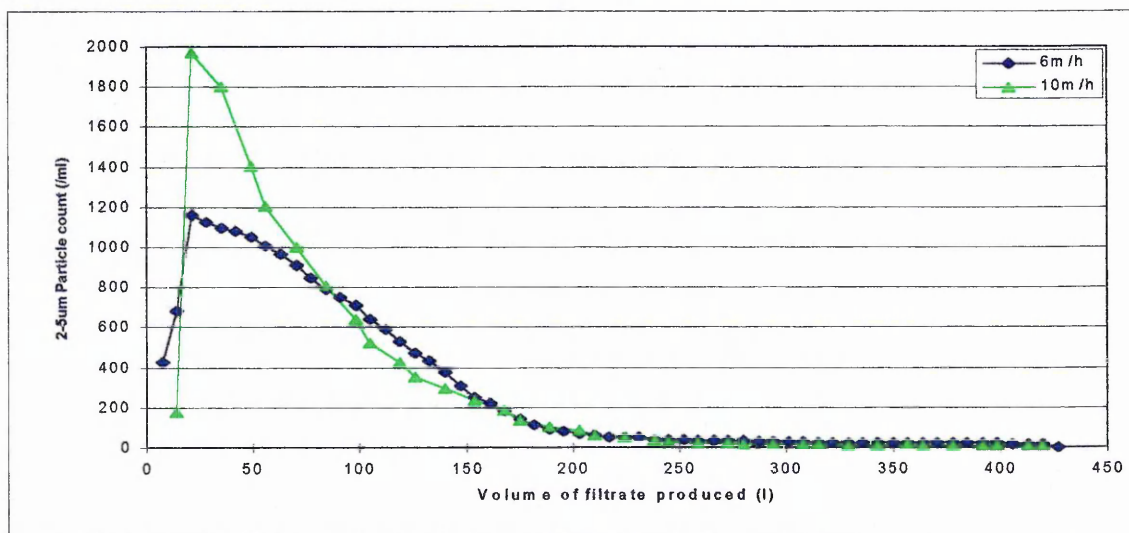


Figure 9.2 Volume corrected filtrate particle count data at 6 and 10m/h (0.5-1.0mm sand)

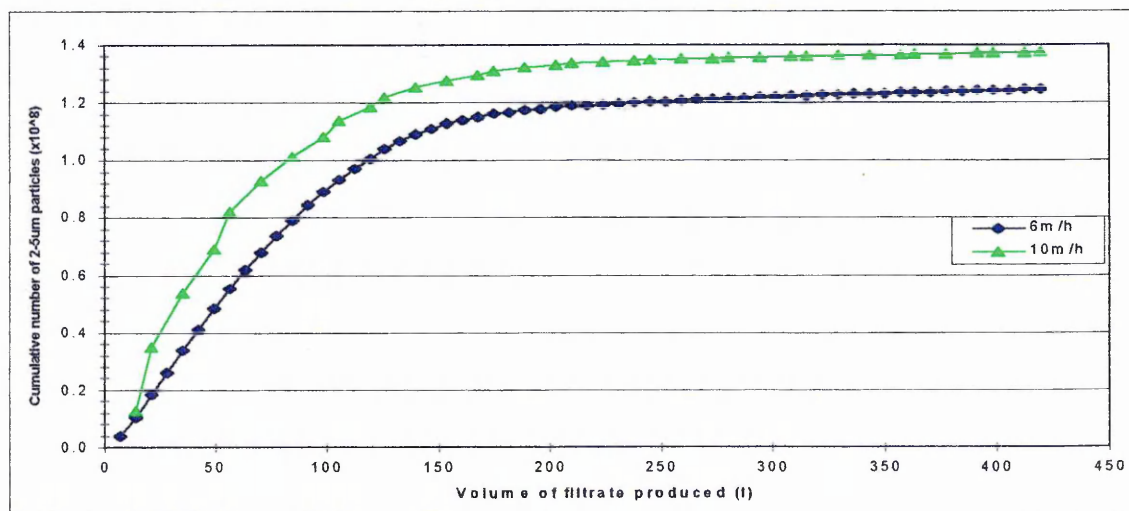


Figure 9.3 Cumulative number of 2-5µm particles in filtrate (0.5-1.0mm sand).

The fact that the 10m/h filter NPF was 110% that of the control filter was consistent for the whole trial, 6 runs, as can be seen in Table 9.3 The mean figure was 110.6 % (s.d = 2.8).

**Table 9.3** The effect of 10m/h filtration rate upon performance of 1m beds of 0.5-1.0mm sand filters during ripening.

Date of run	TNPF - 6m/h (control)	TPNF - 10m/h	10m/h TNPF as % of control TNPF
16/1/96	$5.91 \times 10^7$	$6.76 \times 10^7$	114.3
23/1/96	$9.59 \times 10^7$	$1.05 \times 10^8$	109.2
1/2/96	$1.25 \times 10^8$	$1.36 \times 10^8$	110.4
2/2/96	$1.84 \times 10^8$	$2.08 \times 10^8$	112.9
29/2/96	$1.89 \times 10^8$	$2.00 \times 10^8$	106.2
7/3/96	$1.48 \times 10^8$	$1.64 \times 10^8$	111.1
			Mean = 110.6
			S.d = 2.8

TNPF-total number of 2-5 $\mu$ m particles in first 420l of filtrate; s.d= Std. Deviation.

It can be seen from Figure 9.4 that both the clean bed headloss and rate of headloss development was greater when the filter was run at 10m/h. Clean bed headlosses of 43cm compared to 20cm for the 10m/h and 6m/h filters respectively. The filter operating at 10m/h reached a terminal headloss after only 10.5 hours, whereas the control filter had a total headloss of 124cm of H<sub>2</sub>O after the 24 hours.

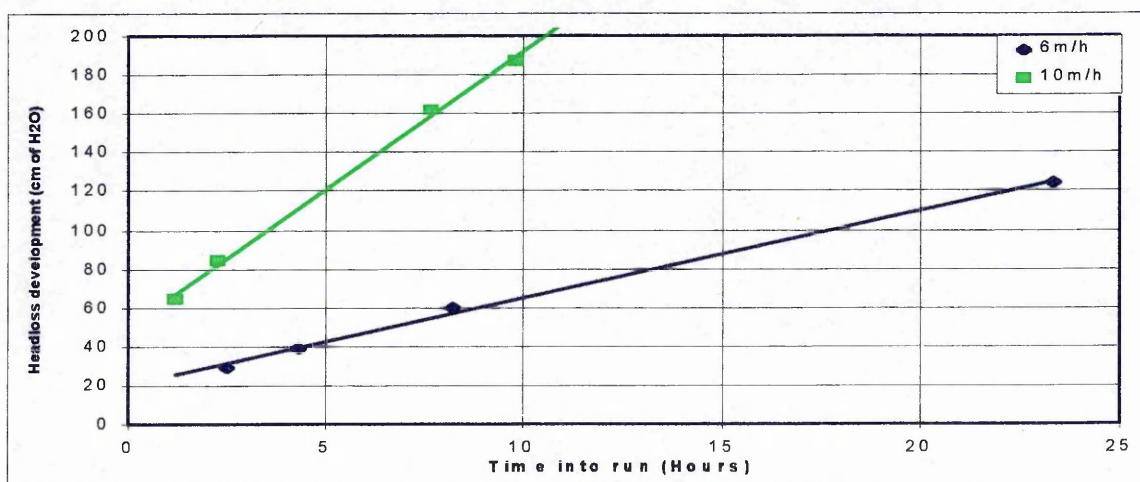


**Figure 9.4** Headloss development at 6 and 10m/h (0.5-1.0mm sand).

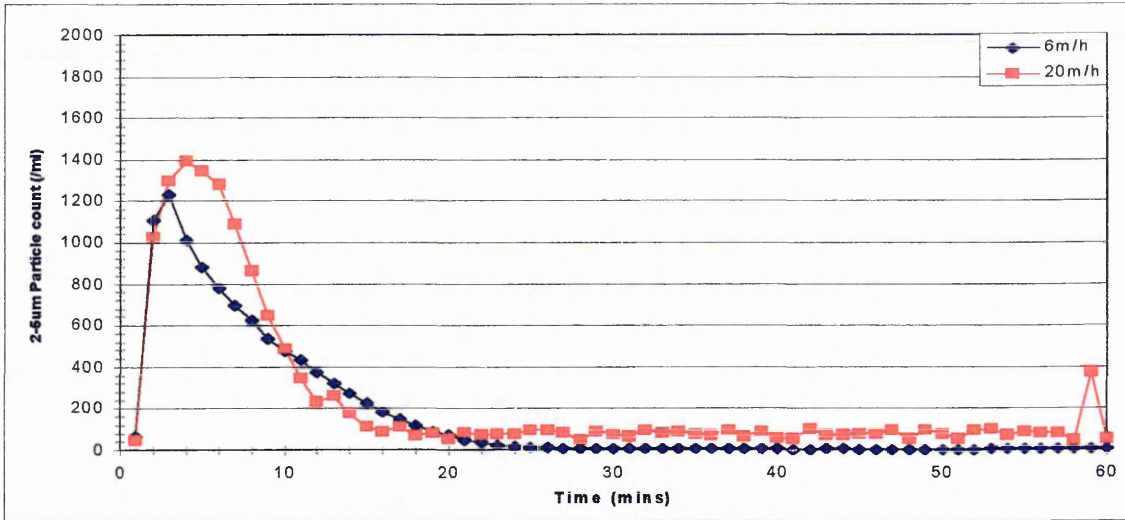


Figure 9.5 Real time filtrate particle count data at 6 and 20m/h (0.5-1.0mm sand).

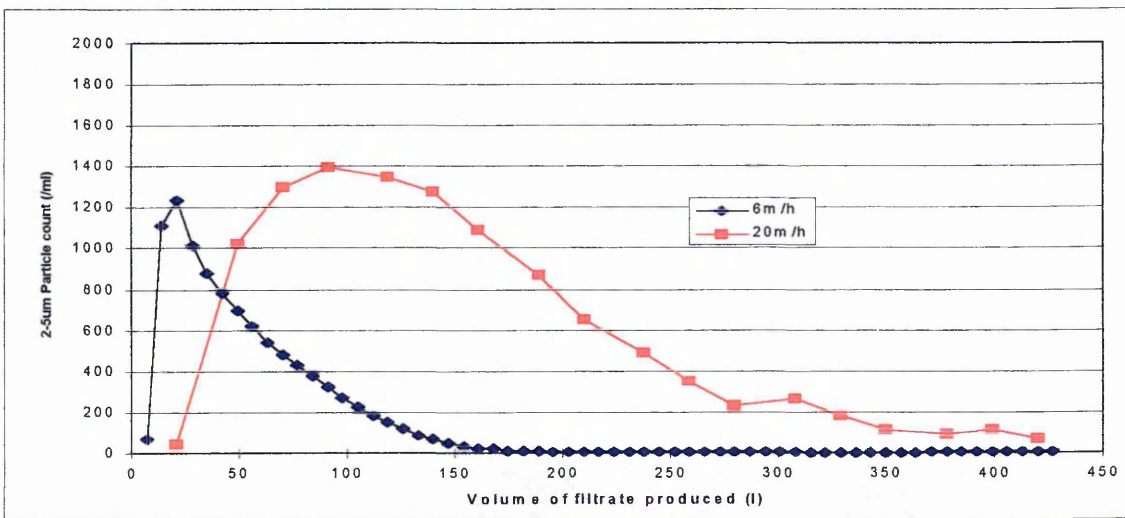


Figure 9.6 Volume corrected filtrate particle count data at 6 and 20m/h (0.5-1.0mm sand)

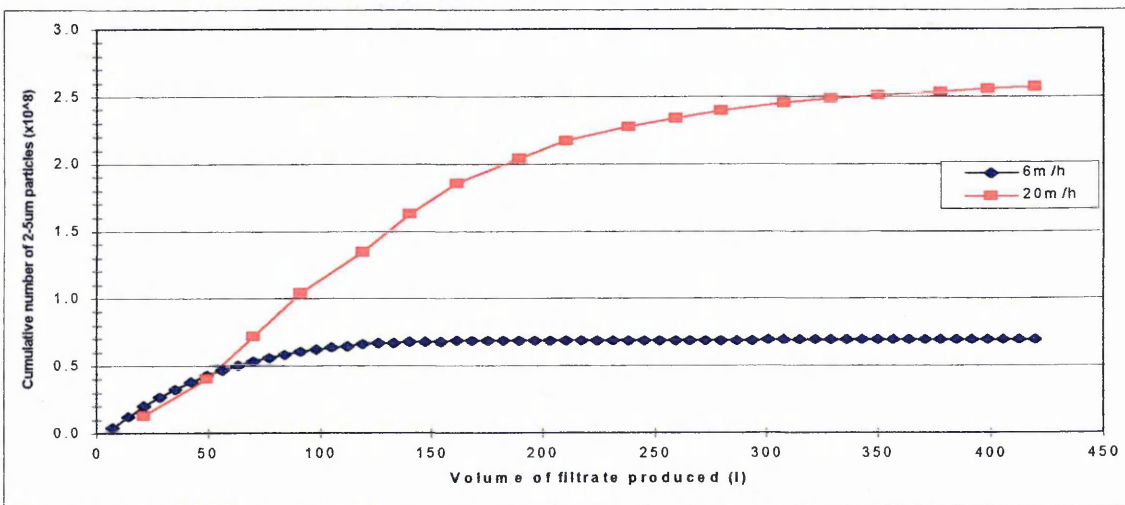


Figure 9.7 Cumulative number of 2-5µm particles in filtrate (0.5-1.0mm sand).

When the filtrate particle counts from filters operating at 6 and 20m/h are examined, Fig. 9.5, a number of observations can be made. The filtrate particle count, of the filter operating at 20m/h, had a slightly higher peak than the control. It ripened more rapidly than the control filter (18 minutes compared to 28minutes) albeit to a higher steady state value (56/ml compared to 11/ml).

When the particle count was plotted against the volume of filtrate produced (Fig 9.6) the effect of the higher filtration rate became clear, a far greater volume of filtrate had to be produced for the 20m/h filter to ripen than for the control filter. This effect upon filtrate quality during ripening was further reflected when the numbers of 2-5 $\mu$ m particles in the filtrate during ripening was examined (Fig 9.7). Apart from the first 50l, the numbers of particles in the control filtrate were very much lower than the 20m/h filtrate. The total NPF for this example was  $6.93 \times 10^7$  compared to  $2.57 \times 10^8$  in the filtrate of the 20m/h filter. The total NPF of the 20m/h filter was 370.9% that of the control filter. The total NPF of all 9 runs are shown in Table 9.4. The mean value for the 20m/h total NPF as a % of the control total NPF was 373.4%.

**Table 9.4 The effect of 20m/h filtration rate upon performance of 1m beds of 0.5-1.0mm sand filters during ripening.**

Date of run	TNPF - 6m/h (control)	TPNF - 20m/h	20m/h TNPF as % of control TNPF
1/4/96	$9.03 \times 10^7$	$2.40 \times 10^8$	265.8
2/4/96	$9.37 \times 10^7$	$2.21 \times 10^8$	235.9
3/4/96	$6.93 \times 10^7$	$2.57 \times 10^8$	370.9
4/4/96	$6.04 \times 10^7$	$2.50 \times 10^8$	413.7
15/4/96	$1.45 \times 10^8$	$5.77 \times 10^8$	399.3
19/4/96	$4.09 \times 10^7$	$1.79 \times 10^8$	436.9
22/4/96	$3.29 \times 10^7$	$1.18 \times 10^8$	358.4
23/4/96	$2.52 \times 10^7$	$1.01 \times 10^8$	400.7
24/4/96	$2.75 \times 10^7$	$1.32 \times 10^8$	478.9
			Mean = 373.4 S.d = 78.2

TNPF- total number of 2-5 $\mu$ m particles in first 420l of filtrate; s.d= Std Deviation.

The further increase in filtration rate from 10 to 20m/h increased the clean bed headloss to 71 cm of H<sub>2</sub>O, compared to the control filters 30cm of H<sub>2</sub>O (Fig 9.8). Terminal headloss was reached after only 4 hours by the 20m/h filter, the control filter had reached a headloss of 60cm at the end of the 6 hr run.

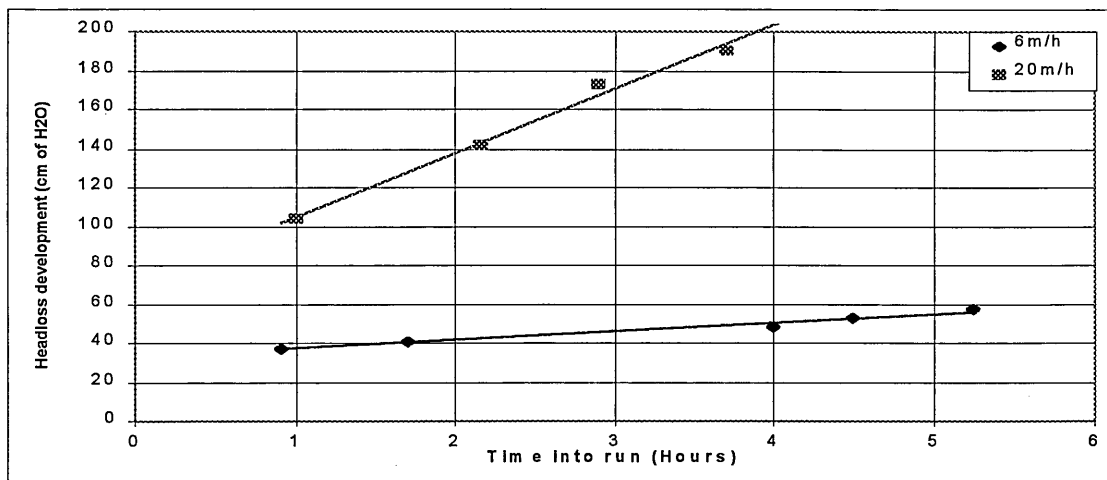


Figure 9.8 Headloss development at 6 and 20m/h (0.5-1.0mm sand).

#### 9.3.2.2 2m beds of 2.0 - 3.35mm sand

The representative run shown in Figures 9.9 to 9.12 was for the 10m/h filtration rate. This run was the only one in which two filters were run at 10m/h simultaneously along side a control. The real-time filtrate particle count (Fig 9.9) showed that the 10m/h filters both had higher peaks than the 6m/h control, between 500 and 700 2-5 $\mu$ m particles/ml higher. Both the 10m/h filters ripened more rapidly, after only 32 minutes compared to 44 minutes by the control filter.

The actual volume of filtrate produced before the filter ripened was found to be the same for all 3 filters, as shown in Fig 9.10. The peaks in filtrate particle count for the two 10m/h filters appeared at the same time and after the same volume of filtrate had been produced, slightly later than that for the control peak. The effect of the increased filtration rate upon the numbers of 2-5 $\mu$ m particles in the filtrate was clearly shown in Fig 9.11. The two 10m/h filters, which showed good correlation, were consistently higher throughout the ripening period. The TNPF (in first 420l of filtrate) were  $1.59 \times 10^8$  and  $1.52 \times 10^8$  for the two 10m/h filters and  $1.21 \times 10^8$  for the control filter. That means the 10m/h filters TNPF were 131% and 125% that of the control TNPF.

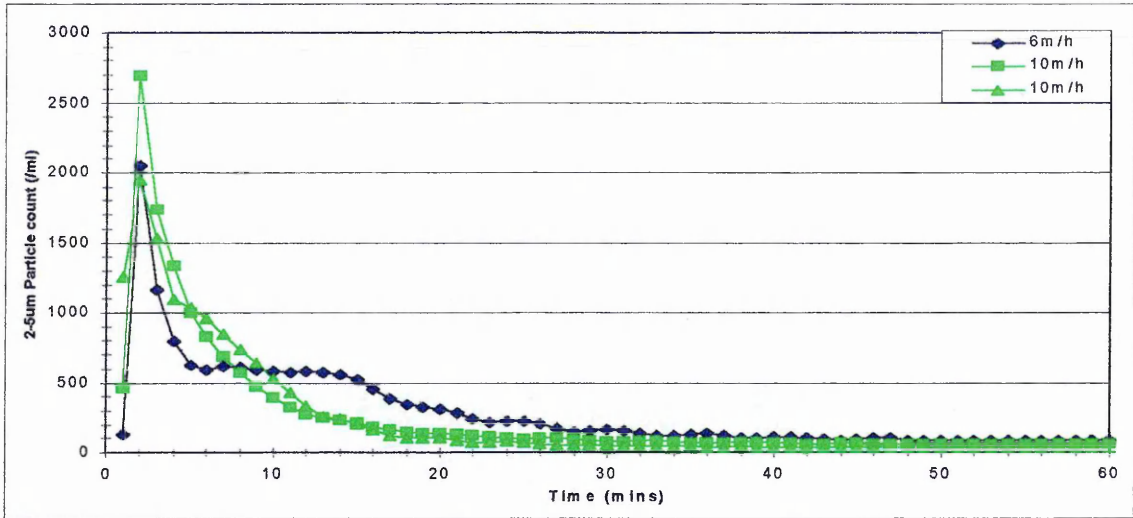


Figure 9.9 Real time filtrate particle count data at 6 and 10m/h (2.0-3.35mm sand).

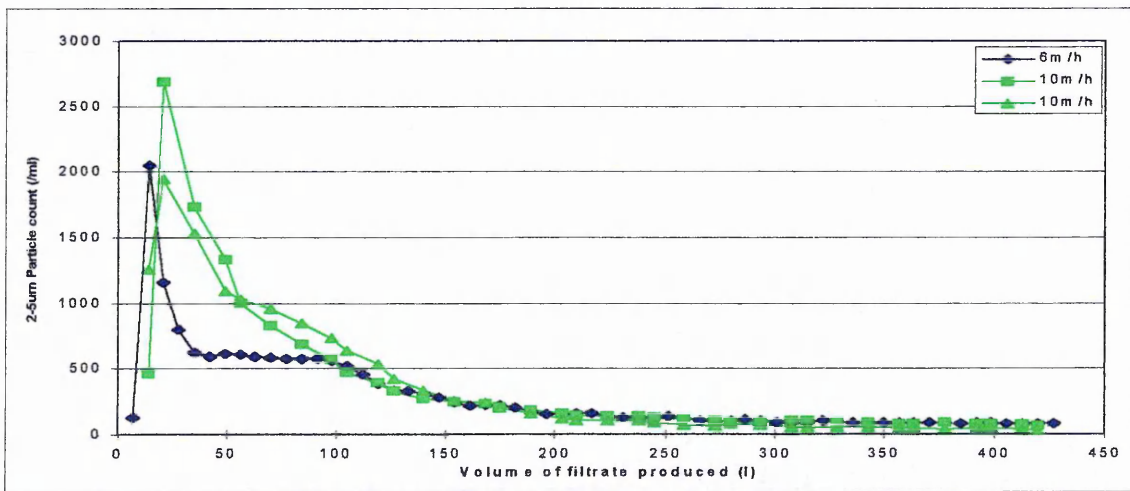


Figure 9.10 Volume corrected filtrate particle count at 6 and 10m/h (2.0-3.35mm sand)

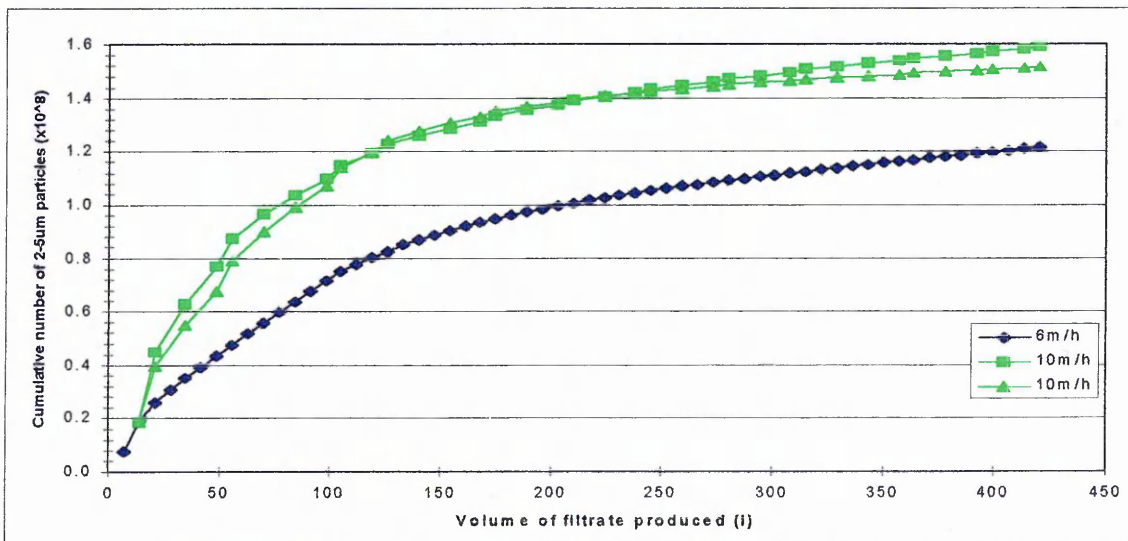


Figure 9.11 Cumulative no. of 2-5µm particles in filtrate at 6, 10m/h (2.0-3.35mm sand).

The TPNF for the other 6 runs operated under the same conditions are shown in Table 9.5. It can be seen that TPNF was consistently higher for the filters operating at 10m/h, but there was a high degree of variability - the mean value was 197% but the Std. Dev was 57.9.

**Table 9.5 The effect of 10m/h filtration rate upon performance of 2m bed of 2.0-3.35mm sand filters during ripening.**

Date of run	TPNF - 6m/h (control)	TPNF - 10m/h	10m/h TPNF as % of control TPNF
23/1/96	$7.13 \times 10^7$	$1.39 \times 10^8$	194.6
1/2/96	$1.21 \times 10^7$	$1.59 \times 10^8$ $1.52 \times 10^8$	131.2 125.1
13/2/96	$9.09 \times 10^7$	$1.74 \times 10^8$	191.9
27/2/96	$9.99 \times 10^7$	$1.67 \times 10^8$	167.9
28/2/96	$6.73 \times 10^7$	$1.80 \times 10^8$	267.9
29/2/96	$8.03 \times 10^7$	$1.72 \times 10^8$	214.3
4/3/96	$7.88 \times 10^7$	$2.25 \times 10^8$	285.2
			Mean = 197.1 S.d = 57.9

TPNF- total number of 2-5 $\mu$ m particles in first 420l of filtrate; S.d = Std. deviation.

The clean bed headloss did not appear to be affected by the increased filtration rate for the run shown in Figure 9.12, it was the same as the control filter, a value of 14cm of H<sub>2</sub>O. However, the rate of headloss development was affected. The estimated run length (extrapolated from run data) was reduced from 250 to 110 hours.

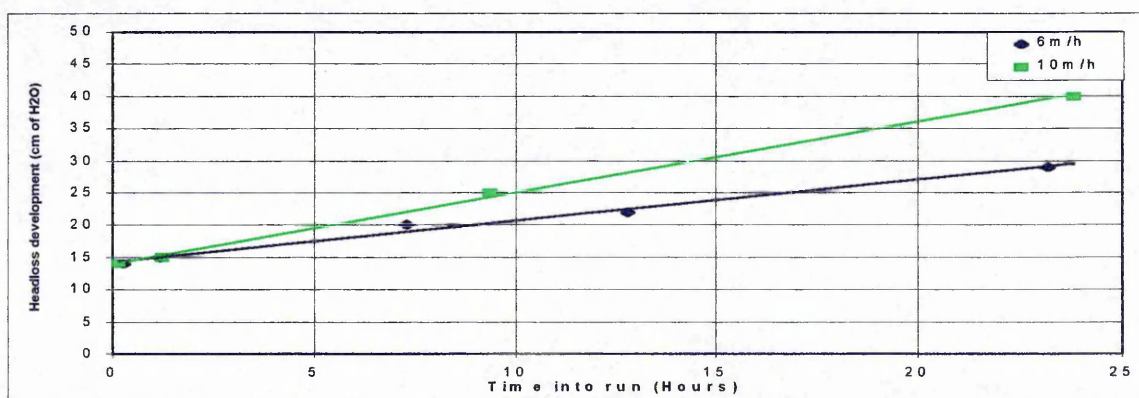


**Figure 9.12 Headloss development at 6 and 10m/h (2.0-3.35mm sand).**



An example of performance at a filtration rate of 20m/h is shown in Figs. 9.13 to 9.16. From Fig. 9.13 it can be seen that the performance of the control filter was improved in this example compared to the previous example (Fig. 9.9), due to varying influent conditions. The peak in filtrate particle count from the control filter was actually higher (1800/ml) than that from the 20m/h filter (1260/ml). The time to ripen for the 20m/h filter was much lower than the control, the steady state values were, however, similar. Interestingly, the double peak in the filtrate particle count from the 20m/h filter was accentuated. This occurred (Fig. 9.14) after 95 l of filtrate had been displaced.

The initial peak in the control filter occurred after a smaller volume of filtrate had been produced (20l), when compared to the 20m/h filter. This was reflected in Fig. 9.15, during the first 40l of filtrate production there were a greater number of 2-5 $\mu$ m particles in the filtrate from the control filter. Thereafter, the numbers present in the filtrate from the 20m/h filter became far greater. After 420l, in this example, the TPNF was  $8.16 \times 10^7$  for the control and  $1.93 \times 10^8$  for the filter running at 20m/h. The 20m/h filters TPNF was therefore 236.7% that of the control. The data for the other 6 runs operated under these conditions is summarised in Table 9.6.

**Table 9.6 The effect of 20m/h filtration rate upon performance of 2m bed of 2.0-3.35mm sand filters during ripening.**

Date of run	TPNF - 6m/h (control)	TPNF - 20m/h	20m/h TPNF as % of control TPNF
1/4/96	$9.20 \times 10^7$	$2.98 \times 10^8$	323.5
2/4/96	$8.16 \times 10^7$	$1.93 \times 10^8$	236.7
3/4/96	$7.58 \times 10^7$	$1.98 \times 10^8$	260.8
19/4/96	$6.60 \times 10^7$	$1.70 \times 10^8$	256.8
22/4/96	$4.53 \times 10^7$	$1.11 \times 10^8$	244.6
23/4/96	$4.10 \times 10^7$	$1.07 \times 10^8$	260.0
25/4/96	$5.11 \times 10^7$	$1.93 \times 10^8$	376.7
			Mean = 279.9
			S.d = 51.1

TPNF- total number of 2-5 $\mu$ m particles in first 420l of filtrate; s.d= Std Deviation.

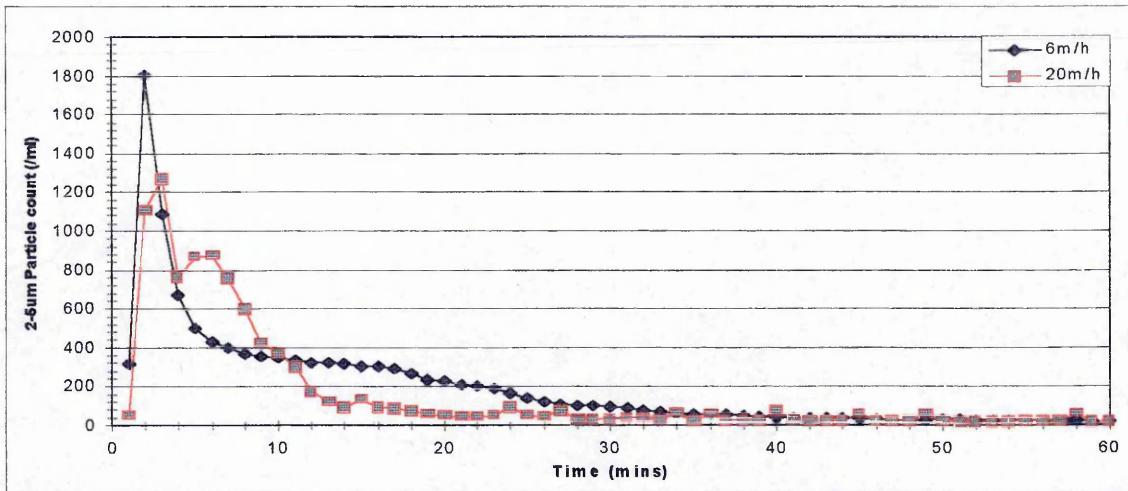


Figure 9.13 Real time filtrate particle count data at 6 and 20m/h (2.0-3.35mm sand).

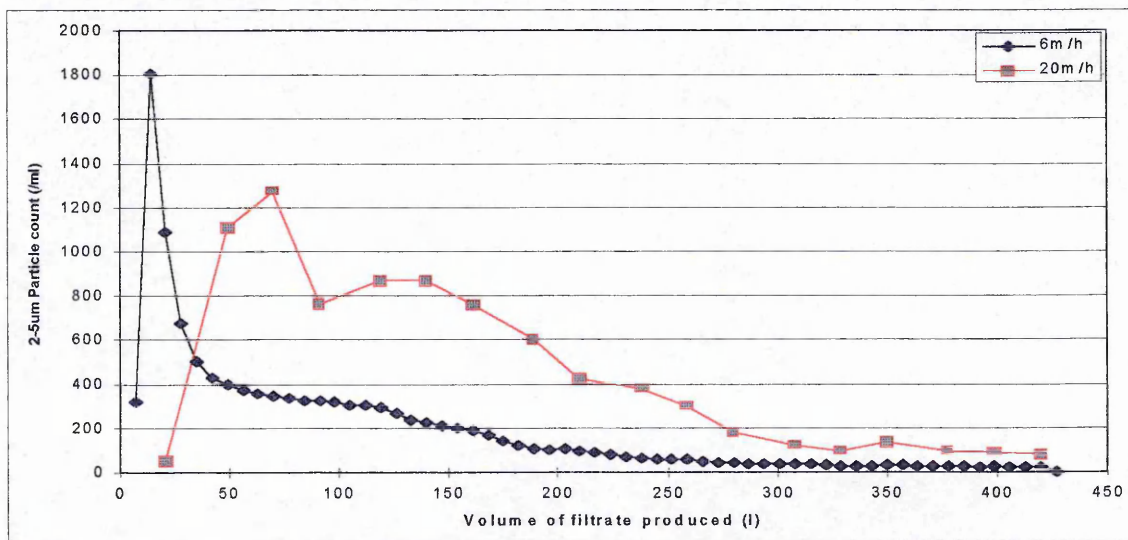


Figure 9.14 Volume corrected filtrate particle count data at 6, 20m/h (2.0-3.35mm sand).

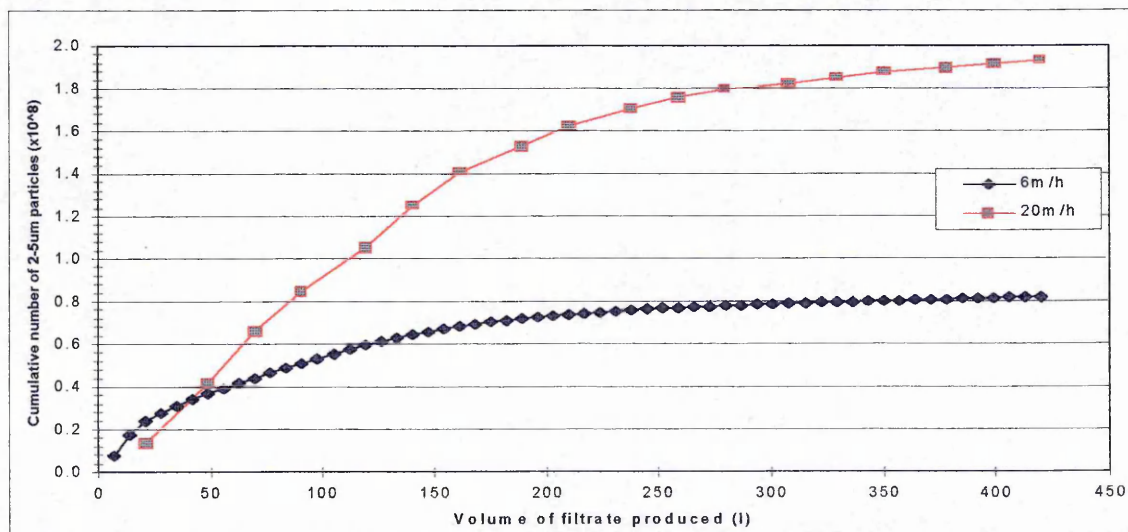


Figure 9.15 Cumulative number of 2-5µm particles in filtrate (2.0-3.35mm sand).

Both the clean bed headloss and rate of headloss development was strongly affected by the 20m/h filtration rate (Fig 9.16). Clean bed headloss had increased from 15cm to about 40cm. Terminal, or 2m headloss was reached after 22 hours.

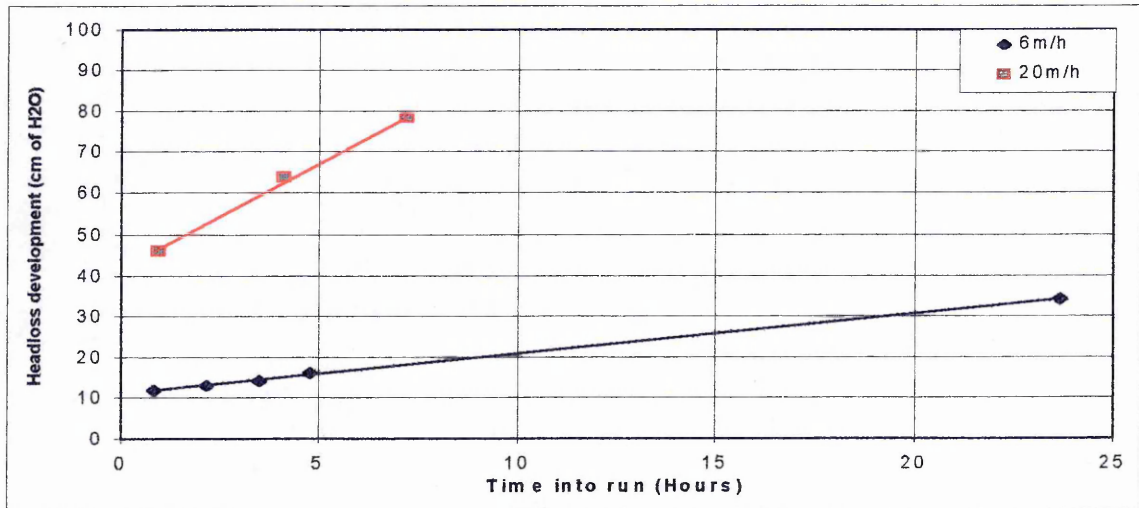


Figure 9.16 Headloss development at 6 and 10m/h (2.0-3.35mm sand).

## 9.4 Discussion

The effect of filtration rate on filtrate quality at steady state and during the ripening period will be discussed initially. The effect on headloss development, run length and water production will then be discussed. Finally, the operational implications of a “fast start” will be reviewed.

### 9.4.1. The effect of filtration rate on filtrate quality

Let us first consider the filtrate quality once the filter had ripened, i.e. at steady state. Theory tells us that removal of particles will be worse at higher filtration rates. Since the filter coefficient,  $\lambda$ , in a first order removal model  $\delta C/\delta L = -\lambda C$  is inversely proportional to both the filtration rate, and grain size of the media. It can be seen from Figure 9.17 and 9.18 that removal ( $C/C_0 \times 100$ ) was higher at 6m/h for both filters. The removal in the 0.5-1.0mm sand bed at 6m/h was greater than that for the 2.0-3.35mm sand. Both of these observations were predicted by theory and shown in previous experimental work (Ives and Sholji, 1965; Kau and Lawler, 1992).

At 10m/h the percentage removal was reduced for both types of filter, more so for the 0.5-1.0mm sand, with the 2-5 $\mu\text{m}$  particles having a removal worse than that of all particles (2-400 $\mu\text{m}$ ). This too was predicted by theory, since 2-5 $\mu\text{m}$  is close to the size of minimum removal efficiency (1 $\mu\text{m}$ ).

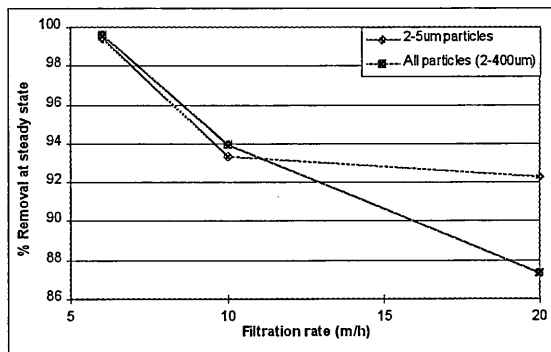


Fig 9.17 % Removal at steady state for a range of filtration rates. (1m of 0.5-1.0 mm sand).

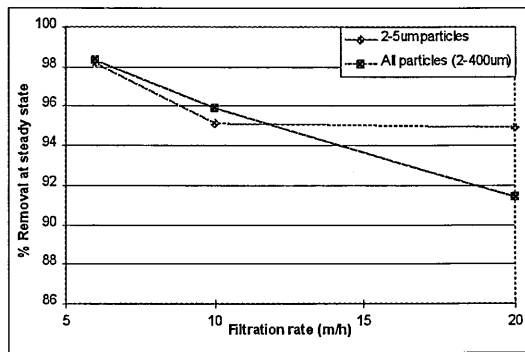


Fig 9.18 % Removal at steady state for a range of filtration rates. (2m of 2.0- 3.35 mm sand).

At 20m/h the removal was significantly reduced when all the particles (2-400 $\mu\text{m}$ ) were considered, especially in the 0.5-1.0mm sand filter. The removal of the 2-5 $\mu\text{m}$  particles was only slightly reduced in both types of filter. It is likely that the phenomenon of floc break-off was occurring, at this filtration rate, especially in the 0.5-1.0mm sand filter. This filter configuration had smaller interstitial pores, and therefore higher shear forces within those pores. A means of approximating shear forces within the filter pores was described in section 8.4, this method has been used to approximate the shear forces under the different filtration rates. The results are shown in Table 9.7, the maximum shear forces ( $\tau_{\text{max}}$ ) are at the media surface, and the mean shear forces ( $\tau_{\text{mean}}$ ) are in the centre of the pores.

**Table 9.7 Approximation of hydraulic shear forces over a range of filtration rates.**

Shear forces	0.5-1.0mm sand			2.0-3.35mm sand		
	6m/h	10m/h	20m/h	6m/h	10m/h	20m/h
$\tau_{\text{(max)}} \text{ (Nm}^{-2}\text{)}$	0.68	1.13	2.25	0.20	0.33	0.66
$\tau_{\text{(mean)}} \text{ (Nm}^{-2}\text{)}$	0.45	0.75	1.50	0.13	0.22	0.44

The high hydraulic shear forces prevalent in the 0.5-1.0mm sand filter at 20 m/h are likely to be causing a greater degree of floc break-off. The phenomenon of floc break-off was described in some detail in section 8.4, where it was occurring during filter ripening. Clark *et al.* (1990) showed that individual particles were captured and then helped to capture other particles; a group of captured particles would then break-off as a floc as the attachment forces were overcome by increasing hydraulic shear forces.

When the removal of 5-400 $\mu\text{m}$  particles is considered at 20m/h (52.3 and 72.8 % for 0.5-1.0mm sand and 2.0-3.35mm sand respectively) the likelihood that floc break-off was occurring after the filter had ripened is reinforced.

Clark *et al.*, (1990) work specifically addressed the ripening period; it was one of the main aims of the trial, detailed in this chapter, to assess the effect of filtration rate on the filtrate quality during the ripening period. Table 9.8 is a summary of the performance data presented in the results section. The values are high rate TNPF as a % of control (6m/h) TNPF.

**Table 9.8 Summary of filter performance during ripening, as a function of filtration rate.**

Filtration rate (m/h)	High rate TPNF as a % of control (6m/h) TPNF	
	1m bed of 0.5-1.0mm sand	2m beds of 2.0-3.35mm sand
10	111.2 (2.1) [6]	197.1 (57.9) [8]
20	357.0 (86.4) [9]	263.5 (30.7) [7]

( ) - Standard deviation of mean; [ ] - number of runs average obtained from.

Generally, as the filtration rate increased, the numbers of 2-5 $\mu$ m particles in the filtrate during the ripening period increased, for both filter configurations. The 10m/h filtration velocity had a detrimental effect on the performance of both media with the greatest effect seen on the coarse 2.0-3.35mm sand. This poor performance was caused by a larger number of particles in the volume of filtrate that corresponded to the backwash remnants. Both filter configurations ripened after the same volume of filtrate had been passed in the control and 10m/h filters.

When the 20m/h filtration rate was considered it was found that a larger volume of filtrate was required for the filters to ripen, this was greater for the 0.5-1.0mm sand filter. This can again be explained by floc break-off. As a floc, or deposit, builds-up on a collector it too becomes a collector, thereby increasing the removal efficiency of the filter. However, when the floc has reached a certain size the attachment forces are not strong enough to overcome the increasing shear forces. When this happens the floc breaks off and the removal efficiency is lowered (Kau and Lawler, 1995). Therefore when floc break-off is occurring the filter takes longer to ripen. Figures 9.19 and 9.20 show the cumulative number of 25-400 $\mu$ m i.e. large particles in the filtrate during ripening at 6 and 20m/h, these figures clearly show that floc break-off was occurring.

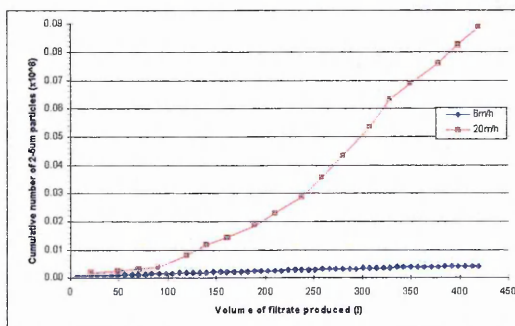


**Figure 9.19 Cumulative no. of 25-400 $\mu$ m particles in filtrate (0.5-1.0mm sand).**

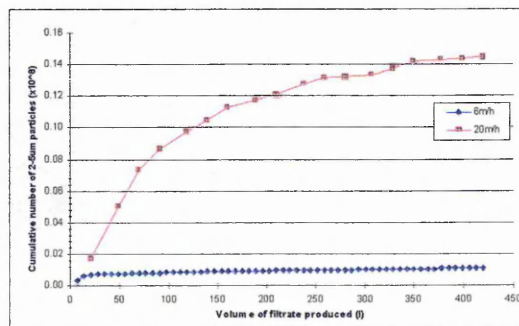


**Figure 9.20 Cumulative no. of 25-400 $\mu$ m particles in filtrate (2.0-3.35mm sand).**

The 2.0-3.35mm sand filter with its greater bed depth appeared to ripen for these large flocs, that is the degree of floc break-off diminished. The 0.5-1.0mm filter, however, did not appear to ripen, the degree of floc break-off was not reduced. Therefore the removal efficiency of the filter was less and it took longer to ripen, resulting in a greater TNPf than in the coarser media.

#### 9.4.2 The effect of filtration rate on runlength

In the results section the headloss data was plotted against time, in order to determine the time to reach terminal headloss. In figures 9.21 to 9.24 the same headloss data has been plotted against the volume of filtrate produced during the filter run.

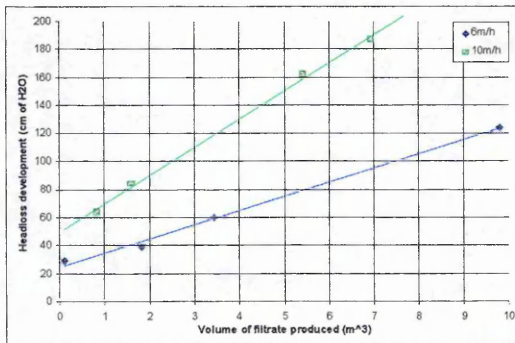


Fig9.21  $\Delta H$  for 0.5-1.0mm sand at 6, 10m/h.

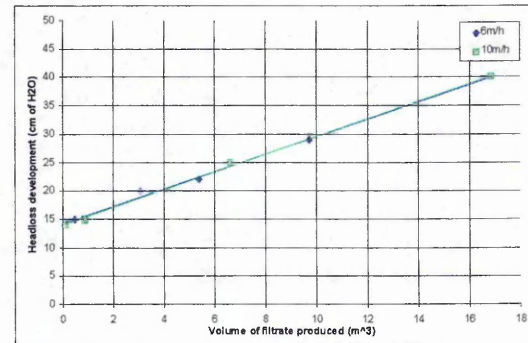


Fig9.23  $\Delta H$  for 2-3.35mm sand at 6, 10m/h.

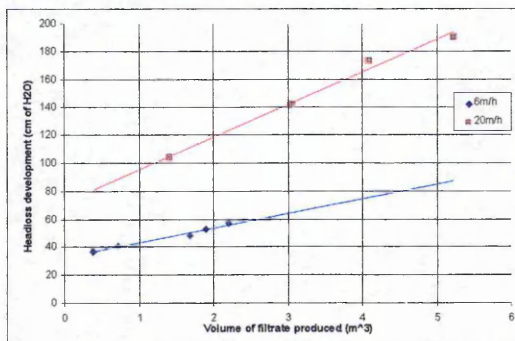


Fig9.22  $\Delta H$  for 0.5-1.0mm sand at 6, 20m/h.

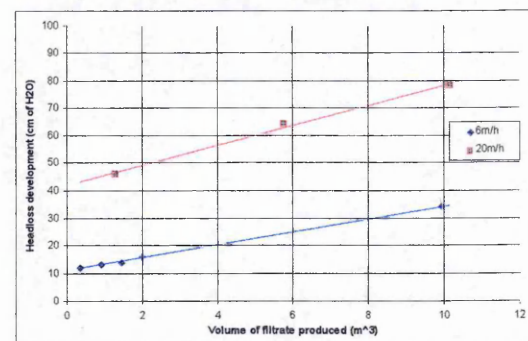


Fig9.24  $\Delta H$  for 2-3.35mm sand at 6, 20m/h.

When the data is plotted in this way the headloss development is normalised in terms of flow, so a direct comparison between the control filter (6m/h) and higher rate filters can be made.

Clean bed headloss is according to theory directly proportional to the filtration velocity. This was the case for the 0.5-1.0mm sand filter at both 10m/h and 20m/h; and for the 2.0-3.35mm sand filter at

20m/h. However, the 10m/h had no effect on the clean bed headloss of this filter, this may be attributed to the greater solid penetration.

Cleasby (1970) stated that the rate of headloss increase during the filter run is roughly proportional to the solids captured by the filter. Assuming essentially complete capture of incoming solids, the headloss will develop in proportion to the filtration rate and the influent suspended solids concentration (constant in this case because washed and ripened on same day). The rate of headloss development is reduced if the solids capture occurs over a greater depth of the medium, rather than in a thin upper layer of the medium. A coarser grain size encourages greater penetration of solids into the bed and thus reduces the rate of headloss development per unit mass of solids captured. This explains why the headloss development is far greater in the 0.5-1.0mm sand filter.

The most common headloss pattern found in filtration, typical for most iron coagulated waters, is linear with respect to volume of filtrate produced (Cleasby, 1970). It can be seen that the data concurs with this pattern. Published results have also shown that the rate of headloss development increases with increasing filtration rate.

#### *9.4.3 The effect of higher filtration rates on water production*

It has been shown that headloss increases at a faster rate per hour at higher filtration rates. The production per unit time, however, also increases, so whilst production per filter run can be diminished, production per day can be substantially increased. As a result the importance attached to filter runlength, in terms of water production, can be misleading. Therefore, the effect of filtration rate on net plant production and production efficiency, as well as filtrate quality needs to be ascertained.

A useful parameter in determining the effect of filtration rate on water production is the unit filter run volume (UFRV). The UFRV is the actual throughput of a filter during one filter run. The following example calculation (adapted from Cleasby, 1970) illustrates how to obtain the UFRV, as well as the net production and plant efficiency. The figures for the two media tested at the different flow rates used are shown in Table 9.9.



Example calculation for 0.5-1.0mm sand at 6m/h:

Runlength = 38 hours - 15 minutes for backwash = 37.75h = 0.63runs/day/filter

Backwash volume =  $3.18 \text{ m}^3/\text{m}^2 \times 0.63 = 2.003 \text{ m}^3/\text{m}^2/\text{day}$

Unit filter run volume =  $37.75 \times 6 = 226.5 \text{ m}^3/\text{m}^2$

Gross volume filtered/ $\text{m}^2/\text{day}$  (GVF) =  $226.5 \times 0.63 = 142.6 \text{ m}^3/\text{m}^2/\text{day}$

Net water production (NWP) =  $142.6 - \text{backwash volume} = 142.6 - 2.003 = 140.6 \text{ m}^3/\text{m}^2/\text{day}$

Production efficiency (PE) expressed as % of gross volume filtered =  $(140.6/142.6) \times 100 = 98.5\%$

**Table 9.9 Effect of filtration rate of water production parameters.**

Filtration rate (m/h)	1m beds of 0.501.0mm sand					2m beds of 2.0 - 3.35mm sand				
	UFRV $\text{m}^3/\text{m}^2/\text{run}$	GVF $\text{m}^3/\text{m}^2/\text{day}$	NWP $\text{m}^3/\text{m}^2/\text{day}$	PE %	No. BW / day	UFRV $\text{m}^3/\text{m}^2/\text{run}$	GVF $\text{m}^3/\text{m}^2/\text{day}$	NWP $\text{m}^3/\text{m}^2/\text{day}$	PE %	No. BW / day
6	226.5	142.6	140.6	98.5	0.63	1498	143.8	143.3	99.6	0.1
10	102.5	234.2	226.9	96.8	2.28	1097	239.7	237.7	99.1	0.22
20	75.0	450.9	430.9	95.8	6.0	435	474.1	467.8	98.6	1.09

From Table 9.9 it was apparent that the filters showed the general trends that were expected, the UFRV were diminished, and the NWP were substantially increased as filtration rate increased. Also included in Table 9.9 is the number of backwashes per day required running at each flowrate. This is a very important parameter because it is directly related to the number of particles entering into supply, since after each backwash, the filter has to go through the ripening period. Take for example, the 0.5-1.0 mm sand operating at 20m/h, it has already been shown that the TNPF under these conditions is on average 3.5 times that of the same filter running at 6m/h. The same filter will backwash 10 times more frequently so the number of 2-5 $\mu\text{m}$  particles entering supply during the ripening period of the 20m/h will be approximately 30 times greater /day.

## 9.5 Conclusions

Under the operating conditions used in these trials and from the results obtained the following conclusions can be made:

At high filtration rates (10 and 20m/h) the TNPF during ripening was greatly increased when compared to a conventional filtration rate (6m/h). Therefore a fast filter start would not be a viable option, unless a filter to waste period was employed.

High filtration rates (10 and 20m/h) greatly increased headloss development and therefore decreased filter runlengths, especially for the 1m beds of 0.5-1.0mm sand filters.

The UFRV was reduced by increased filtration rate, however the NWP per day was greatly increased. Conversely, production efficiency was reduced by higher rates.

# *CHAPTER 10*

## ECONOMIC ASSESSMENT OF TECHNICAL OPTIONS

### 10.1 Introduction

The aim of the technical study was to minimise the number of *Cryptosporidium* oocyst sized particles passing through rapid gravity filters into water supply. This aim was met by assessing a number of technical options.

It was the aim of this non-technical study to cost those technical options and perform a cost benefit analysis to determine the optimum solution in terms of both performance and economics. The study addressed the research drivers - why the water industry, and North West Water in particular, had to carry-out this research and implementation programme. The performance measure for the technical options is defined and discussed. The technical options were costed in terms of both capital and operating costs and a cost benefit analysis was carried-out.

### 10.2 The Research Drivers - Water quality regulations and regulators

In 1974 the water industry underwent major re-organisation when the Water Act was introduced. Overall responsibility for water supply was taken over by 10 Water Authorities, with 29 water companies continuing to supply water in their own areas on the Water Authorities behalf.

In 1989 the water industry was privatised, the 10 Water Authorities became water and sewerage companies. This resulted in major changes in the legislation dealing with the control of water quality in England and Wales. The Water Act 1989 largely replaced the 1974 Act in England and Wales. A number of regulatory bodies were set-up to monitor the companies and enforce the main regulatory instrument which was the Water Act (1989) itself.

The Office of Water Services (OFFWAT) was essentially an economic regulator. The new water and sewerage companies were effectively monopolies and as such had few "pure" market pressures on them. The purpose of OFFWAT was to protect the interests of consumers of water and sewerage services. The objective of the Director General of OFFWAT was to achieve through regulation the same balance as would otherwise be achieved by competitive markets. The

main control which the Director General can exercise is to limit the prices the companies can charge to their customers.

The National Rivers Authority (NRA) is responsible for environmental regulation.

The Secretary of State for the Environment was made responsible for drinking water quality. Within the Department of the Environment the Drinking Water Inspectorate (DWI) was set-up, it was responsible for checking that water supplied by the water companies was fit to drink where it reached the customers home.

Water undertakers were required by the Water Act (1989) to supply only water which was wholesome when they supplied water to any premises for domestic purposes. Standards of wholesomeness had been defined and laid down in regulations. The Water Supply (Water Quality) Regulations 1989 were concerned with the quality of water supplied in England and Wales for drinking, washing and cooking. They gave effect in part to certain EC Directives on drinking water quality. Although, in some cases tougher standards were set (e.g. in relation to lead) than in those EC Directives. Part II of the Water Supply Regulations prescribed standards of wholesomeness in respect to water supplied by water undertakers for certain domestic purposes. In particular it provided that water was to be regarded as wholesome if it contained concentrations or values in respect of various elements, organisms and properties which were consistent with prescribed maximum, and in some cases minimum concentrations or values.

In general, water must not contain any element, organism or substance (other than a specified parameter) at a concentration or value which would be detrimental to public health; nor may it contain any combination of elements, organisms or substances (whether or not specified parameters) which would be detrimental to public health.

In 1989 the DWI published "Guidance on safeguarding the quality of public supply". It stated that water should be wholesome against standards and for anything else that might be there, including organisms detrimental to public health. This document was the first to address the threat of *Cryptosporidium*, a number of appendices detailed the then current knowledge.

*Cryptosporidium* was refereed to because it had become a key issue within the industry since a waterborne outbreak of the disease cryptosporidiosis in Swindon at the end of 1988 (up to 500 people were affected). As a result of this outbreak the Department of Environment and Department of Health set-up an expert group chaired by Sir John Badenoch to address the problem. They published a report in 1990 which made a number of recommendations with respect to water treatment.

The main recommendation and the one that is relevant to this research was the installation of slow-start on all rapid gravity filters (see section 1.5).

### **10.3 Public Health Risk - The Threat of *Cryptosporidium***

*Cryptosporidium parvum* is a coccidian parasite with a world wide distribution. The parasite is transmitted in the oocyst stage by the faecal-oral route. Water is important in disseminating the oocysts which are resistant to many potable water treatment processes and waterborne outbreaks are increasingly reported.

#### *10.3.1 Occurrence of oocysts in raw water*

A number of reviews on the occurrence of oocysts in U.S environmental waters have been published ( Ongerth and Stibbs, 1987; Madore, 1987; Rose, 1987 and Rose, 1988). Oocysts were found in nearly all waters but in varying concentrations. An average concentration of 0.91 oocysts /l was recorded for reservoirs and 0.94/l for surface waters.

A survey of monitoring practices employed by water utilities in the U.K. and the oocyst counts obtained, carried out by Quennell and West (1995), found that oocysts occurred fairly often, but usually at low concentrations and rarely above one oocyst per litre. The data for oocyst occurrence during a 12 month period that spanned 1993 and 1994 is summarised in Table 10.1.

**Table 10.1** Counts of *Cryptosporidium* oocysts from the National Monitoring Survey (Quennell and West, 1995).

Type of sample	No. of samples per year	No. of positive samples	Maximum no. of oocysts found per litre, and date
<b>Source Waters</b>			
Lowland river	2074	254 (12.2%)	5.7 (June 1994)
Upland reservoir/lake	1593	135 (8.5%)	2.74 (May/October 1993)
Borehole	605	6 (1.0%)	1.0 (November 1993)
Springs	376	30 (8.0%)	0.45 (November 1993)
<b>Treated waters</b>			
Ex-treatment works	2132	42 (2.0%)	2.72 (June 1994)
Service reservoirs	378	21 (5.6%)	0.18 (June 1993)
Customers' taps	109	5 (4.6%)	0.05 (October 1994)
<b>Miscellaneous</b>			
Filtered, unchlorinated water	44	0	-
Filter backwash water	50	5 (10.0%)	10 (No date given)
Waterworks sludge	19	0	-
Sewage effluent	48	36 (75.0%)	166 (September 1993)

Typical counts in North West Waters upland lake sources are 0.1-0.2 oocysts/l, with a maximum of 0.6 oocysts/l.

### 10.3.2 Epidemiology of cryptosporidiosis

The zoonotic component of the epidemiology of cryptosporidiosis is well recognised and domestic cattle have been implicated in both direct (faecal-oral) and independent (via water) human infection outbreaks (Tzipori, 1983).

When cryptosporidiosis is introduced into a community, through the water supply, it can then be readily transmitted from person to person. Therefore outbreaks are likely to be community propagated outbreaks initiated by water. What is meant by an outbreak? Some epidemiological

definitions (Casemore, 1994) are:

- Two or more associated cases sharing a common source of infection (horizontal exposure).
- Two or more associated cases derived from a single source (vertical exposure - propagated outbreak).
- An increase in incidence above the expected (background) level (5000 cases of cryptosporidiosis per year in the UK).

### *10.3.3 History of waterborne cryptosporidiosis outbreaks*

The most common symptom of cryptosporidiosis is a persistent diarrhoea, which is usually self-limiting in immunocompetent patients. This means that medical aid is not usually sought and the existence of the infection is not brought to the attention of the authorities. Thus the detection of the small number of cases that are likely to occur during an outbreak in a population with a high level of immunity is difficult (Casemore, 1995).

Consequently, it is usually large outbreaks that are reported. The following section contains a brief chronological history of major outbreaks.

The first reported outbreak occurred in a small community in Texas, USA, during 1984. The artesian well that supplied the community was believed to have been subjected to ingress of human sewage. The rate of diarrhoea was 12 times greater than that in nearby communities. *Cryptosporidium* oocysts were detected in the stool samples of 59% of diarrhoea patients (D'Antonio, 1985).

A large outbreak occurred in Carrollton, Georgia, USA during 1987. Up to 13,000 people were infected. The overall attack rate was believed to be 40%. Operational difficulties at the local water treatment works were believed to have been responsible (Hayes *et al.*, 1989).

In February 1989, the first major outbreak occurred in the U.K. Swindon and parts of Oxfordshire, supplied by the same treatment works, were affected. There were 500 confirmed cases of cryptosporidiosis. The outbreak was attributed to poor raw water quality and operational difficulties at the plant, namely ineffective backwash water treatment.



In 1992, in Jackson County, Oregon, USA, 15,000 people developed symptoms (10% of the population). Several treatment plants, operating in the same catchment area were believed to be involved. The outbreak was attributed to poor raw water quality and poor operation of the treatment plants.

The biggest waterborne outbreak reported to date occurred in early 1993 in Milwaukee, Wisconsin, USA where water from one of the two plants serving the city was contaminated. It was estimated that 400,000 people showed symptoms and 10% were hospitalised. The attack rate was 52% of the population served by the affected treatment plant. One of the plants was experiencing operational difficulties with its coagulant doses and it is believed that this in combination with poor raw water quality was responsible.

#### *10.3.4 Infectious dose of *Cryptosporidium* oocysts*

Human feeding trials on the dose-response relationships carried out by Haas and Rose (1994) showed that a dose of 30 oocysts would initiate infection in 20% of those exposed. The probability of infection after exposure to 1 oocyst is  $4.7 \times 10^{-3}$ . The results of these trials in combination with the dose-response data from outbreaks, especially the Milwaukee outbreak, have been used to develop risk estimates for microbiological infections after exposure to contaminated water. These models have been used to set treatment goals in the USA under the environmental protection agency (EPA)'s "surface water treatment rule". The rule established a goal of 1:10,000 ( $10^{-4}$ ) annual risk of infection from drinking water supplies.

The minimum concentration of oocysts that could be present in drinking water and still meet the annual risk safety level of  $10^{-4}$  was found by Haas *et al.* (1996) to be  $3.27 \times 10^{-5}$  oocysts / litre. Because the acceptable finished water concentration for controlling the endemic risk of cryptosporidiosis is so low, use of direct finished water sampling is impractical. Sample volumes of 100,000L would be required. Therefore, the assessment of whether or not a given finished water may be acceptable from a microbiological viewpoint can only be made based on influent analysis and assessment of reduction via treatment. Haas *et al.*, (1996), using this approach, developed a graph (shown in Fig 10.1) of the log reduction required for treatment as a function of influent water quality to achieve the stipulated acceptable risk.

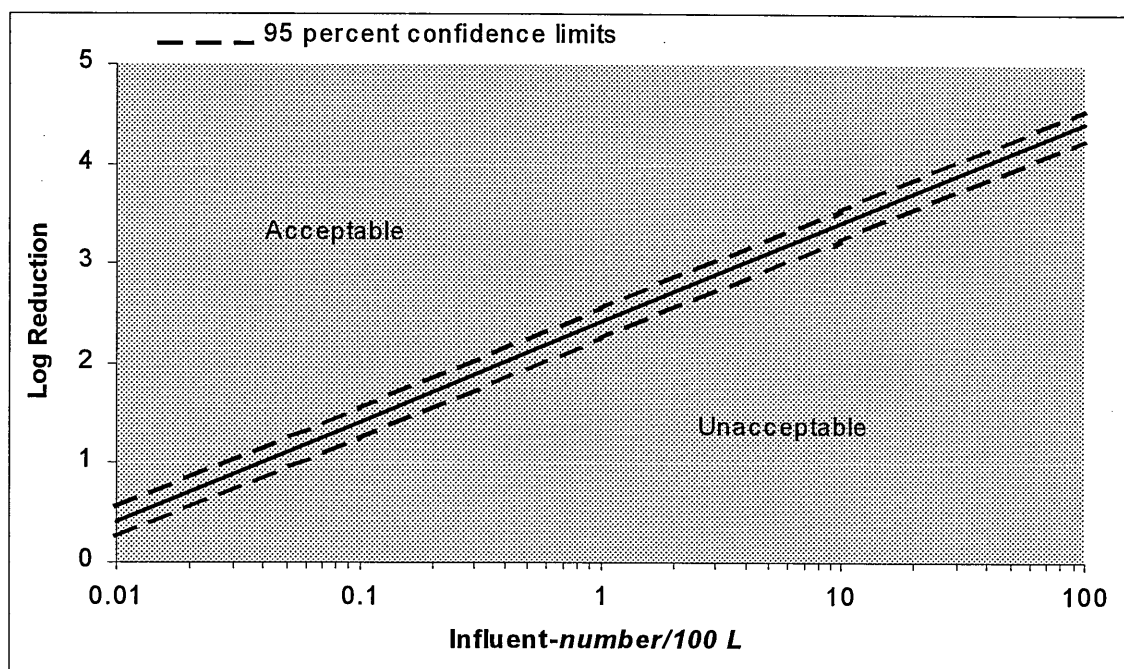


Figure 10.1 Relationship of influent *Cryptosporidium* concentration and log reduction by treatment necessary to produce acceptable water (Haas *et al.*, 1996).

### 10.3.5 Surrogate measures of water quality that allow assessment of public health risk

Surrogate indicators have long been used in water quality monitoring as a substitute for a specific pathogen, an indicator of microbiological purity or filtration efficiency (Jakubowski *et al.*, 1996). A reliable surrogate should be at least as abundant as the pathogen and should be present whenever the pathogen is present in numbers that have a direct relationship to the pathogen. It is important that a surrogate is easy to enumerate by methods that are sensitive. A reliable surrogate for the presence of *cryptosporidium* in drinking water has not been identified. However, various indicators are useful for evaluating water quality and filtration efficiency. The strengths and weaknesses of these indicators have been reviewed by Jakubowski *et al.*, (1996):

Turbidity in water is caused by suspended matter. It is affected by the size, shape, and refractive index of the particulates. Although it is used as a general measure of water quality, it is not specific to biological pathogens. Measurement is simple and in-line monitors permit real-time monitoring. Turbidity does not fully evaluate biological risk, it is also insensitive to oocyst sized particles (Gregory *et al.*, 1994).

Particle counters both count and size inorganic and organic particles. Particle counters and particle size distribution analysers have many applications, including determining filter breakthrough, optimising processes and determining process efficiency. Real-time monitoring and response is possible. LeChevallier *et al.*, (1991) found a good correlation ( $R^2 = 0.83$ ,  $p < 0.01$ ) between log removal of oocysts and 5-15 $\mu\text{m}$  particles. Interferences such as extraneous particles, gas bubbles, and electronic noise can lead to inaccurate counts. Also, calibration standards are not based on real particles, this can result in natural particles with lower refractive index than the calibration materials (usually latex spheres) been undersized.

Microscopic particulate analysis (MPA) compares the type, size and quantities of bioindicators and inert particles found in raw waters with those found in treated water, thus providing critical information about the types of organisms and particulates in waters. Real-time monitoring is not possible, large samples are required and the test is expensive.

Coliform monitoring and heterotrophic plate counts is a useful method for evaluating the degree of pollution and sanitary quality of water. The test is relatively fast, simple and inexpensive. However, coliforms were only detected in 33% of samples collected during protozoan disease outbreaks (88% for bacterial and viral outbreaks).

*Clostridium perfringens* and aerobic spores, primarily of the genus *Bacillus* can both be used as indicators. *C. perfringens* is present in large numbers in human and animal wastes, and its spores are resistant to treatment practices and environmental stress. Aerobic spores are present in most surface waters, they are not faecal indicators. The tests are simple and inexpensive, although not real-time. Removals of *Bacillus* closely parallel both total particle counts and counts in the 3-7 $\mu\text{m}$  size range.

#### 10.4 Treatment Options

Minimising the passage of particulates into supply during filter re-start reduces the chance of *Cryptosporidium* oocysts entering supply. In the technical part of this project a number of treatment options were assessed and optimised so as to provide the greatest physical barrier to oocysts. Two main areas were assessed: backwash optimisation and start-up strategies. A brief

summary of each of the technical options is presented.

#### *10.4.1 Option 1 - Water only backwash*

Water only backwash is the traditional backwash regime and is still used on many plants. In this study it will be used as a benchmark, both in terms of performance and cost.

#### *10.4.2 Option 2 - Air followed by water backwash*

If a treatment plant does not have an air backwash system retro-fit options are available. The filter under drains can be replaced and fitted with filter nozzles; or a laterally branched system of pipes can be fitted above the filter floor (this system is currently undergoing tests at full-scale).

During the pilot trials introduction of an air scour facilitated longer runs, because it was a more effective backwash. However, performance during the ripening period was worse than the water only wash, with a greater number of 2-5 $\mu$ m particles entering into supply.

#### *10.4.3 Option 3 - Combined air/water "collapse-pulsing" backwash*

A retro-fitted air-scour capability could be used to perform a combined air/water backwash at flowrates to achieve collapse-pulsing (CP). During the trials, CP backwash was found to be the most effective, in terms of both runlength and minimising the passage of 2-5 $\mu$ m particles into the filtrate.

#### *10.4.4 Option 4 - Backwash (Opt 3) duration optimisation*

The most effective backwash was CP, different durations of this backwash were assessed in order to determine an optimum. The optimised CP backwash could then be utilised in the start-up strategy trials.

#### *10.4.5 Options 5 and 6 - Backwash optimisation and Delayed start*

Two main start-up strategies were assessed: delayed start and slow start. Delayed start was achieved by retaining the backwash remnants in the filters for a set duration and then starting them in the normal manner. Option 6 was a 1/2 hour delayed start and Option 7 was a 1 hour delayed start.

Generally, delayed start was found to have a beneficial affect upon performance. During the course of the start-up strategy assessment the opportunity arose to evaluate performance under extreme conditions due to severe drought. The delayed start performed well under these more stressful conditions.

#### *10.4.6 Options 7 and 8 - Backwash optimisation and Slow-start*

Slow start, a recommendation in the original Badenoch report (DOE/DOH, 1990), requires sophisticated valves and control systems and is therefore a more expensive option. Option 7 was a 1/2 hour slow start and Option 8 was a 1 hour slow start. Slow start performed well under normal conditions, lower numbers of 2-5 $\mu$ m particles entered the filtrate during ripening. However, runlengths were reduced, meaning more ripening periods. Under the more stressful drought conditions slow start performed badly.

### **10.5 Treatment option costing system**

In order to cost the treatment options it was assumed that a full scale (200MLD) plant already existed at Lostock, treating water from lake Thirlmere, and retro-fitting was necessary. This was more applicable because the vast majority of plants in the NWW region will have to be retro-fitted, very few new plants are planned.

The capital costs of retro-fitting the plant in order to achieve the treatment options was calculated. The operating cost in terms of backwash costs and loss of water production caused by the treatment options was also calculated.

### 10.5.1 Full-scale plant details

Filtration rate = 6m/h

Water production = 8333 m<sup>3</sup>/h

Number of filters = 14

Surface area per filter = 99 m<sup>2</sup>

Total filter area = 1386 m<sup>2</sup>

Costs have been calculated for both the 1m beds of 0.5-1.0mm sand and 2.0m beds of 2.0-3.35mm quartz sand. A water only backwash, for both types of media, was assumed to be the existing backwash regime at the plant.

### 10.5.2 Capital cost of treatment options

The costing system employed is that used by North West Water, cost data has been supplied by Bechtel Engineering (formerly North West Water Engineering).

#### 10.5.2.1 Option 1 - Water only backwash

Since it was assumed that this was the backwash regime already in place at the fictional Lostock plant no capital cost is involved.

#### 10.5.2.2 Option 2 - Air followed by water backwash

The cost of installing an air system above the filter floor was supplied by Roberts Filter Company, Darby, Pennsylvania, USA. The cost per m<sup>2</sup> of filter was inclusive of media removal and replacement, and supply of compressor.

Cost / m <sup>2</sup>	= £710.28	
Total cost	= £710.28 x 1386m <sup>2</sup>	= £984,448

### 10.5.2.3 Option 3 - Combined air/water collapse-pulsing backwash

The capital cost of this option will be the same as that for Option 2.

### 10.5.2.4 Option 4 - Backwash (Opt 3) duration optimisation

No extra capital costs will be incurred in optimising the CP backwash.

### 10.5.2.5 Option 5 and 6 - Backwash optimisation and Delayed start

The capital cost of retro-fitting the fictional Lostock plant for a delayed start capability is made up of control software and instrumentation modifications. The capital cost breakdown is shown in Table 10.2.

**Table 10.2 Capital cost for installation of delayed start control systems.**

Description	Cost (£)
Preliminaries	500.00
Electrical design	1200.00
Software design and testing	1300.00
Electrical installation	5000.00
<b>TOTAL</b>	<b>8000.00</b>

The total capital cost of the delayed start modifications = £8000  
 Capital cost of backwash modifications and delayed start modifications = £984,448 + £8,000  
 = £992,448

### 10.5.3.3 Option 7 and 8 - Backwash optimisation and Slow-start

The capital cost of fitting a slow-start capability is made up of mechanical (valves, actuators etc.), electrical and control system modifications. The cost breakdown is shown in Table 10.3.

**Table 10.3 Capital costs for installation of slow start valves and control systems.**

Description	Cost (£)
Preliminaries	8650.00
Mechanical design	600
Electrical design	21600.00
Software design and testing	1520.00
Factory test mechanical equipment	5400.00
Factory test electrical hardware	-
Site test	-
Supply and deliver inlet valves and actuators (14 x 350mm)	12600.00
Supply and deliver outlet valves and actuators (14 x 500mm)	106000.00
Sampling system	2400.00
Install inlet arrangement	9750.00
Install outlet arrangement	9750.00
Install sampling system	680.00
Removal of redundant equipment	-
Supply and deliver instrumentation	3600.00
Supply and deliver cabling system	9500.00
Supply and deliver panels	7000.00
Supply and deliver PLC/control system hardware	11800.00
Electrical installation	32250.00
Civil works	27900.00
O and M manuals	2750.00
Commissioning	18500.00
Other items	7200.00
<b>TOTAL</b>	<b>299,450.00</b>



The total capital cost of the slow start modifications	= £299,450
Capital cost of backwash modifications and slow start modifications	= £984448+ £299450
	= £1,283,898

#### 10.5.4 Operating costs of treatment options

Two types of operating cost have been calculated, the first does not take into account loss or gain in production (designated operating cost (1)), the second does account for production differences (designated operating cost (2)). The operating costs are worked out in terms of cost of backwash water and electrical consumption during backwash for the first type (Unit cost per KWh is £0.06, Unit cost per m<sup>3</sup> of water is £ 0.1), and the loss of water production is costed in the second. The effect of start-up strategies on water production is illustrated in Figure 10.1.

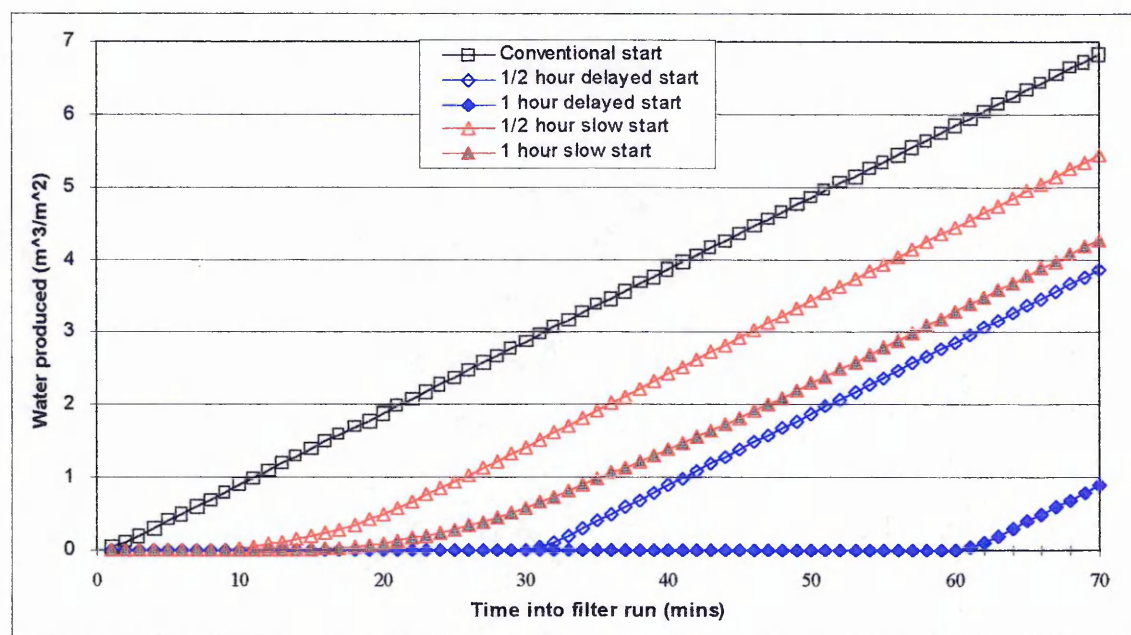


Figure 10.2. How start-up strategies affect water production during the start of a filter run.

Operating costs for both the 1m beds of 0.5-1.0mm sand and the 2m beds of 2.0-3.35mm sand were calculated. Accurate costing was possible for the 1m beds of 0.5-1.0mm sand filters because the exact runlengths were known. These were based on the time to reach 2m headloss,

since particle breakthrough was not occurring. The runlengths, in terms of time to reach terminal headloss for the 2m beds of 2.0-3.35mm media had to be estimated. Runlengths of up to 220 hours were possible, however, particle breakthrough was expected to occur long before this. Due to the experimental procedures used (48 hour runs) it was not known when breakthrough would occur so runlengths were fixed at 70 hours. This fixed runlength did not therefore take into account the effect of different backwash and start-up strategies upon headloss development.

#### 10.5.4.1 Operating cost of different backwash regimes - Options 1,2 and 3.

It was first necessary to calculate both water production and backwash usage per m<sup>2</sup> of bed, as shown in Table 10.4. The corrected runlength incorporates time taken for the backwash.

**Table 10.4. Water production and backwash consumption - 1m 0.5-1.0mm sand filter.**

Filter statistics	Backwash regime		
	Option 1	Option 2	Option 3
Filtration rate (m <sup>3</sup> /m <sup>2</sup> /h)	6	6	6
Average runlength (h)	24.5	33	44
Water produced /run (m <sup>3</sup> /m <sup>2</sup> )	147	198	264
Backwash volume /run (m <sup>3</sup> /m <sup>2</sup> )	5.0	2.5	3.2
Corrected runlength (h)	24.75	33.25	44.23
Number of runs / year	354	263	198
Water production / year (m <sup>3</sup> /m <sup>2</sup> )	52038	52173	52285
Backwash volume / year (m <sup>3</sup> /m <sup>2</sup> )	1770.1	658.7	627.4
% Backwash	3.4	1.3	1.2

The operating cost of the backwash was then calculated (Table 10.5) by adding the cost of the backwash water to the power consumed during backwashing (at 1.5 KW.h /m<sup>2</sup> for each backwash) for operating cost (1). The loss (or gain) in production relative to the existing treatment (Option 1) was accounted for in calculation operating cost (2).

**Table 10.5 Operating costs for backwash regimes - 1m bed of 0.5-1.0mm sand.**

Filter parameters	Backwash regime		
	Option 1	Option 2	Option 3
Water production / year (ML)	72124	72312	72467
Loss of production / year compared to Option 1 (ML)	-	-188	-343
Cost of lost production (£)		-18800	-34300
Backwash usage / year (ML)	2453	913	870
Cost of backwash water (£)	245300	91300	87000
Total power used (KWh)	735966	546777	411642
Cost of power (£)	44157	32807	24699
Total annual cost (1) (£)	289,457	124,032	111,699
Total annual cost (2) (£)	289,457	105,307	77,399

**Table 10.6. Water production and backwash consumption - 2m 2.0-3.35mm sand filter.**

Filter statistics	Backwash regime		
	Option 1	Option 2	Option 3
Filtration rate (m <sup>3</sup> /m <sup>2</sup> /h)	6	6	6
Estimated runlength (h)	70	70	70
Water produced /run (m <sup>3</sup> /m <sup>2</sup> )	420	420	420
Backwash volume /run (m <sup>3</sup> /m <sup>2</sup> )	9.2	7.7	7.6
Corrected runlength (h)	70.18	70.25	70.22
Number of runs / year	124.8	124.6	124.8
Water production / year (m <sup>3</sup> /m <sup>2</sup> )	52416	52332	52416
Backwash volume / year (m <sup>3</sup> /m <sup>2</sup> )	1148.2	959.4	948.5
% Backwash	2.2	1.8	1.8

**Table 10.7 Operating costs for backwash regimes - 2m bed of 2.0-3.35mm sand.**

Filter parameters	Backwash regime		
	Option 1	Option 2	Option 3
Water production /year (ML)	72648	72532	72648
Loss of production / year compared to Option 1 (ML)	-	116	0
Cost of lost production (£)	-	11600	0
Backwash usage / year (ML)	1591.4	1329.7	1314.6
Cost of backwash water (£)	159140	132970	131460
Total power used (KWh)	259875	259875	259875
Cost of power (£)	15592	15592	15592
Total annual cost (1) (£)	174,732	148562	147052
Total annual cost (2) (£)	174,732	136962	147052

#### 10.5.4.2 Option 4 - Backwash (Opt 3) duration optimisation

The water consumption during each backwash per  $m^2$  of filter are shown in Table 10.8 for the 1m beds of 0.5-1.0mm sand and in Table 10.11 for the 2m beds of 2.0-3.35mm sand. The calculations then followed the same format as in the previous section. Values are shown in Tables 10.9 and 10.10 for the 0.5-1.0mm sand and in Tables 10.12 and 10.13 for the 2.0-3.35mm media.

**Table 10.8. Water consumption's ( $m^3/m^2$ ) during backwashing -1m bed of 0.5-1.0mm sand**

Backwash parameters	Collapse-pulsing backwash duration (mins)				
	1	2	3	4	5
CP flowrate ( $m^3/m^2/h$ )	10	10	10	10	10
CP flowrate ( $m^3/m^2/min$ )	0.167	0.167	0.167	0.167	0.167
CP volume ( $m^3/m^2$ )	0.167	0.334	0.501	0.668	0.835
Rinse flowrate ( $m^3/m^2/h$ )	30	30	30	30	30
Rinse volume ( $m^3/m^2$ )	2.5	2.5	2.5	2.5	2.5
Total volume ( $m^3/m^2$ )	2.667	2.834	3.01	3.168	3.335

**Table 10.9. Water production and backwash consumptions for 1m beds of 0.5-1.0mm sand.**

Filter statistics	Collapse-pulsing backwash duration (mins)				
	1	2	3	4	5
Filtration rate (m <sup>3</sup> /m <sup>2</sup> /h)	6	6	6	6	6
Average runlength (h)	21	27	34	38	44
Water produced /run (m <sup>3</sup> /m <sup>2</sup> )	126	162	204	228	264
Backwash volume /run (m <sup>3</sup> /m <sup>2</sup> )	2.667	2.834	3.01	3.168	3.335
Corrected runlength* (h)	21.18	27.2	34.22	38.23	44.25
Number of runs / year	414	322	256	229	198
Water production / year (m <sup>3</sup> /m <sup>2</sup> )	52,164	52,164	52,224	52,212	52,272
Backwash volume / year (m <sup>3</sup> /m <sup>2</sup> )	1104.1	912.5	770.56	725.4	663.3
% Backwash	2.1	1.75	1.5	1.4	1.3

**Table 10.10 Operating costs for different CP backwash durations - 1m of 0.5-1.0mm sand.**

	Collapse-pulsing backwash duration (mins)				
	1	2	3	4	5
Water production /year (ML)	72299	72299	72382	72365	72449
Cost of lost production /year (£)	-17,500	-17,500	-25800	-24100	-32500
Backwash usage / year (ML)	1530	1265	1068	1005	919
Cost of backwash water (£)	153,000	126,500	106,800	100,500	91,900
Cost of power (£)	51642	40166	31933	28565	24698
<b>Total annual cost (1) (£)</b>	<b>204642</b>	<b>166666</b>	<b>138733</b>	<b>129065</b>	<b>116598</b>
<b>Total annual cost (2) (£)</b>	<b>187142</b>	<b>149166</b>	<b>112933</b>	<b>104965</b>	<b>84098</b>

**Table 10.11. Water consumptions ( $\text{m}^3/\text{m}^2$ ) during backwash -2m bed of 2.0-3.35mm sand.**

Backwash parameters	Collapse-pulsing backwash duration (mins)				
	1	2	3	4	5
CP flowrate ( $\text{m}^3/\text{m}^2/\text{h}$ )	30	30	30	30	30
CP flowrate ( $\text{m}^3/\text{m}^2/\text{min}$ )	0.5	0.5	0.5	0.5	0.5
CP volume ( $\text{m}^3/\text{m}^2$ )	0.5	1.0	1.5	2.0	2.5
Rinse flowrate ( $\text{m}^3/\text{m}^2/\text{h}$ )	92	92	92	92	92
Rinse volume ( $\text{m}^3/\text{m}^2$ )	6.1	6.1	6.1	6.1	6.1
Total volume ( $\text{m}^3/\text{m}^2$ )	6.6	7.1	7.6	8.1	8.6

**Table 10.12 Water production and backwash consumption- 2m bed of 2.0-3.35mm sand.**

Filter statistics	Collapse-pulsing backwash duration (mins)				
	1	2	3	4	5
Filtration rate ( $\text{m}^3/\text{m}^2/\text{h}$ )	6	6	6	6	6
Average runlength (h)	70	70	70	70	70
Water produced /run ( $\text{m}^3/\text{m}^2$ )	420	420	420	420	420
Backwash volume /run ( $\text{m}^3/\text{m}^2$ )	6.6	7.1	7.6	8.1	8.6
Number of runs / year	125	125	125	125	125
Water production / year ( $\text{m}^3/\text{m}^2$ )	52500	52500	52500	52500	52500
Backwash volume / year ( $\text{m}^3/\text{m}^2$ )	825	887	950	1012	1075
% Backwash	1.6	1.7	1.8	1.9	2.0

**Table 10.13 Operating costs for different CP durations -2m of 2.0-3.35mm sand.**

	Collapse-pulsing backwash duration (mins)				
	1	2	3	4	5
Water production /year (ML)	72765	72765	72765	72765	72765
Cost of lost production /year (£)	-11700	-11700	-11700	-11700	-11700
Backwash usage / year (ML)	1143	1230	1317	1403	1489
Cost of backwash water (£)	114300	123000	131700	140000	148900
Cost of power (£)	15592	15592	15592	15592	15592
Total annual cost (1) (£)	129892	138592	147292	155592	164492
Total annual cost (2) (£)	118192	126892	135592	143892	152792

### 10.5.5.2 Options 5 and 6 - Backwash optimisation and Delayed start

Optimum CP backwash durations of 4 and 3 minutes were used for the 0.5-1.0mm sand filters and 2.0-3.35mm sand filters respectively. Water production and backwash consumption's are calculated in Tables 10.14 and 10.16 for the different media. Operating costs are calculated and shown in Tables 10.15 and 10.17 for the different filter media.

**Table 10.14. Water production and backwash usage when using delayed start - 1m beds of 0.5-1.0mm sand.**

Filter statistics	Delayed start duration	
	1/2 hour (Option 5)	1 hour (Option 6)
Water produced /run (m <sup>3</sup> /m <sup>2</sup> )	258	255
Backwash volume /run (m <sup>3</sup> /m <sup>2</sup> )	3.168	3.168
Corrected runlength* (h)	43.78	43.73
Number of runs / year	200	200
Water production / year (m <sup>3</sup> /m <sup>2</sup> )	51,600	51,600
Backwash volume / year (m <sup>3</sup> /m <sup>2</sup> )	633.6	633.6
% Backwash	1.2	1.2

**Table 10.15 Annual operating costs of delayed start options - 1m beds of 0.5-1.0mm sand.**

	1/2 hour delayed start	1 hour delayed start
Water production / year (ML)	71,518	70,686
Loss of production / year (ML)	606	1438
Cost of start-up strategy (£)	60600	143800
Cost of backwash water (£)	87941	87941
Cost of power (£)	24948	24948
Total annual cost (£)	112889	112889
Total project cost (£)	173489	256689

**Table 10.16. Water production and backwash usage when using delayed start - 2m beds of 2.0-3.35mm sand.**

Filter statistics	Delayed start duration	
	1/2 hour (Option 7)	1 hour (Option 8)
Water produced /run ( $\text{m}^3/\text{m}^2$ )	420	420
Backwash volume /run ( $\text{m}^3/\text{m}^2$ )	7.6	7.6
Corrected runlength* (h)	70.72	71.22
Number of runs / year	124	123
Water production / year ( $\text{m}^3/\text{m}^2$ )	52080	51660
Backwash volume / year ( $\text{m}^3/\text{m}^2$ )	942.4	934.8
% Backwash	1.8	1.8

**Table 10.17 Annual operating costs of delayed start options - 2m beds of 2.0-3.35mm sand.**

	1/2 hour delayed start	1 hour delayed start
Water production / year (ML)	72183	71601
Loss of production / year (ML)	465	1047
Cost of start-up strategy (£)	46500	104700
Cost of backwash water (£)	130616	129563
Cost of power (£)	15467	15343
Total annual cost (1) (£)	146083	144906
Total annual cost (2) (£)	192583	249606

#### 10.5.5.3 Options 7 and 8 - Backwash optimisation and Slow-start

The water production and backwash consumption when using slow-start strategies are shown in Tables 10.18 and 10.20 for the 0.5-1.0mm sand filters and 2.0-3.35mm sand filters respectively. The operating costs for the two media are in Tables 10.19 and 10.21.



**Table 10.18. Water production and backwash consumption figures when using slow-start options - 1m beds of 0.5-1.0mm sand.**

Filter statistics	Slow start duration	
	1/2 hour (Option 7)	1 hour (Option 8)
Water produced /run ( $\text{m}^3/\text{m}^2$ )	236.1	229.2
Backwash volume /run ( $\text{m}^3/\text{m}^2$ )	3.168	3.168
Corrected runlength* (h)	39.83	38.93
Number of runs / year	220	225
Water production / year ( $\text{m}^3/\text{m}^2$ )	51942	51570
Backwash volume / year ( $\text{m}^3/\text{m}^2$ )	696.9	712.8
% Backwash	1.3	1.41

**Table 10.19 Annual operating costs of slow start options - 1m beds of 0.5-1.0mm sand.**

	1/2 hour slow start	1 hour slow start
Water production / year (ML)	71992	71476
Loss of production / year (ML)	132	648
Cost of start-up strategy (£)	13200	64800
Cost of backwash water (£)	96590	98794
Cost of power (£)	27442	28066
Total annual cost (1) (£)	124032	126860
Total annual cost (2) (£)	137232	191660

**Table 10.20. Water production and backwash consumption figures when using slow-start options - 2m beds of 2.0-3.35mm sand.**

Filter statistics	Slow start duration	
	1/2 hour	1 hour
Water produced /run ( $\text{m}^3/\text{m}^2$ )	418.5	417
Backwash volume /run ( $\text{m}^3/\text{m}^2$ )	7.6	7.6
Corrected runlength* (h)	70.22	70.22
Number of runs / year	125	125
Water production / year ( $\text{m}^3/\text{m}^2$ )	52312	52125
Backwash volume / year ( $\text{m}^3/\text{m}^2$ )	950	950
% Backwash	1.8	1.8

**Table 10.21 Annual operating costs of slow start options - 2m beds of 2.0-3.35mm sand.**

	1/2 hour delayed start	1 hour delayed start
Water production / year (ML)	72504	72245
Loss of production / year (ML)	144	403
Cost of start-up strategy (£)	14400	40300
Cost of backwash water (£)	131670	131670
Cost of power (£)	15592	15592
Total annual cost (1) (£)	147262	147262
Total project cost (2) (£)	161662	187562

*10.5.6 Total cost of treatment options for 5 year period*

In the previous sections capital costs and annual operating costs have been calculated. These are summarised in Table 10.22 for the 1m beds of 0.5-1.0mm sand, and Table 10.23 for the 2m beds of 2.0-3.35mm sand. A 5 year project cost (corresponding to an Asset Management Period) was then calculated incorporating both capital and operating costs. This was performed using both types of operating cost, resulting in Total 5 year project cost (1) - not incorporating production - and Total 5 year project cost (2) - incorporating production.

**Table 10.22 Summary of operating and capital costs - 1m beds of 0.5-1.0mm sand**

Technical Option	Annual operating cost (1) (£)	Annual operating cost (2) (£)	Capital cost (£)	Total 5 year plant cost (1) (£)	Total 5 year plant cost (2) (£)
1	289457	289457	-	1447285	1447285
2	124107	105307	984448	526535	620535
3	111699	77399	984448	386995	558495
4	129065	104965	984448	524825	645325
5	112889	173489	992448	867445	564445
6	112889	256689	992448	1283445	564445
7	124302	137232	1283898	686160	620160
8	126860	191660	1283898	958300	634300

**Table 10.23 Summary of operating and capital costs - 2m beds of 2.0-3.35 mm sand**

Technical Option	Annual operating cost (1) (£)	Annual operating cost (2) (£)	Capital cost (£)	Total 5 year plant cost (1) (£)	Total 5 year plant cost (2) (£)
1	174732	174732	-	873660	873660
2	148562	136962	984448	1727258	1669258
3	147052	147052	984448	1719708	1719708
4	147292	135592	984448	1720908	1662408
5	146083	192583	992448	1722863	1955363
6	144906	249606	992448	1716978	2240428
7	147262	161662	1283898	2020208	2092208
8	147262	187562	1283898	2020208	2221708

### 10.6 Performance measure

Filter performance was measured in terms of the number of 2-5 $\mu$ m particles in the filtrate during ripening. This figure was then scaled-up and extrapolated over 1 year (taking into account the number of backwashes and thus ripening periods). The NPF over 1 year for each Technical Option was then divided by the NPF of Option 1. Therefore performance was relative to Option 1 (Option 1 =1.0). The performance data used are composites since they were relative to Option 1. In the technical trials local controls were used to assess performance. For example, a 1/2 hour slow start on the 0.5-1.0mm sand was assessed relative to a conventionally started filter. Under normal operating conditions, its performance was 0.69 times that of the control. Relative to Option 1 the performance was 0.69 x 0.32 since an optimised backwash was used. The performance data is summarised in Tables 10.24 and 10.25.

Performance data was mostly for normal operating conditions (1000-2500 particles/ml). However, more extreme conditions were encountered during the start-up strategy trials (>2500 particles /ml) and these have also been incorporated into the cost benefit analysis. This is particularly pertinent because the public health was at greater risk during these extreme conditions.

**Table 10.24 Relative performance of Technical Options - 1m beds of 0.5-1.0mm sand**

Technical Option	Performance of Option relative to local control	Performance of Option relative to Option 1
1	1.0	1.0
2	1.36	1.36
3	0.44	0.44
4	0.73	0.32
5	0.78 (0.62)	0.25 (0.20)
6	0.91 (0.40)	0.29 (0.13)
7	0.69 (0.88)	0.22 (0.28)
8	0.40 (0.75)	0.13 (0.24)

Figures in brackets are for performance under extreme (drought) conditions.

**Table 10.25 Relative performance of Technical Options - 2m beds of 2.0-3.35mm sand**

Technical Option	Performance of Option relative to local control	Performance of Option relative to Option 1
1	1.0	1.0
2	1.09	1.09
3	0.96	0.96
4	0.69	0.66
5	1.75 (1.48)	1.16 (0.98)
6	0.85 (0.35)	0.57 (0.23)
7	0.56 (0.97)	0.37 (0.64)
8	0.39 (1.21)	0.26 (0.80)

### 10.7 Cost Benefit Analysis

The capital costs, operating costs ((1) and (2)), and performance of the Technical Options are shown graphically for both types of filter. A cost benefit analysis was carried-out for both types of filter using Total 5 year project costs (1) and (2) and performance data.

### 10.7.1 1m beds of 0.5-1.0mm sand

The capital costs (Fig. 10.5) of options 2 and 3 are the same, this is the cost of the Robert's air distribution system. A very small additional amount of capital is required for the installation of delayed start. The installation of slow start, however, would take a considerable capital investment.

Major differences in the operating cost were apparent when the two costing methods were compared. However, both costing methods showed that the installation of the air distribution system provided major operational savings. Without taking into account differences in production operating costs were more than halved (Fig. 10.3). Options 4, 7 and 8 were slightly higher than 2,3,5 and 6 but the differences were relatively small.

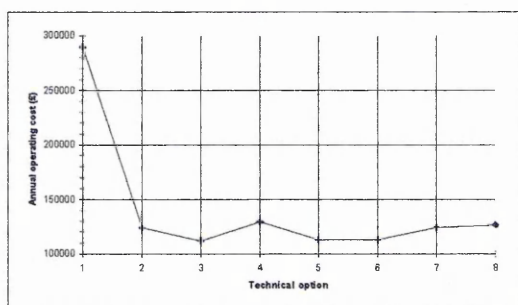


**Figure 10.3** Annual operating costs, not incorporating production - 1m 0.5-1.0mm sand filters

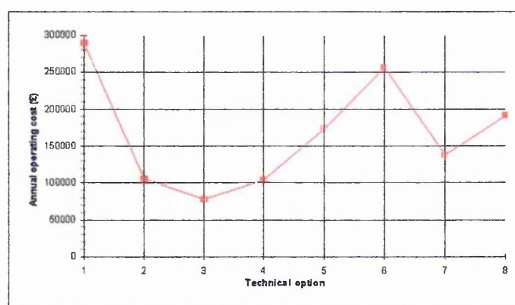


**Figure 10.4** Annual operating costs, incorporating production - 1m 0.5-1.0mm sand filters

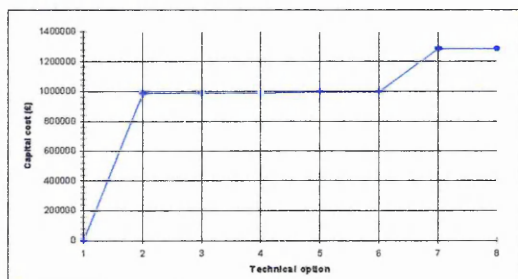


**Figure 10.5** Capital costs of technical options - 1m 0.5-1.0mm sand filter.

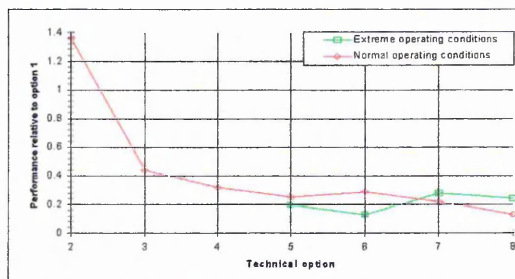


**Figure 10.6** Performance of technical options - 1m 0.5-1.0mm sand filters

When differences in water production, relative to Option 1, were accounted for (Fig. 10.4) the air distribution system resulted in much greater water production, thus facilitating greater savings. This effect was negated by the start-up strategies which resulted in a decrease in production and

hence an increase in operating costs. Option 6, a 1 hour delayed start had the greatest production loss and hence higher operating costs, they were however, still less than Option 1. The result of the operational savings by the installation of an air distribution system mean that the system will pay for itself over a number of years. The pay-back time was calculated for both operating cost systems and is shown in Table 10.26.

The capital invested in the air distribution systems would be recovered after 6.1 years when using an optimised backwash (Option 4), if production were not accounted for. However, if production was accounted for, pay-back would occur in only 5.3 years. The longest pay-back time was for a 1 hour delayed start (Option 6), when incorporating production losses.

**Table 10.26 Pay-back time for invested capital - 1m 0.5-1.0mm sand filter**

Technical Option	Pay-back time (y)	Pay-back time (y)
	Op cost (1)	Op cost (2)
2	5.9	5.3
3	5.5	4.6
4	6.2	5.3
5	5.6	8.5
6	5.6	30.3
7	7.8	8.4
8	7.9	13.1

The performance of the technical Options is shown in Fig. 10.6. Option 2 performed worse than Option 1, the water only backwash. The remaining options provided substantial benefits. The greatest reduction, under normal conditions was by Option 8, a 1 hour slow start. However, under extreme conditions Option 6, the 1 hour delayed start provided the greatest reduction in TNPF.

The cost benefit analysis shown is shown in Figs 10.7 and 10.8. Fig 10.7 shows the cost benefit analysis when production was not accounted for; Fig 10.8 takes account for production. From Fig 10.7 it can be seen that under normal operating conditions, Options 4, 5, 6, 7 and 8 all provide a major improvement in performance, at varying cost. Option 8 provides the greatest improvement, under normal conditions, but at a cost nearly five times that of Options 5 and 6.

Under extreme conditions Options 5 and 6 perform better than Options 7 and 8.

With production relative to Option 1 accounted for, savings are provided by Options 3. Options 2 and 4 incurred little cost over 5 years and Option 4 provided considerable benefit. The performance of Option 4, the optimised backwash also provides a 65% improvement in performance relative to Option 1. The start-up strategies Options 5-8 provide a further improvement in performance but at a cost. Option 8 (1 hour slow start) provides the greatest benefit under normal conditions, but Option 6 (1 hour delayed start) provides the same benefit under extreme conditions at the same cost.

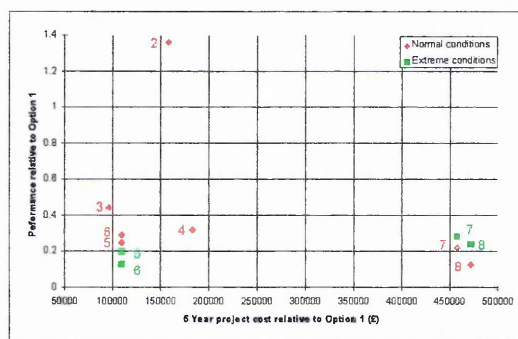


**Figure 10.7** Cost benefit analysis not incorporating production - 1m 0.5-1.0mm sand filter.

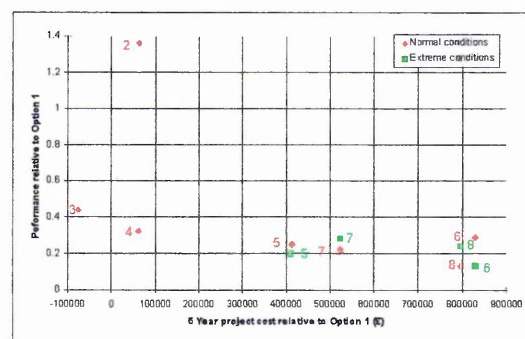


**Figure 10.8** Cost benefit analysis incorporating production - 1m 0.5-1.0mm sand filter.

#### 10.7.2 2m beds of 2.0-3.35mm sand

The operating costs for the, not incorporating production, are shown in Fig. 10.9. All the Options are cheaper than Option 1, and since there were no differences in runlength the operating costs were virtually the same. When production was accounted for (Fig. 10.10), the losses caused by employing a delayed or slow start negated any savings. Options 5, 6 and 8 were more expensive than Option 1. This is reflected in the pay-back times, shown in Table 10.27.

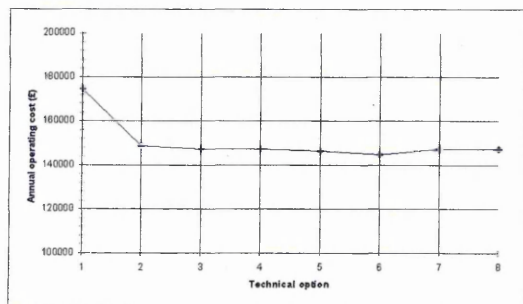


**Figure 10.9** Annual operating costs, not incorporating production - 2m 2.0-3.35 mm sand filters

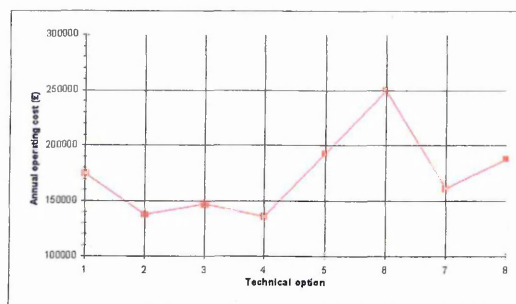


**Figure 10.10** Annual operating costs, incorporating production - 2m 2.0-3.35 mm sand filters

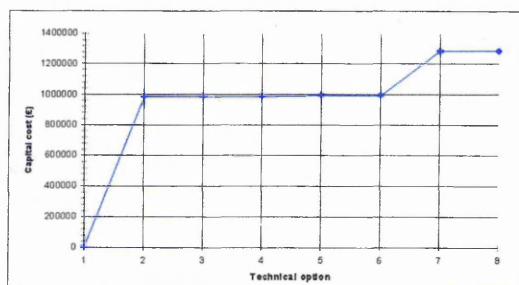


**Figure 10.11** Capital costs of technical options - 2m 2.0-3.35mm sand filter.

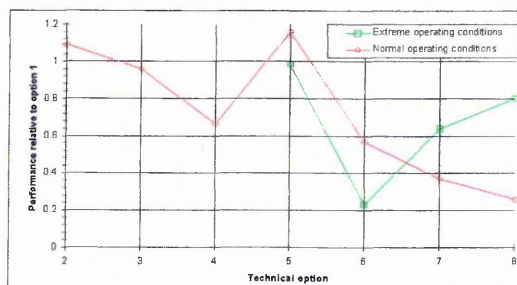


**Figure 10.12** Performance of technical options - 2m 2.0-3.35mm sand filters

The pay-back times, not accounting for production, are all very similar and are also much higher than for the 1m beds of 0.5-1.0mm sand. When production was accounted for it could be seen that Options 5, 6 and 8 did not have a pay-back time, since no annual savings were made. Option 7 did not effectively have a pay-back time. This left Options 2, 3 and 4, the lowest of which was 4 at 25.2 years.

The performance of the Technical Options (Fig. 10.10), under normal conditions, generally improved the higher the Option number, with the notable exception of Option 5. Under extreme conditions Option 6 performed the best and the performance of Options 7 and 8 was substantially affected.



**Table 10.27 Pay-back time for invested capital - 2m 2.0-3.35mm sand filter**

Technical Option	Pay-back time (y)	Pay-back time (y)
	Op cost (1)	Op cost (2)
2	37.6	26.1
3	35.5	35.6
4	35.8	25.2
5	34.6	-
6	33.3	-
7	46.7	98.2
8	46.7	-

The cost benefit analysis, not incorporating production, shown in Fig. 10.13 showed that Option 2-6 would all cost virtually the same. Out of these Options 4 and 6 provided the most benefit, under normal conditions, not as much as Option 7 and 8 but these incurred much greater costs. Under extreme conditions, Fig. 10.14, a lot of variance is seen in the cost. Option 6 would cost as much as Option 8 under these conditions. Option 4 would provide a benefit at a low cost.

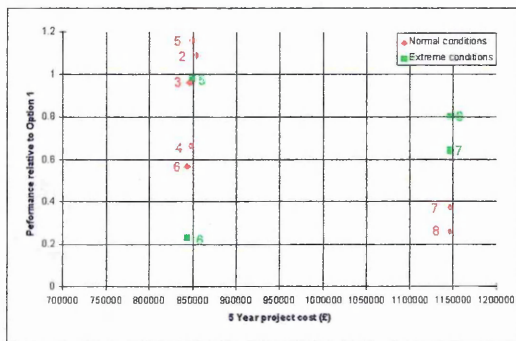


**Figure 10.13 Cost benefit analysis not incorporating production - 2m 2.0-3.35 mm sand filter.**

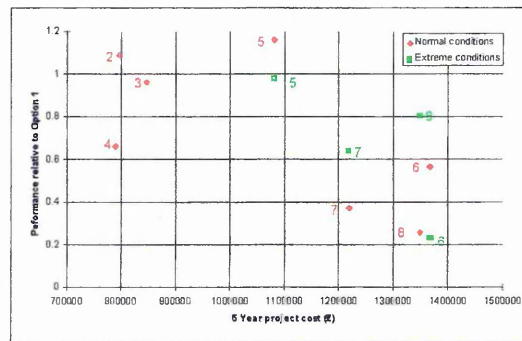


**Figure 10.14 Cost benefit analysis incorporating production - 2m 2.0-3.35 mm sand filter.**

## 10.8 Conclusions/Recommendations

In the original Badenoch report (DOE/DOH, 1990) installation of slow start was suggested as a way of reducing the risk of oocyst penetration into supply during filter ripening. The government, acting on this, asked water companies for their co-operation on the matter. Thus, widespread adoption of slow start occurred.

The technical component of this work showed that a slow start could reduce the numbers of particles entering the filtrate during ripening under "normal" conditions. However, the effect was variable, and under more extreme conditions (in terms of solids loading) slow start made little or no reduction. This was recognised by a re-convened meeting of the Badenoch Group of Experts. As a result they emphasised best-practice when operating filters in the second Badenoch report (DOE/DOH, 1995), recommendation 22 states:

"Water utilities should ensure that the design and operation of treatment plants is optimised in a cost effective way for particle removal taking into account the level of risk identified at each plant."

Although vague, this basically means both operational and capital improvements should be considered at plants, the level of which is dependent on levels of oocysts in raw waters. Thus a plant that treats a high risk water should get both operational and capital improvements in order to provide the greatest possible *Cryptosporidium* barrier. This is where cost effectiveness becomes important, since no Water Utility wants to implement an extensive capital programme. Therefore cost effective solutions are important, this work has shown that backwash optimisation and delayed start can provide considerable benefit at a price far cheaper than slow start. Delayed start is an especially attractive option since it reduces the component of greatest risk (particles retained in the media after backwash) under stressful raw water conditions.

# *CHAPTER 11*

## CONCLUDING DISCUSSION

The research presented in this thesis was carried-out on an operational site, treating “real” raw water from an upland lake source. This resulted in a number of problems due to the inherent variability of natural systems. However, with plant and experimental modifications these were turned into benefits. The nature of the site and the raw water quality allowed confident translation of results from pilot-scale to full-scale.

### 11.1 Problems encountered working under “real” conditions.

The trials were completed over a period of two years and during this time two major environmental problems were encountered. The first was a landslide into lake Thirlmere (15/2/95), which resulted in a huge deterioration in raw water quality that took 4 months to recover, as shown in Fig 11.1. At this time the experimental design did not have sufficient control features in it to deal with such large changes. There was only one column of each media type and 48 hours between runs. Large changes in raw water quality could take place between supposedly duplicate runs. Therefore, data obtained during this period could not be used with any confidence. At this stage the pilot plant was re-fitted to enable more experimental control in the event of future environmental problems.

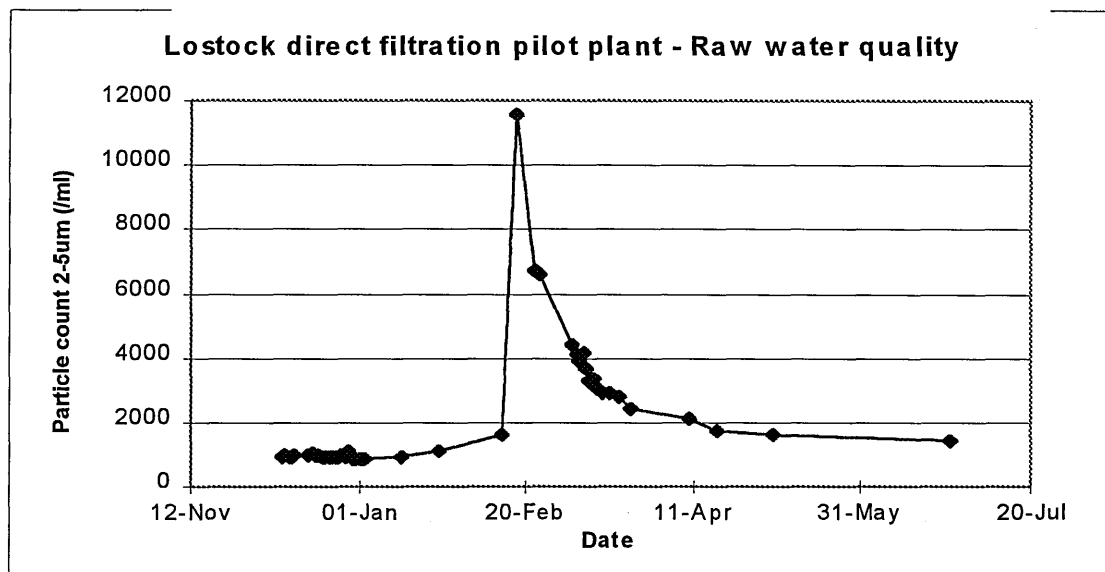


**Figure 11.1 Effect of landslide at lake Thirlmere on raw water quality.**

The second major problem was drought conditions during the summer of 1995, water levels in lake Thirlmere had become so low that the supply had to be augmented by water taken from alternative lakeland sources. This time control filters washed within hours of test filters and therefore valuable data on the effect of variables under alternative raw water conditions was obtained.

The long term nature of the study resulted in changes in filtrate quality during ripening from the same filters under comparable raw water conditions. This is sometimes noticeable when performance of a filter is compared between trials. However, the experimental controls meant that only relative changes in performance were recorded.

A number of observations were made that are interesting from both an operational and academic viewpoint. The derogatory effect of low temperatures on removal at steady state has been reported before (Tebbutt, 1984), and is attributable to an increase in water viscosity. The effect of temperature on particle counts during ripening is rarely discussed. The filtrate quality from a 1m bed of 0.5-1.0mm sand is shown in Fig 11.2 for comparable raw water particle counts at 4 and 17°C.

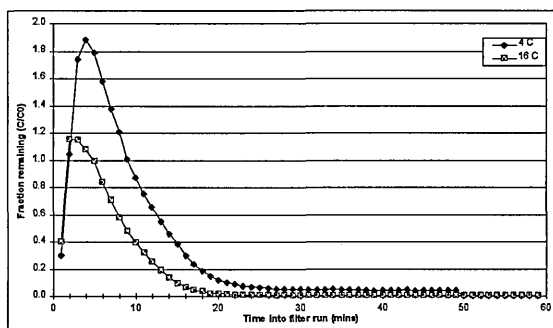


**Figure 11.2** The effect of temperature on filtrate quality during ripening.

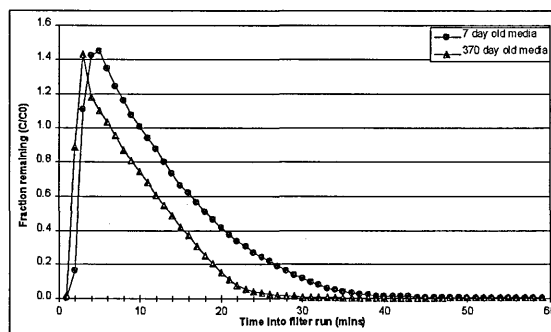


**Figure 11.3** The effect of media age on filtrate quality during ripening.

The effect of media maturation on filter performance during the ripening period is another often overlooked area. Media maturation is reported to occur over 35 years, with noticeable changes occurring after 2 years (Ludyanskiy and Pasichny, 1991). Physical changes in the media occur due to formation of a film composed of organic materials and metals. At Lostock media samples were not taken and hence no analysis was carried-out, however, from the performance results it appears some form of media maturation had occurred in just one year in the 1m bed of 0.5-1.0mm sand filter, as shown in Fig. 11.3

## 11. Implications of the work

During the research and operational development carried-out in this study a greater understanding of the filter ripening phenomenon, its components and the effect variables have upon it has been gained. Strategies for reducing particulate passage into supply during ripening have been tested, optimised and costed. The findings have been incorporated into NWW operational practices.

The effect of ripening of single filters upon the combined filtrate quality of a plant is not normally detected by turbidity monitoring, as recognised in the first Badenoch report. One of the principal recommendations in the report was the installation of turbidity monitors on individual filters. However, the vast majority of plants still only have combined filtrate turbidity monitoring. As a result the risk associated with filter ripening (with respect to *Cryptosporidium* oocyst penetration into supply) is generally overlooked. Particle monitoring at full-scale on the filtrate from individual filters and from as many as thirty filters has illustrated the impact filter ripening can have on overall filtrate quality. This is shown in Figs 11.4 and 11.5, Fig 11.4 is the particle count during the ripening of a single full-scale sand filter, the impact this and two other ripening filters has on the combined filtrate particle count, from thirty filters, is shown in Fig 11.5.

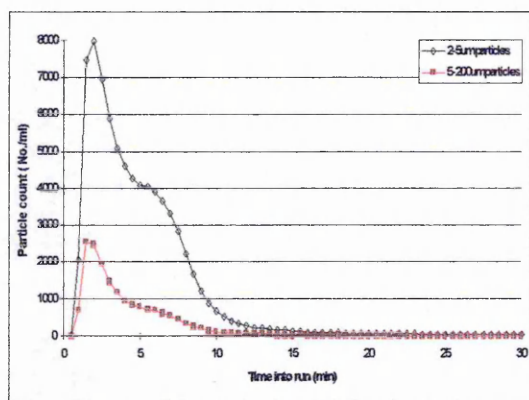


Figure 11.4. Particle count during ripening.

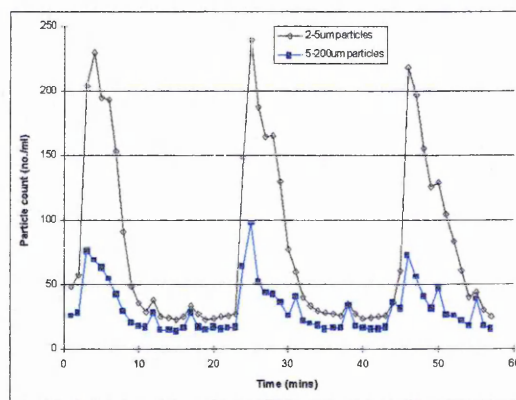


Figure 11.5 Combined filtrate particle count

The numbers of particles entering the filtrate from individual filters clearly has to be reduced to minimise the impact and risk on the combined filtrate. This work has confirmed that the initial peak in filtrate quality during ripening is caused by backwash remnants retained within the filter bed. This component must surely pose the greatest risk to public health since it is likely to contain more *Cryptosporidium* oocysts (if they are present in raw waters). This component was found to cause higher peaks and contribute more particles to the filtrate than the backwash remnants above the media (and the interface with the influent).

Whilst reducing the numbers of particles entering the filtrate during the whole ripening was the overall objective of the research, it was recognised that a reduction in the number of particles in the backwash remnants retained in the bed would also facilitate a considerable risk reduction.

Generally, the collapse-pulsing backwash regime, and both delayed and slow-start resulted in lower numbers of particles entering the filtrate during ripening as a whole and as the backwash remnants from within the filter media were displaced. Slow-start, however, did not provide any reduction when the pilot plant was challenged by a higher solids loading rate, conversely delayed start provided a considerable reduction. When a plant is under such "stress" the risk to public health is greater since more oocysts are likely to enter into supply. Indeed, many of the major outbreaks have occurred when the treatment plant supplying the water has been challenged by influent of very poor quality. Under these circumstances delayed start resulted in a large reduction in risk.

Delayed start was found to be a more attractive option than slow start when the capital cost of retro-fitting existing plant was calculated. Delayed start also facilitated operational savings if the loss of production was discounted. If lost production was included in the operating cost delayed start becomes more expensive. However, within the current climate it is capital cost that is considered important, an increase in operating cost is easily absorbed, whereas major capital is hard to obtain.

The second Badenoch report (DOE/DOH, 1995), withdrew the recommendation that slow-start should be fitted to all filters. Instead, the emphasis was on best-practice when operating filters, recommendation 22 states:

"Water utilities should ensure that the design and operation of treatment plants is optimised in a cost effective way for particle removal taking into account the level of risk identified at each plant."

This recommendation is very vague and open to abuse but the general outcome has been a search for cheap solutions to provide optimum removal of particulate matter. The amount of money invested obviously depends on the perceived risk at individual plants. NWW, which has a number of very high risk sites and many high risk sites, has to do more than provide operators with a stick to measure media height (which could arguably be a form of optimisation and thus best practice). Plans have been shelved to retro-fit four plants with slow-start. At a plant where slow-start had been fitted a trial was carried-out to compare slow-start with delayed start.

Delayed start performed better than slow start in terms of reducing the numbers of particles entering supply during ripening. The result has been a widespread adoption, across the NWW region, of delayed start.



# *CHAPTER 12*

### **FURTHER WORK**

Time and occasionally equipment limitations prevented a number of areas from being investigated. In addition the research highlighted areas where further investigations are required. These are listed below.

1. Although seven media types/configurations were investigated, they were selected on the needs of NWW. A number of other filter types, especially dual media combinations, along with different bed depths of existing media should be investigated.
2. Extended CP backwash durations up to 10 minutes should be investigated, especially for the 2m beds of 2.0-3.35mm sand.
3. The effect of polyelectrolyte addition during the rinse phase of backwash on filter performance during ripening should be investigated. Also the rate of backwash valve closure following the water rinse phase of backwash should be investigated.
4. The effect of start-up strategies should be investigated on different media, and at different filtration rates. Endoscopic observations could be carried-out to observe the deposit morphology, especially in the top layers of the bed, during start-up.
5. Finally, trials on backwash optimisation and start-up strategies should be performed at full-scale to determine how confidently finding at pilot-scale can be translated up to full-scale.

**LIST OF SYMBOLS**

Symbol		Dimension
a	Constant (Equation 2.11, 2.13)	m
b	Constant (Equation )	m
C	Influent concentration	l
d <sub>c</sub>	Collector (media grain) diameter	m
d <sub>p</sub>	Particle diameter	m
g	Acceleration of gravity	ms <sup>-2</sup>
H	Head of water column	m
J	Hydraulic gradient?	
k <sub>1</sub>	Constant (Equation 2.2 )	-
k	Kozeny constant (Equation 2.8)	-
k	Detachment coefficient (Equation )	-
k	Hydraulic permeability	l
K	Boltzmann constant	NmK <sup>-1</sup>
l	Bed depth	m
N	Number of collectors	l
N <sub>Pe</sub>	Peclet number	l
P	Pressure	Nm <sup>-2</sup>
Q	Flowrate	m <sup>3</sup> s <sup>-1</sup>
Q <sub>A</sub>	Air flowrate	m <sup>3</sup> s <sup>-1</sup>
T	Absolute temperature	K
V	Filtration/ backwash rate	ms <sup>-1</sup>
V <sub>mf</sub>	Minimum fluidisation velocity	ms <sup>-1</sup>
α	Attachment efficiency factor	l
α <sub>p</sub>	Particle-particle attachment efficiency factor	l
γ <sub>1</sub>	Constant (Equation 2.10.)	-
ΔH	Loss of head across filter bed	m
ΔH <sub>0</sub>	Loss of head across clean filter bed	m
ΔP	Loss of pressure across filter bed	Nm <sup>-2</sup>
ε	Porosity of filter bed	l
ε <sub>0</sub>	Porosity of clean filter bed	l
η	Single collector efficiency	l
η <sub>I</sub>	Single collector efficiency for interception	l
η <sub>S</sub>	Single collector efficiency for sedimentation	l
η <sub>D</sub>	Single collector efficiency for diffusion	l
η <sub>r</sub>	Resultant single collector efficiency during ripening	l
η <sub>p</sub>	Particle to particle collector efficiency	l
λ	Filter coefficient	m <sup>-1</sup>
λ <sub>0</sub>	Clean bed filter coefficient	m <sup>-1</sup>
ρ <sub>L</sub>	Liquid density	kg m <sup>-3</sup>
ρ <sub>P</sub>	Particle density	kg m <sup>-3</sup>
σ	Specific deposit	l
μ	Dynamic viscosity	kg m <sup>-1</sup> s <sup>-1</sup>
μm	Micrometers	m

**LIST OF ABBREVIATIONS**

<b>BV</b>	Bed volumes
<b>BW</b>	Backwash
<b>CP</b>	Collapse-pulsing
<b>GVF</b>	Gross volume filtered
<b>NPF</b>	Number of particles in filtrate
<b>NPFR</b>	Number of particles in filtrate during ripening
<b>NWP</b>	Net water production
<b>NWW</b>	North West Water
<b>PE</b>	Production efficiency
<b>TNPFR</b>	Total number of particles in filtrate during ripening
<b>UFRV</b>	Unit filter run volume

### REFERENCES

- Adin, A., Baumann, E. R., and Cleasby J. L., (1979). The application of filtration theory to pilot plant design. *J.A.W.W.A.*, 71 No.1, 17-27.
- Adin, A., and Rebhun, M., (1974). High-rate contact flocculation-filtration with cationic polyelectrolytes. *J.A.W.W.A.* 66, No. 2, 109-117.
- Amirtharajah, A., (1978). Optimum backwashing of sand filters. *J. Env. Eng.*, No. EE5, 917-932.
- Amirtharajah, A., (1979). Discussion of "Effectiveness of backwashing for wastewater filters" by J.L. Cleasby. *J.Env. Eng.*, ASCE, 105, p440.
- Amirtharajah, A., (1982). Studies on loss of media during air scour. Proceeding of AWWA Annual Conf. Montana, USA, 387-405.
- Amirtharajah, A., (1984). Fundamentals and theory of air scour. *J. Env. Eng.*, 110, No. 3 573-590.
- Amirtharajah, A., (1988). Some theoretical and conceptual views of filtration. *J.A.W.W.A. Res. and Tech.* 80, no.12 pp 36-46.
- Amirtharajah, A., (1993). Optimum backwashing of filters with air scour: A review. *Water Science and Tech.* 27, No. 10, 195-211.
- Amirtharajah, A., and Giourgis, A. J., (1981). Theory for particle detachment from sand grains during backwashing of filters. Proceedings of International Symposium, Patras, Greece.
- Amirtharajah, A., McNelly, N., Page, G., and McLeod, J., (1991). Optimum backwashing of dual media filters and GAC filter-adsorbers with air scour. AWWA Research Foundation. Denver, Colorado.

Amirtharajah, A., and Tussler, S., (1982). Studies on loss of media during air scour. Proc. of AWWA Annual conference, Montana, USA.

Amirtharajah, A., and Wetstein, D. P., (1980). Initial degradation of effluent quality during filtration. *J.A.W.W.A.* 72, No. 9, 518-524.

Bablon, G.P., Ventresque, C., and Ben Aim, R. (1988). Developing a sand-GAC filter to achieve high-rate biological filtration. *J.AWWA.*, 80, pp 47-53.

Baker, M.N., (1949). The quest for pure water. AWWA, New York.

Bayfield, P. (1993). Factors affecting filter backwashing. M.Sc Thesis, School of Water Sciences, Cranfield University, Bedford.

Bayliss, J.R., (1956). Seven years of high rate filtration. *J.AWWA.*, 48, no.5, p585.

Bayliss, J.R., (1959). Nature and effect of filter backwashing. *J.A.W.W.A.*, 51, pp 126-156.

Beard II, J. B., and Tanaka, T. S., (1977). A comparison of particle counting and nephelometry in evaluating filtration plant performance. *J.A.W.W.A.*, 69, No. 10, 533-538.

Bhargava, D. S., and Ojha, S. P., (1989). Theoretical analysis of backwash time in rapid sand filters. *Water Research*, 23, No. 5, 581-587.

Bishop, S.L., (1981). Methods for evaluating performance of filter media. *J. New. England Water Works Assn.*, 193-207.

Brown, W.G., (1955). High-rate filtration experience at Durham, N.C. *J.AWWA.*, 47, no. 3, p243.

Bucklin, K. E., McFeters, G. A., and Amirtharajah, A., (1991). Penetration of coliforms through municipal drinking water filters. *Water Research*, 25, No. 8, 1013-1017.

Camp, T. R., (1964). Theory of water filtration. *J. San. Eng. Div.* SA4 1-29.

Camp, T. R., (1965). Discussion of "Theory of water filtration." *J. San. Eng. Div.*, 91, SA2 74-80.

Camp, T. R., Graber, S. D., and Conklin, G. F., (1971). Backwashing of granular water filters. *J. Env. Eng. Div.*, 97, SA6 903-926.

Carns, K. E., and Dickson Parker, J., (1985). Using polymers with direct filtration. *J.A.W.W.A.*, 85, 44-49.

Casson, L.W., and Lawler, D.F., (1990). Flocculation in turbulent flow: measurement and modelling of particle size distributions. *J.A.W.W.A.*, 82, pp 54-68.

Chippis, M.J., Bauer, M.J., and Bayley, R.G., (1995). Achieving enhanced filter backwashing with combined air scour and sub-fluidising water at pilot and operational scale. *Filtration and Separation*, 32, No. 1, 55-62.

Clark, S., Lawler, D. F., and Cushing, R. S., (1992). Contact filtration: Particle size and ripening. *J.A.W.W.A.*, 82, No. 3, 61-71.

Cleasby, J.L., Arboleda, J., Burns, D.E., Prendiville, P.W., and Savage, E.S., (1977). Backwashing of granular filters. *J.A.W.W.A.*, 69, pp115-126.

Cleasby, J. L., and Fan, K. S., (1981). Predicting fluidisation and expansion of filter media. 455-471.

Cleasby, J.L., and Lorence, J.C., (1980). Effectiveness of backwashing for wastewater filters. *J. Env. Eng. Div. ASME*, 104, No. EE4, pp 749-765.

Cleasby, J. L., Stanygl, E. W., and Rice, G. A., (1975). Development in backwashing of granular filters. *J.A.W.W.A.*, 101, EE5, 713-727.

Cleasby, J. L., and Williamson, M. M., (1963). Effect of rate changes on filtered water quality. *J.A.W.W.A.*, 55, No. 7, 869-877.

Conley, W. R., (1961). Experience with anthracite sand filters. *J.A.W.W.A.*, 53, S.1473-S.1483.

Cookson, J.T., (1970). Removal of submicron particles in packed beds. *Env. Sci. Tech*, 4, p 128.

Cranston, K.O and Amirtarajah (1987). Improving the initial effluent quality of a dual media filter by coagulants in backwash. *J.AWWA.*, 79, no 12., p 50.

Cross, J., and Rossi, P., (1992). Out for the count-Using particle counters to optimise the performance of municipal water treatment plants. *Wat. Serv. J.*, March.

Culp, R. L., (1977). Direct filtration. *J.A.W.W.A.*, 69, No. 7, 375-378.

D'Antonio, R.G., (1985). A waterborne outbreak of cryptosporidiosis in normal hosts. *Ann. Intern. Med.*, 103, p-886.

Darby, J. L., Attanasio, R. E., and Lawler, D. F., (1992). Filtration of heterodisperse suspensions: Modelling of particle removal and headloss. *Water Research*, 26, No. 6, 711-726.

Darby, J. L., and Lawler, D. F., (1989). Filter ripening: Measurement and predictions from a particle perspective. Proceedings of the AWWA Annual Conf., Los Angeles, California, USA.

Darby, J. L., and Lawler, D. F., (1990). Ripening in depth filtration. *Environmental Science and Technology*, 24, 1069-1079.

Davis, E., and Borchardt, J. A., (1966). Sand Filtration of particulate matter. *J. San. Eng. Div.*, 92, SA5, 47-60.

Department of Environment and Department of Health (1990). *Cryptosporidium* in water supplies. HMSO. London.



Department of Environment and Department of Health (1995). Second report on *Cryptosporidium* in water supplies. HMSO. London

Dharmarajah, A. H., and Cleasby, J. L., (1986). Predicting the expansion behaviour of filter media. *J.A.W.W.A.*, 78, No. , 66-76.

Entwistle, T.M., and Murray, B.A., (1993). Particle counting in contact filtration. Poster paper 15th Federal Convention, Australian Water and Wastewater Association, Queensland, 18th-23 April, 1993.

Fair, G.M., and Geyer, J.C., (1968). In: Water supply and wastewater Engineering. John Wiley and Sons, Inc.

Fitzpatrick, C.S.B. (1990). Detachment of deposits by fluid shear during filter backwashing. *W.Supply.*, 9 no 1.

Fitzpatrick, C.S.B., (1991). Backwashing mechanisms. PhD thesis. University of London.

FitzPatrick, J.A., (1982). Direct filtration. Proceedings, 24<sup>th</sup> Annual public water supply engineers' conference, University of Illinois at Urbana-Champaign, Ill., pp33-47.

Galvin, R. M., (1992). Ripening of silica sand used for filtration. *Water Research*, 26, No. 5, 683-688.

Garcia-Rubio, L.H., (1987). Averages from turbidity measurements. In: Particle size distribution assessment and characterisation. T. Provder (ed.) Symposium Series 332. American Chemical Society, Washington D.C. pp 161-178.

Ghosh, M.M., Jordan, T.A., and Porter, R.L., (1975). Physiochemical approach to water and wastewater filtration. *J.Environ. Eng. Div.*, 101, 71.

Ginn Jr., T. M., Amirtharajah, A., and Karr, P. R., (1992). Effects of particle detachment in granular media filtration. *J.A.W.W.A. Res. Tech.*, 84, No. 2, 66-76.

Glasser, H.T. and Edzwald, J.K., (1978). Coagulation and direct filtration of humic substances with polyethylenimine. *Env. Sci.Tech*, 13.

Graham, N. J. D., (1988). Filter pore flocculation as a mechanism in rapid filtration. *Water Research*, 22, No. 10, 1229-1238.

Gregory, J. (1986). The action of polymeric flocculants. In: Flocculation, sedimentation and consolidation. B.M Moudgil and P. Somasundaran, Eds. Engrg. Foundation, New York.

Gregory, J., Ives, K.J., Scutt, J.E., and Makanjuola, D.B. (1991). Removal of *Cryptosporidium* oocysts by water treatment methods at laboratory scale. In *Cryptosporidium* in water supplies. The second report of the group of experts. HMSO, London, 1995.

Gregory, J., (1994). *Cryptosporidium* in water treatment and monitoring methods. *Filt. and Separation.*, 31, No.3, pp 283-289.

Haarhoff, J., and Malan, W. M., (1983). The disturbance of sand filters supporting layers by air scouring. *Water South Africa*, 9, No. 2, 41-49.

Haas, C.N., Crockett, C.S., Rose, J.B., Gerba, P., and Fazil, A.M. (1996). Assessing the risk posed by oocysts in drinking water. *J.AWWA.*, 88, no.9, 131-135.

Habibian, M. T., and O'Melia, C. R., (1975). Particles, polymers and performance in filtration. *J. Env. Eng. Div.*, 101, 567-583.

Hall, T., and Pressdee, J.R, (1995). Removal of *Cryptosporidium* during water treatment. Proceedings of Workshop on treatment optimisation for *Cryptosporidium* removal from water supplies. HMSO, London.

Hargeshiemer, E. E., Lewis, C. M., Yentsch, C. M., Satchwill, T., and Mielke, J. L., (1991). Pilot scale evaluation of filtration processes using particle counting. Proceedings of the AWWA Water Quality Tech. Conf., San Diego, California, USA, 323-344.

Hargeshiemer, E. E., Lewis, C. M., and Yentsch, C. M., (1992). Evaluation of particle counting as a measure of treatment plant performance. J.A.W.W.A. Res. Fdn., USA.

Hargeshiemer, E.E. and Lewis, C.M., (1995). A practical guide to on-line particle counting. AWWA Research Foundation and AWWA. Denver, Colorado.

Hayes, E.B., Matte, T.D., O'Brien, T.R., McKinley, T.W., Logsdon, G.S., Rose, J.B., (1989). Large community outbreaks of Cryptosporidiosis due to contamination of a filtered public water supply. *N.Engl.J.Med.*, 320, pp 1372-1376.

Happel, J., (1958). Viscous flow in multiparticle systems: slow motion of fluids relative to beds of spherical particles. *A.I.Ch.E.J.*, 4, 197.

Hewitt, A.M., and Amirtharajah, A., (1984). Air dynamics through filter media during air scour. *J.Env. Eng.*, 110, No. 3, 591-603.

Hilmore, D. J., and Cleasby, J. L., (1986). Comparing constant-rate and declining-rate direct filtration of a surface water. *J.A.W.W.A.*, 26-34.

Huang, J. Y. C., and Basagoiti, J., (1989). Effect of solids property on rates of solids dislodgement. *J. Env. Eng.*, 115, No. 1, 3-19.

Humby, W.S., (1994). Attrition of granular media during backwashing. M.Sc Thesis, School of Water Sciences, Cranfield University, Bedford.

Hutchinson, C. W., (1985). On-line particle counting improves filter efficiency. *Water Eng. Management*, 20-25.

Hutchinson, C. W., (1985). On-line particle counting for filtration. *ISA Transcriptions*, 24, No. 3, 75-82.

Hutchinson, W. R., and Foley, P. D., (1974). Operational and experimental results of direct filtration. *J.A.W.W.A.*, 66, No. 2, 79-87.

Ison, C.R., and Ives, K.J. (1969). Removal mechanisms in deep bed filtration. *Chemical Eng. Sci.*, 24, 717-729.

Ives, K.J., (1960). Rational design of filters. *Proc. Inst. Civ. Eng.*, 16, 163.

Ives, K.J. (1982). Fundamentals of filtration. *Proc. Of Sym. On Water Filtration*. European Federation of Chem. Engrg, Antwerp, Belgium.

Ives, K.J. (1989). Filtration studied with endoscopes. *Water Research*, 23, No.7, 861-866.

Ives, K.J., and Fitzpatrick, C.S.B. (1989). Detachment of deposits from sand grains. *Colloids and Surfaces*, 39, 239-253.

Ives., K.J., and Gregory, J., (1967). Basic concepts of filtration. *J.Proc. Soc. Wat. Treat. Exam* 16, no. 147.

Ives, K.J., Gregory, J., Scutt, J., and Pugh, H. (1993). A microsphere in water: *Cryptosporidium parvum*. Presented at 6th World Filtration Congress, Nagoya.

Ives, K.J., and Sholji, I., (1965). Research on variables affecting filtration. *J.Sanit. Eng. Div. ASCE.*, 91, no.4, p1.

Iwasaki,T., (1935). Some notes on sand filtration. *J.AWWA.*, 29, 1591.

Jackubowski, W., Boutros, S., Faber, W., Fayer, R., Ghiorse, W., LeChevallier, M., Rose, J., Schaub, S., Singh, A., and Stewart, M. (1996). Environmental methods for *Cryptosporidium*. *J.AWWA.*, 88, no.9, pp 107-112.

Johnson, R.L., and Cleasby, J.L., (1966). Effect of backwash on filter effluent quality. *ASCE J.Sanit. Eng. Div.*, 92, pp 215-218.

Kau, D.C., and Lawler, D.F., (1992). Wastewater filtration: Particle size, ripening and break-off. *Advances in filtration and separation, Volume 5: Separation problems and the environment*. Amer. Fed. Filt. Soc, Houston, Texas.

Kavanaugh, M.C., Tate, C.H., Trussell, A., Trussell., R.R., and Treweek, G.P. (1980). Use of particle size measurement for water treatment plant process selection and control. *Amer. Chem. Soc.*, 18, No.1, 246-249.

Lechevallier, M.W., Norton, W.D., and Lee, R.G. (1991a). Occurrence of Giardia and Cryptosporidium in surface water supplies. *Applied Environmental Microbiology*, 57, 2610-2616.

Lechevallier, M.W., Norton, W.D., and Lee, R.G. (1991b). Giardia and Cryptosporidium in filtered drinking water supplies. *Applied Environmental Microbiology*, 57, 2617-2621.

Lechevallier, M.W., Norton, W.D. (1992). Examining relationships between particle counts and Giardia, Cryptosporidium and turbidity. *J.A.W.W.A. Res. Tech.*, 84, 54-60.

Lewis, C.M., Hargesheimer, E.E., and Yentsch, C.M. (1991). Quality control for particle counting in water treatment plant process monitoring. Proceedings of A.W.W.A. Water Tech. conference, Orlando, Florida. 187-205.

Lewis, C.M., Hargesheimer, E.E., Yentsch, C.M., and mayberry, P.E. (1991). Selecting and evaluating particle counters for discrete sample analysis. Proceedings of A.W.W.A. annual conference, Vancouver, Canada. 363-386.

Lewis, C.M., Hargesheimer, E.E., and Yentsch, C.M. (1992). Selecting particle counters for process monitoring. *J.A.W.W.A.*, 84, No.12, 46-53.

Lewis, C.M., and Manz, D.H. (1991). Light-scatter particle counting. Improving filtered-water quality. *Journal of Environmental Engineering*, 117, No.2, 209-223.

Logsdon, G.S., Symons, J.M., Hoyer Jr. J.L., and Arozarena, M.M. (1981). Removal of Giardia cysts and cyst models by filtration. *J.A.W.W.A.* 73, No.2, 111-118.

Mackie, R.J., and Bai, R., (1992). Suspended particle size distribution and the performance of deep bed filters. *Wat. Res.*, 26, No.12, 1571-1575.

Mackie, R.I., Horner, R.M., and Jarvis R.J., (1987). Dynamic modelling of deep bed filtration. *A.i.Ch.E.Jl*, 33, pp 1761-1775.

Madore, M.S., (1987). Occurrence of *Cryptosporidium* oocysts in sewage effluents and select surface waters. *J. Protozool.*, 34, No. 1, p 28.

McDowell-Bowyer, L.M., (1992). Chemical mobilisation of micron sized particles in saturated porous media under steady flow conditions. *Env. Sci. Tech.*, 26, no.3, pp 586-593.

McNelly, N.A., and Amirhajah, A. (1991). Optimization of the filter backwashing process as determined by collapse-pulsing. Proceedings of A.W.W.A. annual conference, Orlando, Florida.

Mints, D.M., and Krishtal, V.P., (1960). Investigation of the process of filtration of a suspension in a granular bed. *Zhurnal Priskladnoi Khimi* (English translation) 33, No.2 pp304-316.

Moll, H.G. (1986). Expansion of filter media material during backwashing. Proceedings of 4th World filtration congress. 8.7-8.11.

Moll, H.G. (1990). Effectiveness of backwashing with air and water. Proceedings of 5th World filtration congress, Nice, France. 117-121.

- Moll, H.G. (1996). Effectiveness of backwashing with air and water. Proceedings of 7th World filtration congress, Budapest, Hungary. 369-374.
- Monscivitz, J.T., and Rexing, D.J. (1983). Direct filtration control by particle counting. Proceedings A.W.W.A. annual conference, Denver, Colorado. 47-74.
- Moran, M.C., Moran, D.C., Cushing, R.S., and Lawler, D.F. (1993a). Particle behaviour in deep bed filtration: Part 1. Ripening and breakthrough. *J.AWWA*. 85, no. 12, pp 69-81.
- Moran, M.C., Moran, D.C., Cushing, R.S., and Lawler, D.F. (1993b). Particle behaviour in deep bed filtration: Part 2. Particle detachment. *J.AWWA*. 85, no. 12, pp 82-93.
- Mosher, R.R., and Hendricks, D.W. (1986). Rapid rate filtration of low turbidity water using field-scale pilot filters. *J.A.W.W.A. Res Tech.*, 78.
- O'Melia, C.R., and Ali, W. (1978). The role of retained particles in deep bed filtration. *Progress in Water Technology*, 10, No.5/6, 167-182.
- O'Melia, C.R., and Crapps, D.K. (1964). Some chemical aspects of rapid sand filtration. *J.A.W.W.A.*, 56, No.10, 1326-1344.
- O'Melia, C.R., and Stumm, W., (1967). Theory of water filtration. *J.AWWA*, 59, 1393-1412.
- O'Neil, S.E., (1993). Jar testing of upland waters. Msc. Thesis, School of Water Sciences, Cranfield University, Bedford.
- Ongerth, J.E., (1989). Giardia cyst concentrations in river water. *Appl. Env. Microbiol.*, 53, pp 671-676.
- Ongerth, J.E. and Stibbs, H.H., (1987). Identification of *Cryptosporidium* oocysts in river water. *Appl. Env. Microbiol. Rev.*, 53, p687.

- Paytakes, A.C., Park, H.Y., and Petrie, J., (1981). A visual study of particle deposition and reentrainment during depth filtration of hydrosols with polyelectrolyte. *Chem.Eng.Sci.*, 36, 1319.
- Pugh, H., (1995). Deposition and adhesion of *Cryptosporidium* oocysts to surfaces. PhD Thesis. University of London.
- Quennell, S. and West, P.A., (1995). *Cryptosporidium* monitoring in the U.K. Proceedings of workshop on treatment optimisation for *Cryptosporidium* removal from water supplies. HMSO, London.
- Qureshi, N. (1982). The effect of backwashing rate on filter performance. *J.A.W.W.A.*, 74, No.5, 242-248.
- Rajagopalan, R. and Tien, C., (1976). Trajectory analysis of deep bed filtration with the sphere-in-cell porous media model. *A.I.Ch.E.J.*, 22, 523.
- Raveedran, P., and Amirtharajah, A., (1995). Role of short-range forces in particle detachment during filter backwashing. *J. Chem. Eng.*, 121, No.3, 860-868.
- Regan, M.M., and Amirtharajah, A., (1984). Optimization of particle detachment by collapse-pulsing during air scour. Proceedings of AWWA annual conference, Dallas, Texas, USA.
- Robeck, B.B., Dostal, K.A., and Woodward, R.L., (1964). Studies of modification in water filtration. *J.AWWA.*, 56, no. 2, p198.
- Roberts, J. (1986). Collapse-pulsing in sand filters using air/water combinations. CHEMECA, Adelaide, Australia. 19th-22nd August, 1986.
- Rose, J.B., (1987). Detection of *Cryptosporidium* and *Giardia* in environmental waters. Advances in water analysis and treatments. AWWA, Denver, Colorado.



Rose, J.B. (1988). Occurrence and significance of *Cryptosporidium* in water. *J.A.W.W.A. Res. Tech.*, February, 1988.

Ryan, J.N., and Gschwend, P.M., (1994). Effects of ionic strength and flow rate on colloid release: relating kinetics to interface potential energy. *J.Colloid and Interface Sci.* 164, no. 1, pp 21-34.

Sharma, M.M., Chamoun, H., Sita Ramma Sarma, D.S.H., and Schechter, R.S. (1992). Factors controlling the hydrodynamic detachment of particles from surfaces. *J.Colloid and Interface Sci.* 149, no. 1, pp 121-134.

Srivastava, R.M. (1993). Effect of sequence of measurement on particle count and size measurements using a light blockage (Hiac) particle counter. Technical Note, *Water Research*, 27, No.5, 939-942.

Suthaker, S., Smith, D.W., and Stanley, S.J., (1995). Evaluation of filter media for upgrading existing filter performance. *Env.Tech.*, 6, pp 625-643.

Tare, V., and Venobachar, C. (1985). New conceptual formulation for predicting filter performance. *Env. Sci and Tech*, 19, No. 6, 497-499.

Tate, C.H., Lang, J.S., and Hutchinson, C.W. (1977). Pilot plant tests on direct filtration. *J.A.W.W.A.*, 69, No.7, 379-384.

Tebbutt, T.H.Y., and Shackleton, R.L. (1984). Temperature effects in filter backwashing. *The Public Health Engineer*, 12, No.3, 174-179.

Tien, C., Wang, G.S., and Barot, D.T. (1977). Chain-like formation of particle deposits in fluid-particle separation. *Science*, 196, 983-985.

Tobiason, J.E., Johnson, G.S., Westerhoff, P.K., and Vigneswaran, B., (1993). Particle size and chemical effects on contact filtration performance. *J.Env. Eng.*, 119, No. 3, 520-539.

Tobiason, J.E., and O'Melia, C.R., (1982). Filtration performance in water and wastewater treatment: Theory and measurement. *National Technical Information*, OWRT A-104-NC(2), 14-34-0001-9035

Tobiason, J.E., and O'Melia, C.R. (1988). Physiochemical aspects of particle removal in depth filtration. *J.A.W.W.A.*, 80, No.12, 54-64.

Tobiason, J.E., Johnson G.S., and Westerhoff, P.K., (1990). Particle size and filter performance: model studies. In *National Conf. Envir.Eng, Proceedings of the special conference*, Arlington, Va, USA., pp 733-739.

Treweek, G.P. and Morgan, J.J., (1980). Prediction of suspension turbidities from aggregate size distribution. In: *Particulates in water*. M.C. Kavanaugh and J.O. Leckie (eds.). *Advances in Chemistry Series 189*. American Chemical Society, Washington D.C., pp 329-352.

Trussell, R.R., Trussell, A.R., Lang, J.S., and Tate, C.H., (1980). Recent developments in filtration system design. *J.AWWA.*, 72, no.12., p705.

Tzipori, S., (1983). Cryptosporidiosis in animals and humans. *Microbiol. Rev.*, 47, p84.

Vigneswaran, S., and Ben Aim, R., (1985). The influence os suspended particle size distribution in deep bed filtration. *A.I.Chem.Eng.J.* 31, 321-324.

Vigneswaran, S., and Chang, J.S., (1986). Mathematical modelling of the entire cycle of deep bed filtration. *Water, Air and Soil Pollution*, 29, pp 155-164.

Vigneswaran, S., Chang, J.S., and Janssens, J.G. (1990). Experimental investigation of size distribution of suspended particles in granular bed filtration. *Water Research*, 24, No.7, 927-930.

Vigneswaran, S., and Tulachan, R.K. (1988). Mathematical modelling of transient behaviour of deep bed filtration. *Water Research*, 22, 1093-1100.

Wang, Z., Tobiason, J.E., and O'Melia, C.R. (1986). Chemical aspects of packed bed filtration in water treatment. Proceedings of 4th World Filtration Congress, part 1, Ostend, Belgium. 8.23-8.27.

Wen, H.Y., and Kasper, G. (1989). On the kinetics of particle reentrainment from surfaces. *Journal of Aerosol Science*, 20, No.4, 483-498.

Wen C.Y., and Yu, y.H (1966). Mechanisms of fluidisation. *Chem. Eng., Prog. Symp. Series* no. 62. New York. AiChE.

Westerhoff, G.P., (1976). Filter loading, performance, and water quality. *JAWWA.*, 68, 310-312.

Yao, K.M., Habibian, M.T., and O'Melia, C.R., (1971). Water and wastewater filtration: Concepts and application. *Env. Sci and Tech.*, 5, 1105-1112.